Impulsive differential equations with applications to infectious diseases

Rachelle Miron

Thesis submitted to the Faculty of Graduate and Postdoctoral Studies
in partial fulfillment of the requirements for the degree of Doctor of Philosophy in Mathematics [1]

Department of Mathematics and Statistics
Faculty of Science
University of Ottawa

[1]The Ph.D. program is a joint program with Carleton University, administered by the Ottawa-Carleton Institute of Mathematics and Statistics

Abstract

Impulsive differential equations are useful for modelling certain biological events. We present three biological applications showing the use of impulsive differential equations in real-world problems. We also look at the effects of stability on a reduced two-dimensional impulsive HIV system. The first application is a system describing HIV induction-maintenance therapy, which shows how the solution to an impulsive system is used in order to find biological results (adherence, etc). A second application is an HIV system describing the interaction between T-cells, virus and drugs. Stability of the system is determined for a fixed drug level in three specific regions: low, intermediate and high drug levels. Numerical simulations show the effects of varying drug levels on the stability of a system by including an impulse. We reduce these two models to a two-dimensional impulsive model. We show analytically the existence and uniqueness of T-periodic solutions, and show how stability changes when varying the immune response rate, the impulses and a certain nonlinear infection term. The third application shows how seasonal changes can be incorporated into an impulsive differential system of Rift Valley Fever, and looks at how stability may differ when impulses are included. The analysis of impulsive differential systems is crucial in developing more realistic mathematical models for infectious diseases.

Acknowledgements

First and foremost, I'd like to thank my Ph.D. supervisor Dr. Robert Smith? for your continuous encouragement and support. I could never even begin to tell you how much I appreciate all your help and guidance throughout our 6 years working together. You have taught me so much about math, biology and about being a great teacher in which I am truly grateful. I'd also like to give a special thanks to Dr. Jane Heffernan for taking the time to read and comment on the final version of my thesis.

Second, I'd like to thank my dad, mom, Sean, Ricky, Renée, Robin and Matt for continuously motivating me at working harder, and always believing that I could accomplish my goal of becoming a doctor. In particular I'd like to give an extra thanks to my dad... even though you know nothing more than extremely basic math, you always read my manuscripts and never failed to give great critiques, which helped me improve as a writer.

And last, I'd like to thank the University of Ottawa MathBio team. In particular, thank you to Dr. Frithjof Lutscher, Dr. Benoit Dionne, Dr. Jing Li, Rolina van Gaalen, Jeff Musgrave, Carley Rogers, Nyuk Sian Chong and Kevin Church for your continuous inspiring ideas and help along my journey.

Dedication

"I learned that courage was not the absence of fear, but the triumph over it. The brave man is not he who does not feel afraid, but he who conquers that fear."

- *Nelson Mandela*

For mom and dad. You are my heroes.

Contents

List of Figures

Chapter 1

Introduction

Impulses in differential equations are used to describe instantaneous changes in the behaviour of a system. They aid in describing biological events that undergo sudden perturbations more precisely. It is known, for example, that many biological phenomena involving thresholds — such as drug resistance models in medicine and biology — do exhibit impulsive effects. We develop and analyze three impulsive differential systems, two of which describe the dynamics of the human immunodeficiency virus (HIV) with impulsive drug effects and one that describes the dynamics of the Rift Valley Fever (RVF) virus to seasonal changes. We also analyze a two-dimensional reduced impulsive HIV system, and see the effects that an impulse and a nonlinear term may have on the stability of the system.

We first include an overview of impulsive differential equations (Chapter 2). The information is a summary of results from *Impulsive Differential Equations: Periodic Solutions and Applications* and *Theory of Impulsive Differential Equations* [1, 2]. It describes the different outcomes that occur when including an impulse in a differential system and analyzes solutions to linear homogenous, linear non-homogenous and nonlinear periodic equations.

Chapter 3 includes two applications describing the immunological effects of HIV.

First there is a short overview of HIV. The interested reader is referred to Appendix A for more information on the immunology and microbiology of the virus, drug therapy, incidence, worldwide issues, and new and ongoing prevention strategies of HIV. Two manuscripts are presented next. The first is published in the journal *Biomed Central Infectious Diseases* [3] (Section 3.1), and the second is published in the *Bulletin of Mathematical Biology* [4] (Section 3.2). The first application describes the effects of induction-maintenance therapy. The impulsive differential system includes ten ordinary differential equations. The drug dynamics occur at fixed times, where an instantaneous increase occurs when a drug is taken. Between drug intakes, the drug decays exponentially, meaning it is cleared from the body depending on its half-life. The impulsive differential system (ordinary differential equations involving impulse effects) is solved in order to view the effects of imperfect adherence to a protease-inhibitor-sparing HIV drug regimen. The number of doses allowed during a drug holiday was calculated in order to avoid drug resistance. Simulation details and extra comments for the manuscript, as well as sensitivity analysis can be found in Appendix B. The second application describes the interaction that occurs in an HIV-positive individual between T-cells, virus and protease inhibitor drugs. The impulsive differential system includes thirteen ordinary differential equations with the impulse occurring when a drug is taken. Stability analysis shows the interaction between the wild-type and resistant virus for a fixed drug level at either low, intermediate or high concentration (see Appendices C, D, E, F for more details on the development of results for different regions). Numerical simulations show the outcome when the drug concentration varies. Simulation details and extra comments for the manuscript can be found in Appendix G.

Chapter 4 introduces a two-dimensional impulsive differential system. The equations are derived from the models presented in the two manuscripts in Chapter 3. The impulsive system is an approximated HIV model including only one class of T cells and virus. We develop a general two-dimensional system where all but one term

is linear (there is only one nonlinear infection term). The importance of the nonlinear infection term has caused debate when modelling infectious diseases since some research suggests that it can be omitted while others demonstrate that results change when it is not included. We use our two-dimensional impulsive system to analyze the effects of stability when this non-infection term is either included or not. We first prove that, for a general linear impulsive system, the immune response rate (rate at which the immune system reacts when virus is present) and the parameter chosen for our impulse change the regions of stability. We also numerically show that, for specific parameters, when the nonlinear infection term is included, the regions of stability appear to change. We also look at two subcases of the general impulsive system in order to analytically show the effects of the nonlinear infection term.

Chapter 5 includes an application describing the epidemiological effects of RVF. First there is a short overview of RVF. The interested reader is referred to Appendix H for more information on the etiology of the virus, the vectors that transmit the virus, the viable hosts and the epidemiology of the virus. The manuscript is presented next (Section 5.1). This paper is in press in the journal *Mathematical Population Studies* [5]. The model shows the effects of seasonal changes to a system including human, livestock and mosquito populations. The one-season model is presented first. It is a system of eleven ordinary differential equations. Stability analysis is computed for the disease-free equilibrium, and the basic reproductive number is found. Impulses are then included to analyze the multiple-season outcome. The winter season allows the host populations to increase and the mosquito population to decrease. These outcomes are described by a system of impulses. Numerical simulations show the changes that may occur when multiple seasons are included. Simulation details and extra comments for the manuscript can be found in Appendix I.

Chapter 6 concludes the thesis with a discussion, conclusion and future work.

Chapter 2

Overview of impulsive differential equations

2.1 Review of Impulsive Differential Equations

Differential equations can be used to model the dynamics of many real-world phenomena. Many evolutionary processes are characterized by the fact that at certain moments of time they experience an abrupt change of state. These processes are subject to short-term perturbations whose duration is negligible in comparison with the duration of the process. Consequently, it is natural to assume that these perturbations act instantaneously; that is, in the form of impulses. Thus, impulsive differential equations — that is, differential equations involving impulse effects — appear as a natural description of observed evolutionary phenomena of several real-world problems. All the information provided in this chapter is a summary of the books *Impulsive Differential Equations: Periodic Solutions and Applications* and *Theory of Impulsive Differential Equations* [1, 2].

2.1.1 Definition of Impulsive Differential Equations

Each system is given by an ordinary differential equation coupled with relations defining the jump condition. Assume that the law of evolution of the process is described by a differential equation

$$\frac{dx}{dt} = f(t, x),$$

where $t \in \mathbb{R}$, $x \in \Omega \subset \mathbb{R}^n$, $f : \mathbb{R} \times \Omega \to \mathbb{R}^n$ and the moments of the impulse effect for the solution $x(t)$ occurs at $t = \tau_k$ $(k \in \mathbb{N})$.

Denote $I(t, x) : \mathbb{R} \times \Omega \to \Omega$, where

$$(t, x) \to (t, x + I(t, x))$$

is the mapping of the solution before the impulse, $x(\tau_k^-)$, to after the impulse effect, $x(\tau_k^+)$. Then

$$\Delta x(\tau_k) = I(\tau_k^-, x(\tau_k^-)),$$

where $\Delta x(\tau_k) = x(\tau_k^+) - x(\tau_k^-)$.

2.1.2 Classes of Impulsive Differential Equations

There are three classes of impulsive differential equations:

Class 1: Equations with fixed moments of the impulse effect

$$\begin{aligned} \frac{dx}{dt} &= f(t, x) \qquad t \neq \tau_k \\ \Delta x &= I_k(x) \qquad t = \tau_k. \end{aligned} \tag{2.1.1}$$

The impulse is fixed beforehand by defining the sequence $\tau_k : \tau_k < \tau_{k+1}$ $(k \in K \subset \mathbb{Z})$. For $t \in (\tau_k, \tau_{k+1}]$ the solution $x(t)$ of equation (2.1.1) satisfies the equation $dx/dt =$

$f(t,x)$, and for $t=\tau_k$, $x(t)$ satisfies the relation $x(\tau_k^+)=x(\tau_k^-)+I_k(x(\tau_k^-))$.

Class 2: Equations with state-dependent moments of the impulse effect

$$\begin{aligned} \frac{dx}{dt} &= f(t,x) \qquad t \neq \tau_k(x) \\ \Delta x &= I_k(x) \qquad t=\tau_k(x), \end{aligned} \tag{2.1.2}$$

where $\tau_k : \Omega \to \mathbb{R}$ and $\tau_k < \tau_{k+1}$ ($k \in K \subset \mathbb{Z}$, $x \in \Omega$). The impulse occurs when the mapping point (t,x) meets some hypersurface σ_k of the equation $t=\tau_k(x)$.

Class 3: Autonomous impulsive equations

$$\begin{aligned} \frac{dx}{dt} &= f(x) \qquad x \notin \sigma \\ \Delta x &= I_k(x) \qquad x \in \sigma, \end{aligned} \tag{2.1.3}$$

where σ is an $(n-1)-$dimensional manifold contained in the phase space $\Omega \subset \mathbb{R}^n$. The impulse occurs when the solution $x(t)$ meets the manifold σ.

2.1.3 Example

Before we look at the existence and uniqueness of solutions, we present a simple example of an impulsive differential equation with state-dependent moments of the impulse effect.

Consider

$$\begin{aligned} \frac{dx}{dt} &= 0 \qquad t \neq \tau_k(x) \\ \Delta x &= x^2 sgn(x) - x \qquad t=\tau_k(x), \end{aligned} \tag{2.1.4}$$

where $t \geq 0$, $x \in \mathbb{R}$ and $\tau_k(x) = x + 6k$ for $|x| < 3$ ($k = 0, 1, 2, \dots$).

Starting at a point $(0, x_0)$ with $|x_0| \geq 3$, there is no impulsive effect since the integral curve does not intersect the hypersurface σ (see Figure 2.1).

Starting at a point $(0, x_0)$ with $1 < |x_0| < 3$, the integral curve is subject to an impulse effect finitely many times. For instance, starting at a point $(0, \sqrt[4]{2})$, the integral curve first hits the hypersurface at $\tau_1 = x_0$ (since $k = 0$) and is subject to an impulse $\Delta x = x_0^2 \text{sgn}(x_0) - x_0$. Then we solve $dx/dt = 0$ with the new initial condition $x(\tau_1^+) = x(\tau_1^-) + x_0^2 \text{sgn}(x_0) - x_0 = \sqrt{2}$. Once the integral curve hits the hypersurface for the second time, τ_2^-, it undergoes a second impulse $\Delta x = x(\tau_2^-)^2 \text{sgn}(x(\tau_2^-)) - x(\tau_2^-) = 2 - \sqrt{2}$ and again we solve the ODE $dx/dt = 0$ with the new initial condition $x(\tau_2^+) = 2$. This process continues till the integral curve no longer hits the hypersurface. In this case, we have 3 impulses and, after moment $\tau_3 = 2$, the integral curve no longer intersects the hypersurface σ_k (see Figure 2.2).

Starting at a point $(0, x_0)$ with $0 < x_0 < 1$, the integral curve is subject to an impulse effect infinitely many times for which we have $\lim_{k\to\infty} \tau_k = \infty$, $\lim_{k\to\infty} x(\tau_k) = 0$ (see Figure 2.3).

Starting at a point $(0, x_0)$ with $-1 < x_0 < 0$, the integral curve is subject to an impulse effect infinitely many times but $\lim_{k\to\infty} x(\tau_k) = 0$, $\lim_{k\to\infty} \tau_k = 6$ (see Figure 2.4). This phenomena is called beating.

The points $(0, 0)$, $(0, 1)$ and $(0, -1)$ also intersect the hypersurfaces σ_k infinitely many times, but at fixed points of the expression $x^2 \text{sgn}(x)$ (see Figure 2.4).

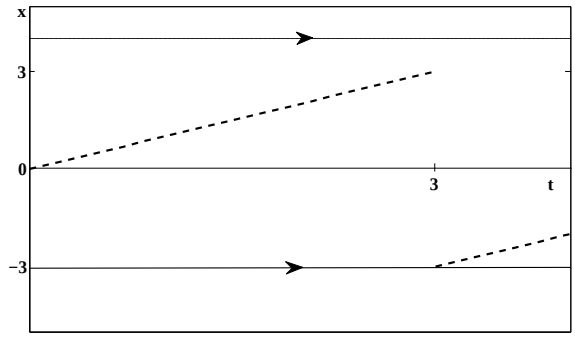

Figure 2.1: The solution of the impulsive differential equation (2.1.4) has no impulse effect for $|x_0| \geq 3$. For $|x_0| > 3$ the integral curve does not hit the hypersurface σ_k. Here, the dotted lines are the hypersurfaces σ_k and the solid line is the integral curve.

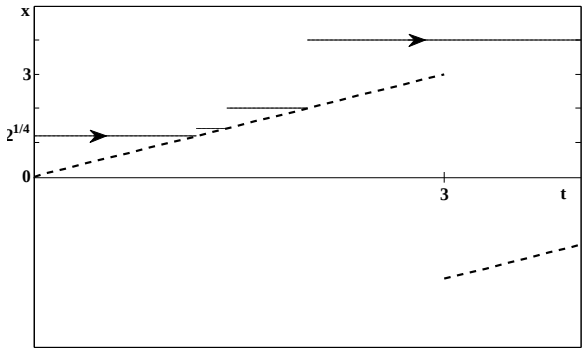

Figure 2.2: The solution of the impulsive differential equation (2.1.4) hits the hypersurface finitely many times for $1 < |x_0| < 3$ and undergoes a finite number of impulses. Here, the dotted lines are the hypersurfaces σ_k and the solid line is the integral curve.

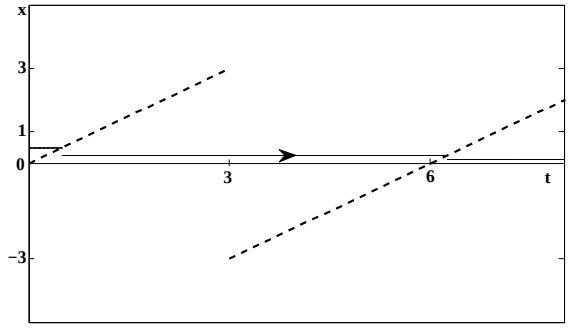

Figure 2.3: The solution of the impulsive differential equation (2.1.4) hits the hypersurface infinitely many times for $0 < x_0 < 1$ but the solution tends towards zero. Here, the dotted lines are the hypersurfaces σ_k and the solid line is the integral curve.

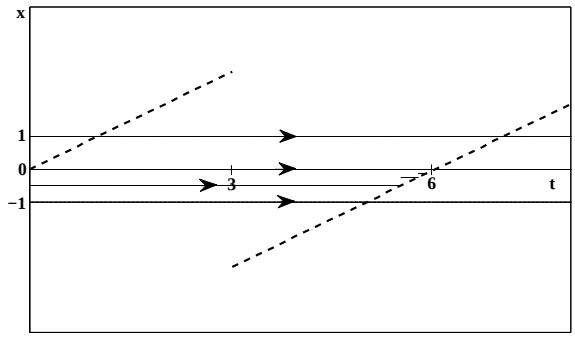

Figure 2.4: The solution of the impulsive differential equation (2.1.4) can (a) hit the hypersurface finitely many times for $x_0 = 0, 1, -1$ but does not undergo an impulse (since these are fixed points of the system), or (b) hits the hypersurface infinitely many times for $-1 < x_0 < 0$ and undergoes an infinite amount of impulses (beating occurs in this case). Here, the dotted lines are the hypersurfaces σ_k and the solid line is the integral curve.

2.2 Existence and Uniqueness Theorems

2.2.1 State-dependent moments of impulse effect

Let $\Omega \subset \mathbb{R}^n$ be an open set. Suppose that, for each $k \in \mathbb{Z}$, the functions $\tau_k : \Omega \to \mathbb{R}$ are continuous in Ω and satisfy

$$\tau_k(x) < \tau_{k+1}(x), \quad \lim_{k \to \pm\infty} \tau_k(x) = \infty$$

for $x \in \Omega$. Let $f : \mathbb{R} \times \Omega \to \mathbb{R}^n$, $I_k : \Omega \to \mathbb{R}^n$, $(t_0, x_0) \in \mathbb{R} \times \Omega$ and $\alpha < \beta$ $(\alpha, \beta \in \mathbb{R})$.

Consider the impulsive differential equation

$$\begin{aligned} \frac{dx}{dt} &= f(t,x) \qquad t \neq \tau_k(x) \\ \Delta x &= I_k(x) \qquad t = \tau_k(x), \end{aligned} \tag{2.2.1}$$

with initial condition

$$x(t_0^+) = x_0. \tag{2.2.2}$$

First we define a solution to the impulsive differential equation where it is continuous and differentiable between impulses.

Definition 2.2.1 *The function $\varphi : (\alpha, \beta) \to \mathbb{R}^n$ is said to be a solution of equation (2.2.1) if:*

1. *$(t, \varphi(t)) \in \mathbb{R} \times \Omega$ for $t \in (\alpha, \beta)$;*

2. *for $t \in (\alpha, \beta)$, $t \neq \tau_k(\varphi(t))$, $k \in \mathbb{Z}$, the function $\varphi(t)$ is differentiable and $\frac{d\varphi}{dt}(t) = f(t, \varphi(t))$;*

3. *the function* $\varphi(t)$ *is continuous from the left in* (α, β) *and if* $t \in (\alpha, \beta)$, $t = \tau_k(\varphi(t))$ *and* $t \neq \beta$, *then* $\varphi(t^+) = \varphi(t^-) + I_k(\varphi(t^-))$ *and, for each* $j \in \mathbb{Z}$ *and some* $\delta > 0$, $s \neq \tau_j(\varphi(s))$ *for* $t < s < t + \delta$.

Definition 2.2.2 *Each solution* φ *of (2.2.1) which is defined in an interval of the form* (t_0, β) *and satisfies the condition (2.2.2) is said to be a solution of the initial value problem (2.2.1)-(2.2.2).*

If $t_0 \neq \tau_k(x_0)$ for $k \in \mathbb{Z}$, then the existence and uniqueness conditions of the solution of the initial value problem (2.2.1)-(2.2.2) depends only on the properties of the function f. If $t_0 = \tau_k(x_0)$ for some k, then we need to impose additional conditions on f and τ_k to guarantee the existence of a solution. The following theorem provides such conditions to guarantee a finite impulse.

Theorem 2.2.3 *Let the following conditions hold.*

1. *The function* $f : \mathbb{R} \times \Omega \to \mathbb{R}^n$ *is continuous in* $t \neq \tau_k(x)\,(k \in \mathbb{Z})$.

2. *For any* $(t, x) \in \mathbb{R} \times \Omega$ *there exists a locally integrable function* $l : \mathbb{R} \to \mathbb{R}$ *such that, in a small neighbourhood of* (t, x),

$$|f(s, y)| \leq l(s).$$

3. *For each* $k \in \mathbb{Z}$, *the condition* $t_1 = \tau_k(x_1)$ *implies the existence of* $\delta > 0$ *such that*

$$t \neq \tau_k(x)$$

for all $0 < t - t_1 < \delta$ *and* $|x - x_1| < \delta$.

Then for each $(t_0, x_0) \in \mathbb{R} \times \Omega$, *there exists a solution* $\varphi : (t_0, \beta) \to \mathbb{R}^n$ *of the initial value problem (2.2.1)-(2.2.2) for some* $\beta > t_0$.

Note that the solution $x(t)$ of the initial value problem (2.2.1)-(2.2.2) is unique if there is a unique solution for the initial value problem $dx/dt = f(t, x)$, $x(t_0) = x_0$; that is, if f is locally Lipschitz continuous with respect to x in a neighbourhood of (t_0, x_0).

If the impulses occur at fixed times, then the system is significantly simpler and a great deal more can be said about continuation of solutions (Section 2.2.2). With variable impulse times, different solutions will generally undergo impulsive effects at different times, so we cannot ordinarily expect solutions to depend continuously on initial data. For an example see Section 2.1.3, where initial conditions can either hit a hypersurface or not for different initial conditions. The next sections will discuss continuity of initial conditions for fixed impulse effect.

2.2.2 Fixed moments of impulse effect

Consider the impulsive differential equation

$$\begin{aligned} \frac{dx}{dt} &= f(t, x) \qquad t \neq \tau_k \\ \Delta x &= I_k(x) \qquad t = \tau_k, \end{aligned} \tag{2.2.3}$$

where $\tau_k < \tau_{k+1}$ $(k \in \mathbb{Z})$ and $\lim_{k \to \pm\infty} \tau_k = \pm\infty$.

The following theorem guarantees that, for a finite impulse effect, a solution exists after the impulse.

Theorem 2.2.4 *Let the function $f : \mathbb{R} \times \Omega \to \mathbb{R}^n$ be continuous in the sets $(\tau_k, \tau_{k+1}] \times \Omega$ $(k \in \mathbb{Z})$. For each $k \in \mathbb{Z}$ and $x \in \Omega$, suppose there exists the finite limit of $f(t, y)$ as $(t, y) \to (\tau_k, x)$, $t > \tau_k$.*

Then, for each $(t_0, x_0) \in \mathbb{R} \times \Omega$, there exists $\beta > t_0$ and a solution $\varphi : (t_0, \beta) \to \mathbb{R}^n$ of the initial value problem (2.2.2)-(2.2.3).

If, moreover, the function f is locally Lipschitz continuous with respect to x in $\mathbb{R} \times \Omega$, then this solution is unique.

Now we consider the problem of continuability to the right of a given solution $\varphi(t)$ of equation (2.2.3). The following theorem imposes conditions such that $\varphi(t)$ is continuous after the impulse.

Theorem 2.2.5 (continuation of solutions) *Let the following conditions hold.*

1. *The function $f : \mathbb{R} \times \Omega \to \mathbb{R}^n$ is continuous in the sets $(\tau_k, \tau_{k+1}] \times \Omega$ $(k \in \mathbb{Z})$ and, for each $k \in \mathbb{Z}$, the limit of $f(t, y)$ as $(t, y) \to (\tau_k, x)$, $t > \tau_k$ exists and is finite.*

2. *The function $\varphi : (\alpha, \beta) \to \mathbb{R}^n$ is a solution of (2.2.3).*

Then the solution $\varphi(t)$ is continuable to the right of β if and only if the limit

$$\lim_{t \to \beta^-} \varphi(t) = \eta$$

exists, and one of the following conditions is fulfilled:

(a) $\beta \neq \tau_k$ for any $k \in \mathbb{Z}$ and $\eta \in \Omega$;

(b) $\beta = \tau_k$ for some $k \in \mathbb{Z}$ and $\eta + I_k(\eta) \in \Omega$.

Theorem 2.2.6 (right maximal interval) *Let the following conditions hold.*

1. *Condition 1 of Theorem (2.2.5) is satisfied.*

2. *The function f is locally Lipschitz continuous with respect to x in $\mathbb{R} \times \Omega$.*

3. *$\eta + I_k(\eta) \in \Omega$ for each $k \in \mathbb{Z}$ and $\eta \in \Omega$.*

Then, for any $(t_0, x_0) \in \mathbb{R} \times \Omega$, there exists a unique solution of the initial value problem (2.2.2)-(2.2.3) which is defined in an interval of the form (t_0, β) and is not continuable to the right of β.

Under the conditions of Theorem (2.2.6), for each $(t_0, x_0) \in \mathbb{R} \times \Omega$, there exists a unique solution $x(t; t_0, x_0)$ of the initial value problem (2.2.2)-(2.2.3) which is defined on the interval (a, b) and is not continuable to the right of b or the left of a. Denote by $J(t_0, x_0)$ the maximal interval of the solution, and set $J^- = J^-(t_0, x_0) = (a, t_0]$ and $J^+ = J^+(t_0, x_0) = [t_0, b)$. Then

$$x(t) = \begin{cases} x_0 + \displaystyle\int_{t_0}^{t} f(s, x(s))ds + \sum_{t_0 < \tau_k < t} I_k(x(\tau_k)) & \text{for } t \in J^+ \\ x_0 + \displaystyle\int_{t_0}^{t} f(s, x(s))ds - \sum_{t \leq \tau_k \leq t_0} I_k(x(\tau_k)) & \text{for } t \in J^- \ . \end{cases}$$

Below is a straightforward verification of this solution.

Consider the impulsive differential equation with fixed moment of impulse effect (2.2.3). For $t_0^+ < t < t_1^-$, the solution is

$$x(t) - x_0 = \int_{t_0}^{t} f(s, x(s))ds$$
$$x(t) = x_0 + \int_{t_0}^{t} f(s, x(s))ds.$$

This means that

$$x(t_1^-) = x_0 + \int_{t_0}^{t_1} f(s, x(s))ds.$$

After the impulse, we get

$$x(t_1^+) = x_0 + \int_{t_0}^{t_1} f(s, x(s))ds + I_1(x(t_1)).$$

For $t_1^+ < t < t_2^-$, the solution is

$$\begin{aligned} x(t) &= x(t_1^+) + \int_{t_1}^{t} f(s, x(s))ds \\ &= x_0 + \int_{t_0}^{t_1} f(s, x(s))ds + I_1(x(t_1)) + \int_{t_1}^{t} f(s, x(s))ds. \end{aligned}$$

This means that

$$x(t_2^-) = x_0 + \int_{t_0}^{t_2} f(s, x(s))ds + I_1(x(t_1)).$$

After the impulse, we get

$$x(t_2^+) = x_0 + \int_{t_0}^{t_2} f(s, x(s))ds + I_1(x(t_1)) + I_2(x(t_2)).$$

For $t_2^+ < t < t_3^-$, the solution is

$$\begin{aligned} x(t) &= x(t_2^+) + \int_{t_2}^{t} f(s, x(s))ds \\ &= x_0 + \int_{t_0}^{t_2} f(s, x(s))ds + I_1(x(t_1)) + I_2(x(t_2)) + \int_{t_2}^{t} f(s, x(s))ds. \end{aligned}$$

This means that

$$x(t_3^-) = x_0 + \int_{t_0}^{t_2} f(s, x(s))ds + I_1(x(t_1)) + I_2(x(t_2)) + \int_{t_2}^{t_3} f(s, x(s))ds.$$

After the impulse, we get

$$x(t_3^+) = x_0 + \int_{t_0}^{t_3} f(s, x(s))ds + I_1(x(t_1)) + I_2(x(t_2)) + I_3(x(t_3)).$$

Assume

$$x(t_k^+) = x_0 + \int_{t_0}^{t_k} f(s, x(s))ds + I_1(x(t_1)) + I_2(x(t_2)) + \cdots + I_k(x(t_k)).$$

Then for $t_k^+ < t < t_{k+1}^-$, the solution is

$$\begin{aligned} x(t) &= x(t_k^+) + \int_{t_k}^{t} f(s, x(s))ds \\ &= x_0 + \int_{t_0}^{t_k} f(s, x(s))ds + I_1(x(t_1)) + I_2(x(t_2)) + \cdots + I_k(x(t_k)) + \int_{t_k}^{t} f(s, x(s))ds \\ &= x_0 + \int_{t_0}^{t} f(s, x(s))ds + I_1(x(t_1)) + I_2(x(t_2)) + \cdots + I_k(x(t_k)). \end{aligned}$$

Therefore, by mathematical induction, for $t_0^+ < t < b$, the solution is

$$x(t) = x_0 + \int_{t_0}^{t} f(s, x(s))ds + \sum_{t_0 < t_k < t} I_k(x(t_k)).$$

2.2.3 Continuity, differentiability and dependence on initial data, on parameters

Consider the impulsive differential equation

$$\frac{dx}{dt} = f(t, x, \lambda) \qquad \phi(t, x, \lambda) \neq 0 \tag{2.2.4}$$

$$\Delta x = I_k(t, x, \lambda) \qquad \phi(t, x, \lambda) = 0, \tag{2.2.5}$$

where $t \in \mathbb{R}$, $x \in \mathbb{R}^n$ and $\lambda \in \Lambda \subset \mathbb{R}^m$ is a parameter.

Denote by $x(t; t_0, y, \lambda)$ the solution of the equation (2.2.4)-(2.2.5) satisfying the initial condition

$$x(t_0^+; t_0, y, \lambda) = y. \tag{2.2.6}$$

Let $\phi(t_0, x_0, \lambda_0) \neq 0$ and $\varphi(t) = x(t; t_0, x_0, \lambda_0)$ be a solution of (2.2.4)-(2.2.5) for $\lambda = \lambda_0$ that is defined in the interval $[t_0, t_1]$ and satisfies the relations

$$\varphi(t_0) = x_0 \qquad \phi(t_1, \varphi(t_1), \lambda_0) \neq 0.$$

We shall discuss the conditions under which the solution $x(t; t_0, y, \lambda)$ is a continuous function at the point $(t_1; t_0, y, \lambda)$.

Denote by $u(t; t_0, y, \lambda)$ the solution of the initial value problem

$$\frac{du}{dt} = f_1(t, u, \lambda) \qquad u(t_0) = y,$$

where $f_1 : \mathbb{R} \times \mathbb{R}^n \times \Lambda \to \mathbb{R}^n$, and consider the equation

$$\phi(t, u(t; t_0, y, \lambda), \lambda) = 0.$$

An immediate consequence of the implicit function theorem is the following lemma, which imposes that f be continuous and that the jump condition be continuously differentiable.

Lemma 2.2.7 *Let the following conditions hold.*

1. *The function* $f_1 : \mathbb{R} \times \mathbb{R}^n \times \Lambda \to \mathbb{R}^n$ *is continuous in* $\mathbb{R} \times \mathbb{R}^n \times \Lambda$.

2. *The function* $\phi : \mathbb{R} \times \mathbb{R}^n \times \Lambda \to \mathbb{R}$ *is continuously differentiable in a neighbourhood of the point* (τ_1, x_1, λ_0), *where* $\tau_1 > t_0$ *and* $x_1 = u(\tau_1; t_0, x_0, \lambda_0)$.

3. $\phi(\tau_1, x_1, \lambda_0) = 0$

4. $\dfrac{\partial \phi}{\partial t}(\tau_1, x_1, \lambda_0) + \dfrac{\partial \phi}{\partial x}(\tau_1, x_1, \lambda_0) f_1(\tau_1, x_1, \lambda_0) \neq 0.$

Then there exists a neighbourhood U *of the point* (t_0, x_0, λ_0) *and a unique function* $T = T(\tau, y, \lambda)$ *which is continuous in* U *and such that*

$$T(t_0, x_0, \lambda_0) = \tau_1$$

$$\phi(T(\tau, y, \lambda), u(T(\tau, y, \lambda); \tau, y, \lambda), \lambda) \equiv 0 \qquad (\tau, y, \lambda) \in U.$$

Corollary 2.2.8 *The function* $T(\tau, y, \lambda)$ *is Lipschitz continuous with respect to* $(\tau, y, \lambda) \in U$ *if* f_1 *is continuously differentiable in* $\mathbb{R} \times \mathbb{R}^n \times \Lambda$.

Introduce the following conditions that take the entire solution and split it up between each impulse and then impose conditions for f and I to be continuous in each partition.

H2.1 The function $\phi : \mathbb{R} \times \mathbb{R}^n \times \Lambda \to \mathbb{R}$ is continuously differentiable in $\mathbb{R} \times \mathbb{R}^n \times \Lambda$ and there exists $\delta > 0$ such that for $|\lambda - \lambda_0| < \delta$ the equation $\phi(t, x, \lambda) = 0$ defines a smooth hypersurface $S(\lambda)$ which partitions the space $\mathbb{R} \times \mathbb{R}^n$ into a finite number of disjoint domains $D_1(\lambda), \ldots, D_{N+1}(\lambda)$ such that

$$D_1(\lambda) \cup \cdots \cup D_{N+1}(\lambda) \cup S(\lambda) = \mathbb{R} \times \mathbb{R}^n.$$

H2.2 The solution $\varphi(t) = x(t; t_0, x_0, \lambda_0)$ is defined for $t \in [t_0, t_1]$, has moments of impulse effect $\tau_k = \tau_k(t_0, x_0, \lambda_0)$ $(k = 1, \ldots, N)$ and the relations

$$(t, \varphi(t)) \in D_k(\lambda_0), \qquad t \in \triangle_k \quad (k = 1, \ldots, N + 1)$$

hold, where $\triangle_1 = [t_0, \tau_1)$, $\triangle_{N+1} = (\tau_N, t_1]$, $\triangle_k = (\tau_{k-1}, \tau_k]$ $(k = 2, \ldots, N)$.

H2.3 $\dfrac{\partial \phi}{\partial t}(\tau_k, \varphi(\tau_k), \lambda_0) + \dfrac{\partial \phi}{\partial x}(\tau_k, \varphi(\tau_k), \lambda_0) f(\tau_k, \varphi(\tau_k), \lambda_0) \neq 0$ $(k = 1, \ldots, N)$.

Under these conditions, there exists a $\delta > 0$ such that for $|\lambda - \lambda_0| < \delta$ the sets

$$S_k(\lambda) = \{(t, x) \in \mathbb{R} \times \mathbb{R}^n : \phi(t, x, \lambda) = 0, |t - \tau_k| < \delta, |x - \varphi(\tau_k)| < \delta\} \quad (k = 1, \ldots, N)$$

are open smooth n-dimensional manifolds.

H2.4 There exists a $\delta > 0$ such that for $|\lambda - \lambda_0| < \delta$ and $|y - x_0| < \delta$ the solution $x(t) = x(t; t_0, y, \lambda)$ is defined for $t \in [t_0, t_1]$ and the integral curve $(t, x(t))$ for $t \in [t_0, t_1]$ meets each successive $S_k(\lambda)$ $(k = 1, \ldots, N)$ just once.

H2.5 In the domain $D_k(\lambda)$ $(k = 1, \ldots, N + 1)$, the function $f(t, x, \lambda)$ coincides with some function $f_k : \mathbb{R} \times \mathbb{R}^n \times \Lambda \to \mathbb{R}$, which is continuous in $\mathbb{R} \times \mathbb{R}^n \times \Lambda$.

H2.6 The function $I : \mathbb{R} \times \mathbb{R}^n \times \Lambda \to \mathbb{R}$ is continuous in $\mathbb{R} \times \mathbb{R}^n \times \Lambda$.

The following theorem is based on Lemma (2.2.7).

Theorem 2.2.9 *Let conditions H2.1-H2.6 hold. Then the solution $x(t; \tau, y, \lambda)$ of the initial value problem (2.2.4)-(2.2.6) is a continuous function in some neighbourhood of $(t_1, t_0, x_0, \lambda_0)$.*

Moreover, the moments of the impulse effect $\tau_k(\tau, y, \lambda)$ $(k = 1, \ldots, N)$ of this solution are continuous functions in some neighbourhood of (t_0, x_0, λ_0).

Now let us consider the question of the differentiability of the solution $x(t; \tau, y, \lambda)$ at the point of the impulse $(t_1, t_0, x_0, \lambda_0)$ and consider the dependence on initial data and parameters.

Introduce the following conditions.

H2.7 In the domain $D_k(\lambda)$ $(k = 1, \ldots, N + 1)$, the function $f(t, x, \lambda)$ coincides with some function $f_k : \mathbb{R} \times \mathbb{R}^n \times \Lambda \to \mathbb{R}$, which is continuously differentiable in $\mathbb{R} \times \mathbb{R}^n \times \Lambda$.

H2.8 The function $I : \mathbb{R} \times \mathbb{R}^n \times \Lambda \to \mathbb{R}$ is continuously differentiable in $\mathbb{R} \times \mathbb{R}^n \times \Lambda$.

The following theorem is based on Lemma (2.2.7) as well.

Theorem 2.2.10 *Let conditions H2.1-H2.4, H2.7 and H2.8 hold. Then:*

1. *The solution $x(t;\tau,y,\lambda)$ of the initial value problem (2.2.4)-(2.2.6) is a continuously differentiable function in some neighbourhood of (t_1,t_0,x_0,λ_0) and the moments of the impulse effect $\tau_k(\tau,y,\lambda)$ $(k=1,\dots,N)$ of this solution are continuously differentiable functions in some neighbourhood of (t_0,x_0,λ_0).*

2. *The derivative $u = \dfrac{\partial x}{\partial x_0}(t;t_0,x_0,\lambda_0)$ is a solution of the initial value problem*

$$\begin{aligned} \frac{du}{dt} &= \frac{\partial f}{\partial x}(t,\varphi(t),\lambda_0)\,u && t \neq \tau_k \\ \Delta u &= \frac{\partial I}{\partial x}\,u + \Big[f^+ - f - \frac{\partial I}{\partial t} - \frac{\partial I}{\partial x}f\Big]\frac{\dfrac{\partial \phi}{\partial x}\,u}{\dfrac{\partial \phi}{\partial x}f + \dfrac{\partial \phi}{\partial t}} && t = \tau_k \\ u(t_0^+) &= E_n. \end{aligned}$$

3. *The derivative $v = \dfrac{\partial x}{\partial \lambda}(t;t_0,x_0,\lambda_0)$ is a solution of the initial value problem*

$$\begin{aligned} \frac{dv}{dt} &= \frac{\partial f}{\partial x}(t,\varphi(t),\lambda_0)\,v + \frac{\partial f}{\partial \lambda}(t,\varphi(t),\lambda_0) && t \neq \tau_k \\ \Delta v &= \frac{\partial I}{\partial x}v + \frac{\partial I}{\partial \lambda} + \Big[f^+ - f - \frac{\partial I}{\partial t} - \frac{\partial I}{\partial x}f\Big]\frac{\dfrac{\partial \phi}{\partial x}\,v + \dfrac{\partial \phi}{\partial \lambda}}{\dfrac{\partial \phi}{\partial x}f + \dfrac{\partial \phi}{\partial t}} && t = \tau_k \\ v(t_0^+) &= 0. \end{aligned}$$

Here $\frac{\partial I}{\partial x}$, $\frac{\partial I}{\partial \lambda}$, $\frac{\partial I}{\partial t}$, $\frac{\partial \phi}{\partial x}$, $\frac{\partial \phi}{\partial \lambda}$, $\frac{\partial \phi}{\partial t}$ are computed at the point $(\tau_k,\varphi(\tau_k),\lambda_0)$ and $f = f_k(\tau_k,\varphi(\tau_k),\lambda_0)$, $f^+ = f_{k+1}(\tau_k,\varphi(\tau_k^+),\lambda_0)$.

2.2.4 Definition of stability

The discontinuous nature of solutions of systems with impulsive effect means that we must adjust our definitions of stability. Consider the impulsive system

$$\begin{aligned} \frac{dx}{dt} &= f(t,x) \qquad t \neq \tau_k(x) \\ \Delta x &= I_k(x) \qquad t = \tau_k(x) \\ x(t_0^+) &= x_0. \end{aligned} \tag{2.2.7}$$

The standard definitions are modified so that we can choose initial points suitably close together so that trajectories remain arbitrarily close for all time, except in any neighbourhood of the impulse points, no matter how small.

Definition 2.2.11 *Let $\bar{x} = x(t;t_0,y_0)$ be a given solution of (2.2.7) existing for $t \geq t_0$ and suppose that $\bar{x}(t)$ hits the surfaces $S_k : t = \tau_k(x)$ at the moments t_k such that $t_k < t_{k+1}$ and $t_k \to \infty$ as $k \to \infty$. Then the solution $\bar{x}(t)$ of (2.2.7) is said to be*

$(S_{1\eta})$ *stable, if, for each $\epsilon > 0$, $\eta > 0$ and $t_0 \in \mathbb{R}^+$, there exists a $\delta = \delta(t_0,\epsilon,\eta) > 0$ such that $|x_0 - y_0| < \delta$ implies $|x(t) - \bar{x}(t)| < \epsilon$ for $t \geq t_0$ and $|t - t_k| > \eta$, where $x(t) = x(t;t_0,x_0)$ is any solution of (2.2.7) existing for $t \geq t_0$;*

$(S_{2\eta})$ *uniformly stable, if δ in $(S_{1\eta})$ is independent of t_0;*

$(S_{3\eta})$ *attractive, if, for each $\epsilon > 0$, $\eta > 0$ and $t_0 \in \mathbb{R}^+$, there exist $\delta_0 = \delta_0(t_0) > 0$ and a $T = T(t_0,\epsilon,\eta) > 0$ such that $|x_0 - y_0| < \delta_0$ implies $|x(t) - \bar{x}(t)| < \epsilon$ for $t \geq t_0 + T$ and $|t - t_k| > \eta$;*

$(S_{4\eta})$ *uniformly attractive, if δ_0 and T in $(S_{3\eta})$ are independent of t_0;*

$(S_{5\eta})$ *asymptotically stable, if $(S_{1\eta})$ and $(S_{3\eta})$ holds;*

$(S_{6\eta})$ *uniformly asymptotically stable, if $(S_{2\eta})$ and $(S_{4\eta})$ holds.*

In the case of fixed moments of impulse, $\tau_k(x) = \tau_k$, definition (2.2.11) remains the same except the values of η are omitted. For example, $(S_{1\eta})$ becomes (S_1); that is, the solution to equation (2.2.7) with fixed moment of impulse is stable if for any $\epsilon > 0$ and $t_0 \in \mathbb{R}^+$, there exists a $\delta = \delta(t_0, \epsilon) > 0$ such that $|\bar{x}| < \delta$ implies $|x(t)| < \epsilon$ for $t \geq t_0$.

2.3 Linear systems with fixed moments of impulse effect

2.3.1 Existence and uniqueness of solutions

Let τ_k $(k \in \mathbb{Z})$ be fixed and satisfy

H3.1 $\tau_k < \tau_{k+1}$ $(k \in \mathbb{Z})$, $\lim_{k\to\pm\infty} \tau_k = \pm\infty$.

Let $m, n \in \mathbb{N}$. Denote by $PC(D, F)$, the set of functions $\psi : D \to F$ which are continuous for $t \in D$, $t \neq \tau_k$, are continuous from the left for $t \in D$, and have discontinuities at the points $\tau_k \in D$.

Consider the linear homogeneous impulsive equation

$$\begin{aligned} \frac{dx}{dt} &= A(t)x \qquad t \neq \tau_k \\ \Delta x &= B_k x \qquad t = \tau_k, \end{aligned} \tag{2.3.1}$$

with the condition

H3.2 $A \in PC(\mathbb{R}, \mathcal{L}(\mathbb{R}^n))$, $B_k \in \mathcal{L}(\mathbb{R}^n)$ $(k \in \mathbb{Z})$.

Theorem 2.3.1 *Let H3.1, H3.2 hold. Then, for any $(t_0, x_0) \in \mathbb{R} \times \mathbb{C}^n$, there exists a unique solution $x(t)$ of equation (2.3.1) with $x(t_0^+) = x_0$, and this solution is defined for all $t > t_0$.*

If, moreover, $det(E + B_k) \neq 0$ $(k \in \mathbb{Z})$, where E is the $n \times n$ identity matrix, then the solution is defined for all $t \in \mathbb{R}$.

The solutions of equation (2.3.1) can be written as:

$$x(t; t_0, x_0) = W(t, t_0^+)x_0, \tag{2.3.2}$$

where

$$W(t,s) = \begin{cases} U_k(t,s) & \text{for } t,s \in (\tau_k, \tau_{k+1}] \\ U_{k+1}(t,\tau_k^+)(E+B_k)U_k(\tau_k,s) & \text{for } \tau_{k-1} < s \leq \tau_k < t \leq \tau_{k+1} \\ U_k(t,\tau_k)(E+B_k)^{-1}U_{k+1}(\tau_k^+,s) & \text{for } \tau_{k-1} < t \leq \tau_k < s \leq \tau_{k+1} \\ U_{k+1}(t,\tau_k^+)\prod_{j=k}^{i+1}(E+B_j)U_j(\tau_j,\tau_{j-1}^+)(E+B_i)U_i(\tau_i,s) & \text{for } \tau_{i-1} < s \leq \tau_i < \tau_k < t \leq \tau_{k+1} \\ U_i(t,\tau_i)\prod_{j=i}^{k+1}(E+B_j)^{-1}U_{j+1}(\tau_j^+,\tau_{j+1})(E+B_k)^{-1}U_{k+1}(\tau_k^+,s) & \text{for } \tau_{i-1} < t \leq \tau_i < \tau_k < s \leq \tau_{k+1} \end{cases}$$

and where $U_k(t,s)$ is the Cauchy matrix for the linear homogeneous equation when $t \neq \tau_k$. The Cauchy matrix is defined in the same manner as the fundamental matrix in ODEs (i.e. $U(t,s) = X(t)X^{-1}(s)$ where $X(t)$ is the fundamental matrix of a homogeneous system). For a linear system with constant coefficients, the Cauchy operator is defined by $X(t,s) = e^{A(t-s)}$. We will see more about the fundamental matrix in the next section.

Note that $W(t,s)$ is split into five cases. The first is without impulses; the second is with one impulse going forward in time; the third is with one impulse going backward in time; the fourth is with several impulses going forward in time, and the fifth is with several impulses going backward in time.

2.3.2 Fundamental matrix

Definition 2.3.2 *Let $x_1(t), ..., x_n(t)$ be solutions to (2.3.1) defined on the interval $(0, \infty)$. Let $X(t) = \{x_1(t), ..., x_n(t)\}$ be a matrix-valued function whose columns are*

these solutions. Then $x_1(t), ..., x_n(t)$ *are linearly independent if and only if* $\det X(t_0^+) \neq 0$. *In this case, we say that* $X(t)$ *is a* fundamental matrix *of (2.3.1).*

We also have the following analogue of Liouville's formula for linear equations:

$$\det W(t,t_0) = \begin{cases} \prod\limits_{t_0<\tau_k<t} \det(E+B_k) \exp\Big(\int_{t_0}^{t} \mathrm{Tr}A(s)\,ds\Big) & \text{for } t > t_0 \\ \prod\limits_{t\leq\tau_k\leq t_0} \det(E+B_k)^{-1} \exp\Big(\int_{t_0}^{t} \mathrm{Tr}A(s)\,ds\Big) & \text{for } t \leq t_0\,, \end{cases}$$

where $\mathrm{Tr}A(t)$ is the trace of the matrix $A(t)$.

Lemma 2.3.3 *Suppose H3.1, H3.2 hold and* $\lim\limits_{k\to\infty} t_k = \infty$. *Let* $X(t)$ *be a fundamental matrix of (2.3.1) in* $\mathbb{R}_+$. *Then*

1. *For any constant matrix* $M \in \mathcal{L}(\mathbb{C}^n)$, $X(t)M$ *is also a solution of (2.3.1).*
2. *If* $Y : \mathbb{R} \to \mathcal{L}(\mathbb{C}^n)$ *is a solution of (2.3.1), there exists a unique matrix* M *such that* $Y(t) = X(t)M$. *Furthermore, if* $Y(t)$ *is also a fundamental matrix, then* $\det M \neq 0$.

2.3.3 Variation of constants formula for non-homogeneous equations

Consider the linear non-homogeneous impulsive equation

$$\begin{aligned} \frac{dx}{dt} &= A(t)x + g(t) \qquad t \neq \tau_k \\ \Delta x &= B_k x + h_k \qquad t = \tau_k, \end{aligned} \tag{2.3.3}$$

where $g(\cdot) \in PC(\mathbb{R}, \mathbb{C}^n)$, $h_k \in \mathbb{R}^n$ $(k \in \mathbb{Z})$.

The solution $x(t)$ of equation (2.5.1) using the variation of parameters formula is:

$$x(t) = \begin{cases} W(t,t_0^+)x(t_0^+) + \displaystyle\int_{t_0}^{t} W(t,s)g(s)ds + \sum_{t_0<\tau_k<t} W(t,\tau_k^+)h_k & \text{for } t > t_0 \\ W(t,t_0^+)x(t_0^+) + \displaystyle\int_{t_0}^{t} W(t,s)g(s)ds - \sum_{t\le\tau_k\le t_0} W(t,\tau_k^+)h_k & \text{for } t \le t_0. \end{cases}$$

In general, if $\det(E+B_k) \neq 0$ ($k \in \mathbb{Z}$) and $\phi(t)$ is the fundamental solution to (2.3.1), then the function

$$x = c_1\varphi_1(t) + \cdots + c_n\varphi_n(t)$$

is a solution of (2.3.1), and the general solution of (2.5.1) has the form

$$x = c_1\varphi_1(t) + \cdots + c_n\varphi_n(t) + x_p(t)$$

where $x_p(t)$ is a particular solution of (2.5.1).

2.4 Linear homogeneous periodic equations

Consider the linear T-periodic system with fixed moments of impulsive effect

$$\begin{aligned} \frac{dx}{dt} &= A(t)x \qquad t \neq \tau_k \\ \Delta x &= B_k x \qquad t = \tau_k, \end{aligned} \tag{2.4.1}$$

subject to the following assumptions:

H4.1 The matrix $A(\cdot) \in PC(\mathbb{R}, \mathcal{L}(\mathbb{C}^n))$ and $A(t+T) = A(t)$ for $t \in \mathbb{R}$.

H4.2 $\tau_k < \tau_{k+1}$ for $k \in \mathbb{Z}$, $B_k \in \mathcal{L}(\mathbb{C}^n)$ and $\det(E + B_k) \neq 0$.

H4.3 There exists an integer $q > 0$ such that $B_{k+q} = B_k$, $\tau_{k+q} = \tau_k + T$ for $k \in \mathbb{Z}$ and $q \in \mathbb{N}$.

Theorem 2.4.1 *Suppose conditions H4.1-H4.3 hold. Then each fundamental matrix of (2.4.1) can be represented in the form*

$$X(t) = \varphi(t)e^{\Lambda t} \qquad (t \in \mathbb{R})$$

for a non-singular, T-periodic matrix $\varphi(\cdot) \in PC^1(\mathbb{R}, \mathcal{L}(\mathbb{C}^n))$ and a constant matrix $\Lambda \in \mathcal{L}(\mathbb{C}^n)$.

To the fundamental matrix $X(t)$ there corresponds a unique matrix M such that $X(t+T) = MX(t)$ for all $t \in \mathbb{R}$. Here, M is called the monodromy matrix of equation (2.4.1). The eigenvalues $\mu_1, \ldots, \mu_n$ of M are called *Floquet multipliers* of (2.4.1). The eigenvalues $\lambda_1, \ldots, \lambda_n$ of Λ are called the *characteristic exponents* of (2.4.1).

Remark 2.4.2 In order to calculate the multipliers $\mu_1, \ldots, \mu_n$ of (2.4.1), we have to choose an arbitrary fundamental matrix $X(t)$ of (2.4.1) and calculate the eigenvalues of the matrix

$$M = W(t_0 + T, t_0) = X(t_0 + T)X^{-1}(t_0) \tag{2.4.2}$$

where $t_0 \in \mathbb{R}$ is fixed. If $X(0) = E$ then we can choose $M = X(T)$ as the monodromy matrix.

See Chapter 4 for an application of a linear impulsive system.

Theorem 2.4.3 *Let conditions H4.1-H4.3 hold. Then $\mu \in \mathbb{C}$ is a Floquet multiplier of (2.4.1) if and only if there exists a non-trivial solution $\varphi(t)$ such that $\varphi(t + T) = \mu\varphi(t)$ for all $t \in \mathbb{R}$.*

Theorem 2.4.4 *Let conditions H3.1-H3.3 hold. Then equation (2.4.1) has a non-trivial kT-periodic solution if and only if the k^{th} power of at least one of its multipliers equals 1.*

Now we consider stability of the linear T-periodic impulsive equation. The multipliers of equation (2.4.1) completely characterize its stability. This is seen from the following theorem and the relation

$$\frac{1}{T}\ln|\mu_j| = Re(\lambda_j) \quad (j = 1, \ldots, n)$$

between the multipliers μ_j of the monodromy matrix M, and the real parts of the eigenvalues λ_j of the matrix Λ.

Theorem 2.4.5 *Suppose conditions H4.1-H4.3 hold. Then the solution to equation (2.4.1) is*

1. *stable if and only if all multipliers μ_j satisfy $|\mu_j| \leq 1$; for those multipliers for which $|\mu_j| = 1$, the corresponding characteristic exponent (which has zero real part) is a simple zero of the characteristic polynomial of Λ,*
2. *asymptotically stable if and only if all multipliers satisfy $|\mu_j| < 1$, and*
3. *unstable if $|\mu_j| > 1$ for some j.*

2.4.1 Example

Linear homogeneous example using monodromy matrix

Consider

$$\begin{aligned} &\frac{dx}{dt} = \omega y \qquad \frac{dy}{dt} = -\omega x \qquad t \neq \tau_k \qquad (t \in \mathbb{R}) \\ &\Delta x = 0 \qquad \Delta y = \frac{a}{\omega}x + by \qquad t = \tau_k \qquad (k \in \mathbb{Z}). \end{aligned} \tag{2.4.3}$$

Denote

$$A = \begin{bmatrix} 0 & \omega \\ -\omega & 0 \end{bmatrix}, \qquad B = \begin{bmatrix} 0 & 0 \\ \frac{a}{\omega} & b \end{bmatrix}, \qquad E = \begin{bmatrix} 1 & 0 \\ 0 & 1 \end{bmatrix}.$$

The monodromy matrix is

$$\begin{aligned} M &= W(\tau_0 + T, \tau_0^+) \\ &= (E + B)e^{AT} \\ &= \begin{bmatrix} 1 & 0 \\ \dfrac{a}{\omega} & 1+b \end{bmatrix} \begin{bmatrix} \cos(\omega T) & \sin(\omega T) \\ -\sin(\omega T) & \cos(\omega T) \end{bmatrix} \\ &= \begin{bmatrix} \cos(\omega T) & \sin(\omega T) \\ \dfrac{a}{\omega}\cos(\omega T) - (b+1)\sin(\omega T) & \dfrac{a}{\omega}\sin(\omega T) + (b+1)\cos(\omega T) \end{bmatrix} \end{aligned}$$

and its multipliers μ_j $(j = 1, 2)$ satisfy the equation

$$\mu^2 - \Big[\frac{a}{\omega}\sin(\omega T) + (b+2)\cos(\omega T)\Big]\mu + b + 1 = 0. \tag{2.4.4}$$

By means of Theorem 2.4.4, we shall investigate the existence of T- and $2T$-periodic solutions.

(i) Existence of T-periodic solutions. From Theorem 2.4.4, system (2.4.3) has non-trivial T-periodic solutions if and only if $\mu = 1$ is a root of (2.4.4); that is, if

$$\frac{a}{\omega}\sin(\omega T) + (b+2)\cos(\omega T) = b + 2 \tag{2.4.5}$$

or

$$\sin\Big(\frac{1}{2}\omega T\Big)\Big[\frac{a}{\omega}\cos\Big(\frac{1}{2}\omega T\Big) - (b+2)\sin\Big(\frac{1}{2}\omega T\Big)\Big] = 0. \tag{2.4.6}$$

Let $x = x(t)$, $y = y(t)$ be a T-periodic solution of (2.4.3) and $x(\tau_0^+) = x_0$, $y(\tau_0^+) = y_0$. Then $z_0 = [x_0 \quad y_0]^T$ must satisfy the system $Mz_0 = z_0$ (since, by Theorem 2.4.4, $\mu = 1$) or, in detail, the system

$$\begin{aligned} \Big(\cos(\omega T) - 1\Big)x_0 + \sin(\omega T)y_0 = 0 \\ \Big[\frac{a}{\omega}\cos(\omega T) - (b+1)\sin(\omega T)\Big]x_0 \\ + \Big[\frac{a}{\omega}\sin(\omega T) + (b+1)\cos(\omega T) - 1\Big]y_0 = 0. \end{aligned} \tag{2.4.7}$$

The following cases are possible.

(i.1) Let $\sin\left(\frac{1}{2}\omega T\right) = 0$; that is, $T = 2k\pi/\omega$ ($k \in \mathbb{N}$). Condition (2.4.6) is satisfied and system (2.4.7) is reduced to the equation

$$\frac{a}{\omega}x_0 + by_0 = 0.$$

For $\tau_j < t \leq \tau_{j+1}$, we have a solution

$$\begin{bmatrix} x(t) \\ y(t) \end{bmatrix} = e^{(t-\tau_j)A} \begin{bmatrix} x_0 \\ y_0 \end{bmatrix}.$$

Solving, we get

$$\begin{aligned} x(t) &= x_0 \cos\omega(t-\tau_j) + y_0 \sin\omega(t-\tau_j) \\ y(t) &= -x_0 \sin\omega(t-\tau_j) + y_0 \cos\omega(t-\tau_j), \end{aligned}$$

where $x(\tau_{j+1}^-) = x_0$, $y(\tau_{j+1}^-) = y_0$ due to periodicity. Thus, for $t = \tau_{j+1}$,

$$\Delta x = 0, \qquad \Delta y = \frac{a}{\omega}x_0 + by_0 = 0;$$

that is, the T-periodic solutions starting at $t = \tau_0^+$ from the point (x_0, y_0) of the straight line $(a/\omega)x + by = 0$ are continuous.

(i.2) Let $\sin\frac{1}{2}\omega T \neq 0$, $a = 0$ and $b = -2$. Condition (2.4.6) is satisfied for each $T > 0$, $T \neq 2k\pi/\omega$ and, from condition (2.4.7), we have

$$\begin{aligned} \Big(\cos(\omega T) - 1\Big)x_0 + \sin(\omega T)y_0 &= 0 \\ \sin(\omega T)x_0 - \Big(\cos(\omega T) - 1\Big)y_0 &= 0. \end{aligned}$$

Using the identities

$$\begin{aligned} \cos a + 1 &= 2\cos^2\frac{a}{2} \\ \sin a &= 2\sin\frac{a}{2}\cos\frac{a}{2}, \end{aligned}$$

the T-periodic solutions start at $t = \tau_0^+$ from the point (x_0, y_0) of the straight line

$$-x_0 + \cot\Big(\frac{1}{2}\omega T\Big)y_0 = 0.$$

(i.3) Let $\sin\frac{1}{2}\omega T \neq 0$, $a \neq 0$ and let T satisfy the condition

$$\cot\frac{1}{2}\omega T = \frac{(b+2)\omega}{a}.$$

Then, from the first equation in condition (2.4.7), and the fact that $1 - \cos a = 2\sin^2\frac{a}{2}$, the T-periodic solutions of (2.4.3) start from the points (x_0, y_0) for which

$$-ax_0 + (b+2)\omega y_0 = 0.$$

(ii) $2T$-periodic solutions of system (2.4.3). From Theorem 2.4.4, there exists a non-trivial $2T$-periodic solution if and only if the second power of at least one of its multipliers equals 1. The eigenvalues of the matrix M^2 are $m_j = \mu_j^2$ $(j = 1, 2)$, where μ_j are the eigenvalues of the monodromy matrix M and satisfy equation (2.4.4). Hence they must satisfy $m^2 + (m_1 + m_2)m + m_1 m_2 = 0$, where

$$\begin{aligned} m_1 + m_2 = \mu_1^2 + \mu_2^2 &= (\mu_1 + \mu_2)^2 - 2\mu_1\mu_2 \\ &= \Big[\frac{a}{\omega}\sin(\omega T) + (b+2)\cos(\omega T)\Big]^2 - 2(b+1) \\ m_1 m_2 = \mu_1^2\mu_2^2 &= (b+1)^2; \end{aligned}$$

that is, m_j $(j = 1, 2)$ satisfy the equation

$$m^2 - \Big\{\Big[\frac{a}{\omega}\sin(\omega T) + (b+2)\cos(\omega T)\Big]^2 - 2(b+1)\Big\}m + (b+1)^2 = 0. \tag{2.4.8}$$

System (2.4.3) has non-trivial $2T$-periodic solutions if and only if $m = 1$ is a solution of (2.4.8); that is, if

$$\Big[\frac{a}{\omega}\sin(\omega T) + (b+2)\cos(\omega T)\Big]^2 = (b+2)^2. \tag{2.4.9}$$

Then $z_0 = [x_0 \quad y_0]^T$ must satisfy the system $M^2 z_0 = z_0$ or $(M - M^{-1})z_0 = 0$. In view of

$$M^{-1} = \frac{1}{b+1}\begin{bmatrix} \dfrac{a}{\omega}\sin(\omega T) + (b+1)\cos(\omega T) & -\sin(\omega T) \\ -\dfrac{a}{\omega}\cos(\omega T) + (b+1)\sin(\omega T) & \cos(\omega T) \end{bmatrix},$$

the system $(M - M^{-1})z_0 = 0$ takes the form

$$\begin{aligned} \sin(\omega T)\Big[\frac{a}{\omega}x_0 + (b+2)y_0\Big] &= 0 \\ (b+2)\Big[\frac{a}{\omega}\cos(\omega T) - (b+1)\sin(\omega T)\Big]x_0 & \\ +\Big[(b+1)\frac{a}{\omega}\sin(\omega T) + b(b+2)\cos(\omega T)\Big]y_0 &= 0. \end{aligned} \tag{2.4.10}$$

The following cases are possible.

(ii.1) Let $\sin\omega T = 0$; that is, $T = k\pi/\omega$ ($k \in \mathbb{N}$). In this case, condition (2.4.9) is satisfied and system (2.4.10) is reduced to the equation

$$(b+2)\Big(\frac{a}{\omega}x_0 + by_0\Big) = 0.$$

Then

(ii.1.1) If $b = -2$, then all solutions of (2.4.3) are periodic with period $T_1 = 2T = 2k\pi/\omega$.

(ii.1.2) If $b \neq -2$, then $T_1 = 2k\pi/\omega$ is the period of the solutions starting at $t = \tau_0^+$ from the points (x_0, y_0) of the straight line $(a/\omega)x + by = 0$. These motions are continuous (case (i.1)).

(ii.2) Let $\sin\omega T \neq 0$, $a = 0$ and $b = -2$. Then conditions (2.4.9) and (2.4.10) are satisfied and all solution of (2.4.3) have period $T_1 = 2T \neq 2k\pi/\omega$.

(ii.3) Let $\sin\omega T \neq 0$, $a \neq 0$ and $b \neq -2$ and let T satisfy condition (2.4.9) which can

be written in the form

$$\frac{a^2}{\omega^2}\sin^2(\omega T) + 2\frac{a}{\omega}(b+2)\sin(\omega T)\cos(\omega T) = (b+2)^2(\cos^2(\omega T)+1)$$
$$2\omega a(b+2)\cos(\omega T)\sin(\omega T) = \sin^2(\omega T)\omega^2(b+2)^2 - \sin^2(\omega T)a^2$$
$$\cot(\omega T) = \frac{\omega^2(b+2)^2 - a^2}{2\omega a(b+2)}.$$

Then equation (2.4.3) has $2T$-periodic solutions starting from the points (x_0, y_0) of the straight line

$$\frac{a}{\omega}x - (b+2)y = 0.$$

This is calculated using the first equation in condition (2.4.10).

When the solutions have a period of T (or $2T$), then the multipliers of equation (2.4.3) are $\mu_1 = 1$, $\mu_2 = b+1$ (or $m_1 = 1$, $m_2 = (b+1)^2$). (These are found by substituting equation (2.4.5) into equation (2.4.4) and solving $\mu^2 - (b+2)\mu + (b+1) = 0$.) These periodic motions are stable if $|b+1| < 1$ or $-2 < b < 0$.

Biological example: solving for a T-periodic solution

Consider a simple two-compartmental model of drug distribution in the human body. It is assumed that the drug, which is administered orally, is first dissolved in the gastro-intestinal tract. The drug is then absorbed into the so-called apparent volume of distribution, and finally is eliminated from the system by the kidneys. Let $x(t)$ and $y(t)$ denote, respectively, the amount of the drug at time t in the gastro-intestinal tract and the apparent volume of distribution, and let $\mu > 0$ and $\lambda > 0$ be relevant rate constants. Then the dynamical system of this model is

$$\frac{dx}{dt} = -\mu x \qquad \frac{dy}{dt} = \mu x - \lambda y.$$

At the moments of time τ_n ($\tau_n < \tau_{n+1}, n \in \mathbb{N}$), let the sick person take doses $\delta_n > 0$ of the medicine so that

$$\Delta x = \delta_n \qquad \triangle y = 0 \qquad t = \tau_n. \tag{2.4.11}$$

For some diseases, it is necessary that the doses of medicine be taken periodically ($\tau_n = nT$) and be fixed: $\delta_n = \delta$ ($n \in \mathbb{N}$). Some constraints are usually imposed on the value of the dose δ. On the one hand, it must be large enough to produce the desired therapeutic effect; on the other hand, it cannot exceed a certain bound to avoid harmful effects of overdose of the medicine. The following problem arises: *Determine the dose $\delta > 0$ so that the T-periodic solution $x(t)$, $y(t)$ of the impulsive system*

$$\begin{array}{lll} \dfrac{dx}{dt} = -\mu x & \dfrac{dy}{dt} = \mu x - \lambda y & t \neq nT \\ \Delta x = \delta & \triangle y = 0 & t = nT, \end{array} \tag{2.4.12}$$

satisfies the inequalities

$$x(t) \leq x^* \qquad y(t) \geq y^*, \tag{2.4.13}$$

where $0 < y^* < x^*$. We choose these inequalities so that the amount of drug dissolved in the intestinal tract is small and that the amount of drug absorbed in the volume of distribution (the entire body) is large. We set $y^* < x^*$ so that the amount of drug absorbed in the body is larger than the amount of drug being dissolved in the intestinal tract.

Denote

$$z = \begin{bmatrix} x \\ y \end{bmatrix}, \qquad A = \begin{bmatrix} -\mu & 0 \\ \mu & -\lambda \end{bmatrix}, \qquad b = \begin{bmatrix} \delta \\ 0 \end{bmatrix}, \qquad z_0^+ = z(0^+) = \begin{bmatrix} x_0^+ \\ y_0^+ \end{bmatrix}.$$

First, note that the eigenvalues $-\mu$ and $-\lambda$ of the matrix A are negative. Then the homogeneous system $z' = Az$ is exponentially stable and has no non-trivial T-periodic solution.

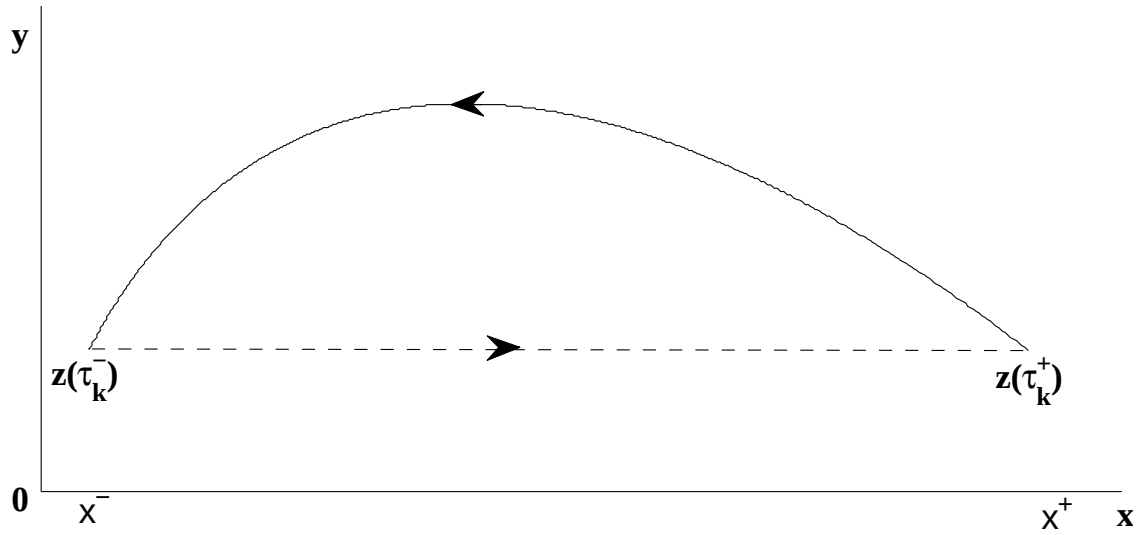

Figure 2.5: Solution to the periodic orbit of equation (2.4.12), where the dotted line is the impulse.

Solving for the fundamental matrix, we have

$$e^{At} = \begin{bmatrix} e^{-\mu t} & 0 \\ \dfrac{\mu}{\lambda - \mu}(e^{-\mu t} - e^{-\lambda t}) & e^{-\lambda t} \end{bmatrix}.$$

In order to determine the initial value, we use the condition of T-periodicity $z(T^+) = z(0^+)$ (see Figure 2.5), and the fact that $z_1^- = e^{AT} z_0^+$ and $z_1^+ = z_0^+$, which implies that

$$z_1^+ - z_1^- = \begin{bmatrix} \delta \\ 0 \end{bmatrix} = b$$

$$z_0^+ - e^{AT} z_0^+ = b$$

$$(E - e^{AT}) z_0^+ = b.$$

Now we can determine z_0^+, which allows us to determine, for $t \in (0, T]$, the T-periodic solution of (2.4.12), which has the form $z(t) = e^{At} z_0^+$ since there are no nonlinear terms

and we only have one impulse for $t \in (0, T]$. We have

$$z_0^+ = \frac{1}{(1-e^{-\mu T})(1-e^{-\lambda T})} \begin{bmatrix} 1-e^{-\lambda T} & 0 \\ \dfrac{\mu}{\lambda-\mu}(e^{-\lambda T}-e^{-\mu T}) & 1-e^{-\mu T} \end{bmatrix} \begin{bmatrix} \delta \\ 0 \end{bmatrix}$$

and so

$$z(t) = e^{At} \frac{\delta}{(1-e^{-\mu T})(1-e^{-\lambda T})} \begin{bmatrix} 1-e^{-\lambda T} \\ \dfrac{\mu}{\lambda-\mu}(e^{-\lambda T}-e^{-\mu T}) \end{bmatrix}.$$

Thus our solution is

$$\begin{aligned} x(t) &= \frac{\delta}{1-e^{-\mu T}} e^{-\mu t} \\ y(t) &= \frac{\delta\mu}{\lambda-\mu}\Big[\frac{e^{-\mu t}}{1-e^{-\mu T}} - \frac{e^{-\lambda t}}{1-e^{-\lambda T}}\Big], \end{aligned}$$

for $0 \le t \le T$. We have that $x(t) \le x(0^+)$ and $y(t) \ge y(0^+)$ since

$$\begin{aligned} (x+y)' &= -\lambda z \\ &\ge \lambda(x+y), \end{aligned}$$

and

$$(x+y) \ge (x_0+y_o)e^{-\lambda t},$$

meaning the $\min(x+y) = (x_0+y_0)$, and

$$\begin{aligned} x(t)+y(t) &\ge x_0+y_0 \\ y(t) &\ge y_0+x_0-x(t) \end{aligned}$$

gives $y(t) \ge y(0^+)$ since $x(t) \le x(0^+)$. Thus, conditions (2.4.13) are met if

$$y^* \frac{(\lambda-\mu)(1-e^{-\mu T})(1-e^{-\lambda T})}{\mu(e^{-\mu T}-e^{-\lambda T})} \le \delta \le x^*(1-e^{-\mu T}).$$

2.5 Linear non-homogeneous periodic equations

Consider the linear non-homogeneous T-periodic impulsive differential equation

$$\begin{aligned} \frac{dx}{dt} &= A(t)x + g(t) \qquad t \neq \tau_k \\ \Delta x &= B_k x + h_k \qquad\quad t = \tau_k. \end{aligned} \tag{2.5.1}$$

Suppose that conditions H4.1-H4.3 hold, as well as the following condition:

H5 $g(\cdot) \in PC(\mathbb{R}, \mathbb{C}^n)$, $h_k \in \mathbb{C}^n$ $(k \in \mathbb{Z})$ and

$g(t+T) = g(t)$, $h_{k+q} = h_k$ $(t \in \mathbb{R}, k \in \mathbb{Z})$.

We shall investigate the question of existence of a T-periodic solution of equation (2.5.1).

From the variation of constants formula in Section 2.3.3, it follows that the solution $x(t)$ of (2.5.1) has the form

$$x(t) = X(t)x(0) + \int_0^t X(t)X^{-1}(s)g(s)ds + \sum_{0 \leq \tau_k < t} X(t)X^{-1}(\tau_k^+)h_k, \tag{2.5.2}$$

where $X(t) = W(t,0)$ is the normalized (at $t_0 = 0$) fundamental matrix of equation (2.4.1).

The solution $x(t)$ will be T-periodic if $x(T) = x(0)$, or if

$$(E - X(T))x(0) = \int_0^T X(T)X^{-1}(s)g(s)ds + \sum_{0 \leq \tau_k < T} X(T)X^{-1}(\tau_k^+)h_k. \tag{2.5.3}$$

2.5.1 Non-critical case: $\det(E - X(T)) \neq 0$

We have, from Remark 2.4.2, that $M = X(T)$ is the monodromy matrix of the homogeneous equation (2.4.1) since $t_0 = 0$. The condition $\det(E - X(T)) \neq 0$ means that all multipliers of equation (2.4.1) are distinct from 1; that is, equation (2.4.1) has no T-periodic solutions other than $x \equiv 0$. In this case, equation (2.5.3) has a

unique solution

$$x(0) = [E - X(T)]^{-1}\Big[\int_0^T X(T)X^{-1}(s)g(s)ds + \sum_{0\le\tau_k<T} X(T)X^{-1}(\tau_k^+)h_k\Big]. \quad (2.5.4)$$

Hence, equation (2.5.1) has a unique T-periodic solution

$$\begin{aligned}\bar{x}(t) =& X(t)[E - X(T)]^{-1}\Big[\int_0^T X(T)X^{-1}(s)g(s)ds + \sum_{0\le\tau_k<T} X(T)X^{-1}(\tau_k^+)h_k\Big] \\ &+ \int_0^t X(t)X^{-1}(s)g(s)ds + \sum_{0\le\tau_k<t} X(t)X^{-1}(\tau_k^+)h_k.\end{aligned} \quad (2.5.5)$$

Theorem 2.5.1 *Suppose conditions H4.1-H4.3 and H5 hold and let the homogeneous equation (2.4.1) have no non-trivial T-periodic solutions. Then the non-homogeneous equation (2.5.1) has a unique T-periodic solution $\bar{x}(t)$.*

Remark 2.5.2 If all multipliers μ_j of equation (2.4.1) are such that $|\mu_j| < 1$, $j = 1, \ldots, n$, then the T-periodic solution $\bar{x}(t)$ of (2.5.1) is exponentially stable.

See Chapter 4 for an application of a nonlinear impulsive system.

2.5.2 Critical case: $\det(E - X(T)) = 0$

Consider the so-called critical case when the homogeneous equation (2.4.1) has a nontrivial T-periodic solution; that is, when at least one of the multipliers of equation (2.4.1) equals 1. Then $\det(E - X(T)) = 0$ and equation (2.5.3) may have no solution. In this case, equation (2.5.1) will not have a T-periodic solution either. The existence of such a solution is determined by relations between the free terms $g(t)$ and h_k of equation (2.5.1) and the T-periodic solution of the adjoint equation with respect to equation (2.4.1):

$$\begin{aligned}\frac{dy}{dt} &= -A^*(t)y && t \neq \tau_k \\ \Delta y &= -(E + B_k^*)^{-1}B_k^* y && t = \tau_k,\end{aligned} \quad (2.5.6)$$

where $A^*(t)$ and B_k^* are the conjugate transposes of $A(t)$ and B_k, respectively.

Note that the adjoint equation is a linear differential equation usually derived integration by parts. If $H(t,s)$ is the Cauchy matrix of the adjoint equation, then $H(t,s) = [U^*(t,s)]^{-1}$ where $U(t,s)$ is the Cauchy matrix of the homogeneous equation (2.4.1).

Lemma 2.5.3 *Let $A \in PC(\mathbb{R}, \mathcal{L}(\mathbb{C}^n))$, $B_k \in \mathcal{L}(\mathbb{C}^n)$ and $\det(E + B_k) \neq 0$ $(k \in \mathbb{Z})$. Then:*

1. *For any two solutions $x(t)$ and $y(t)$ of the mutually adjoint equations (2.4.1) and (2.5.6), the following identity is valid*

$$(x(t)|y(t)) = const. = (x(0)|y(0)) \qquad (t \in \mathbb{R}), \tag{2.5.7}$$

   where $(x|y) = \sum_{i=1}^{n} x_i y_i^*$ is the scalar product in $\mathbb{C}^n$.

2. *Two fundamental matrices $X(t)$ and $Y(t)$ of the mutually adjoint equations (2.4.1) and (2.5.6) satisfy the identity*

$$Y^*(t)X(t) \equiv C \qquad (t \in \mathbb{R}), \tag{2.5.8}$$

   where $C \in \mathcal{L}(\mathbb{C}^n)$ is a constant matrix.

3. *If identity (2.5.8) is valid, where $X(t)$ is a fundamental matrix of equation (2.4.1), $C \in \mathcal{L}(\mathbb{C}^n)$ is a non-singular matrix, then $Y(t)$ is a fundamental matrix of equation (2.5.6).*

Consider the following linear algebraic equations:

$$Ax = b \tag{2.5.9}$$

$$Ay = 0 \tag{2.5.10}$$

$$A^*z = 0 \tag{2.5.11}$$

where $A \in \mathcal{L}(\mathbb{C}^n)$ and $b, x, y, z \in \mathbb{C}^n$.

Lemma 2.5.4 *The following assertions are valid.*

1. *The mutually adjoint homogeneous equations (2.5.10) and (2.5.11) have the same number, m, of linearly independent solutions, and*

$$m = n - rank(A) = n - rank(A^*).$$

2. *If $z_1, \ldots, z_m$ are the linearly independent solutions of equation (2.5.11), then the non-homogeneous equation (2.5.9) has a solution if and only if*

$$(z_j|b) = 0 \qquad (j = 1, \ldots, m).$$

3. *If $(z_j|b) = 0$ $(j = 1, \ldots, m)$, then there exists a unique solution $x = \bar{x}$ of equation (2.5.9) which satisfies the conditions*

$$(y_j|\bar{x}) = 0 \qquad (j = 1, \ldots, m),$$

where $y_1, \ldots, y_m$ are linearly independent solutions of equation (2.5.10). This solution is defined by the formula

$$\bar{x} = Q^{-1}b,$$

where $Q = A - ZY^*$, $Z = [z_1, \ldots, z_m] \in \mathcal{L}(\mathbb{C}^n, \mathbb{C}^m)$ and $Y = [y_1, \ldots, y_m] \in \mathcal{L}(\mathbb{C}^n, \mathbb{C}^m)$.

This lemma comes directly from linear algebra. It allows us to take the solutions of the homogeneous and adjoint equations and find a solution to the non-homogeneous equation (assertion 3). Next we look at a similar theorem for an impulsive differential equation with T-periodic solutions.

Theorem 2.5.5 *Let conditions H4.1-H4.3 and H5 hold and let the homogeneous equation (2.4.1) have m linearly independent T-periodic solutions $\varphi_1(t), \ldots, \varphi_m(t)$ $(1 \leq m \leq n)$. Then:*

1. *The adjoint equation (2.5.6) also has m linearly independent T-periodic solutions $\psi_1(t), \dots, \psi_m(t)$.*

2. *Equation (2.5.1) has a T-periodic solution if and only if the following conditions are met*

$$\int_0^T \psi_j^*(t)g(t)dt + \sum_{0\le\tau_k<T} \psi_j^*(\tau_k^+)h_k = 0 \qquad (j = 1, \dots, m). \tag{2.5.12}$$

3. *If conditions (2.5.12) are met, then each T-periodic solution of equation (2.5.1) has the form*

$$x(t) = c_1\varphi_1(t) + \cdots + c_m\varphi_m(t) + x_p(t),$$

where $x_p(t)$ is a particular T-periodic solution of (2.5.1).

4. *If conditions (2.5.12) are met, then equation (2.5.1) has a unique T-periodic solution $\bar{x}(t)$ which satisfies the condition*

$$(\varphi_i(0)|\bar{x}(0)) = 0 \qquad (i = 1, \dots, m). \tag{2.5.13}$$

2.5.3 Examples

Scalar form

Consider the case when the T-periodic equation (2.5.1) is scalar; that is, it has the form

$$\begin{aligned} \frac{dx}{dt} &= a(t)x + g(t) \qquad && t \ne \tau_k \\ \Delta x &= b_k x + h_k && t = \tau_k,\ k \in \mathbb{Z}, \end{aligned} \tag{2.5.14}$$

where $a(\cdot),\ g(\cdot) \in PC(\mathbb{R}, \mathbb{C})$; $b_k,\ h_k \in \mathbb{C}$, $1 + b_k \ne 0$ $(k \in \mathbb{Z})$.

The Cauchy matrix for the corresponding homogeneous equation

$$\begin{aligned} \frac{dx}{dt} &= a(t)x \qquad && t \ne \tau_k \\ \Delta x &= b_k x && t = \tau_k \end{aligned} \tag{2.5.15}$$

is given by

$$X(t,s) = \prod_{s\le\tau_k<t}(1+b_k)\exp\Big(\int_s^t a(u)du\Big) \qquad (-\infty < s \le t < \infty).$$

From Remark 2.4.2, the unique multiplier of equation (2.5.15) is calculated by solving for the eigenvalues of $M = W(t_0+T, t_0)$, where $t_0 + T = \tau_q^+$ and $t_0 = \tau_0^+$ for a periodic solution with q impulses, and $W(t,s)$ is the Cauchy matrix of equation (2.5.15).

Thus the multiplier of equation (2.5.15) is

$$\mu = X(\tau_q^+, \tau_0^+) = \prod_{k=1}^{q}(1+b_k)\exp\Big(\int_{\tau_0}^{\tau_q} a(u)du\Big). \tag{2.5.16}$$

Case 1. If $\mu \neq 1$, then the homogeneous equation of (2.5.15) has no periodic solutions and the non-homogeneous equation (2.5.14) has a unique T-periodic solution

$$\begin{aligned}\bar{x}(t) = &X(t,\tau_0^+)\frac{1}{1-\mu}\Big[\int_{\tau_0}^{\tau_q} X(\tau_q^+, s)g(s)ds + \sum_{k=1}^{q} X(\tau_q^+, \tau_k^+)h_k\Big] \\ &+ \int_{\tau_0}^{t} X(t,s)g(s)ds + \sum_{\tau_0<\tau_k<t} X(t,\tau_k^+)h_k.\end{aligned} \tag{2.5.17}$$

Moreover, the solution $\bar{x}(t)$ is exponentially stable if $|\mu| < 1$ and unstable if $|\mu| > 1$.

Note that $\bar{x}(t)$ is calculated using the properties of the fundamental matrix; ie, $X(t,s) = X(t)X^{-1}(s)$ and $X(0) = E$ and without loss of generality the property $x(\tau_0^+) = 1$, which is an assumption made later in this thesis.

Case 2. If $\mu = 1$, then all solutions of (2.5.15) are T-periodic. Then all solutions of the adjoint equation

$$\begin{aligned}\frac{dy}{dt} &= -a^*(t)y \qquad t \neq \tau_k \\ \Delta y &= -\frac{b_k^*}{1+b_k^*}y \qquad t = \tau_k\end{aligned} \tag{2.5.18}$$

are also T-periodic (from Theorem 2.5.5). In particular, the function

$$y = \Psi(t) = \prod_{\tau_0 \le \tau_k < t} \frac{1}{1 + b_k^*} \exp\Big(- \int_{\tau_0}^{t} a^*(u)du \Big)$$

is a T-periodic solution of (2.5.18) for which $\Psi(\tau_q^+) = \Psi(\tau_0^+) = 1$. This is a solution to (2.5.18), since it is a form of the Cauchy matrix for the adjoint equation; ie, a fundamental solution.

If, in this case, Condition 2 in Theorem 2.5.5

$$\int_{\tau_0}^{\tau_q} \Psi^*(t)g(t)dt + \sum_{k=1}^{q} \Psi^*(\tau_k^+)h_k = 0 \tag{2.5.19}$$

is met, then all solutions of equation (2.5.14)

$$x(t) = X(t, \tau_0^+)x(0) + \int_{\tau_0}^{t} X(t,s)g(s)ds + \sum_{\tau_0 < \tau_k < t} X(t, \tau_k^+)h_k$$

are T-periodic and stable.

Matrix form

Consider the second-order impulsive differential equation

$$\begin{aligned} \ddot{x} + 2\alpha\dot{x} + \beta^2 x &= f(t) \qquad t \neq \tau_k \\ \Delta x &= g_k \qquad t = \tau_k \\ \Delta\dot{x} &= h_k \qquad t = \tau_k, \end{aligned} \tag{2.5.20}$$

where $x, \alpha, \beta, g_k, h_k \in \mathbb{R}$, $f(\cdot) \in PC(\mathbb{R}, \mathbb{R})$.

In matrix form, equation (2.5.20) can be written

$$\begin{aligned} \frac{dz}{dt} &= Az + F(t) \qquad t \neq \tau_k \\ \Delta z &= I_k \qquad t = \tau_k, \end{aligned} \tag{2.5.21}$$

where

$$z = \begin{bmatrix} x \\ \dot{x} \end{bmatrix}, \quad A = \begin{bmatrix} 0 & 1 \\ -\beta^2 & -2\alpha \end{bmatrix}, \quad F(t) = \begin{bmatrix} 0 \\ f(t) \end{bmatrix}, \quad I_k = \begin{bmatrix} g_k \\ h_k \end{bmatrix}.$$

The eigenvalues $\lambda_{1,2}$ of the matrix A are determined from the characteristic equation

$$\lambda^2 + 2\alpha\lambda + \beta^2 = 0, \tag{2.5.22}$$

so that $\lambda_{1,2} = -\alpha \pm \sqrt{\alpha^2 - \beta^2}$. The normalized (at $t = 0$) fundamental matrix $\Phi(t)$ of the homogeneous equation

$$\frac{d\Phi}{dt} = A\Phi \tag{2.5.23}$$

is determined in the various cases by the following formulae.

(i) If $\alpha^2 - \beta^2 > 0$, then the roots of (2.5.22) are real and distinct, and

$$\Phi(t) = \begin{pmatrix} \dfrac{\lambda_1 e^{\lambda_2 t} - \lambda_2 e^{\lambda_1 t}}{\lambda_1 - \lambda_2} & \dfrac{e^{\lambda_1 t} - e^{\lambda_2 t}}{\lambda_1 - \lambda_2} \\ -\lambda_1\lambda_2 \dfrac{e^{\lambda_1 t} - e^{\lambda_2 t}}{\lambda_1 - \lambda_2} & \dfrac{\lambda_1 e^{\lambda_1 t} - \lambda_2 e^{\lambda_2 t}}{\lambda_1 - \lambda_2} \end{pmatrix} \tag{2.5.24}$$

(ii) If $\alpha^2 = \beta^2$, then the roots of (2.5.22) are real, $\lambda_1 = \lambda_2 = -\alpha$ and

$$\Phi(t) = \begin{pmatrix} (1 + \alpha t)e^{-\alpha t} & te^{-\alpha t} \\ -\alpha^2 te^{-\alpha t} & (1 - \alpha t)e^{-\alpha t} \end{pmatrix} \tag{2.5.25}$$

(ii) If $\omega^2 = \beta^2 - \alpha^2 > 0$, then the roots of (2.5.22) are complex, $\lambda_1 = \lambda_2^* = -\alpha + i\omega$ and

$$\Phi(t) = \begin{pmatrix} \dfrac{e^{-\alpha t}}{\omega}[\omega\cos\omega t + \alpha\sin\omega t] & \dfrac{e^{-\alpha t}}{\omega}\sin\omega t \\ -\dfrac{\omega^2 + \alpha^2}{\omega}e^{-\alpha t}\sin\omega t & \dfrac{e^{-\alpha t}}{\omega}[\omega\cos\omega t - \alpha\sin\omega t] \end{pmatrix}. \tag{2.5.26}$$

The solution $z(t)$ of (2.5.21) with $z(\tau_0^+) = \begin{bmatrix} x_0 \\ \dot{x}_0 \end{bmatrix}$ has the form

$$z(t) = \Phi(t-\tau_0)z(\tau_0^+) + \int_{\tau_0}^{t} \Phi(t-s)F(s)ds + \sum_{\tau_0<\tau_k<t} \Phi(t-\tau_k)I_k \qquad (t > \tau_0)$$

from which we find the solution $x(t)$ of (2.5.20) with $x(\tau_0^+) = x_0$, $\dot{x}(\tau_0^+) = \dot{x}_0$ is

$$\begin{aligned} x(t) = &\varphi_{11}(t-\tau_0)x_0 + \varphi_{12}(t-\tau_0)\dot{x}_0 + \int_{\tau_0}^{t} \varphi_{12}(t-s)f(s)ds \\ &+ \sum_{\tau_0<\tau_k<t} [\varphi_{11}(t-\tau_k)g_k + \varphi_{12}(t-\tau_k)h_k] \qquad (t > \tau_0) \end{aligned} \tag{2.5.27}$$

where φ_{ij}, $i, j = 1, 2$, are the entries of the matrix $\Phi(t)$ defined by one of the formulae (2.5.24), (2.5.25) or (2.5.26).

Let us discuss the question of the existence of T-periodic solutions of equation (2.5.20) under the assumption that it is T-periodic; that is, that there exists a $q \in \mathbb{N}$ such that

$$\tau_{k+q} = \tau_k + T, \quad g_{k+q} = g_k, \quad h_{k+q} = h_k, \quad f(t+T) = f(t) \quad (t \in \mathbb{R}, k \in \mathbb{Z}).$$

The equation for the initial condition $z(\tau_0^+)$ of the T-periodic solution of (2.5.21) is

$$(E - \Phi(T))z(\tau_0^+) = \int_{\tau_0}^{\tau_q} \Phi(\tau_q - s)F(s)ds + \sum_{k=1}^{q} \Phi(\tau_q - \tau_k)I_k. \tag{2.5.28}$$

or in coordinate form

$$(1 - \phi_{11}(T))x_0 - \phi_{12}(T)\dot{x}_0 = Q_1 \tag{2.5.29}$$

$$-\phi_{21}(T))x_0 + (1 - \phi_{22}(T))\dot{x}_0 = Q_2, \tag{2.5.30}$$

where

$$Q_1 = \int_{\tau_0}^{\tau_q} \phi_{12}(\tau_q - s)f(s)ds + \sum_{k=1}^{q} [\phi_{11}(\tau_q - \tau_k)g_k + \phi_{12}(\tau_q - \tau_k)h_k]$$

$$Q_2 = \int_{\tau_0}^{\tau_q} \phi_{22}(\tau_q - s)f(s)ds + \sum_{k=1}^{q} [\phi_{21}(\tau_q - \tau_k)g_k + \phi_{22}(\tau_q - \tau_k)h_k].$$

The following cases are possible.

(i) $\lambda_1 \neq 2m\pi i/T$, $\lambda_2 \neq 2m\pi i/T$ for each $m \in \mathbb{Z}$. Then the multipliers $\mu_i = e^{\lambda_i T}$ of equation (2.5.23) are distinct from 1, and equation (2.5.20) has a unique T-periodic solution. The initial values x_0, $\dot{x}_0$ of this equation are determined from system (2.5.28).

(ii) λ_1 and λ_2 are real and $\lambda_1\lambda_2 = 0$. The following subcases are possible.

(ii.1) $\lambda_1 = \lambda \neq 0$ and $\lambda_2 = 0$. Then equation (2.5.23) has one linearly independent T-periodic solution

$$\Phi_1(t) = \begin{bmatrix} 1 \\ 0 \end{bmatrix}.$$

The adjoint equation to (2.5.23), $\Psi' = -A^*\Psi$, also has one linearly independent T-periodic solution

$$\Psi_1(t) = \begin{bmatrix} 1 \\ -\dfrac{1}{\lambda} \end{bmatrix}$$

and the compatibility condition from Theorem 2.5.5 takes the form (with $\Psi^*(t)$ the matrix transpose of $\Psi(t)$)

$$-\int_{\tau_0}^{\tau_q} \frac{f(u)}{\lambda} du + \sum_{k=1}^{q} g_k - \sum_{k=1}^{q} \frac{h_k}{\lambda} = 0. \tag{2.5.31}$$

If condition (2.5.31) is met, then the system (2.5.28) for the determination of x_0, $\dot{x}_0$, using the fact that

$$\Phi(t) = \begin{bmatrix} 1 & \dfrac{e^{\lambda t} - 1}{\lambda} \\ 0 & e^{\lambda t} \end{bmatrix},$$

is reduced to the equation

$$(1 - e^{\lambda T})\dot{x}_0 = \int_{\tau_0}^{\tau_q} e^{\lambda(\tau_q - u)} f(u) du + \sum_{k=1}^{q} e^{\lambda(\tau_q - \tau_k)} h_k,$$

where x_0 can be arbitrary. Thus, in this case, equation (2.5.20) has a one-parameter family of T-periodic solutions.

(ii.2) $\lambda_1 = \lambda_2 = 0$. In this case, equation (2.5.23) and the adjoint equation $\Psi' = -A^*\Psi$ each have one linearly independent T-periodic solution

$$\Phi_1(t) = \begin{bmatrix} 1 \\ 0 \end{bmatrix} \quad \text{and} \quad \Psi_1(t) = \begin{bmatrix} 0 \\ 1 \end{bmatrix},$$

respectively. The compatibility condition from Theorem 2.5.5 takes the form

$$\int_{\tau_0}^{\tau_q} f(u)du + \sum_{k=1}^{q} h_k = 0. \tag{2.5.32}$$

If condition (2.5.32) is met, then x_0 can be arbitrary and we have, from equation (2.5.30),

$$T\dot{x}_0 = \int_{\tau_0}^{\tau_q} uf(u)du + \sum_{k=1}^{q} \tau_k h_k - \sum_{k=1}^{q} g_k.$$

Consequently, also in this case, equation (2.5.20) has a one-parameter family of T-periodic solutions.

(iii) $\lambda_1 = \lambda_2^* = i\omega = 2m\pi i/T$ for some $m \in \mathbb{Z}$ ($\alpha = 0$). Equation (2.5.23) and the adjoint equation $\Psi' = -A^*\Psi$ each have two linearly independent T-periodic solutions; or, more concretely,

$$\Phi(t) = \begin{bmatrix} \cos\omega t & \dfrac{1}{\omega}\sin\omega t \\ -\omega\sin\omega t & \cos\omega t \end{bmatrix}, \quad \Psi(t) = \begin{bmatrix} \cos\omega t & \omega\sin\omega t \\ -\dfrac{1}{\omega}\sin\omega t & \cos\omega t \end{bmatrix}.$$

The compatibility condition from Theorem 2.5.5 takes the form

$$\int_{\tau_0}^{\tau_q} \cos\omega u \cdot f(u)du + \sum_{k=1}^{q} \omega\sin\omega\tau_k \cdot g_k + \sum_{k=1}^{q} \cos\omega\tau_k \cdot h_k = 0,$$

$$\int_{\tau_0}^{\tau_q} \sin\omega u \cdot f(u)du - \sum_{k=1}^{q} \omega\cos\omega\tau_k \cdot g_k + \sum_{k=1}^{q} \sin\omega\tau_k \cdot h_k = 0.$$

If these conditions are met, then system (2.5.20) is satisfied for all x_0, $\dot{x}_0$. Consequently, in this case, all solutions of equation (2.5.28) are T-periodic.

2.6 Nonlinear equations

Consider the T-periodic impulsive equation with unfixed moment of impulse effect

$$\begin{aligned} \frac{dx}{dt} &= f(t,x,\epsilon) \qquad t \neq \tau_k(x,\epsilon) \\ \Delta x &= I_k(x,\epsilon) \qquad t = \tau_k(x,\epsilon), \end{aligned} \tag{2.6.1}$$

where $\epsilon \in J = (-\bar{\epsilon}, \bar{\epsilon})$ is a small parameter and $\tau_k(x,\epsilon) < \tau_{k+1}(x,\epsilon)$ for $x \in \mathbb{R}^n$, $\epsilon \in J$. Suppose that for $\epsilon = 0$, equation (2.6.1) has a T-periodic solution $x = \phi(t)$ with moments of impulse effect τ_k.

We associate with the solution $\phi(t)$ the variational equation

$$\begin{aligned} \frac{dz}{dt} &= \frac{\partial f}{\partial x}(t,\phi(t),0)z \qquad t \neq \tau_k \\ \Delta z &= L_k z \qquad\qquad\qquad\quad t = \tau_k, \end{aligned} \tag{2.6.2}$$

where

$$L_k = \frac{\partial I_k}{\partial x} + \Big[\frac{\partial I_k}{\partial x} f_k + f_k - f_k^+\Big] \frac{\dfrac{\partial \tau_k}{\partial x}}{1 - \dfrac{\partial \tau_k}{\partial x} f_k},$$

and

$$\begin{aligned} f_k &= f(\tau_k^-, \phi(\tau_k^-), 0) \qquad f_k^+ = f(\tau_k^+, \phi(\tau_k^+), 0) \\ \frac{\partial I_k}{\partial x} &= \frac{\partial I_k}{\partial x}(\phi(\tau_k^-), 0) \qquad \frac{\partial \tau_k}{\partial x} = \frac{\partial \tau_k}{\partial x}(\phi(\tau_k^-), 0). \end{aligned}$$

Remark 2.6.1 In the non-critical case, if the variational equation (2.6.2) is exponentially stable then the T-periodic solution $\phi(t)$ of equation (2.6.1) is also exponentially stable.

The following is valid to show sufficient conditions of the existence of a unique T-periodic solution.

Consider the T-periodic impulsive equation

$$\begin{aligned} \frac{dx}{dt} &= A(t)x + g(t) + f(t,x,\epsilon) \qquad t \neq \tau_k(x,\epsilon) \\ \Delta x &= B_k x + h_k + I_k(x,\epsilon) \qquad\quad t = \tau_k(x,\epsilon), \end{aligned} \tag{2.6.3}$$

where $t \in \mathbb{R}$, $k \in \mathbb{Z}$, $x \in B_H = B_H(0) \subset \mathbb{R}^n$ and $\epsilon \in J = (-\bar{\epsilon}, \bar{\epsilon})$ is a small parameter, and $A(t)$, B_k, $g(t)$ and h_k satisfy conditions H4.1-H4.3 and H5, in which $\mathbb{C}$ is replaced by $\mathbb{R}$.

Introduce the following conditions.

H6.1 The function $f : \mathbb{R} \times B_H \times J \to \mathbb{R}^n$ is continuous in the sets $(\tau_k, \tau_{k+1}] \times B_H \times J$ $(k \in \mathbb{Z})$, and for each $k \in \mathbb{Z}$, $x \in B_H$ and $\epsilon \in J$ there exists a finite limit of $f(t, y, u)$ as $(t, y, u) \to (\tau_k, x, \epsilon)$, $t > \tau_k$. Moreover,

$$f(t + T, x, \epsilon) = f(t, x, \epsilon) \quad (t \in \mathbb{R}, x \in B_H, \epsilon \in J).$$

H6.2 The functions $I_k : B_H \times J \to \mathbb{R}^n$ are continuous in $B_H \times J$ and

$$I_{k+q}(x, \epsilon) = I_k(x, \epsilon) \quad (k \in \mathbb{Z}, x \in B_H, \epsilon \in J).$$

H6.3 There exists a non-negative function $\mu(\epsilon)$ such that $\lim_{\epsilon \to 0} \mu(\epsilon) = \mu(0) = 0$ and

$$|f(t, x, \epsilon)| \leq \mu(\epsilon), \qquad |I_k(x, \epsilon)| \leq \mu(\epsilon),$$

for $t \in \mathbb{R}$, $k \in \mathbb{Z}$, $x \in B_H$ and $\epsilon \in J$.

H6.4 There exists a non-negative function $\lambda(\epsilon)$ such that $\lim_{\epsilon \to 0} \lambda(\epsilon) = \lambda(0) = 0$ and

$$|f(t, x, \epsilon) - f(t, y, \epsilon)| \leq \lambda(\epsilon)|x - y|$$
$$|I_k(x, \epsilon) - I_k(y, \epsilon)| \leq \lambda(\epsilon)|x - y|,$$

for $t \in \mathbb{R}$, $k \in \mathbb{Z}$, $x, y \in B_H$ and $\epsilon \in J$.

The following theorem is valid.

Theorem 2.6.2 *Let the following conditions hold.*

1. *Conditions H4.1-H4.3, H5 and H6.1-H6.4 are met.*

2. *The homogenous equation (2.4.1) has no non-trivial T-periodic solutions.*

3. The following inequality is valid:

$$m = \sup_{t\in[0,T]} \left| \int_0^T G(t,s)g(s)\,ds + \sum_{k=1}^{q} G(t,\tau_k^+)h_k \right| < H$$

where $G(t,s)$ is the Green's function of the homogenous equation (2.4.1).

Then there exists $\epsilon_0 \in (0,\bar{\epsilon})$ such that for $|\epsilon| \le \epsilon_0$ equation (2.6.3) has a unique T-periodic solution $x_\epsilon(t)$ satisfying the inequality

$$|x_\epsilon(t) - x_0(t)| < H - m.$$

Note that the Green's function for the homogenous equation (2.4.1) is defined by

$$G(t,s)=\begin{cases} X(t)[E-X(T)]^{-1}X^{-1}(s) & 0<s<t\le T \\ X(t+T)[E-X(T)]^{-1}X^{-1}(s) & 0<t\le s\le T \\ G(t-kT,s-jT) & (kT<t\le kT+T \\ & jT<s\le jT+T \\ & k\in\mathbb{Z}, j\in\mathbb{Z}) \end{cases}$$

2.7 Nonlinear autonomous equations

Consider the autonomous impulsive equation

$$\begin{aligned} \frac{dx}{dt} &= f(x,\epsilon) \qquad x \notin \sigma(\epsilon) \\ \Delta x &= I_k(x,\epsilon) \qquad x \in \sigma(\epsilon), \end{aligned} \tag{2.7.1}$$

where $\epsilon \in J = (-\bar{\epsilon},\bar{\epsilon})$ is a small parameter and, for each $\epsilon \in J$, the set $\sigma(\epsilon)$ is a hypersurface in $\mathbb{R}^n$.

Suppose that $\sigma(\epsilon)$ consists of q non-intersecting smooth hypersurfaces $\sigma_k(\epsilon)$ that are given by the equations $\phi_k(x,\epsilon) = 0$ $(k = 1,\dots,q)$. For $\epsilon = 0$, let equation (2.7.1)

have a T_0-periodic solution $x = \varphi(t)$ with moments of an impulse effect τ_k and

$$\begin{aligned} \tau_{k+q} &= \tau_k + T_0 \quad (k \in \mathbb{Z}), \\ \phi_k(\varphi(\tau_k)) &= 0 \qquad\quad (k = 1, \dots, q). \end{aligned}$$

Associate with the solution $\varphi(t)$ the variational equation

$$\begin{aligned} \frac{dz}{dt} &= \frac{\partial f}{\partial x}(\varphi(t), 0)z \qquad t \neq \tau_k \\ \Delta z &= N_k z \qquad\qquad\quad t = \tau_k, \end{aligned} \tag{2.7.2}$$

where

$$N_k = \frac{\partial I_k}{\partial x} + \Big[f^+ - f - \frac{\partial I_k}{\partial x} f\Big] \frac{\dfrac{\partial \phi}{\partial x}}{\dfrac{\partial \phi}{\partial x} f}$$

and

$$\begin{aligned} f &= f(\varphi(\tau_k^-), 0), \qquad & f^+ &= f(\varphi(\tau_k^+), 0), \\ \frac{\partial I_k}{\partial x} &= \frac{\partial I_k}{\partial x}(\varphi(\tau_k^-), 0), \qquad & \frac{\partial \phi}{\partial x} &= \frac{\partial \phi}{\partial x}(\varphi(\tau_k^-), 0). \end{aligned}$$

Note that the variation equation is similar to a linearized system. We will use this fact in order to look at stability of a periodic orbit.

A peculiarity of the autonomous equation (2.7.1) is that the derivative $\varphi'(t)$ of the solution $\varphi(t)$ is a solution of the variational equation (2.7.2). Indeed, for $t \neq \tau_k$ we have

$$[\varphi'(t)]' = [f(\varphi(t), 0)]' = \frac{\partial f}{\partial x}(\varphi(t), 0)\varphi'(t)$$

and for $t = \tau_k$ we successively obtain

$$\frac{\partial \phi_k}{\partial x}(\varphi(\tau_k^-), 0)\varphi'(\tau_k^-) = \frac{\partial \phi_k}{\partial x}(\varphi(\tau_k^-), 0) f(\varphi(\tau_k^-), 0),$$

$$\begin{aligned} N_k \varphi'(\tau_k^-) &= \frac{\partial I_k}{\partial x}\varphi'(\tau_k^-) + \Big[f^+ - f - \frac{\partial I_k}{\partial x} f\Big] \frac{\dfrac{\partial \phi}{\partial x}\varphi'(\tau_k^-)}{\dfrac{\partial \phi}{\partial x} f} \\ &= f(\varphi(\tau_k^+), 0) - f(\varphi(\tau_k^-), 0), \end{aligned}$$

$$\triangle\varphi'(\tau_k) = \varphi'(\tau_k^+) - \varphi'(\tau_k^-) = f(\varphi(\tau_k^+), 0) - f(\varphi(\tau_k^-), 0) = N_k\varphi'(\tau_k^-).$$

If $\varphi'(t) \not\equiv 0$, then $\varphi'(t)$ is a non-zero T_0-periodic solution of (2.7.2), and then equation (2.7.2) has a multiplier $\mu_1 = 1$.

We will consider the non-critical case when equation (2.7.2) has no nontrivial T_0-periodic solutions other than $\varphi'(t)$; ie, just one of the multipliers of equation (2.7.2) equals 1.

2.7.1 Stability in $\mathbb{R}^2$

Consider the two dimensional autonomous system

$$\begin{array}{lll} \dfrac{dx_1}{dt} = P(x_1, x_2) & \dfrac{dx_2}{dt} = Q(x_1, x_2) & \phi(x_1, x_2) \neq 0 \\ \Delta x_1 = a(x_1, x_2) & \Delta x_2 = b(x_1, x_2) & \phi(x_1, x_2) = 0, \end{array} \tag{2.7.3}$$

where $t \in \mathbb{R}$.

Let $\vec{x} = \varphi(t)$, $t \in \mathbb{R}_+$ be a solution of (2.7.3), with instants of impulsive effect τ_k, such that

$$0 < \tau_1 < \tau_2 < ... \qquad \lim_{k\to\infty} \tau_k = \infty$$

and let $L_+ = \{\vec{x} \in \mathbb{R}^2 : \vec{x} = \varphi(t), t \in \mathbb{R}_+\}$. Denote by $J^+(t_0, x_0)$ the maximal interval of the form (t_0, ω) in which the solution $x(t; t_0, z_0)$ of (2.7.3) is defined.

Let $B_\eta(\gamma(\tau_1))$ be the ball of radius η centered at $\varphi(\tau_1)$.

Definition 2.7.1 *The solution $\vec{x} = \varphi(t)$ of (2.7.3) is called*

1. orbitally stable *if, for all $\epsilon > 0$, $\eta > 0$ and $t_0 \in \mathbb{R}_+$, there exists $\delta > 0$ such that for all $x_0 \in \mathbb{R}^2$, $d(x_0, L^+) < \delta$ and $x_0 \notin \bar{B}_\eta(\varphi(\tau_k)) \cup \bar{B}_\eta(\varphi(\tau_k^+))$ implies $d(x(t), L^+) < \epsilon$ for $t \in J^+(t_0, x_0)$ and $|t - t_k| > \eta$, where $x(t) = x(t; t_0, x_0)$ is any solution of (2.7.3) for which $x(t_0^+; t_0, x_0) = x_0$.*

2. orbitally attractive *if, for all $\epsilon > 0$, $\eta > 0$ and $t_0 \in \mathbb{R}_+$, there exists $\delta > 0$ and $T > 0$ such that $t_0 + T \in J^+(t_0, x_0)$ and $d(x_0, L^+) < \delta$ and $x_0 \notin \bar{B}_\eta(\varphi(\tau_k)) \cup$*

$\bar{B}_\eta(\varphi(\tau_k^+))$ *implies* $d(x(t), L^+) < \epsilon$ *for* $t \geq t_0 + T$, $t \in J^+(t_0, x_0)$ *and* $|t - \tau_k| > \eta$, *where* $x(t) = x(t; t_0, x_0)$ *is any solution of (2.7.3) for which* $x(t_0^+; t_0, x_0) = x_0$.

3. orbitally asymptotically stable *if it is orbitally stable and orbitally attractive.*

Definition 2.7.2 *The solution* $\vec{x} = \varphi(t)$ *of (2.7.3) has the property of* asymptotic phase *if, for all* $\epsilon > 0$, $\eta > 0$ *and* $t_0 \in \mathbb{R}_+$, *there exists* $\delta > 0$, $c > 0$ *and* $T > |c|$ *such that* $t_0 + T \in J^+(t_0, x_0)$ *and* $|x_0 - \varphi(t_0)| < \delta$ *implies* $|x(t + c) - \varphi(t)| < \epsilon$ *for* $t \geq t_0 + T$, $t \in J^+(t_0, x_0)$ *and* $|t - \tau_k| > \eta$, *where* $x(t) = x(t; t_0, x_0)$ *is any solution of (2.7.3) for which* $x(t_0^+; t_0, x_0) = x_0$.

Asymptotic phase is a nice property in which cycle times come into phase with the period of the periodic orbit.

Suppose (2.7.3) has a T-periodic solution

$$p(t) = \begin{bmatrix} \xi(t) \\ \eta(t) \end{bmatrix},$$

with

$$\left|\frac{d\xi}{dt}\right| + \left|\frac{d\eta}{dt}\right| \neq 0.$$

Assume further that the periodic solution $\vec{p}(t)$ has q instants of impulsive effect in the interval $(0, T)$. Since we have a periodic orbit, one multiplier is equal to 1. The other is calculated according to the formula

$$\mu_2 = \prod_{k=1}^{q} \Delta_k \exp\Big[\int_0^T \Big(\frac{\partial P}{\partial x}(\xi(t), \eta(t)) + \frac{\partial Q}{\partial y}(\xi(t), \eta(t))\Big) dt\Big], \tag{2.7.4}$$

where

$$\Delta_k = \frac{P_+\left(\frac{\partial b}{\partial y}\frac{\partial \phi}{\partial x} - \frac{\partial b}{\partial x}\frac{\partial \phi}{\partial y} + \frac{\partial \phi}{\partial x}\right) + Q_+\left(\frac{\partial a}{\partial x}\frac{\partial \phi}{\partial y} - \frac{\partial a}{\partial y}\frac{\partial \phi}{\partial x} + \frac{\partial \phi}{\partial y}\right)}{P\frac{\partial \phi}{\partial x} + Q\frac{\partial \phi}{\partial y}}.$$

P, Q, $\dfrac{\partial a}{\partial x}$, $\dfrac{\partial b}{\partial x}$, $\dfrac{\partial a}{\partial y}$, $\dfrac{\partial b}{\partial y}$, $\dfrac{\partial \phi}{\partial x}$ and $\dfrac{\partial \phi}{\partial y}$ are computed at the point $(\xi(\tau_k^-), \eta(\tau_k^-))$ and $P_+ = P(\xi(\tau_k^+), \eta(\tau_k^+))$, $Q_+ = Q(\xi(\tau_k^+), \eta(\tau_k^+))$.

We then have the following theorem, from Bainov and Simeonov [1], which is an analogue of the Poincaré criterion.

Theorem 2.7.3 *The T-periodic solution $\vec{p}(t)$ of (2.7.3) is orbitally asymptotically stable and has the property of asymptotic phase if the multiplier μ_2 calculated by (2.7.4) satisfies the condition $|\mu_2| < 1$.*

The Floquet theory for impulsive dynamical systems in $\mathbb{R}^n$, $n \geq 3$, is also developed in Bainov and Simeonov [1] but calculation of the multipliers is much more difficult. In practice, the theory is only useful in low-dimensional systems. If we are in $\mathbb{R}^2$ or the system can be reduced to a two-dimensional system, then we can apply the results in this section.

2.7.2 Examples: Species-food example

In an isolated medium, let a given species be bred, being fed with a certain resource. We assume that in the absence of the species the quantity of resource does not change, and in the absence of resource the species dies out.

If we denote by $y(t)$ and $x(t)$ the absolute or relative quantities of the species and the resource at the moment t, then the dynamics of the species-food system can be simulated by the system of ordinary differential equations

$$\frac{dx}{dt} = -\gamma xy \qquad \frac{dy}{dt} = -y(\epsilon - \delta x), \tag{2.7.5}$$

where $(x, y) \in \mathbb{R}^2_+$ and $\gamma > 0$, $\delta > 0$ are constants.

If $x(0) = x_0 > 0$ and $y(0) = y_0 > 0$, then the solution of system (2.7.5) remains in $\mathbb{R}^2_+$ (Figure 2.6) and

$$\lim_{t \to +\infty} x(t) = x_\infty \qquad \lim_{t \to +\infty} y(t) = 0$$

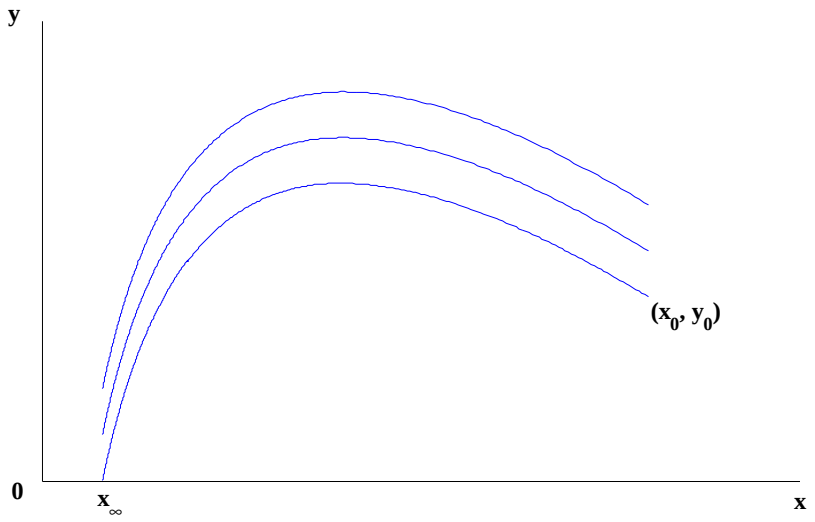

Figure 2.6: The solution to the differential equation (2.7.5) with no impulses. Given an x_0 and y_0, the species, y, dies out if the food, x, is not regenerated.

[1]. This means that, if the resource is not regenerated, the species dies out. It turns out, however, that under appropriately chosen impulse effects on the species-food system a periodic regime of development of the species is possible.

Consider the following two cases.

Case 1: At certain moments, let the species-food system be subject to an impulsive effect such that the quantity of food is increased by the amount $\lambda > 0$ and the population of the species is decreased by αy. Assume that $0 < \alpha < 1$; that is, the whole species is not exhausted at any time. This system could be applied to water filtration. A certain species is added to a specific amount of water containing waste (food eaten by the species). At a specific time, a certain amount of the water containing species is removed and new water containing waste is added. Thus, the amount of species decreases while the amount of food increases at specific times.

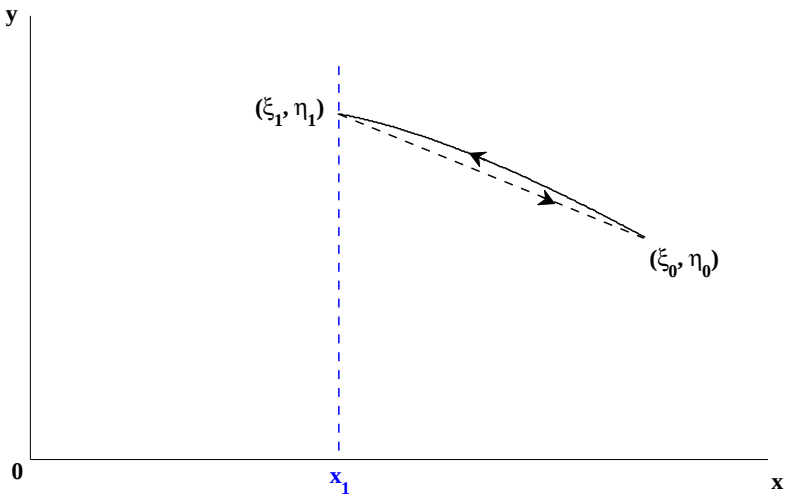

Figure 2.7: Periodic orbit to equation (2.7.6) with an impulse at x_1.

Let these impulse effects occur when the quantity of food reaches a given level $x_1 > 0$. Thus we obtain the following impulsive system

$$\begin{aligned} &\frac{dx}{dt} = -\gamma xy \qquad \frac{dy}{dt} = -y(\epsilon - \delta x) \qquad \text{if } x \neq x_1 \\ &\Delta x = \lambda \qquad\quad \triangle y = -\alpha y \qquad\quad\ \ \text{if } x = x_1. \end{aligned} \tag{2.7.6}$$

Note that this is a state-dependent impulsive system and that the cycle time becomes a dependent variable.

Let us investigate the questions of the existence of a T-periodic solution of system (2.7.6) with one impulse effect per period and of the stability of this solution.

Let $x = \xi(t)$, $y = \eta(t)$ be such a T-periodic solution. Introduce the notation $\xi_0^+ = \xi(0^+)$, $\eta_0^+ = \eta(0^+)$, $\xi_1^- = \xi(T^-)$, $\eta_1^- = \eta(T^-)$, $\xi_1^+ = \xi(T^+)$, $\eta_1^+ = \eta(T^+)$. Then, from the condition of T-perodicity, $\xi_1^+ = \xi_0^+$, $\eta_1^+ = \eta_0^+$, we obtain

$$\xi_1^- + \lambda = \xi_0^+ \qquad (1-\alpha)\eta_1^- = \eta_0^+, \tag{2.7.7}$$

since $\eta^+ = -\alpha\eta^- + \eta^-$.

For $t \in (0, T]$, the solution $x = \xi(t)$, $y = \eta(t)$ of system (2.7.6) satisfies the

relation

$$\dot{y} = -\epsilon y + \delta x y$$
$$\gamma \dot{y} = \Big(\frac{\epsilon}{x} - \delta\Big)\dot{x}$$

and integrating we get

$$\gamma(y - y_0^+) = \epsilon \ln\Big(\frac{x}{x_0^+}\Big) - \delta(x - x_0^+) \tag{2.7.8}$$
$$e^{\gamma(\eta(t)-\eta_0^+)} = \Big(\frac{x_1}{\xi_0^+}\Big)^{\epsilon} e^{-\delta(\xi(t)-\xi_0^+)}. \tag{2.7.9}$$

In particular, for $t = T$, we have (since $\eta(T) = \eta_1^-$ and $\xi(T) = \xi_1^- = x_1$)

$$e^{\gamma(\eta_1^- - \eta_0^+)} = \Big(\frac{x_1}{\xi_0^+}\Big)^{\epsilon} e^{-\delta(x_1-\xi_0^+)},$$

and, in view of (2.7.7), we obtain

$$\eta_0^+ = \frac{1-\alpha}{\alpha\gamma}\Big(\epsilon \ln\frac{x_1}{x_1+\lambda} + \delta\lambda\Big).$$

From (2.7.7), it follows that η_0^+ is positive if

$$x_1 > x^* = \frac{\lambda \exp(-\delta\lambda/\epsilon)}{1 - \exp(-\delta\lambda/\epsilon)}. \tag{2.7.10}$$

Thus, if condition (2.7.10) holds, then system (2.7.6) has a unique periodic solution with one impulse effect per period. The period T of this solution can be found, taking into account the first equation of (2.7.6), (2.7.8) and (2.7.9):

$$\begin{aligned} T = \int_0^T dt &= \int_{x_1}^{x_1+\lambda} \frac{1}{-\gamma x y} dx \\ &= \int_{x_1}^{x_1+\lambda} \frac{dx}{\Big(\gamma\eta_0^+ + \epsilon \ln\frac{x}{x_1+\lambda} - \delta(x - x_1 - \lambda)\Big)x}. \end{aligned} \tag{2.7.11}$$

The trajectory of the solution $x = \xi(t)$, $y = \eta(t)$ is given in Figure 2.7.

From formula (2.7.4), we compute the multiplier μ_2 of the system in variations corresponding to the T-periodic solution $x = \xi(t)$, $y = \eta(t)$:

$$\frac{\partial P}{\partial x} = -\gamma y \qquad \frac{\partial Q}{\partial y} = -\epsilon + \delta x$$

$$\frac{\partial a}{\partial x} = 0 \qquad \frac{\partial a}{\partial y} = 0$$

$$\frac{\partial b}{\partial x} = 0 \qquad \frac{\partial b}{\partial y} = -\alpha$$

$$\frac{\partial \phi}{\partial x} = 1 \qquad \frac{\partial \phi}{\partial y} = 0$$

$$\begin{aligned}
\triangle_1 &= \frac{P_+(-\alpha+1)}{P} \\
&= \frac{P(\xi_0^+, \eta_0^+)(1-\alpha)}{P(\xi_1^-, \eta_1^-)} \\
&= \frac{-\gamma \xi_0^+ \eta_0^+ (1-\alpha)}{-\gamma \xi_1^- \eta_1^-} \\
&= \frac{\xi_0^+ \eta_0^+ (1-\alpha)}{\xi_1^- \eta_1^-}
\end{aligned}$$

$$\begin{aligned}
\int_0^T \Big(\frac{\partial P}{\partial x} + \frac{\partial Q}{\partial y}\Big) dt &= \int_0^T (-\gamma \eta(t) - \epsilon + \delta \xi(t)) dt \\
&= \int_0^T \Big[\frac{\xi'(t)}{\xi(t)} + \frac{\eta'(t)}{\eta(t)}\Big] dt \\
&= \int_0^T \frac{d}{dt}\big(\ln(\xi(t)) + \ln(\eta(t))\big) dt \\
&= \int_0^T d \ln(\xi(t)\eta(t))) \\
&= \ln \frac{\xi_1^- \eta_1^-}{\xi_0^+ \eta_0^+}
\end{aligned}$$

$$\begin{aligned}
\mu_2 &= \triangle_1 \exp\Big\{ \int_0^T \Big(\frac{\partial P}{\partial x} + \frac{\partial Q}{\partial y}\Big) dt \Big\} \\
&= (1-\alpha) \frac{\xi_0^+ \eta_0^+}{\xi_1^- \eta_1^-} \frac{\xi_1^- \eta_1^-}{\xi_0^+ \eta_0^+} \\
&= 1 - \alpha.
\end{aligned}$$

Since $\mu_2 = 1 - \alpha \in (0, 1)$, the T-periodic solution $x = \xi(t)$, $y = \eta(t)$ of system (2.7.6) is orbitally asymptotically stable.

Case 2: Let the species-food system be subject to an impulse effect when the quantity of food reaches the level x_1 satisfying condition (2.7.10). Let $n > 0$ be an integer and assume that the quantity of food increases by λ under each impulse effect, while the population of the species decreases by jumps only at the moments of the impulse effect τ_k whose ordinal number k is a multiple of n; that is,

$$\begin{aligned} &\triangle x(\tau_k^-) = \lambda, \\ &\triangle y(\tau_k^-) = \begin{cases} 0, & \text{if } k \text{ is not divisible by } n, \\ -\alpha y(\tau_k^-), & \text{if } k \text{ is divisible by } n. \end{cases} \end{aligned} \tag{2.7.12}$$

First, we shall discover under what initial conditions $x(0) = x_0 > 0$ and $y(0) = y_0$ the impulsive system (2.7.5), (2.7.12) has a periodic solution with period $T = \tau_n$. Let $x_k^- = x(\tau_k^-)$, $x_k^+ = x(\tau_k^+)$, $y_k^- = y(\tau_k^-)$, $y_k^+ = y(\tau_k^+)$ and $\tau_0 = 0$.

In view of (2.7.12), the condition of T-periodicity of $x_n^+ = x_0^+$, $y_n^+ = y_0^+$ yields

$$x_n^- + \lambda = \xi_0^+, \qquad (1 - \alpha) y_n^- = y_0^+. \tag{2.7.13}$$

From equation (2.7.9), it follows that

$$e^{\gamma(y_k^- - y_{k-1}^+)} = \left(\frac{x_k^-}{x_{k-1}^+}\right)^{\epsilon} e^{-\delta(x_k^- - x_{k-1}^+)} \qquad (k = 1, \ldots, n)$$

and, in view of (2.7.12) and (2.7.13), we find successively

$$\begin{aligned} y_k^- - y_{k-1}^+ &= \frac{1}{\gamma}\Big(\epsilon \ln \frac{x_1}{x_1 + \lambda} + \delta\lambda\Big) \equiv z \qquad (k = 1, \ldots, n), \\ y_k^- &= y_0^+ + kz \qquad (k = 1, \ldots, n), \\ y_0^+ &= \frac{(1 - \alpha) n z}{\alpha}. \end{aligned}$$

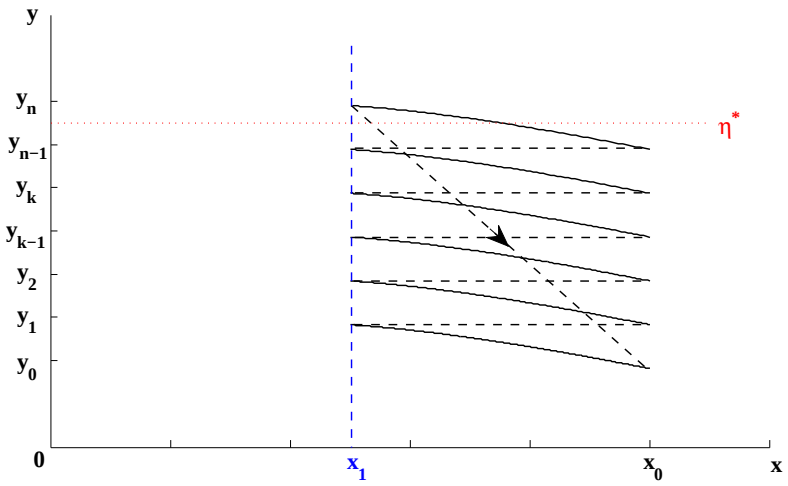

Figure 2.8: Solution to equation (2.7.14) with an impulse at x_1. Here η^* is a threshold value.

From (2.7.10), it follows that y_0 is positive. Hence, the solution $x = \xi(t)$, $y = \eta(t)$ of system (2.7.5), (2.7.12) satisfying the initial condition $\xi(0^+) = x_0$, $\eta(0^+) = y_0$ is the unique nontrivial T-periodic solution of this system with n impulse effects per period.

Let us choose a level $\eta^* = \frac{1}{2}(y_{n-1} + y_n) = z(\frac{n}{\alpha} - \frac{1}{2})$ as the threshold which causes the species to return back to the initial condition. Then $x = \xi(t)$, $y = \eta(t)$ is a τ_n-periodic solution of the following autonomous impulsive system

$$\begin{aligned} &\frac{dx}{dt} = -\gamma xy \qquad \frac{dy}{dt} = -y(\epsilon - \delta x) && \text{if} \quad x \neq x_1 \\ &\Delta x = \lambda \qquad \Delta y = \begin{cases} 0 & \text{if } y < \eta^* \\ -\alpha y & \text{if } y > \eta^* \end{cases} && \text{if} \quad x = x_1. \end{aligned} \tag{2.7.14}$$

The trajectory of this solution is represented in Figure 2.8.

From formula (2.7.4), we compute the multiplier μ_2 of the system in variations corresponding to the τ_n-periodic solution $x = \xi(t)$, $y = \eta(t)$ of system (2.7.14):

$$\frac{\partial P}{\partial x} = -\gamma y \qquad \frac{\partial Q}{\partial y} = -\epsilon + \delta x$$

$$\frac{\partial a}{\partial x} = 0 \qquad \frac{\partial a}{\partial y} = 0$$

$$\frac{\partial \phi}{\partial x} = 1 \qquad \frac{\partial \phi}{\partial y} = 0$$

$$\frac{\partial b}{\partial x} = 0 \qquad \frac{\partial b}{\partial y} = \begin{cases} 0 & \text{if } y < \eta^* \\ -\alpha y & \text{if } y > \eta^* \end{cases}$$

$$\begin{aligned} \Delta_k &= \frac{P(\xi(\tau_k^+), \eta(\tau_k^+))}{P(\xi(\tau_k^-), \eta(\tau_k^-))} \qquad (k = 1, \ldots, n-1) \\ &= \frac{P(x_k^+, y_k^+)}{P(x_k^-, y_k^-)} \\ &= \frac{-\gamma x_k^+ y_k^+}{-\gamma x_k^- y_k^-} = \frac{x_0^+}{x_1^-} \\ \Delta_n &= \frac{P(x_n^+, y_n^+)(-\alpha + 1)}{P(x_n^-, y_n^-)} \qquad (k = 1, \ldots, n-1) \\ &= (1-\alpha)\frac{-\gamma x_n^+ y_n^+}{-\gamma x_n^- y_n^-} \\ &= (1-\alpha)\frac{x_0^+ y_0^+}{x_1^- y_n^-} \end{aligned}$$

$$\begin{aligned} \int_0^T \Big(\frac{\partial P}{\partial x} + \frac{\partial Q}{\partial y}\Big) dt &= \int_{\tau_{k-1}}^{\tau_k} (-\gamma y - \epsilon + \delta x) dt \\ &= \ln \frac{x_k^- y_k^-}{x_{k-1}^+ y_{k-1}^+} = \ln \frac{x_1^- y_k^-}{x_0^+ y_{k-1}^+} \end{aligned}$$

$$\begin{aligned} \mu_2 &= \prod_{k=1}^{n} \Delta_k \exp\Big\{ \int_{\tau_{k-1}}^{\tau_k} \Big(\frac{\partial P}{\partial x} + \frac{\partial Q}{\partial y}\Big) dt \Big\} \\ &= \Big(\frac{x_0}{x_1} \cdot \frac{x_1 y_1}{x_0 y_0}\Big)\Big(\frac{x_0}{x_1} \cdot \frac{x_1 y_2}{x_0 y_1}\Big) \cdots \Big(\frac{x_0}{x_1} \cdot \frac{x_1 y_{n-1}}{x_0 y_{n-2}}\Big)\Big(\frac{(1-\alpha)x_0 y_0}{x_1 y_n} \cdot \frac{x_1 y_n}{x_0 y_{n-1}}\Big) \\ &= 1 - \alpha. \end{aligned}$$

Since $\mu_2 = 1 - \alpha \in (0, 1)$, the τ_n-periodic solution $x = \xi(t)$, $y = \eta(t)$ of system (2.7.6) is orbitally asymptotically stable. The period of this solution can be calculated from the formula

$$T = \sum_{k=1}^{n} \int_{x_1}^{x_1+\lambda} \frac{dx}{\Big(\gamma y_{k-1} + \epsilon \ln \frac{x}{x_1+\lambda} - \delta(x - x_1 - \lambda)\Big)x}.$$

Chapter 3

Applications of impulsive differential equations to the Human Immunodeficiency Virus

Human Immunodeficiency Virus (HIV) is one of the most dangerous sexually transmitted infections ever encountered. There have been many attempts to control the virus (condoms, drugs, vaccines, microbicides, male circumcision, education). At the end of 2010, an estimated 34 million people (31.6 million–35.2 million) were living with HIV worldwide, up 17% from 2001 [6]. There were 2.7 million new HIV infections in 2010, which was 15% less than in 2001, and 21% below the number of new infections at the peak of the epidemic in 1997 [6]. Of the 33.3 million infected, approximately 390 thousand are children [6, 7]. The number of people dying of AIDS-related causes fell to 1.8 million in 2010, down from a peak of 2.2 million in the mid-2000s [6, 8]. Sub-Saharan Africa has the largest population of seropositive individuals, accounting for approximately 70% of new infections in 2010 [6]. This extremely high number of HIV cases is largely due to the lack of education, the high number of rape cases, globalization, lack of resources, capitalism, poverty, etc [9, 10, 11]. Antiretroviral drugs

have decreased the number of deaths by diminishing the viral load levels in infected individuals. Unfortunately, the costs of antiretroviral drugs limit the number of HIV-positive individuals in poor countries who can efficiently take therapy. More than 5 million people in low- and middle-income countries were receiving antiretroviral therapy by the end of 2009, but that left more than 9 million untreated HIV-positive people in these countries [8].

HIV is an infection that is accompanied by a profound depletion in the number of $CD4^+$ T lymphocytes, and can be transmitted by blood or other body fluids. The number of years it takes HIV to cause a large depletion in T cells and lead to AIDS (Acquired Immunodeficiency Syndrome) varies between individuals, but is approximately 10 to 12 years [12].

The virus is carried in infected $CD4^+$ T cells, dendritic cells and macrophages [12]. It is also a free virus in blood, semen, vaginal fluids and breast milk, meaning the virus can easily travel without integrating into a cell [12]. HIV is most commonly spread by sexual intercourse, contaminated needles used for drug injections and from mother to foetus [12]. Mothers with HIV who breastfeed transmit HIV 40% of the time [12]. In 2009, around 53% of the 1.4 million HIV-positive, pregnant women in low- and middle-income countries received antiretroviral therapy to prevent the transmission of HIV to their babies [8].

Once a person is affected with HIV/AIDS, they are infected for life; there is no cure for this disease. More people than ever are living with HIV, largely due to greater access to treatment [6]. The antiretroviral coverage is increasing in sub-Saharan Africa, raising 20% between 2009 and 2010 [6]. There are a number of antiretroviral drugs that have been created in order to keep the $CD4^+$ T cells at a high enough level in order to combat any other antigen that may be encountered by an HIV-positive patient. Drugs such as reverse transcriptase inhibitors, protease inhibitors, integrase inhibitors and fusion inhibitors will stop the production of new infectious virions [14]. Reverse transcriptase inhibitors (RTIs) aim to stop the viral reverse transcriptase

which is required for synthesis of the provirus. Protease inhibitors (PIs) aim to stop the viral protease, which cleaves polyproteins to produce the virion proteins and viral enzymes. PIs act at a very late maturation stage of the virus, producing non-infectious virions. Integrase inhibitors block the integration of the viral DNA into the host DNA. Fusion inhibitors block the fusion of the virus to the host, which blocks viral entry.

For more information on the immunology and microbiology of the virus, drug therapy, incidence, worldwide issues, and new and ongoing prevention strategies of HIV, see Appendix A.

3.1 Modelling imperfect adherence to HIV induction therapy

Adherence to drug regimens is crucial in order to be certain a virus is being controlled. Studies have shown that patients must have 95% adherence to drug therapy in order to prevent biological resistance [15]. They also show that 40–60% of patients are less than 90% adherent to their drugs, and adherence decreases over time [15]. Smith? [16] developed an impulsive differential system answering an adherence question of how many doses can be missed before drug-resistance emerges. He included susceptible and infected T cells, virus and drug in his model. He was able to calculate the number of doses that can be missed before drug-resistance emerges.

Many different HIV drug cocktails are being prescribed in order to minimize the likelihood of mutant development and minimize the number of drugs a patient must consume. Induction-maintenance therapy is a new form of treatment where patients begin with an intense course of drugs for a short period of time (the induction phase), followed by a long-term course of treatment that is less intense (maintenance). Since patients take a more intense course of treatment during the induction phase, pill

fatigue is more likely, thus causing imperfect adherence.

Previous mathematical work with induction therapy failed due to uncalculated latently infected cells and imperfect adherence [17, 18]. Recently, however, Curlin et al. [19] have shown that a longer induction phase decreases the probability that viruses resistant to maintenance therapy will emerge. Their studies have shown that the probability of success (maintaining a suppressed, circulating, free-virus population for a period of at least 3 years after the end of induction therapy) varies with the length and time of the induction phase [19]. Using a stochastic model, it was shown that induction therapy would have to last at least 180 days for cocktails containing two RTI-like drugs and a PI-like drug [19, 20].

We use impulsive differential equations to investigate the effect of imperfect adherence during the induction phase. We answer not only the question of how many doses can be missed during a drug holiday, but also how many drug holidays can be taken during a finite time. Since previous work showed that induction therapy failed due to latently infected cells, we extended the model presented in Smith? [16] by including latently infected cells. The model is composed of ten ordinary differential equations describing the interaction between T-cells (susceptible, infected and latently infected), virus and drug, coupled with a difference equation describing the drug behaviour.

By solving for the endpoints of the impulsive periodic orbit, we were able to theoretically determine the maximal length of a possible drug holiday and the minimal number of doses that must subsequently be taken while still avoiding drug resistance. We can then determine the number of drug holidays that can be taken during a 180-day induction phase. We have found that a patient can take several drug holidays, but then has to follow each drug holiday with a strict drug-taking regimen. These results differ from that found by Smith? [16]; a much more strict drug-taking regimen is required in order to avoid drug-resistance since the threshold is calculated in a tighter way. We calculated the length and number of drug holidays for all fifteen

protease-sparing triple-drug cocktails that have been approved by the US Food and Drug Administration. Numerical simulations show that if the drug holidays are taken as prescribed, resistant virus will not emerge. Simulation details, errata and extra comments for the manuscript, as well as sensitivity analysis can be found in Appendix B.

The contribution by each author is as follows. The first author developed and analyzed the model, performed numerical simulations and wrote the manuscript. The second author designed the project and edited the manuscript.

This paper is published in the journal Biomed Central Infectious Diseases [3];
Miron, R.E., Smith?, R.J. 2010. Modelling imperfect adherence to HIV induction therapy. *BMC Infectious Diseases* **10**:6.

Modelling imperfect adherence to HIV induction therapy

Rachelle E. Miron[1] and Robert J. Smith?*[2]

[1]Department of Mathematics, The University of Ottawa, 585 King Edward Ave, Ottawa ON K1N 6N5, Canada
[2]Department of Mathematics and Faculty of Medicine, The University of Ottawa, 585 King Edward Ave, Ottawa ON K1N 6N5, Canada

Email: Rachelle E. Miron - rmiro082@uottawa.ca; Robert J. Smith?*- rsmith43@uottawa.ca;

*Corresponding author

Abstract

Background: Induction-maintenance therapy is a treatment regime where patients are prescribed an intense course of treatment for a short period of time (the induction phase), followed by a simplified long-term regimen (maintenance). Since induction therapy has a significantly higher chance of pill fatigue than maintenance therapy, patients might take drug holidays during this period. Without guidance, patients who choose to stop therapy will each be making individual decisions, with no scientific basis.

Methods: We use mathematical modelling to investigate the effect of imperfect adherence during the inductive phase. We address the following research questions: 1. Can we theoretically determine the maximal length of a possible drug holiday and the minimal number of doses that must subsequently be taken while still avoiding resistance? 2. How many drug holidays can be taken during the induction phase?

Results: For a 180 day therapeutic program, a patient can take several drug holidays, but then has to follow each drug holiday with a strict, but fairly straightforward, drug-taking regimen. Since the results are dependent upon the drug regimen, we calculated the length and number of drug holidays for all fifteen protease-sparing triple-drug cocktails that have been approved by the US Food and Drug Administration.

Conclusions: Induction therapy with partial adherence is tolerable, but the outcome depends on the drug cocktail. Our theoretical predictions are in line with recent results from pilot studies of short-cycle treatment interruption strategies and may be useful in guiding the design of future clinical trials.

Background

Currently, 33 million people worldwide are infected with HIV/AIDS, of whom 2.7 million were infected in 2007 [1]. HIV is a disease that is accompanied by a profound depletion in the number of $CD4^+$ T cells and can be transmitted by blood or other body fluids [2]. Most patients with HIV/AIDS are prescribed a triple-drug cocktail with either three nucleoside-analogue reverse transcriptase inhibitors (RTIs), or two RTIs and one protease inhibitor (PI) [3]. However, PI-sparing cocktails have been shown to have equivalent potency to PI-containing cocktails [4] and may reduce the risk of metabolic and potential cardiovascular consequences of PI-containing therapy, while providing similar or improved virologic control and durability of effect [5].

The importance of adherence to HIV drug regimens presents challenges that arise from the biology of HIV, the magnitude of the required therapeutic effort and the changing demography of HIV infection [6]. In order to determine regimens for partial adherence, a number of mathematical models have attempted to quantify how drug concentration levels in the body of an HIV patient affect viral replication [7–13]. Adherence to drug therapy is necessary in order to control HIV, but sometimes-overwhelming side effects, as well as the inconvenience of following a strict regimen, deter patients from taking their drugs [14]. Imperfect or partial adherence can facilitate the emergence of drug-resistant mutations [15].

Induction therapy is a HIV/AIDS treatment regime that hopes to benefit patients by decreasing drug resistance and reducing the overall number of drugs that must be taken. In order to minimise drug resistance, induction-maintenance (IM) therapy strategies begin with a period of intensified antiretroviral therapy (induction phase), followed by a simplified, long-term regimen (maintenance phase) [16–19]. Previous work with induction therapy failed due to uncalculated latently infected cells and imperfect adherence [17, 19]. Recently, however, Curlin *et al.* [20] have shown that a longer induction phase decreases the probability that viruses resistant to maintenance therapy will emerge. Their studies have shown that the probability of success (maintaining a suppressed, circulating, free-virus population for a period of at least 3 years after the end of induction therapy) varies with the length and time of the induction phase [20]. Using a stochastic model, it was shown that induction therapy would have to last at least 180 days for cocktails containing two RTI-like drugs and a PI-like drug [20, 21].

Imperfect adherence has led to failure in suppressing viral replication and often mutations develop before or during induction therapy [6]. Since induction therapy has a significantly higher chance of pill fatigue than maintenance therapy, it is likely the patients will take some holidays during this period. Scientific literature cautions patients against taking any holidays while on therapy [22], but many patients are underadherent or nonadherent [23, 24]. Without guidance, patients who choose to stop therapy will each be making individual decisions, with no scientific basis. Recently, the question of short-term holidays (such as weekends) have been examined. Patients were highly adherent to five days on/ two days off (FOTO) therapy. When asked about their preference for this type of therapy versus continuous HAART (Highly Active Antiretroviral Therapy), on a 10-point scale, the mean response was 9.7 [25].

Here, we examine the effects of imperfect adherence during the induction phase using a mathematical model of impulsive differential equations. We use the model to address the following research questions: 1. Can we determine the maximal length of a drug holiday and the number of subsequent doses that must be taken to avoid resistance? 2. How many drug holidays can be taken during the induction phase?

Methods

Modelling drug therapy

When modelling drug therapy and trying to approximate the number of doses a patient can miss without gaining drug resistance, it is important to have a reliable threshold that will guarantee that viral replication will not exceed a safe limit and so that the mutant strain will not appear. The inhibition of viral replication, s, can be described by

$$s(t) \quad = \quad \frac{R(t)}{R(t) + IC_{50}},$$

where $R(t)$ is the drug and IC_{50} is the concentration of drug which inhibits viral replication by 50% [7]. Thus, when $s \approx 0$, the drug has no effect, while if $s \approx 1$, the drug completely inhibits viral replication. See Figure 1.

Thus, the antiretroviral drug effect can be split into three regions: in Region 1, drug levels are insufficient to control either the wild-type or the mutant strain. In Region 2, drug levels are sufficient to control the wild-type strain but not a 10-fold mutant strain of the virus (ie a mutant strain that requires ten times the amount of drug to be controlled). In Region 3, drug levels are sufficient to control replication of both virus strains. These findings provide a threshold above which resistant viruses will be eradicated. We let R_2 be the threshold between Regions 2 and 3.

The mathematical model

We adapt the mathematical model used from Smith & Wahl [26], to include latently infected cells [27]:

$$\begin{aligned}
\frac{dV_I}{dt} &= n_I\omega T_I - d_V V_I - r_I T_S V_I \\
\frac{dV_Y}{dt} &= n_I\omega T_Y - d_V V_Y - r_Y T_S V_Y - r_Y T_{RI} V_Y \\
\frac{dV_{NI}}{dt} &= n_I(1-\omega)(T_I + T_Y) - d_V V_{NI} \\
\frac{dT_S}{dt} &= \lambda - r_I T_S V_I - r_Y T_S V_Y - d_S T_S - \theta r_P r_R T_S R + m_{RI} T_{RI} \\
\frac{dT_I}{dt} &= (1-\psi) r_I T_S V_I - d_I T_I + p_L T_{LI} \\
\frac{dT_{LI}}{dt} &= \psi r_I T_S V_I - d_S T_{LI} - p_L T_{LI} \\
\frac{dT_Y}{dt} &= (1-\psi) r_Y T_S V_Y - d_I T_Y + (1-\psi) r_Y T_{RI} V_Y + p_L T_{LY} \\
\frac{dT_{LY}}{dt} &= \psi r_Y T_S V_Y - d_S T_{LY} - p_L T_{LY} + \psi r_Y T_{RI} V_Y \\
\frac{dT_{RI}}{dt} &= \theta r_P r_R T_S R - r_Y T_{RI} V_Y - (d_S + m_{RI}) T_{RI} + m_{RY} T_{RY} - \eta r_Q T_{RI} R \\
\frac{dT_{RY}}{dt} &= \eta r_Q T_{RI} R - (d_S + m_{RY}) T_{RY}
\end{aligned}$$

for $t \neq t_k$, where

$$\theta = \begin{cases} 0 & \text{if } R < R_1 \\ 1/r_R & \text{if } R_1 < R < R_2 \\ 1/r_P & \text{if } R > R_2\,, \end{cases}$$

$$\eta = \begin{cases} 0 & \text{if } R < R_2 \\ 1 & \text{if } R > R_2\,. \end{cases}$$

In these equations, V_I and V_Y denote the wild-type and mutant virus respectively, V_{NI} denotes the non-infectious virus, T_S denotes the susceptible CD4$^+$ T cells, T_I denotes CD4$^+$ T cells infected by the wild-type virus, T_{LI} denotes CD4$^+$ T cells latently infected by the wild-type virus, T_Y denotes CD4$^+$ T cells infected by the mutant virus, T_{LY} denotes CD4$^+$ T cells latently infected by the mutant virus, T_{RI} denotes the noninfected CD4$^+$ T cells which have absorbed enough drug so the wild-type strain is inhibited, but not enough to prevent infection from the mutant strain, T_{RY} denotes the noninfected CD4$^+$ T cells which have absorbed enough drug to prevent infection from both virus strains, t is the time in days, n_I is the number of virions produced per infected cell per day, ω is the fraction of virions produced per day by an infected CD4$^+$ T cell, d_V is the clearance rate of free virus, r_I is the rate at which a susceptible cell becomes infected by the wild-type strain, r_Y is the rate at which a susceptible cell becomes infected by the mutant strain, d_S is the death rate of noninfected CD4$^+$ T cells, d_I is the death rate of infected CD4$^+$ T

cells, ψ is the proportion of cells which become latently infected, p_L is the rate at which latently infected cells become productive, r_P is the rate at which the drug inhibits the wild-type T cells when drug concentrations are in Region 2, and r_R and r_Q are the rates at which the drug inhibits the wild- type and drug-resistant T cells, respectively, when drug concentrations are in Region 3. The constant λ is the birth rate of $CD4^+$ T cells, while m_{RI} and m_{RY} are the rates at which the drug is cleared from the intracellular compartment for intermediate and high drug concentrations, respectively. For parameter values and references, see [26].

The dynamics of a drug can be modelled using impulsive differential equations. The exponential decay can be written as a differential equation, where $R(t)$ is the drug concentration during induction therapy. The dynamics of the drug are

$$\frac{dR}{dt} = -d_r R, \qquad t \neq t_k$$

with impulsive conditions, at times $t = t_k$,

$$\triangle R = \begin{cases} R^i, & \text{if a dose is taken,} \\ 0, & \text{if no dose is taken.} \end{cases}$$

The rate at which the drug is cleared is d_r and R^i is the dosage. Assuming a drug is taken at time t_k, by the definition of an impulsive effect, we have

$$R(t_k^+) = R(t_k^-) + R^i \,.$$

Determining the Region 2 threshold

To find R_2, the Region 2 threshold, we determined the time taken for resistance levels to reach a minimum. The drug levels at this time were evaluated from the antiretroviral effect curves and used as the R_2 threshold. This ensures that, when a drug holiday occurs, resistance levels are guaranteed to be low. Missing several doses increases resistance, but, by using the local minimum values, we ensure that resistance cannot emerge when patients are not taking a drug holiday.

To determine the threshold, note that

$$\begin{aligned} V_Y'(0) &= r_I T_Y(0) - d_V V_Y(0) - r_Y V_Y(0) T_S(0) - r_Y V_Y(0) T_{RI}(0) \\ &< 0 \end{aligned}$$

since $T_Y(0) = 0$ at the beginning of infection. It follows that the viral load is initially decreasing.

If the viral load reaches a minimum at time $\bar{t}$, then define $R_2 = R(\bar{t})$. This ensures that $V_Y'(t) < 0$ for $0 < t < \bar{t}$. If the viral load decreases indefinitely, then we could define R_2 to be any value of R less than the trough value of the periodic orbit of the drug dynamics. However, this case is not realistic, since the virus does not clear on its own.

We define R_1 to be the value of R such

$$\frac{R_1}{R_1 + IC_{50}} = \frac{R_2}{R_2 + 10IC_{50}}\,.$$

Thus, $R_1 = 0.1R_2$. See Figure 1.

Impulsive differential equations

The dynamics of both the wild-type and the resistant strains can be modelled using impulsive differential equations. Impulsive differential equations consist of a system of ordinary differential equations (ODEs), together with difference equations. Between "impulses", t_k, the system is continuous, behaving as a system of ODEs. At the impulse points, there is an instantaneous change in state in some or all of the variables. This instantaneous change can occur when certain spatial, temporal or spatio-temporal conditions are met. We refer the interested reader to Bainov & Simeonov [28–30] and Lakshmikantham et al. [31] for more details on the theory of impulsive differential equations.

The change in drug concentration depends on whether a drug is taken or not. There is an instantaneous increase in the drug concentration immediately after a dose is taken and then an exponential decay while the drug is being absorbed in the body. The case of perfect adherence is illustrated in Figure 2A. However, as long as the drug concentration level does not drop below R_2, there is a sufficient amount of drug to control both viral strains. We can thus determine the number of doses that can be missed and the number of doses subsequently taken in order to stay above the R_2 threshold. See Figure 2B.

The differential equations describing the virus and T cells depend on the dynamic behaviour of the drugs. Thus, for example, the rate of change of susceptible T cells decreases in Regions 2 or 3 (at different rates), but not in Region 1. The T cell and virus dynamics are continuous, but their derivatives are not, since those derivatives depend on the drugs, which are discontinuous. Since the drug equations decouple from the remaining equations, we develop theoretical results using the drug equations and apply those results numerically to the entire model.

Results

Theoretical results

We used our model to examine the effects of imperfect adherence on the induction phase of IM therapy. First, it is necessary to model perfect adherence to locate the impulsive periodic orbit in the drug levels. This provides a region where the drug concentration level must reach in order to sustain a low viral load. As can be seen in Figure 2, drug levels start at zero during induction therapy (since induction therapy starts at the beginning of drug therapy). Each time a drug is taken, the dose decays at a rate of $R(t) = R(t_k^+)e^{-d_r(t-t_k)}$, where $R(t_1^+)$ is the value at which the drug starts to decay instantaneously after the drug is ingested. Since we assume perfect adherence, we get

$$\begin{aligned}
R(t_1^-) &= 0 \\
R(t_1^+) &= R(t_1^-) + R^i \\
&= R^i \\
R(t_2^-) &= R(t_1^+)e^{-d_r(t_2-t_1)} \\
&= R^i e^{-d_r(t_2-t_1)} \\
R(t_2^+) &= R(t_2^-) + R^i \\
&= R^i[e^{-d_r(t_2-t_1)} + 1] \\
R(t_3^-) &= R(t_2^+)e^{-d_r(t_3-t_2)} \\
&= R^i[e^{-d_r(t_2-t_1)} + 1]e^{-d_r(t_3-t_2)} \\
&\vdots \\
R(t_n^-) &= R^i e^{-d_r\tau}(1 + e^{-d_r\tau} + e^{-2d_r\tau} + e^{-3d_r\tau} + \cdots + e^{-(n-1)d_r\tau}) \\
&= R^i e^{-d_r\tau}\frac{1 - e^{-nd_r\tau}}{1 - e^{-d_r\tau}}
\end{aligned}$$

where $\tau = t_{k+1} - t_k$ is the (fixed) time between doses for perfect adherence. We thus have

$$\lim_{n\to\infty} R(t_n^-) = \frac{R^i e^{-d_r\tau}}{1 - e^{-d_r\tau}}\,.$$

Furthermore,

$$\begin{aligned}
R(t_n^+) &= R(t_n^-) + R^i \\
&= R^i\frac{1 - e^{-(n+1)d_r\tau}}{1 - e^{-d_r\tau}} \\
&\to \frac{R^i}{1 - e^{-d_r\tau}}
\end{aligned}$$

as $n \to \infty$.

Therefore, assuming perfect adherence, the impulsive orbit has endpoints

$$\frac{R^i}{1-e^{-d_r\tau}} \qquad \text{and} \qquad \frac{R^i e^{-d_r\tau}}{1-e^{-d_r\tau}}\,.$$

Knowing the values of the endpoints for the impulsive orbit after $n = n_1$ doses, we are able to incorporate imperfect adherence and see its effects. In order to avoid Region 2 after missing many doses and to maintain an average drug concentration level within Region 3, we impose conditions to ensure proper therapy. To guarantee successful induction therapy, after the first n_1 doses are taken, we will force the lower endpoint of the drug concentration to be within a tolerance ϵ_1 of the impulsive orbit. Thus, we require

$$\begin{aligned}
R(t_{n_1}^-) &> \frac{R^i e^{-d_r\tau}}{1-e^{-d_r\tau}} - \epsilon_1 \\
R^i e^{-d_r\tau}\frac{1-e^{-n_1 d_r\tau}}{1-e^{-d_r\tau}} &> \frac{R^i e^{-d_r\tau}}{1-e^{-d_r\tau}} - \epsilon_1 \\
-R^i\frac{e^{-(n_1+1)d_r\tau}}{1-e^{-d_r\tau}} &> -\epsilon_1 \\
n_1 &> \frac{1}{d_r\tau}\ln\left[\frac{R^i}{\epsilon_1(1-e^{-d_r\tau})}\right] - 1\,.
\end{aligned}$$

Once the drug concentration level has reached the impulsive orbit, a patient may take a drug holiday. If h_1 doses are subsequently missed (see Figure 2B), then

$$\begin{aligned}
R(t_{n1+h1}^-) &= R(t_{n1}^+)e^{-h_1 d_r\tau} \\
&= R^i e^{-h_1 d_r\tau}\frac{1-e^{-(n_1+1)d_r\tau}}{1-e^{-d_r\tau}}\,.
\end{aligned}$$

In order to avoid Region 2 after h_1 doses are missed, we impose the condition $R(t_{n_1+h_1}^-) > R_2$. This will allow us to find the maximum number of doses a patient can miss after being ϵ_1 away from the impulsive orbit. This results in

$$\begin{aligned}
R^i e^{-h_1 d_r\tau}\frac{1-e^{-(n_1+1)d_r\tau}}{1-e^{-d_r\tau}} &> R_2 \\
e^{-h_1 d_r\tau} &> \frac{R_2}{R^i}\left(\frac{1-e^{-d_r\tau}}{1-e^{-(n_1+1)d_r\tau}}\right) \\
\frac{1}{d_r\tau}\ln\left[\frac{R^i}{R_2}\left(\frac{1-e^{-(n_1+1)d_r\tau}}{1-e^{-d_r\tau}}\right)\right] &> h_1\,. \qquad (1)
\end{aligned}$$

After a patient has missed h_1 doses, in order to keep the viral replication low, they must take enough doses, n_2, to return to the impulsive orbit. In the worst-case scenario, the exponential decay has reached

Region 2; thus, starting at R_2, we get

$$\begin{aligned}
R(t^-_{n1+h1}) &= R_2 \\
R(t^+_{n1+h1}) &= R_2 + R^i \\
R(t^-_{n1+h1+1}) &= (R_2 + R^i)e^{-d_r\tau} \\
R(t^+_{n1+h1+1}) &= R_2 e^{-d_r\tau} + R^i(1 + e^{-d_r\tau}) \\
R(t^-_{n1+h1+2}) &= R_2 e^{-2d_r\tau} + R^i e^{-d_r\tau}(1 + e^{-d_r\tau}) \\
R(t^+_{n1+h1+2}) &= R_2 e^{-2d_r\tau} + R^i(1 + e^{-d_r\tau} + e^{-2d_r\tau}) \\
R(t^-_{n1+h1+3}) &= R_2 e^{-3d_r\tau} + R^i e^{-d_r\tau}(1 + e^{-d_r\tau} + e^{-2d_r\tau}) \\
&\vdots \\
R(t^-_{n1+h1+n2}) &= R_2 e^{-n_2 d_r\tau} + R^i e^{-d_r\tau}(1 + e^{-d_r\tau} + \cdots + e^{-(n_2-1)d_r\tau}) \\
R(t^-_{n1+h1+n2}) &= R_2 e^{-n_2 d_r\tau} + R^i e^{-d_r\tau}\Big(\frac{1 - e^{-n_2 d_r\tau}}{1 - e^{-d_r\tau}}\Big).
\end{aligned}$$

After n_2 doses are taken, we must impose a new condition that forces the drug concentration level to be ϵ_2 away from the impulsive orbit. We need

$$\begin{aligned}
R(t^-_{n_1+h_1+n_2}) &> \frac{R^i e^{-d_r\tau}}{1 - e^{-d_r\tau}} - \epsilon_2 \\
R_2 e^{-n_2 d_r\tau} + R^i e^{-d_r\tau}\frac{1 - e^{-n_2 d_r\tau}}{1 - e^{-d_r\tau}} &> \frac{R^i e^{-d_r\tau}}{1 - e^{-d_r\tau}} - \epsilon_2 \\
R_2 e^{-n_2 d_r\tau} - R^i\frac{e^{-(n_2+1)d_r\tau}}{1 - e^{-d_r\tau}} &> -\epsilon_2 \\
e^{-n_2 d_r\tau} &> -\frac{\epsilon_2(1 - e^{-d_r\tau})}{R_2(1 - e^{-d_r\tau}) - R^i e^{-d_r\tau}} \\
n_2 &> \frac{1}{d_r\tau}\ln\left[\frac{R^i e^{-d_r\tau} - R_2(1 - e^{-d_r\tau})}{\epsilon_2(1 - e^{-d_r\tau})}\right].
\end{aligned} \tag{2}$$

In order to determine the number of times a patient can miss a fixed amount of doses, we must verify if missing h_2 doses is the same as missing h_1 doses. After missing h_2 doses, we have

$$\begin{aligned}
R(t^+_{n1+h1+n2}) &= R(t^-_{n1+h1+n2}) + R^i \\
&= R_2 e^{-n_2 d_r\tau} + R^i\Big(1 + e^{-d_r\tau}\frac{1 - e^{-n_2 d_r\tau}}{1 - e^{-d_r\tau}}\Big) \\
R(t^-_{n1+h1+n2+h2}) &= R_2 e^{-(n_2+h_2)d_r\tau} + R^i e^{-h_2 d_r\tau}\Big(1 + e^{-d_r\tau}\frac{1 - e^{-n_2 d_r\tau}}{1 - e^{-d_r\tau}}\Big).
\end{aligned}$$

Patients are able to miss h_2 doses as long as their drug concentration levels do not drop below Region 2.

Thus we repeat the same condition on h_2:

$$\begin{aligned}
R(t^-_{n_1+h_1+n_2+h_2}) &> R_2 \\
R_2 e^{-(n_2+h_2)d_r\tau} + R^i e^{-h_2 d_r\tau}\Big(1 + e^{-d_r\tau}\frac{1-e^{-n_2 d_r\tau}}{1-e^{-d_r\tau}}\Big) &> R_2 \\
e^{-h_2 d_r\tau}\left(R_2 e^{-n_2 d_r\tau} + R^i\Big(1 + e^{-d_r\tau}\frac{1-e^{-n_2 d_r\tau}}{1-e^{-d_r\tau}}\Big)\right) &> R_2 \\
\frac{1}{d_r\tau}\ln\left[e^{-n_2 d_r\tau} + \frac{R^i}{R_2}\Big(1 + e^{-d_r\tau}\frac{1-e^{-n_2 d_r\tau}}{1-e^{-d_r\tau}}\Big)\right] &> h_2\,.
\end{aligned}$$

At the end of induction therapy, k doses must be taken to ensure that, before the start of maintenance therapy, there is sufficient drug to control viral replication. After missing h_2 doses and assuming we are at Region 2, k subsequent doses are taken and the drug level becomes

$$\begin{aligned}
R(t^-_{n1+h1+n2+h2}) &= R_2 \\
R(t^+_{n1+h1+n2+h2}) &= R_2 + R^i \\
R(t^-_{n1+h1+n2+h2+1}) &= (R_2 + R^i)e^{-d_r\tau} \\
R(t^+_{n1+h1+n2+h2+1}) &= R_2 e^{-d_r\tau} + R^i(1 + e^{-d_r\tau}) \\
R(t^-_{n1+h1+n2+h2+2}) &= R_2 e^{-2d_r\tau} + R^i e^{-d_r\tau}(1 + e^{-d_r\tau}) \\
R(t^+_{n1+h1+n2+h2+2}) &= R_2 e^{-2d_r\tau} + R^i(1 + e^{-d_r\tau} + e^{-2d_r\tau}) \\
R(t^-_{n1+h1+n2+h2+3}) &= R_2 e^{-3d_r\tau} + R^i e^{-d_r\tau}(1 + e^{-d_r\tau} + e^{-2d_r\tau}) \\
&\vdots \\
R(t^-_{n1+h1+n2+h2+k}) &= R_2 e^{-kd_r\tau} + R^i e^{-d_r\tau}(1 + e^{-d_r\tau} + \cdots + e^{-(k-1)d_r\tau}) \\
R(t^-_{n1+h1+n2+h2+k}) &= R_2 e^{-kd_r\tau} + R^i e^{-d_r\tau}\Big(\frac{1-e^{-kd_r\tau}}{1-e^{-d_r\tau}}\Big)\,.
\end{aligned}$$

As can be seen, because we started at the threshold after missing h_2 doses, $R(t^-_{n1+h1+n2}) = R(t^-_{n1+h1+n2+h2+k})$ as long as $n_2 = k$. Finally, after k doses, a patient needs to return to the periodic orbit. Thus, we impose

$$\begin{aligned}
R(^-_{n_1+h_1+n_2+h_2+k}) &> \frac{R^i e^{-d_r\tau}}{1-e^{-d_r\tau}} - \epsilon_3 \\
k &> \frac{1}{d_r\tau}\ln\left[\frac{R^i e^{-d_r\tau} - R_2(1-e^{-d_r\tau})}{\epsilon_3(1-e^{-d_r\tau})}\right],
\end{aligned}$$

which is the same as the constraint for n_2 as long as $\epsilon_2 = \epsilon_3$. If these conditions are satisfied, we are able to guarantee that the drug concentration levels do not enter Region 2 and significant drug resistance will not emerge.

Imperfect adherence

The number of missable and subsequent doses that must be taken to avoid significant drug resistance for all FDA-approved drugs that are part of a PI-sparing cocktail is shown in Table 1. These are defined by (1) and (2), respectively. However, we stress that these results are theoretical and have not been tested clinically. In particular, it should be noted that pharmacokinetic parameters can vary from patient to patient.

There are fifteen FDA-approved PI-sparing triple-drug cocktails, for which we calculated (a) the initial number of doses that must be taken to be within a prescribed tolerance of perfect adherence, (b) the number of doses that could be missed without significant drug resistance emerging and (c) the number of doses that must be taken subsequently.

To determine the value of the prescribed tolerance, we examined two possibilities: a tolerance of $0.1\mu M$ and a tolerance of $0.01\mu M$. That is, the number of doses is considered sufficient if the trough value of the periodic orbit of the drug dynamics is within $0.01\mu M$ of the trough value of therapy without drug holidays. We imposed a further condition: that the mean drug concentration be larger than the trough value of drugs when no drug holidays are taken. This is illustrated in Figure 3. This ensures that, over the length of the entire induction phase, drugs are maintained at sufficiently high levels (see [26] for more discussion). In Figure 3A, using a tolerance of $0.1\mu M$, the overall mean drug concentration is below the trough value during therapy. Using a tolerance of $0.01\mu M$, as shown in Figure 3B, shows that the overall mean drug concentration is above the trough value during therapy.

For the fifteen FDA-approved PI-sparing triple-drug cocktails, we identified the "weakest" drugs in each cocktail; ie, those for which the least number of doses can be missed. These drugs are Abacavir (ABC), Lamivudine (3TC), Stavudine (d4T), Emtricitabine (FTC), Zidovudine (ZDF), Didanosine (ddI) and Nevirapine (NVP). Thus, for each cocktail, the maximal number of missable doses is the same as that of its "weakest" drug. By combining the steps in (b) and (c) above, it was possible to theoretically calculate the number of drug holidays that could be taken during the inductive phase, based on the regimen for the "weakest" drug. See Table 2.

Since the minimum number of doses required to be taken and the maximum number of doses allowed to be missed follow a reliable pattern, we can extend this to fit into a baseline induction phase of 180 days [20]. This means, for example, that a patient taking the triple-drug cocktail FTC/TDF/EFV can theoretically have a 6 day holiday, as long as each holiday is followed by 17 days of perfect adherence; patients can take seven such holidays during the induction phase, and are thus able to miss a total of 42 days out of 180. A

patient taking ABC/3TC/NVP can theoretically have sixteen drug holidays of 3 days each in a 180 day period, as long as each holiday is immediately followed by a 7 day period of strict adherence.

Numerical simulations

In order to determine the long-term effects of taking the prescribed drug holidays, we simulated the worst-case scenario: monotherapy to the "weakest" drug in each combination from Table 2. This has the effect of overestimating the development of resistance: if no resistance is predicted to emerge during monotherapy, then it is unlikely to emerge during combination therapy. Conversely, if resistance does emerge during monotherapy, then there is no guarantee that it would emerge during combination therapy, due to the presence of the other two drugs.

We considered an extinction threshold of 2×10^{-4} virions/mL. This corresponds to the concentration at which the virus falls below 1 per body. Thus, missing the maximum number of doses would theoretically lead to extinction of both strains (at least up to the level of detection), whereas missing more doses does not. However, it should be noted that we did not curtail the viral dynamics at this threshold.

We used the model in Section (describing the dynamic interaction between virus, T cells and drugs) and the calculations in Section (summarised in Tables 1 and 2) to illustrate our theoretical results. In order to demonstrate the effects of taking the prescribed drug holidays, we first ran simulations where patients missed the maximum number of doses and then took the required number of subsequent doses; this cycle was repeated for 180 days. Next, we ran the same simulations, with the same parameters, except that one additional dose of the drug was skipped during each drug holiday.

We performed these simulations for each of the "weakest" drugs identified in Table 2: ABC (Figure 4), 3TC (Figure 5), d4T (Figure 6), FTC (Figure 7), ZDV (Figure 8), ddI (Figure 9) and NVP (Figure 10). The first figure in each case illustrates the case of missing the maximal drug holiday and taking the minimum number of subsequent doses. The second figure in each case illustrates the same case, except that one additional dose was missed during each drug holiday. The exception is NVP, in which resistance did not emerge until three extra doses were missed (Figure 10B, inset).

For the first case, the wild-type virus oscillated at low levels during each drug holiday, but significant levels of resistance did not appear. Thus, taking the required number of doses successfully keeps the mutant strain at low levels. Conversely, missing one extra dose per holiday (three in the case of NVP) resulted in a significant buildup of resistance by the end of the induction phase.

In this case, there is a tremendous increase in the mutant strain by the end of the inductive phase,

indicating that therapy has failed. Resistance to Abacavir increases from 10^{-3} to 10^{4}; resistance to Lamivudine increased from less than 10^{-3} to 10^{4}; resistance to Stavudine increased from 10^{-3} to 10^{3}; resistance to Emtricitabine increased from 10^{-3} to 10^{4}; resistance to Zidovudine increased from 10^{-3} to 10^{3}; resistance to Didanosine increased from 10^{-3} to 10^{2}; and resistance to Nevirapine increased from 10^{-3} to 10^{4}.

Comparison with clinical results

A number of studies have attempted to characterise the safety of regular (and irregular) treatment interruptions, generally referred to as structured treatment interruptions (STIs). Pai *et al.* [22] summarised the to-date evidence of STIs in patients with chronic unsuppressed HIV infection due to drug-resistant HIV. They concluded that there were no significant virologic or immunologic benefit to STIs and that there is evidence that STIs have a prolonged negative impact on CD4 response and other disease events. Subsequently, the SMART trial [32] examined $CD4^{+}$ guided interruptions, of an average duration of 16 months. The DART trial [33] examined fixed 12 week interruptions. Both trials showed no benefit to these treatment interruptions. Indeed, the SMART trial was halted prematurely, due to significant morbidity and mortality among participants. Holkmann *et al.* [34] reported a two-fold risk of AIDS or death for patients who underwent treatment interruptions that lasted three months or longer.

It should be noted that all these trials involved lengthy periods of treatment interruption, of the order of weeks. Our results here recommend signficantly shorter periods of treatment interruption, of the order of days. Furthermore, our results predict significant increase in resistance if these periods are exceeded, consistent with the results from the majority of trials.

Shorter treatment interruptions have also been investigated. A study comparing interruptions of less than 7 days compared to longer interruptions showed that only 5% of men who discontinued HAART for short periods increased their HIV RNA. Conversely, men with longer interruptions had significantly higher rates (35.7 of HIV RNA increase [35]. Another study investigating cycles of 2-6 week fixed interruptions observed no clinically significant benefit with regard to viral suppression when off HAART, but also observed no evidence for an increase of viral resistance among patients undergoing repeated interruptions [36]. Recently, a pilot study examining five days on, two days off (FOTO) followed patients for 48 weeks [25]. Virologic suppression was maintained in 89.6% of patients. Combinations included 3TC/TDF/EFV, ABC/TDF/EFV, ddI/3TC/EFV and ABC/ddI/TDF/EFV; 100% of subjects on EFV- based regimens on the FOTO treatment schedule maintained virologic suppression at weeks 24 and 48. Combinations also

included nevirapine- based regimens where one subject, on NVP/ABC/3TC/ZDV, had viral rebound at week 12 that was confirmed at week 16 on the FOTO schedule. It was also noted that 30% of the subjects on nevirapine-based regimens had blips of viral increase during therapy. Other combinations included TDF/3TC/NVP, ZDV/ 3TC/NVP, d4T/3TC/TDF/NVP. They also observed excellent adherence to the FOTO treatment schedule and a strong preference for this schedule compared to HAART. None of the observed rebounds in viral load were associated with the reported adherence of more than 2 days off therapy.

These preliminary results are in line with our theoretical recommendations. For regimens that include EFV-based regimens, all therapies included NRTIs and NNRTIs that we recommend a maximum of more than 2 days per drug holiday, followed by at least 5 days of subsequent therapy (Table 2). The NVP-based regimen with viral rebound included ZDV; our results predict that drug holidays on such a regimen should be no longer than 1.33 days (Figure 8). The three other NVP-based regimens with viral blips included ZDV and d4T; our results predict that neither would allow drug holidays as long as two days (Table 1).

Sensitivity to variations

Since individual patients may respond differently to drugs, we explore the sensitivity of the number of missable doses to variations in parameters. The number of missable doses depends on the dosing interval, the drug decay rate, the drug concentration, the Region 2 threshold and the number of initial doses, which itself depends on the prescribed tolerance. Since we have already explored variations in the dosing interval and the prescribed decay rate, we now examine the variation with respect to the other parameters.

Figure 11 demonstrates the effect of variations in the drug decay rate, the Region 2 threshold and the drug concentration. Since the slope of the curves is low for the second and third figures, we conclude that the results are not highly sensitive to variations in the Region 2 threshold or the drug concentration, although small fluctuations may decrease the number of missable days (Figure 11B and Figure 11C). The outcome is more sensitive to variations in the drug decay rates, but is still not highly sensitive (Figure 11A).

Discussion

It is vital to provide HIV patients with an effective drug regimen. Not only is it important that the drugs have a high efficacy, but it is also important that patients follow a regimen that will benefit both their mental and physical states. Since there are such a large number of patients who are unable to take their drugs regularly, it is important to understand the impact of drug holidays upon a patient's ability to

control the virus. Induction therapy provides patients with the chance to submit to a very strict, but short, period of intense drug taking, followed by a long period of less-restrictive and more-relaxed therapy (maintenance therapy). We have demonstrated the effects of taking drug holidays during induction therapy. Instead of taking drugs two to three times a day for the entire length of the induction period, we were able to show that a patient can have drug holidays with sometimes as much as six days off each time. This form of treatment allows patients to take drug holidays with very little negative effect.

However, missing more doses than stated can highly affect the amount of resistant virus created. We have demonstrated that there is a large increase of mutant virus by simply missing one extra dose during each drug holiday (three for the TDF- FTC-NVP combination). Induction therapy with partial adherence works as long as a patient does not exceed the maximum length of the drug holiday; if they follow the prescribed regime, they can control the effects of drug resistance. It should be noted that Curlin *et al.* [20] showed that an induction phase on the order of 180-days was ideal for a triple-drug therapy including two RTI-like drugs and one PI-like drug. Since the results for a triple-drug therapy including three RTIs do not show a dramatic increase in resistant virus while taking the patterns suggested, we used an 180 day induction phase as a baseline.

These results apply to the fifteen FDA-approved, PI-sparing triple-drug cocktails, but simulations were only performed for the drugs with the least number of missable doses: Abacavir, Lamivudine, Stavudine, Emtricitabine, Zidovudine, Didanosine and Nevirapine. Missing one extra doses at the end of each drug holiday (three for Nevirapine) drastically increases the amount of resistant virus. However, it should be noted that the simulations were for monotherapy only and thus, in a triple-drug cocktail, the remaining two drugs inure against resistance.

Efavirenz and nevirapine only require a single mutation to confer resistance, and cross resistance affecting these three NNRTIs is common [37]. Both Lamivudine and Emtricitabine select for the M184V resistance mutation, which confers high-level resistance to both drugs, a modest decrease in susceptibility to Didanosine and Abacavir, and improved susceptibility to Zidovudine, Stavudine and Tenofovir [38]. It should be noted that our model assumes that the mutant is always present. By simulating the results for monotherapy, we illustrated the worst-case scenario; this is illustrated by Figure 10B, which shows that missing one extra dose per holiday is not disastrous; in this example, the mutant only takes hold when three extra doses are missed. Thus, our results are more conservative than is strictly necessary.

Double mutation happens less frequently; emergence of the M184V mutation is less frequent with Tenofovir/Emtricitabine than with Zidovudine/Lamivudine, while selection of the Lamivudine-associated

M184V mutation to the Zidovudine/Lamivudine combination has been associated with increased susceptibility to Zidovudine [37]. It follows that, when the combinations are taken synchronously, the selection of mutants will be signficantly less likely than under monotherapy.

Discontinuous dosing is, of course, not realistic. There is a delay, the time-to- peak, between taking a drug and it reaching peak values in cells. Consequently, estimates based on maximal concentrations and terminal plasma half-lives could overestimate drug exposure. However, such delays can be approximated by an instantaneous change if the time-to-peak is sufficiently short, compared to the time between doses. This approximation has been shown to be robust, even for quite large delays [39].

Other limitations to our model are the assumption that the $CD4^+$ pool of lymphocytes is the most significant source of HIV infection and that maintaining drug concentrations at clinical levels results in maximal control of virus replication. However, not all HIV-susceptible tissues are equally susceptible to antiretroviral drugs. For example, lymphoid cells in the gut are not completely suppressed [40]. These and other reservoirs will contribute to the long-term generation of virus particles, both during therapy and while undergoing a drug holiday. The relative rates of mutation or selection of resistant viruses for the various drugs are modelled via the choice of infection rate, r_Y, compared to the infection rate, r_I, for the wild-type strain. For numerical simulations, we used the intracellular half-life of each drug, if known; in the case of nucleosides, it is the cellular concentration of active nucleotide that is responsible for inhibition of viral reverse transcription. Furthermore, we assume that all tissues harbouring HIV are exposed to the same concentration of drug.

Previously [13], we showed how many doses can be missed for each PI- sparing drug, for only a single drug holiday during any given therapy. Here, we extend this to the case of more than one drug holiday. Furthermore, all previous mathematical models of adherence considered therapy without an endpoint. Since induction therapy only occurs for a finite time, we have to consider the viral load when induction therapy ends. In particular, if a drug holiday coincided with the end of induction therapy, then the induction phase would functionally have ended at an earlier time and may thus be significantly less effective. Some of the key differences between our earlier work and the results provided here occur due to the fact that here we use 10-fold resistance, rather than 50- fold resistance; multiple holidays occur during a finite time interval; and the tolerance used was $0.01\mu M$ instead of 1% of the minimum value of periodic orbit; the tolerance we used here is more conservative.

Future work will investigate the effects of imperfect adherence to triple-drug cocktails involving protease inhibitors. We will also investigate the compounding effects of combination therapy in slowing the

emergence of resistance and the effect of inter-individual variances in pharmacokinetics. Our modelling process could also be extended to additional treatment scenarios in which patients might be tempted to take drug holidays due to a high pill burden, such as booster therapies or the initial year of HAART.

Conclusions

Using readily available pharmacokinetic data, we can theoretically determine the maximal length of drug holidays and the number of subsequent doses that must be taken. Since the induction phase lasts for a finite time, we can thus determine how many drug holidays can be taken within a 180-day induction period. Our theoretical results are in line with recent results concerning five-days-on/two-days-off (FOTO) for most cocktails, suggesting that drug holidays may be limited to very short breaks, rather than the longer holidays previously examined.

We thus conclude that induction therapy with partial adherence is tolerable, but the outcome depends on the drug cocktail. We have also demonstrated a robust method by which to determine therapy guidelines for patients who are unable or unwilling to adhere completely. Treatment interruptions, if they occur, must be short and followed by a strict period of dose taking. Thus, while continuous therapy is preferable, FOTO therapy is acceptable for all RTI cocktails except those containing ZDV, d4T or DLV, which can only tolerate extremely short drug holidays.

Competing Interests

The authors declare that they have no competing interests.

Authors contributions

Both authors wrote the manuscript and performed numerical simulations. RJS designed the study, while REM performed the mathematical analysis. Both authors read and approved the final manuscript.

Acknowledgements

The authors are grateful to Frithjof Lutscher, Lindi Wahl and Jing Li for technical discussions, and to Robert Stengel, Selwyn Hurwitz and John Mittler for their careful reading of the manuscript and constructive comments that greatly improved the final version. RJS is supported by an NSERC Discovery grant, an Early Researcher Award and funding from MITACS.

References

1. Steinbrook R: **The AIDS Epidemic - A Progress Report from Mexico City**. *N Engl J Med* 2008, **359**:885–887.
2. McCune J: **The dynamics of CD4$^+$ T-cell depletion in HIV disease**. *Nature* 2001, **410**:974–979.
3. Yeni PG, Hammer SM, Hirsch M, Saag M, Schechter M, Carpenter CCJ, Fischi MA, Gatell JM, Gazzard BG, Jacobsen D, Katzenstein DA, Montaner JSG, Richman DD, Schooley RT, Thompson MA, Vella S, Volberding PA: **Treatment for adult HIV infection: 2004 recommendations of the International AIDS Society - USA Panel**. *JAMA* 2004, **292**:251–265.
4. Staszewski S, Morales-Ramirez J, Tashima KT, Rachlis A, Skiest D, Stanford J, Stryker R, Johnson P, Labriola DF, Farina D, Manion DJ, Ruiz NM: **Efavirenz plus zidovudine and lamivudine, efavirenz plus indinavir and indinavir plus zidovudine and lamivudine in the treatment of HIV-1 infection in adults**. *N Engl J Med* 1999, **341**:1865–1873.
5. Moyle G: **Protease inhibitor-sparing regimens: new evidence strengthens position**. *J Acq Immun Def Synd* 2003, **33**(Suppl 1):17–25.
6. Atlice FL, Friedland GH: **The era of adherence to HIV therapy**. *Ann Intern Med* 1998, **129**:503–505.
7. Wahl LM, Nowak MA: **Adherence and drug resistance: predictions for therapy outcome**. *Proc R Soc B* 2000, **267**:835–843.
8. Philips AN, Youle M, Johnson M, Loveday C: **Use of stochastic model to develop understanding of the impact of different patterns of antiretroviral drug use on resistance development**. *AIDS* 2001, **15**:2211–2220.
9. Tchetgen E, Kaplan EH, Friedland GH: **Public health consequences of screening patients for adherence to highly active antiretroviral therapy**. *J AIDS* 2001, **26**:118–129.
10. Huang Y, Rosenkranz S, Wu H: **Modeling HIV dynamics and antiviral response with consideration of time-varying drug exposures, adherence and phenotypic sensitivity**. *Math Biosci* 2003, **184**:165–186.
11. Huang Y, Liu D, H W: **Hierarchical Bayesian methods for estimation of parameters in longitudinal HIV dynamic system**. *Biometrics* 2004, **62**:413–423.
12. Ferguson NM, Donnelly CA, Hooper J, Ghani AC, Fraser C, Bartley L: **Adherence to antiretroviral therapy and its impact on clinical outcome in HIV-infected patients**. *J R Soc Interface* 2005, **2**:349–363.
13. Smith RJ: **Adherence to antiretroviral HIV drugs: how many doses can you miss before resistance emerges?** *Proc R Soc B* 2006, **273**:617–624.
14. Krakovska O, Wahl LM: **Optimal drug treatment regimens for HIV depend on adherence**. *J Theor Biol* 2007, **246**:499–509.
15. Friedland GH, Williams A: **Attaining higher goals in HIV treatment: the central importance of adherence**. *AIDS* 1999, **13**(Suppl 1):61–72.
16. Reijers MH, Weverling GJ, Jurriaans S, Wit FW, Weigel HM, Ten Kate RW, Mulder JW, Frissen PH, van Leeuwen R, Reiss P, Schuitemaker H, de Wolf F, Lange JM: **Maintenance therapy after quadruple induction therapy in HIV-1 infected individuals: Amsterdam Duration of Antiretroviral Medication study**. *Lancet* 1998, **352**:185–190.
17. Havlir DV, Marschner IC, Hirsch MS, Collier AC, Tebas P, Bassett RL, Ioannidis JP, Holohan MK, Leavitt R, Coone G, Richman DD: **Maintenance antiretroviral therapies in HIV infected patients with undetectable plasma HIV RNA after triple-drug therapy. AIDS Clinical Trials Group Study 343 Team**. *N Engl J Med* 1998, **339**:1261–1268.
18. Pialoux G, Raffi F, Brun-Vezinet F, Meiffrédy V, Flandre P, Gastaut J, Dellamonica P, Yeni P, Delfraissy J, Aboulker J: **A randomized trial of three maintenance regimens given after three months of induction therapy with zidovudine, lamivudine, and indinavir in previously untreated HIV-1-infected patients. Trilege (Agence Nationale de Recherches sur le SIDA 072) Study Team**. *N Engl J Med* 1998, **339**:1269–1276.

19. Descamps D, Flandre P, Calvez V, Peytavin G, Meiffrédy V, Collin G, Delaugerre C, Robert-Delmas S, Bazin B, Aboulker JP, Pialoux G, Raffi F, Brun-Vézinet F: **Mechanisms of virologic failure in previously untreated HIV-infected patients from a trial of induction-maintenance therapy**. *JAMA* 2000, **283**:205–211.

20. Curlin M, Iyer S, Mittler J: **Optimal timing and duration of induction therapy for HIV-1 infection**. *PLoS Comput Biol* 2007, **3**(7):e133.

21. Havlir D, Hellmann NS, Petropoulos CJ, Whitcomb JM, Collier AC, Hirsch MS, Tebas P, Sommadossi JP, Richman DD: **Drug Susceptibility in HIV infection after Viral Rebound in Patients Recieving Indinavir-Containing Regimens**. *JAMA* 2000, **283**:299–234.

22. Pai N, Lawrence J, Reingold AL, Tulsky J: **Structured treatment interruptions (STI) in chronic unsuppressed HIV infection in adults**. *Cochrane Database of Systematic Reviews* 2006, **3**:Art. No.: CD006148.

23. Chesney MA, Morin M, Sherr L: **Adherence to HIV combination therapy**. *Social Science & Medicine* 2000, **50**:1599–1605.

24. Curlin ME, Wilkin T, Mittler J: **Induction-maintenance therapy for HIV-1 infection**. *Future HIV Therapy* 2008, **2**:175–185.

25. Cohen CJ, Colson AE, Sheble-Hall AG, McLaughlin KA, Morse GD: **Pilot Study of a Novel Short-Cycle Antiretroviral Treatment Interruption Strategy: 48-Week Results of the Five-Days-On, Two-Days-Off (FOTO) Study**. *HIV Clin Trials* 2007, **8**:19–23.

26. Smith RJ, Wahl LM: **Drug resistance in an immunological model of HIV-1 infection with impulsive drug effects**. *Bull Math Biol* 2005, **67**:783–813.

27. Smith? RJ, Aggarwala BD: **Can the viral reservoir of latently infected CD4+ T cells be eradicated with antiretroviral drugs?** *J Math Biol* 2009, **59**:697–715.

28. Bainov DD, Simeonov PS: *Systems with Impulsive Effect*. Chichester: Ellis Horwood Ltd 1989.

29. Bainov DD, Simeonov PS: *Impulsive differential equations: periodic solutions and applications*. Burnt Mill: Longman Scientific and Technical 1993.

30. Bainov DD, Simeonov PS: *Impulsive Differential Equations: Asymptotic Properties of the Solutions*. Singapore: World Scientific 1995.

31. Lakshmikantham V, Bainov DD, Simeonov PS: *Systems with Impulsive Effect*. Singapore: World Scientific 1989.

32. Strategies for Management of Antiretroviral Therapy (SMART) Study Group, El-Sadr WM, Lundgren JD: **CD4+ count-guided interruption of antiretroviral treatment**. *N Engl J Med* 2006, **355**(22):2283–2296.

33. DART Trial Team: **Fixed duration interruptions are inferior to continuous treatment in African adults starting therapy with CD4 cell counts $<$ 200 cells/microl**. *AIDS* 2008, **22**(2):237–247.

34. Holkmann Olsen C, Mocroft A, Kirk O, Vella S, Blaxhult A, Clumeck N, Fisher M, Katlama C, Phillips A, Lundgren J: **Interruption of combination antiretroviral therapy and risk of clinical disease progression to AIDS or death**. *HIV Med* 2007, **8**:96–104.

35. Li X, Margolick J, Conover C, Badri S, Riddler SA, Witt MD, Jacobson LP: **Interruption and Discontinuation of Highly Active Antiretroviral Therapy in the Multicenter AIDS Cohort Study**. *JAIDS* 2005, **38**:320–328.

36. Papasavvas E, Kostman JR, Mounzer K, Grant RM, Gross R, Gallo C, Azzoni L, Foulkes A, Thiel B, Pistilli M, Mackiewicz A, Shull J, Montaner LJ: **Randomized, Controlled Trial of Therapy Interruption in Chronic HIV-1 Infection**. *PLoS Medicine* 2004, **1**(3):e64.

37. **Panel on Antiretroviral Guidelines for Adults and Adolescents. Guidelines for the use of antiretroviral agents in HIV-1-infected adults and adolescents. Department of Health and Human Services. November 3, 2008; 1-139**
[http://www.aidsinfo.nih.gov/ContentFiles/AdultandAdolescentGL.pdf].

38. Ait-Khaled M, Stone C, Amphlett G, Clotet B, Staszewski S, Katlama C, Tisdale M, CNA3002 International Study Team: **M184V is associated with a low incidence of thymidine analogue mutations and low phenotypic resistance to zidovudine and stavudine**. *AIDS* 2002, **16**:1686–1689.

39. Smith? RJ, Schwartz EJ: **Predicting the potential impact of a cytotoxic T-lymphocyte HIV vaccine: how often should you vaccinate and how strong should the vaccine be?** *Math Biosci* 2008, **212**:180–187.

40. Chun TW, Nickle DC, Justement JS, Meyers JH, Roby G, Hallahan CW, Kottilil S, Moir S, Mican JM, Mullins JI, Ward DJ, Kovacs JA, Mannon PJ, Fauci AS: **Persistence of HIV in gut-associated lymphoid tissue despite long-term antiretroviral therapy**. *J Infect Dis* 2008, **197**:714–720.

41. Scott L, Perry C: **Delavirdine - A review of its use in HIV infection**. *Drugs* 2000, **60**:1411–1444.

42. Perry C, Noble S: **Didanosine - An update review of its use in HIV infection**. *Drugs* 1999, **58**:1099–1135.

43. Bhana N, Ormrod D, Perry C, Figgitt D: **Zidovudine - A review of its use in management of vertically-aquired pediatric HIV infection**. *Drugs* 2002, **4**:515–553.

44. Hervey P, Perry C: **Abacavir - A review of its clinical potential in patients with HIV infection**. *Drugs* 2000, **60**:447–479.

45. Frampton J, Perry C: **Emtricitabine - A review of its use in management of HIV infection**. *Drugs* 2006, **65**:1427–1448.

46. Moore KHP, Barrett JE, Shaw S, Pakes GE, Churchus R, Kapoor A, Barry MG, D B: **The pharmacokinetics of lamivudine phosphorylation in peripheral blood mononuclear cells from patients infected with HIV-1**. *AIDS* 1999, **13**:2239–2250.

47. Fletcher C, Brundage R, Remmel R, Page L, Weller D, Calles N, Simon C, Kline M: **Pharmacologic characteristics of indinivir, didanosine, stavudine, in human immunodeficiency virus-infected children receiving combination therapy**. *Antimicrobial Agents and Chemotherapy* 2000, **44**:1029–1034.

48. Hawkins T, Veikley W, St Claire R, Guyer B, Clark N, Kearney B: **Intracellular pharmacokinetics of tenofovir diphosphate, carbovir triphosphate, and lamivudine triphosphate in patients receiving triple-nucleoside regimens**. *J Acquir Defic Syndr* 2001, **39**:406–411.

Figures

Figure 1 - Dose-effect curves

Example of dose-effect curves for the wild-type (solid blue curve) and 10-fold resistance (dashed green curve) virus strains. When drug concentration levels are in Region 1, the amount of drug is insufficient to either control wild-type or mutant strains. When drug concentration levels are in Region 2, the amount of drug is sufficient to block the wild-type virus but resistant virus may emerge. When drug concentration levels are in Region 3, both virus strains are controlled. This example is for the reverse transcriptase inhibitor Stavudine (d4T).

Figure 2 - Drug concentrations

Drug concentrations using impulsive differential equations. A. Example of drug concentration levels with perfect adherence to therapy. Drug concentration levels fluctuate from lower endpoints (t_1^-, t_2^-, $t_3^-\ldots$) to upper endpoints (t_1^+, t_2^+, $t_3^+\ldots$). Drug concentration levels increase instantaneously after a dose is taken and decrease exponentially between doses. If all doses are taken, drug concentration levels monotonically approach an impulsive orbit. B. Example of fluctuating drug concentration levels when missing drug doses.

Once drug concentration levels have reached the impulsive orbit ($t^+_{n_1}$), missing h doses results in a long exponential decay. Subsequent adherence returns drug concentration levels to the impulsive periodic orbit before the next drug holiday occurs ($t^+_{n1+h1+n2}$). In this example, a patient has two drug holidays within a 30 day period.

Figure 3 - Determining the prescribed tolerance

Difference between a prescribed tolerance of (A) $0.1\mu M$ and (B) $0.01\mu M$ for the reverse transcriptase inhibitor Didanosine (ddI). The red line plotted on both graphs is the average drug concentration while taking drug holidays. This was calculated using the data from Table 2. The average drug concentration in (A) is around 11μM and has not reached the trough values when drug holidays are excluded, whereas the average drug concentration in (B) is around 12μM and thus exceeds the trough values during therapy.

Figure 4 - Adherence to ABC monotherapy

A. Long-term effects of adherence to ABC monotherapy, using the prescribed adherence breaks. The wild type (solid blue curve, left axes) and mutant (dashed green curve, right axes) populations are shown. The overall effect of the mutant remains low. Parameters used, in addition to those in Table 1, were $n_I = 262.5$ day^{-1}, $\omega = 0.7$, $r_I = 0.01$ day^{-1}, $r_Y = 0.001$ day^{-1}, $d_V = 3$ day^{-1}, $d_S = 0.1$ day^{-1}, $d_I = 0.5$ day^{-1}, $\psi = 0.2$, $p_L = 0.05$, $r_R = r_Q = 80\ \mu M^{-1}$day^{-1}, $\lambda = 180$ cells μL^{-1} and $m_{RI} = m_{RY} = \log(2)$ day^{-1}. Initial conditions were $V_I(0) = 22000$ virions mL^{-1}, $V_Y(0) = 5 \times 10^{-3}$ virions mL^{-1}, $T_S(0) = 1000$ cells day^{-1} and all other initial conditions were zero. B. The effects of missing one extra dose per drug holiday. The proportions of each type of uninfected T cell at the end of the simulation are shown in the insets.

Figure 5 - Adherence to 3TC monotherapy

A. Long-term effects of effects of adherence to 3TC monotherapy, using prescribed adherence breaks. B. The effects of missing one extra dose. Drug parameters are as in Table 1, while all other parameters are as in Figure 4. The proportions of each type of uninfected T cell at the end of the simulation are shown in the insets.

Figure 6 - Adherence to d4T monotherapy

A. Long-term effects of effects of adherence to d4T monotherapy, using prescribed adherence breaks. B. The effects of missing one extra dose. Drug parameters are as in Table 1, while all other parameters are as

in Figure 4. The proportions of each type of uninfected T cell at the end of the simulation are shown in the insets.

Figure 7 - Adherence to FTC monotherapy

A. Long-term effects of effects of adherence to FTC monotherapy, using prescribed adherence breaks. B. The effects of missing one extra dose. Drug parameters are as in Table 1, while all other parameters are as in Figure 4. The proportions of each type of uninfected T cell at the end of the simulation are shown in the insets.

Figure 8 - Adherence to ZDV monotherapy

A. Long-term effects of effects of adherence to ZDV monotherapy, using prescribed adherence breaks. B. The effects of missing one extra dose. Drug parameters are as in Table 1, while all other parameters are as in Figure 4. The proportions of each type of uninfected T cell at the end of the simulation are shown in the insets.

Figure 9 - Adherence to ddI monotherapy

A. Long-term effects of effects of adherence to ddI monotherapy, using prescribed adherence breaks. B. The effects of missing one extra dose. Drug parameters are as in Table 1, while all other parameters are as in Figure 4. The proportions of each type of uninfected T cell at the end of the simulation are shown in the insets.

Figure 10 - Adherence to NVP monotherapy

A. Long-term effects of effects of adherence to NVP monotherapy, using prescribed adherence breaks. B. The effects of missing one extra dose. Drug parameters as as in Table 1, while all other parameters are as in Figure 4. In this case, both strains are controlled. Inset: The effects of missing three extra doses. In this case, the wild-type strain is controlled, but the resistant strain emerges. The proportions of each type of uninfected T cell at the end of the simulation are shown in the insets.

Figure 11 - Sensitivity to other parameters

Sensitivity of length of drug holiday to (A) the drug decay rate, d_r, (B) the Region 2 threshold, R_2, and (C) the drug concentration, R^i. Dashed lines indicate values used in our calculations. This example is for ABC.

Tables

Table 1 - Missable doses and subsequent adherence

Summary of data and theoretical results for reverse transcriptase inhibitors used for FDA-approved triple-drug therapy. All results are calculated with a mutant that exhibits 10-fold resistance to the drug. The decay rate d_r was calculated using the formula $d_r = 24\log(2)/T_{1/2}$, where $T_{1/2}$ is the half-life. The last two columns are the number of doses that may be missed before significant drug resistance emerges and the number that must subsequently be taken to return to within $0.01\mu M$ of perfect adherence. We used the intracellular half-life for each drug, if known. Data for Column 1 was taken from [41–48], and data from Columns 2 and 3 were taken from the Department of Health and Human Services 2008 Guidelines for the Use of Antiretroviral Agents in HIV-1-Infected Adults and Adolescents [37].

Drug (units)	R^i (μM)	τ (days)	$T_{1/2}$ (hours)	R_1 (μM)	R_2 (μM)	maximum missable days (theoretical)	minimum subsequent days (theoretical)
Abacavir (ABC)	12	1/2	15	$10^{-1.0269}$	$10^{-0.0269}$	3	7
Didanosine (ddI)	4.65	1/2	25	$10^{-1.2218}$	$10^{-0.2218}$	5	7.5
Emtricitabine (FTC)	7.2	1	39	$10^{-0.9788}$	$10^{0.0212}$	6	17
Lamivudine (3TC)	6	1/2	20	$10^{-1.1249}$	$10^{-0.1249}$	3.5	8.5
Stavudine (d4T)	2.144	1/2	7.5	$10^{-1.6383}$	$10^{-0.6383}$	1	2.5
Tenofivir (TDF)	1.184	1	60	$10^{-1.5229}$	$10^{-0.5229}$	10	24
Zidovudine (ZDV)	4.24	1/3	7	$10^{-1.6021}$	$10^{-0.6021}$	1.33	2.67
Delavirdine (DLV)	26.6	1/3	5.8	$10^{-1.4559}$	$10^{-0.4559}$	1.67	2.67
Efavirenz (EFV)	12.9	1	45	$10^{-0.8356}$	$10^{0.1644}$	9	22
Nevirapine (NVP)	7.5	1/2	27	$10^{-1.0088}$	$10^{-0.0088}$	5	12.5

Table 2 - Number of drug holidays

Summary of all FDA-approved, PI-sparing triple-drug combinations. Drugs marked with an asterisk are the drug in their respective cocktail with the least number of doses that may theoretically be missed (see Table 1). The number of drug holidays, the length of each holiday and the minimum number of subsequent days of strict adherence is thus calculated from this drug's missable and subsequent doses.

FDA-approved combination			Number of drug holidays (theoretical)	Length of each holiday (days)	Minimum subsquent therapy (days)
ABC*	3TC	NVP	16	3	7
ABC*	3TC	EFV	16	3	7
TDF	3TC*	EFV	14	3.5	8.5
ddI	3TC*	EFV	14	3.5	8.5
d4T*	3TC	EFV	50	1	2.5
d4T*	3TC	NVP	50	1	2.5
ddI*	FTC	EFV	13	5	7.5
TDF	FTC*	EFV	7	6	17
TDF	FTC	NVP*	9	5	12.5
ZDV*	3TC	ABC	44	1.33	2.66
ZDV*	3TC	EFV	44	1.33	2.66
ZDV*	3TC	NVP	44	1.33	2.66
ZDV*	3TC	TDF	44	1.33	2.66
ZDV*	DLV	3TC	44	1.33	2.66
ZDV*	DLV	ddI	44	1.33	2.66

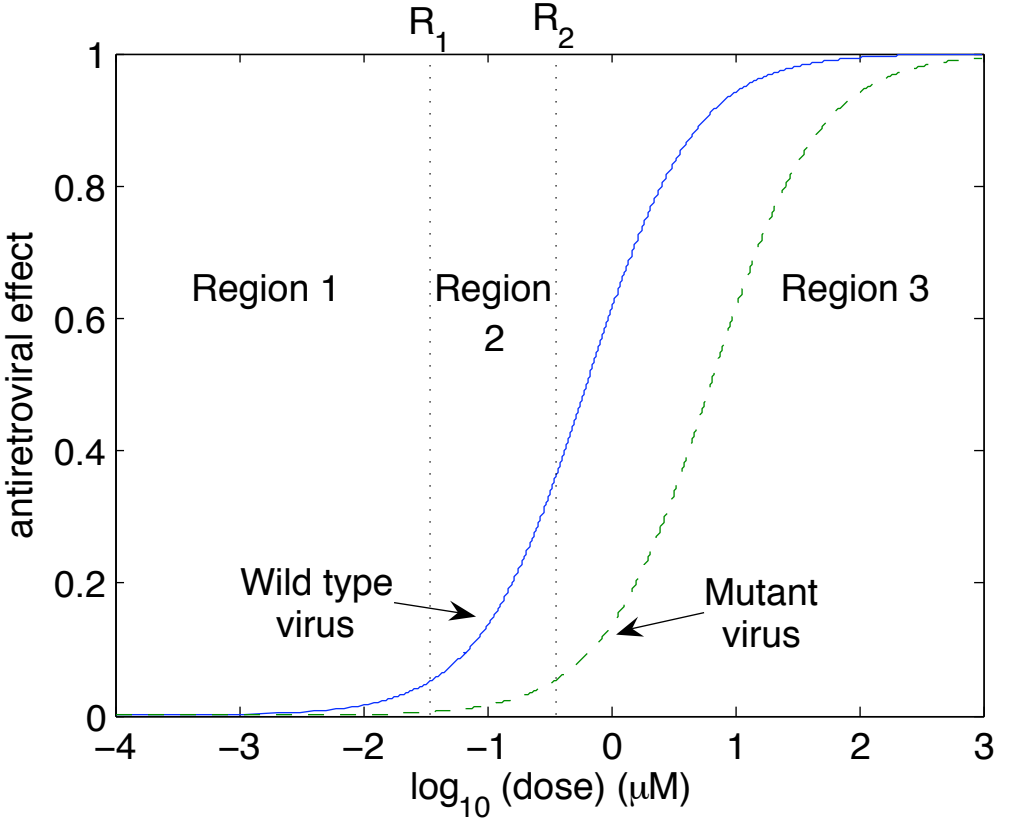
R1
R2
1
0.8
0.6
0.4
0.2
0
antiretroviral effect
Region 1
Region 2
Region 3
Wild type virus
Mutant virus
−4
−3
−2
−1
0
1
2
3
log10 (dose) (μM)

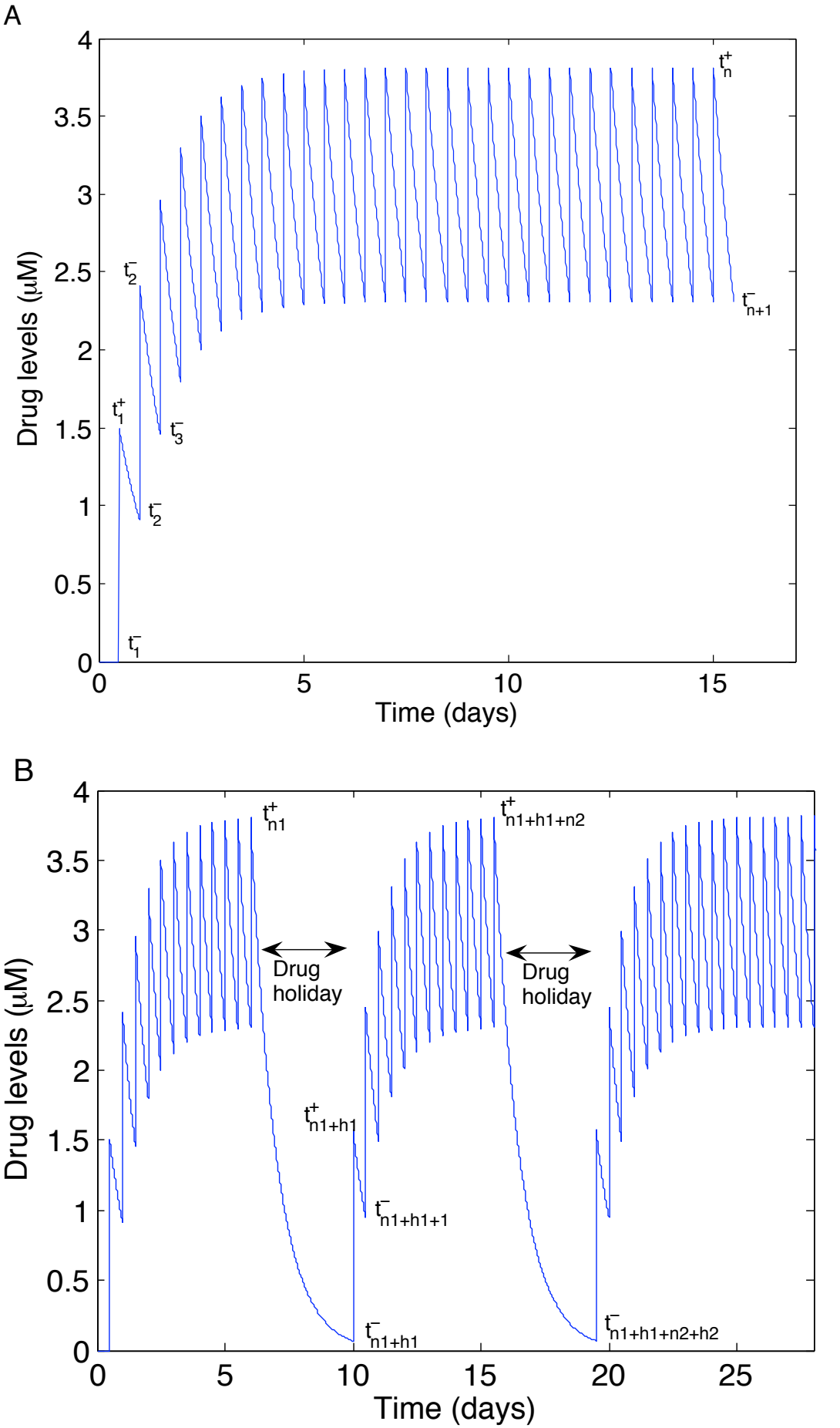
A
Drug levels (μM)
Time (days)
t_1^+
t_1^-
t_2^-
t_2^-
t_3^-
t_n^+
t_{n+1}^-
B
Drug levels (μM)
Time (days)
t_{n1}^+
Drug holiday
t_{n1+h1}^+
t_{n1+h1}^-
$t_{n1+h1+1}^-$
$t_{n1+h1+n2}^+$
Drug holiday
$t_{n1+h1+n2+h2}^-$

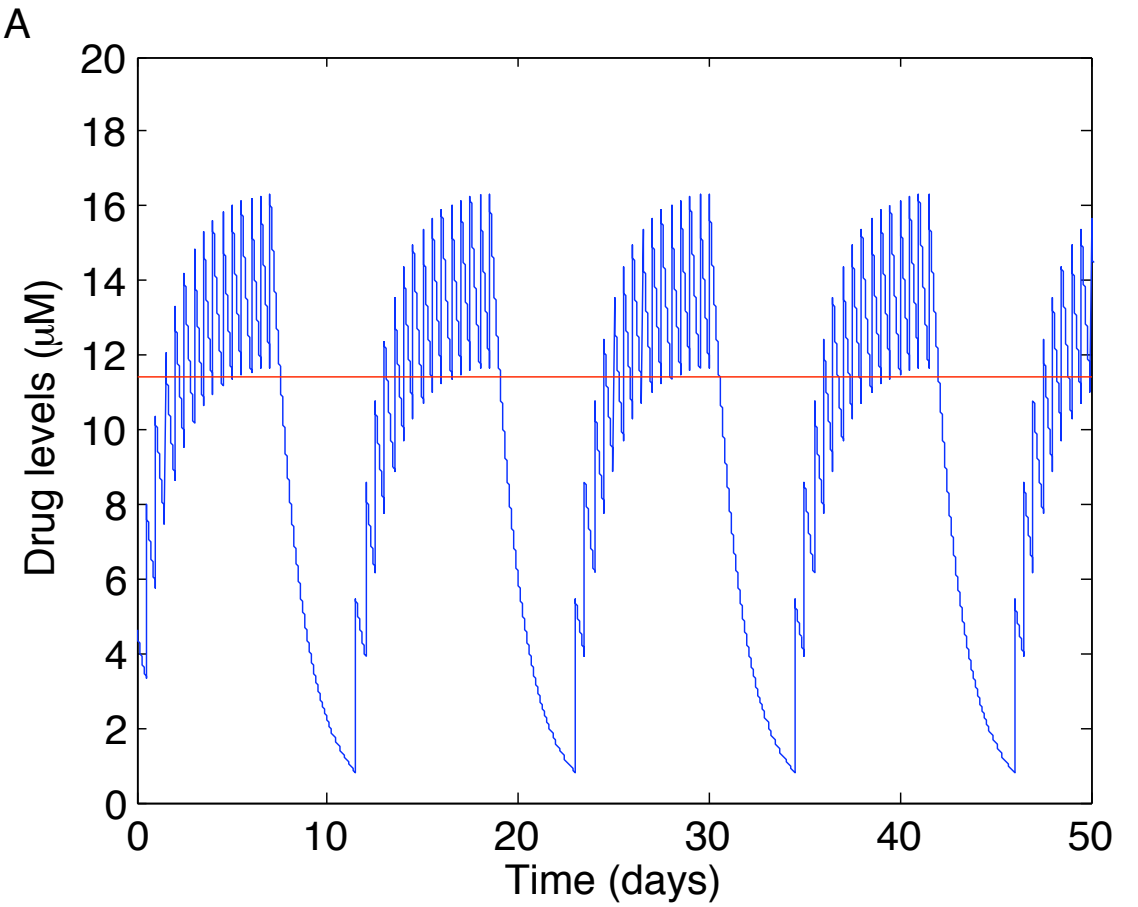
A
Drug levels (μM)
Time (days)
0
2
4
6
8
10
12
14
16
18
20
0
10
20
30
40
50

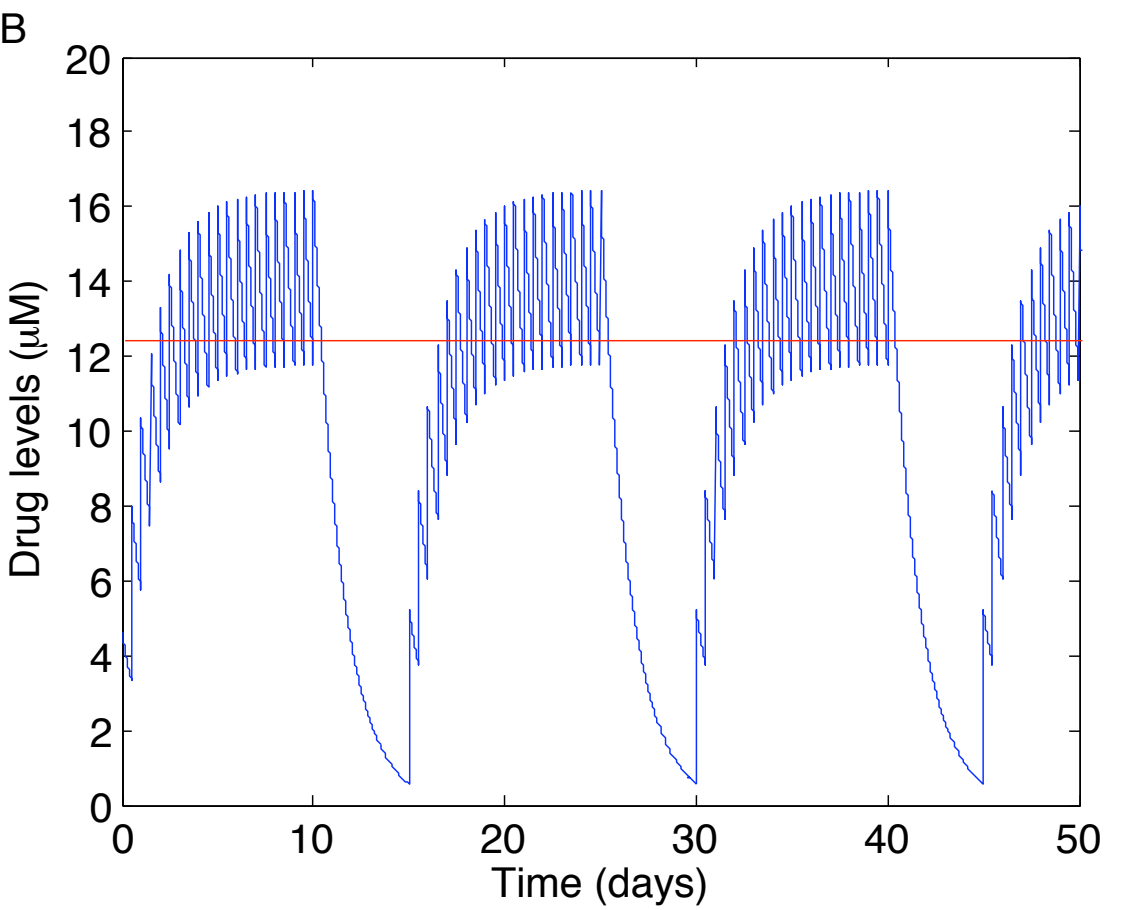
B
Drug levels (μM)
Time (days)
0
2
4
6
8
10
12
14
16
18
20
0
10
20
30
40
50

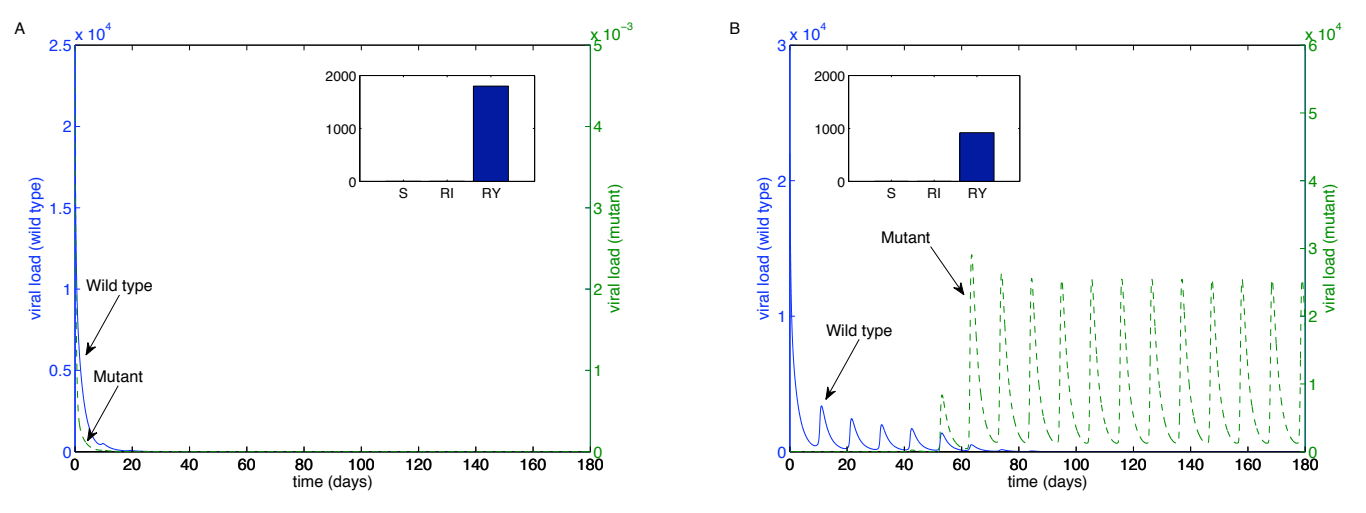
A
x 10^4
2.5
2
1.5
1
0.5
0
viral load (wild type)
x 10^-3
5
4
3
2
1
0
viral load (mutant)
2000
1000
0
S
RI
RY
Wild type
Mutant
0
20
40
60
80
100
120
140
160
180
time (days)
B
x 10^4
3
2
1
0
viral load (wild type)
x 10^4
6
5
4
3
2
1
0
viral load (mutant)
2000
1000
0
S
RI
RY
Mutant
Wild type
0
20
40
60
80
100
120
140
160
180
time (days)

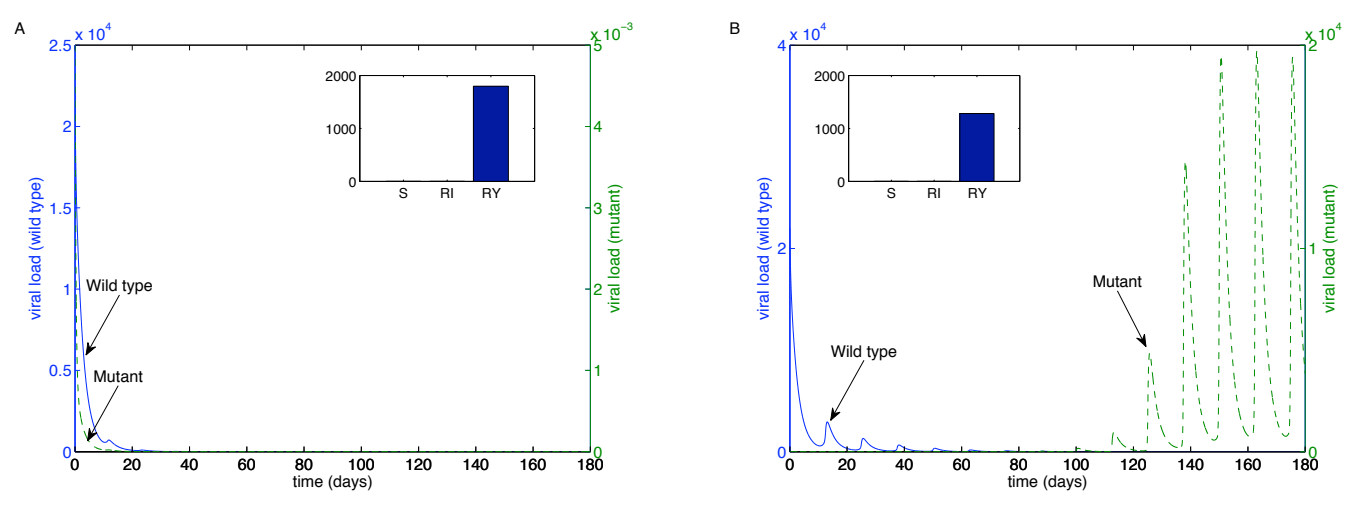
A
x 10^4
2.5
2
1.5
1
0.5
0
viral load (wild type)
x 10^-3
5
4
3
2
1
0
viral load (mutant)
2000
1000
0
S
RI
RY
Wild type
Mutant
0
20
40
60
80
100
120
140
160
180
time (days)
B
x 10^4
4
2
0
viral load (wild type)
x 10^4
2
1
0
viral load (mutant)
2000
1000
0
S
RI
RY
Mutant
Wild type
0
20
40
60
80
100
120
140
160
180
time (days)

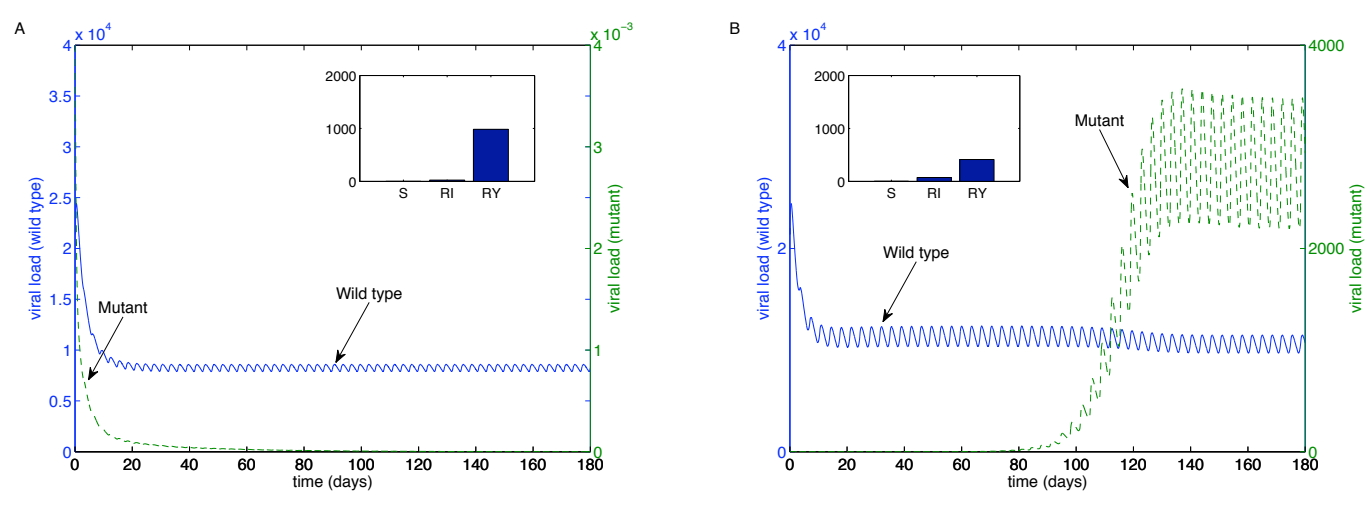
A
x 10^4
x 10^-3
viral load (wild type)
viral load (mutant)
time (days)
Mutant
Wild type
2000
1000
0
S
RI
RY
B
x 10^4
4000
2000
Mutant
Wild type

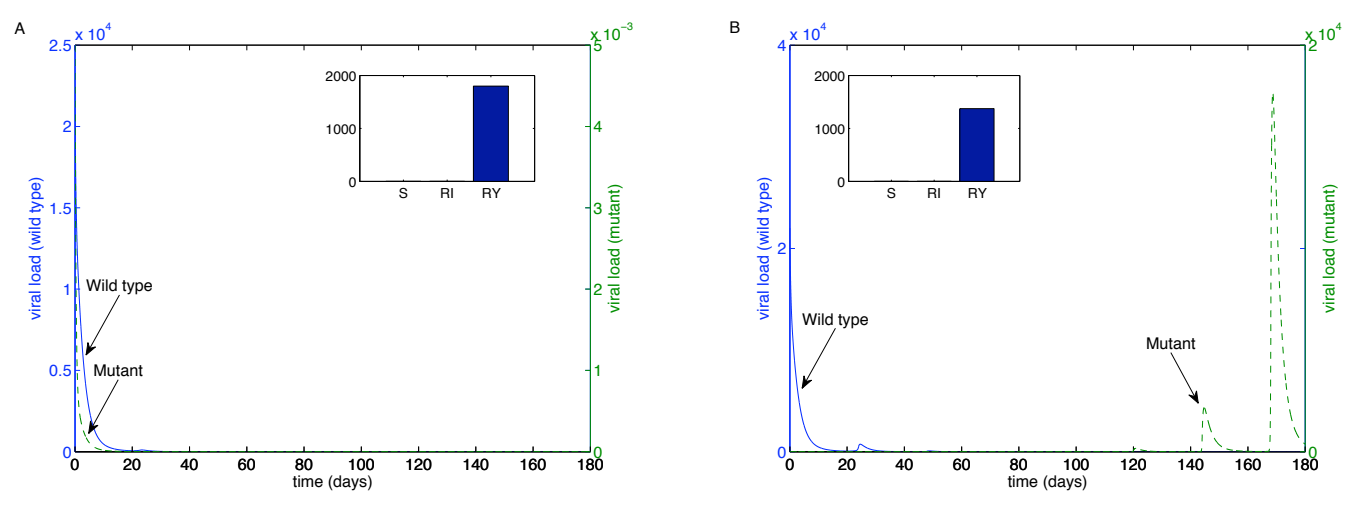
A
x 10^4
2.5
2
1.5
1
0.5
0
viral load (wild type)
x 10^-3
5
4
3
2
1
0
viral load (mutant)
2000
1000
0
S
RI
RY
Wild type
Mutant
0
20
40
60
80
100
120
140
160
180
time (days)
B
x 10^4
4
2
0
viral load (wild type)
x 10^4
2
0
viral load (mutant)
2000
1000
0
S
RI
RY
Wild type
Mutant
0
20
40
60
80
100
120
140
160
180
time (days)

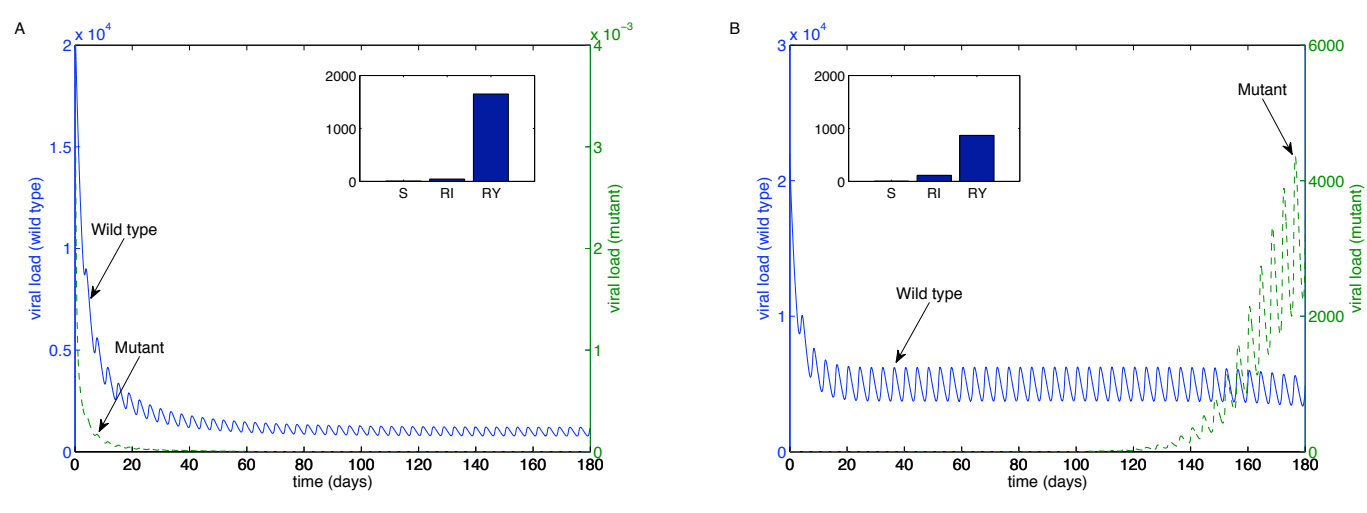
A
x 10^4
x 10^-3
viral load (wild type)
viral load (mutant)
time (days)
Wild type
Mutant
2000
1000
0
S
RI
RY
B
x 10^4
6000
4000
2000
Mutant
Wild type

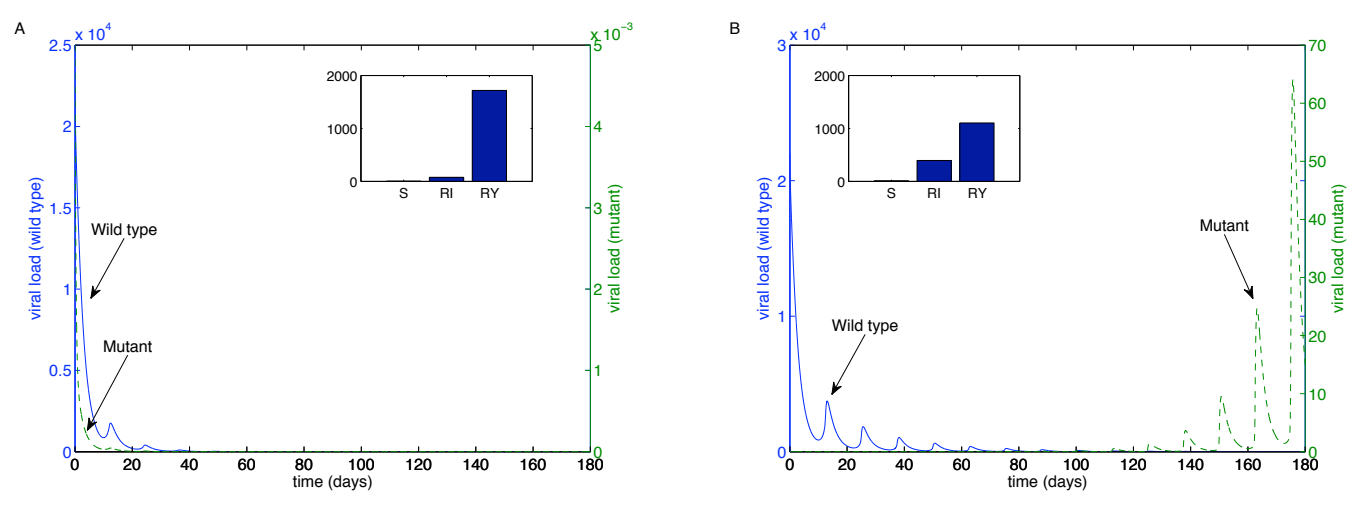
A
x 10^4
2.5
2
1.5
1
0.5
0
viral load (wild type)
x 10^-3
5
4
3
2
1
0
viral load (mutant)
Wild type
Mutant
2000
1000
0
S
RI
RY
0
20
40
60
80
100
120
140
160
180
time (days)
B
x 10^4
3
2
1
0
viral load (wild type)
70
60
50
40
30
20
10
0
viral load (mutant)
Wild type
Mutant
2000
1000
0
S
RI
RY
0
20
40
60
80
100
120
140
160
180
time (days)

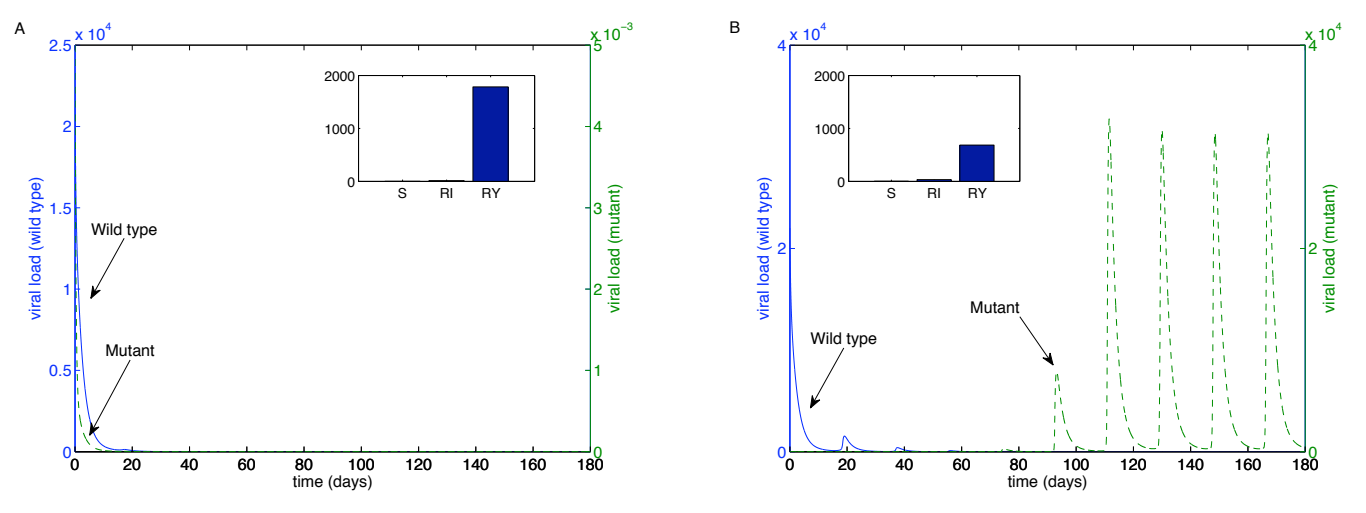
A
x 10^4
2.5
2
1.5
1
0.5
0
viral load (wild type)
x 10^-3
5
4
3
2
1
0
viral load (mutant)
Wild type
Mutant
2000
1000
0
S
RI
RY
0
20
40
60
80
100
120
140
160
180
time (days)
B
x 10^4
4
2
0
viral load (wild type)
x 10^4
4
2
0
viral load (mutant)
Wild type
Mutant
2000
1000
0
S
RI
RY
0
20
40
60
80
100
120
140
160
180
time (days)

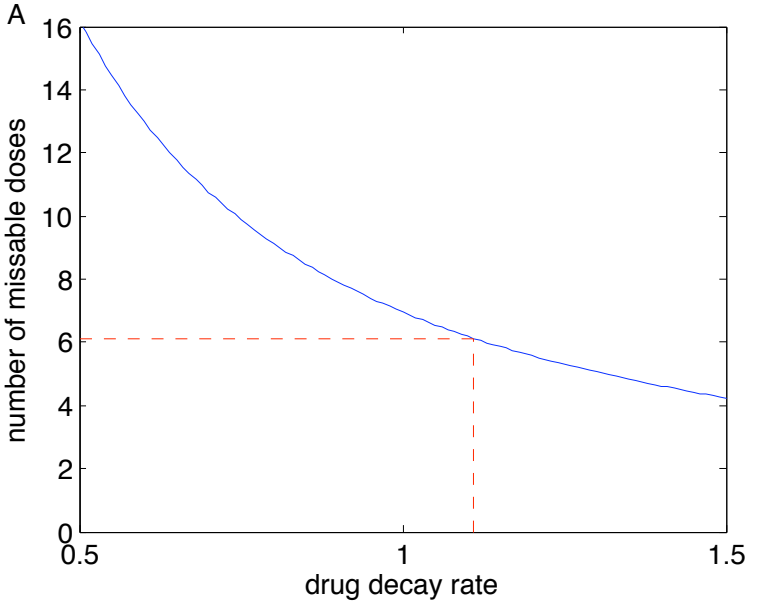
A
number of missable doses
0
2
4
6
8
10
12
14
16
0.5
1
1.5
drug decay rate

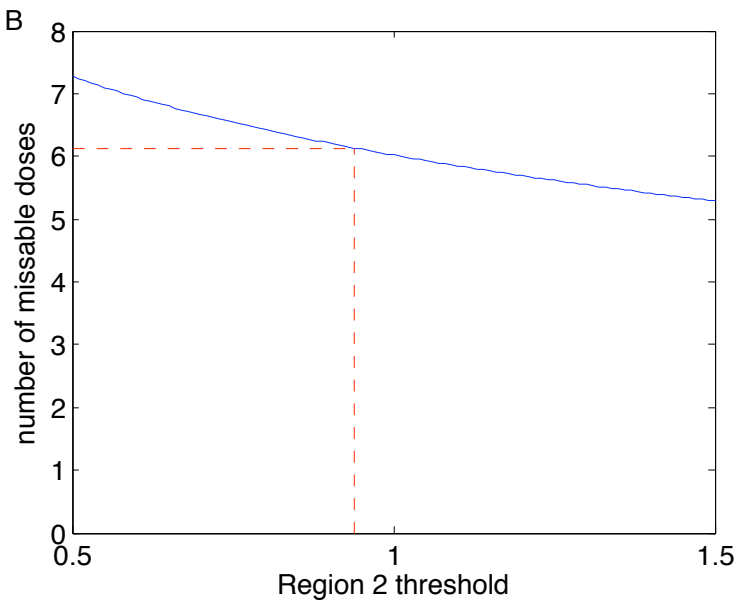
B
number of missable doses
0
1
2
3
4
5
6
7
8
0.5
1
1.5
Region 2 threshold

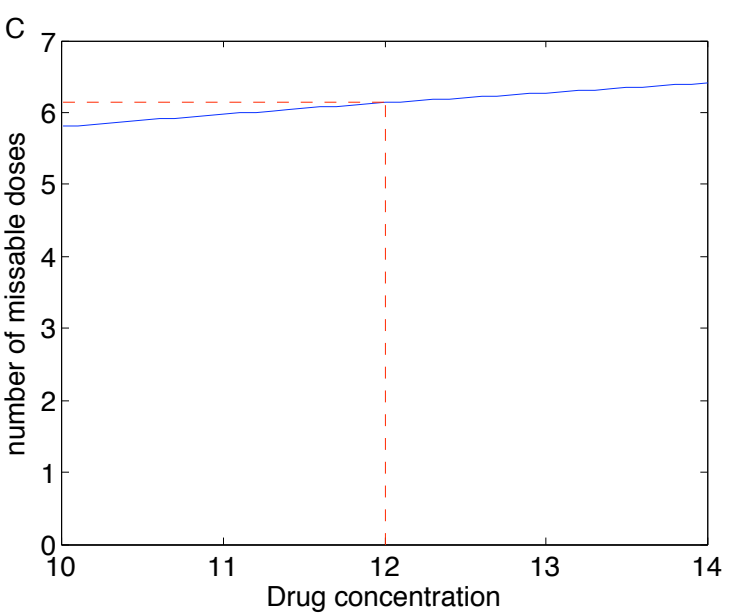
C
number of missable doses
0
1
2
3
4
5
6
7
10
11
12
13
14
Drug concentration

3.2 Resistance to protease inhibitors in a model of HIV-1 infection with impulsive drug effects

The effects of drug resistance have altered the history of disease progression. Drug resistance can emerge with lack of adherence to any strict drug therapy. Mutation development occurs quickly during HIV-1 drug therapy, and thus studying the behaviour of drug-resistant strains is crucial in controlling the spread of HIV.

Smith and Wahl [21] developed an impulsive differential system with one strain of infectious virus, susceptible cells and infected cells. They included the drug dynamics of both reverse transcriptase inhibitors and protease inhibitors by an exponential decay between impulse times and a constant impulse each time a drug is taken. They solved for stability of the non-impulsive system, and showed that insufficient dosing of either drug corresponds to high viral load and large populations of infectious T cells. They also showed that, if physiologically tolerable, sufficiently frequent dosing with the reverse transcriptase inhibitor alone could theoretically maintain the T cell counts close to the T cell count in the uninfected immune system. Later, Smith and Wahl [22] developed a model describing the interactions between $CD4^+$ T-cells, reverse transcriptase inhibitors and two strains of virus: the wild-type strain, which initially dominates in the absence of drugs, and the mutant strain, which is the less efficient competitor, but has more resistance to the drugs. They included low, intermediate and high drug inhibited T cells and T cells infected with a wild-type and mutant strain. They also described three regions of drug behavior: Region 1 describes the dynamics between cells and virus at low drug levels; Region 2 describes the dynamics between cells and virus at an intermediate drug level, and Region 3 describes the dynamics between cells and virus at high drug levels. At an intermediate level of drug, the drug will affect the wild-type strain alone, whereas at high drug levels both strains will be controlled. They used impulsive differential equations to represent the drug

dynamics of each model and the relationship between them. Stability analysis was computed for each region. They showed that it is theoretically possible to eliminate HIV. They also predicted that protease-inhibitors alone could not do the same.

We develop and analyze a model including protease inhibitors, $CD4^+$ T-cells and two strains of virus. The dynamics between T cells and virus change from Smith and Wahl [22] since protease inhibitors do not inhibit the infection of a T cell; they only inhibit viral budding of infectious virions. We also consider the same three regions in order to view the effect of having low, intermediate or high drug levels. Therefore, the model presented in this chapter includes T cells inhibited with low, intermediate and high drug levels, but each of these classes can be infected by either strain of virus; the only difference between the classes is the budding of infectious virus. We use a system of impulsive differential equations to model the drug dynamics as the drug changes from one region to the next. Stability analysis of the ordinary differential equations is computed, including the basic reproductive number for each region, and numerical simulations show the effect of varying the drug with an impulse (see Appendices C, D, E, F for more details on the development of results for each region and errata). We show that Smith and Wahl's [22] prediction about protease inhibitors was incorrect, and that if physiologically tolerable, free-virus elimination is theoretically possible, due to local stability. Simulation details and extra comments for the manuscript can be found in Appendix G.

The contribution by each author is as follows. The first author developed and analyzed the current model, performed numerical simulations and wrote the manuscript. The second author designed the project and edited the manuscript.

This paper is in press in the journal of The Bulletin of Mathematical Biology [4];
Miron, R.E., Smith?, R.J. 2014. Resistance to protease inhibitors in a model of HIV-1 infection with impulsive drug effects. *Bulletin of Mathematical Biology* **76**:1, 59–97.

Resistance to protease inhibitors in a model of HIV-1 infection with impulsive drug effects

Rachelle E. Miron[1] and Robert J. Smith?[1,2]

1. Department of Mathematics, The University of Ottawa, 585 King Edward Ave, Ottawa ON K1N 6N5, Canada
2. Faculty of Medicine, The University of Ottawa, 585 King Edward Ave, Ottawa ON K1N 6N5, Canada

Abstract

Background: The emergence of drug resistance is one of the most prevalent reasons for treatment failure in HIV therapy. This has severe implications for the cost of treatment, survival and quality of life.
Methods: We use mathematical modelling to describe the interaction between T cells, HIV-1 and protease inhibitors. We use impulsive differential equations to examine the effects of different levels of protease inhibitors in a T cell. We classify three different regimes according to whether the drug efficacy is low, intermediate or high. The model includes two strains: the wild-type strain, which initially dominates in the absence of drugs, and the mutant strain, which is the less efficient competitor, but has more resistance to the drugs.
Results: Drug regimes may take trajectories through one, two or all three regimes, depending on the dosage and the dosing schedule. Stability analysis shows that resistance does not emerge at low drug levels. At intermediate drug levels, drug resistance is guaranteed to emerge. At high drug levels, either the drug-resistant strain will dominate or, in the absence of longer-lived reservoirs of infected cells, a region exists where viral elimination could theoretically occur. We provide estimates of a range of dosages and dosing schedules where the trajectories lie either solely within a region or cross multiple regions.
Conclusion: Under specific circumstances, if the drug level is physiologically tolerable, elimination of free virus is theoretically possible. This forms the basis for theoretical control using combination therapy and for understanding the effects of partial adherence.

1 Introduction

The effects of drug resistance have altered the history of disease progression [1]. Drug resistance can emerge with lack of adherence to any strict drug therapy [2]. Mutation development occurs quickly at a rate of approximately 3×10^{-5} per

nucleotide base cycle of replication [2]. Since HIV is highly variable, it rapidly develops resistance to antiretroviral drugs [2]. This results in the spread of a different form of HIV, so that antiretroviral therapy can no longer control the virus [3].

Many mathematical models have been developed to describe drug resistance [4]-[9], but such models have focussed on the emergence of drug resistance during continuous therapy [10]-[17]. A more recent tool to model drug dynamics is impulsive differential equations. Smith and Wahl [18] used impulsive differential equations to model the interaction between cell/virus dynamics and reverse transcriptase inhibitors, integrase inhibitors and fusion inhibitors. Smith and Wahl [19] also used impulsive differential equations to model drug resistance by considering immunological behaviour for HIV dynamics, including the effects of reverse transcriptase inhibitors and other drugs that prevent cellular infection. Smith [20] answered the question of determining how many doses may be skipped before HIV treatment response is adversely affected by the emergence of drug-resistance using impulsive differential equations. Krakovska and Wahl [21] developed a model that predicts optimal treatment regimens, and used this model, coupled with impulsive differential equations, to investigate the effects of adherence. Lou and Smith? [22] developed a mathematical model that describes the binding of the virus to T cells in the presence of the fusion inhibitor enfuvirtide using impulsive differential equations. Lou et al. [23] used impulsive differential equations to develop a rigorous approach to analyze the threshold behaviours of nonlinear virus dynamics models with impulsive drug effects and to examine the feasibility of virus clearance.

The other major class of antiretroviral drugs used to treat HIV-positive patients are protease inhibitors (PIs). PIs aim to stop the viral protease, which cleaves polyproteins to produce the virion proteins and viral enzymes [2]. This decreases the number of infectious virions that bud from the infected $CD4^+$ T cells and increases the number of non-infectious virions, which cannot infect other susceptible T cells [2]. Modelling PIs is significantly different to modelling reverse transcriptase inhibitors, integrase inhibitors and fusion inhibitors, since cells still become infected and still cause budding even with drug present. Here we examine the conditions required for the emergence of drug resistance to protease inhibitors during HIV-1 drug therapy.

We consider two strains: the wild-type strain, which initially dominates in the absence of drugs, and the mutant strain, which is the less efficient competitor, but has more resistance to the drugs. At an intermediate level of drug, the drug will affect the wild-type strain alone, whereas a high level of drug will control both strains [12, 28]. We describe three models for each drug level and use impulsive differential equations to model the drug dynamics flowing between each model.

This paper is organised as follows. In section 2, we present the model describing the interactions between the $CD4^+$ T cells, the wild-type and mutant virus, and the drugs. In section 3, we fix the drug level as a constant and find the equilibrium points, as well as the stability, for all three regions. In section 4, numerical simulations are performed to show the effects of varying drug levels.

We conclude with a discussion.

2 The model

2.1 T cells

We use nine state variables describing $CD4^+$ T cells in a variety of stages during infection and while on drugs. The variable T_S describes susceptible $CD4^+$ T cells, whereas T_I and T_Y describe cells infected by wild-type or mutant virus, respectively. Once an intermediate level of drug has entered the cells, we have three new classes. T_{PN} describes the susceptible cells that have an intermediate level of drug. T_{PI} and T_{PY} describe the cells that are infected with the wild-type or mutant strain, respectively, and that also have an intermediate level of drug. As more drug is taken, a $CD4^+$ T cell is inhibited with a high level of drug. We have three such cell types: susceptible cells inhibited with high drug levels, T_{PPN}; cells infected with the wild-type strain, T_{PPI}; and cells infected with the mutant strain, T_{PPY}. We also describe the virions by V_I and V_Y for the wild-type and mutant strains, respectively. Non-infectious virus is denoted by V_N. The interaction between the cells and virus can be seen in Figure 1, and a description of the state variables is listed in Table 1. When low drug levels are present, there is not enough drug to inhibit the T cells from being infected by either the wild-type or the mutant strains. When intermediate drug levels are present, there is not enough drug in the T cells to inhibit the drug-resistant strain from producing infectious virus, but cells infected with the wild-type strain will only produce non-infectious virus. When high drug levels are present, T cells are unable to produce infectious virus, regardless of whether they are infected with the wild-type or mutant strain.

2.2 Drugs

Similar to Smith and Wahl [18], we use P(t) to denote the intracellular concentration of the drug and its active metabolites. We assume that drugs are taken at (not necessarily fixed) times t_k. The effect of the drugs is assumed to be instantaneous, resulting in a system of impulsive differential equations, whereby solutions are continuous for $t \neq t_k$ (satisfying the associated system of ordinary differential equations) and undergo an instantaneous change in state when $t = t_k$. This can be assumed since the time during which the drug is absorbed is smaller than the time during which the drug is cleared [29].

According to impulsive theory found in the mathematical literature [30]-[33], we can describe the nature of the impulse at time t_k via a difference equation

$$\Delta P \equiv P(t_k^+) - P(t_k^-) = f(t_k, P(t_k^-)). \tag{2.1}$$

where $f(t, P)$ is a mapping of the solution before the impulse, $P(t_k^-)$, to after the impulse effect, $P(t_k^+)$.

To model the effects of resistance mutation on drug efficacy, we consider the dose-effect curve illustrated in Figure 2. Here the solid line shows a dose-effect curve for the wild-type virus, while the dashed line shows the same curve for a drug-resistant strain with 10-fold resistance; drug resistance implies an increase in the half-maximal inhibitory concentration IC_{50} of the drug. The axis, or effect, in the dose-effect curve is the probability that a given T cell absorbs sufficient quantities of the drug to prevent the viral protease from being created in order to stop viral budding. Thus when $P < P_1$ (Region 1), this probability is negligible for both viral strains. In some region $P_1 < P < P_2$ (Region 2), this probability remains negligible for the drug-resistant virus, but grows monotonically with dose for the wild-type. Similarly, when $P > P_2$ (Region 3), the probability of blocking the viral protease is significant for both wild-type and drug-resistant strains, although higher for the wild-type. In all three cases where the probability that the viral protease will be blocked is non-negligible, we assume that the probability grows linearly with increasing dose, although at different rates for different strains and regions (note that the dose-effect curves in these regimes are much closer to linear than suggested by this semilog plot). The Region 1 and Region 2 thresholds (P_1 and P_2, respectively) are calculated similarly to Miron and Smith? [34]. Our model of HIV dynamics therefore consists of three distinct systems in which different drug actions are possible, depending on the drug concentration P (see Figure 1).

2.3 Combining T cell populations with virus and drugs

The dynamics of the CD4$^+$ T cells and virus can be modelled by the following set of ordinary differential equations:

$$\begin{aligned}
\frac{dV_I}{dt} &= n_I\omega T_I - d_V V_I - r_I T_S V_I - r_I T_{PN} V_I - r_I T_{PPN} V_I \\
\frac{dV_Y}{dt} &= n_I\omega(T_Y + T_{PY}) - d_V V_Y - r_Y T_S V_Y - r_Y T_{PN} V_Y - r_Y T_{PPN} V_Y \\
\frac{dV_N}{dt} &= n_I(1-\omega)(T_I + T_Y + T_{PY}) + n_I(T_{PI} + T_{PPI} + T_{PPY}) - d_V V_N \\
\frac{dT_S}{dt} &= \lambda - r_I T_S V_I - r_Y T_S V_Y - d_S T_S - \alpha_1 r_P P T_S + m_P T_{PN} \\
\frac{dT_I}{dt} &= r_I T_S V_I - d_I T_I - \alpha_1 r_P P T_I + m_P T_{PI} \\
\frac{dT_Y}{dt} &= r_Y T_S V_Y - d_I T_Y - \alpha_1 r_P P T_Y + m_P T_{PY} \\
\frac{dT_{PN}}{dt} &= \alpha_1 r_P P T_S - m_P T_{PN} - r_Y T_{PN} V_Y - r_I T_{PN} V_I - d_S T_{PN} - \alpha_2 r_{PP} P T_{PN} + m_{PP} T_{PPN} \\
\frac{dT_{PI}}{dt} &= r_I T_{PN} V_I + \alpha_1 r_P P T_I - m_P T_{PI} - \alpha_2 r_{PP} P T_{PI} + m_{PP} T_{PPI} - d_I T_{PI} \\
\frac{dT_{PY}}{dt} &= r_Y T_{PN} V_Y + \alpha_1 r_P P T_Y - m_P T_{PY} - \alpha_2 r_{PP} P T_{PY} + m_{PP} T_{PPY} - d_I T_{PY} \\
\frac{dT_{PPN}}{dt} &= \alpha_2 r_{PP} P T_{PN} - m_{PP} T_{PPN} - r_Y T_{PPN} V_Y - r_I T_{PPN} V_I - d_S T_{PPN} \\
\frac{dT_{PPI}}{dt} &= r_I T_{PPN} V_I + \alpha_2 r_{PP} P T_{PI} - m_{PP} T_{PPI} - d_I T_{PPI} \\
\frac{dT_{PPY}}{dt} &= r_Y T_{PPN} V_Y + \alpha_2 r_{PP} P T_{PY} - m_{PP} T_{PPY} - d_I T_{PPY},
\end{aligned} \tag{2.2}$$

for $t \neq t_k$ (see impulsive conditions below). This model varies between the three regions mentioned in Section 2.2 by simply changing α_1 and α_2. In Region 1, $\alpha_1 = 0$ and $\alpha_2 = 0$. In Region 2, $\alpha_1 = 1$ and $\alpha_2 = 0$. In Region 3, $\alpha_1 = 1$ and $\alpha_2 = 1$.

Here t is the time in days, n_I is the number of virions produced per day, ω is the proportion of infectious virions produced from an infected CD4$^+$ T cell, and r_I and r_Y are the infection rates of CD4$^+$ T cells with wild-type or mutant virus, respectively. The constant λ is the rate at which new susceptible CD4$^+$ T cells are produced, while the death rates are denoted by d_V, d_S and d_I for the virus, the susceptible and infected CD4$^+$ T cells, respectively. We denote by r_P the rate at which drug inhibits the T cells when drug concentrations are intermediate and the drug concentration is denoted by P. Note that, once the wild-type virus infects T_{PN}, the new infected cell only produces non-infectious virus. The rate m_P is the clearance rate of the drug from an intermediate inhibited cell. The rate at which drug inhibits the T cells when drug concentrations are high is

denoted by r_{PP}. The rate m_{PP} is the clearance rate of the drug from a highly inhibited cell to an intermediate inhibited cell.

All death rates, rates of infection and λ are assumed to be positive. We assume $0 \ll \omega \leq 1$ and $r_I > r_Y$ (i.e., the wild-type is the more infectious strain of the virus). Futhermore, $d_S < d_I < d_V$ [35].

In order to analyze this model, we consider each region separately and look at submodels of system (2.2).

Consider Region 1 ($\alpha_1 = 0$ and $\alpha_2 = 0$). We assume here that the primary difference between wild-type and mutant virus is the rate of infection and that, in the absence of drugs, the wild-type strain is the better competitor. Also, there is not enough drug to inhibit the T cells from being infected by either the wild-type or the mutant strains. In this case, $\frac{dT_{PPN}}{dt}$ is negative, meaning T_{PPN} decays to zero. This also means T_{PN}, T_{PI}, T_{PY}, T_{PPI} and T_{PPY} decay to zero. This then forces all terms in the first six equations of system (2.2) including T_{PN}, T_{PI}, T_{PY}, T_{PPN}, T_{PPI}, and T_{PPY} to decay to zero. Thus our subsystem excludes all the terms including T_{PN}, T_{PI}, T_{PY}, T_{PPN}, T_{PPI} and T_{PPY}.

The same can be concluded for the subsystem for Region 2 ($\alpha_1 = 1$ and $\alpha_2 = 0$). Again $\frac{dT_{PPN}}{dt}$ is negative, meaning T_{PPN} decays to zero. This also means T_{PPI} and T_{PPY} decay to zero. This then forces all terms in the first nine equations of system (2.2) including T_{PPN}, T_{PPI} and T_{PPY} to decay to zero. Thus our subsystem excludes all the terms including T_{PPN}, T_{PPI} and T_{PPY}.

In summary, we have the following subregions of system (2.2), for $t \neq t_k$.

For $P < P_1$ (Region 1, Fig. 1A), the dynamics of the CD4$^+$ T cells and virions are given by

$$\begin{aligned}
\frac{dV_I}{dt} &= n_I \omega T_I - d_V V_I - r_I T_S V_I \\
\frac{dV_Y}{dt} &= n_I \omega T_Y - d_V V_Y - r_Y T_S V_Y \\
\frac{dV_N}{dt} &= n_I (1-\omega)(T_I + T_Y) - d_V V_N \\
\frac{dT_S}{dt} &= \lambda - r_I T_S V_I - r_Y T_S V_Y - d_S T_S \\
\frac{dT_I}{dt} &= r_I T_S V_I - d_I T_I \\
\frac{dT_Y}{dt} &= r_Y T_S V_Y - d_I T_Y.
\end{aligned} \tag{2.3}$$

For $P_1 < P < P_2$ (Region 2, Fig. 1B), the dynamics of the CD4$^+$ T cells

and virions are given by

$$
\begin{aligned}
\frac{dV_I}{dt} &= n_I\omega T_I - d_V V_I - r_I T_S V_I - r_I T_{PN} V_I \\
\frac{dV_Y}{dt} &= n_I\omega(T_Y + T_{PY}) - d_V V_Y - r_Y T_S V_Y - r_Y T_{PN} V_Y \\
\frac{dV_N}{dt} &= n_I(1-\omega)(T_I + T_Y + T_{PY}) + n_I T_{PI} - d_V V_N \\
\frac{dT_S}{dt} &= \lambda - r_I T_S V_I - r_Y T_S V_Y - d_S T_S - r_P P T_S + m_P T_{PN} \\
\frac{dT_I}{dt} &= r_I T_S V_I - d_I T_I - r_P P T_I + m_P T_{PI} \\
\frac{dT_Y}{dt} &= r_Y T_S V_Y - d_I T_Y - r_P P T_Y + m_P T_{PY} \\
\frac{dT_{PN}}{dt} &= r_P P T_S - m_P T_{PN} - r_Y T_{PN} V_Y - r_I T_{PN} V_I - d_S T_{PN} \\
\frac{dT_{PI}}{dt} &= r_P P T_I - m_P T_{PI} + r_I T_{PN} V_I - d_I T_{PI} \\
\frac{dT_{PY}}{dt} &= r_P P T_Y - m_P T_{PY} + r_Y T_{PN} V_Y - d_I T_{PY}.
\end{aligned}
\tag{2.4}
$$

For $P > P_2$ (Region 3, Fig. 1C), the dynamics of the CD4$^+$ T cells and

virions are given by

$$\begin{aligned}
\frac{dV_I}{dt} &= n_I\omega T_I - d_V V_I - r_I T_S V_I - r_I T_{PN} V_I - r_I T_{PPN} V_I \\
\frac{dV_Y}{dt} &= n_I\omega (T_Y + T_{PY}) - d_V V_Y - r_Y T_S V_Y - r_Y T_{PN} V_Y - r_Y T_{PPN} V_Y \\
\frac{dV_N}{dt} &= n_I(1-\omega)(T_I + T_Y + T_{PY}) + n_I(T_{PI} + T_{PPI} + T_{PPY}) - d_V V_N \\
\frac{dT_S}{dt} &= \lambda - r_I T_S V_I - r_Y T_S V_Y - d_S T_S - r_P P T_S + m_P T_{PN} \\
\frac{dT_I}{dt} &= r_I T_S V_I - d_I T_I - r_P P T_I + m_P T_{PI} \\
\frac{dT_Y}{dt} &= r_Y T_S V_Y - d_I T_Y - r_P P T_Y + m_P T_{PY} \\
\frac{dT_{PN}}{dt} &= r_P P T_S - m_P T_{PN} - r_Y T_{PN} V_Y - r_I T_{PN} V_I - d_S T_{PN} - r_{PP} P T_{PN} + m_{PP} T_{PPN} \\
\frac{dT_{PI}}{dt} &= r_I T_{PN} V_I + r_P P T_I - m_P T_{PI} - r_{PP} P T_{PI} + m_{PP} T_{PPI} - d_I T_{PI} \\
\frac{dT_{PY}}{dt} &= r_Y T_{PN} V_Y + r_P P T_Y - m_P T_{PY} - r_{PP} P T_{PY} + m_{PP} T_{PPY} - d_I T_{PY} \\
\frac{dT_{PPN}}{dt} &= r_{PP} P T_{PN} - m_{PP} T_{PPN} - r_Y T_{PPN} V_Y - r_I T_{PPN} V_I - d_S T_{PPN} \\
\frac{dT_{PPI}}{dt} &= r_I T_{PPN} V_I + r_{PP} P T_{PI} - m_{PP} T_{PPI} - d_I T_{PPI} \\
\frac{dT_{PPY}}{dt} &= r_Y T_{PPN} V_Y + r_{PP} P T_{PY} - m_{PP} T_{PPY} - d_I T_{PPY}.
\end{aligned} \tag{2.5}$$

The dynamics of the drug are modelled using impulsive differential equations. The exponential decay can be written as a differential equation, where $P(t)$ is the drug concentration. The dynamics of the drug are

$$\begin{aligned}
\frac{dP}{dt} &= -d_P P \qquad && t \neq t_k \\
\Delta P &= P^i && t = t_k.
\end{aligned} \tag{2.6}$$

The rate at which the drug is cleared is d_P and P^i is the dosage. Assuming a drug is taken at time t_k, by the definition of an impulsive effect, we have

$$P(t_k^+) = P(t_k^-) + P^i\,. \tag{2.7}$$

Here we assume that $P(0) = 0$.

Thus (2.3)-(2.5), together with (2.6) describe our three-regime model of impulsive differential equations. A list and description of all the parameters and state variables can be found in Table 1.

3 Analysis

3.1 Asymptotic Behaviour

In order to interpret system (2.2), we analyze each region separately. We investigate the stability of each equilibrium by fixing the drug concentration level as a constant in order to approximate the effect of the impulsive periodic orbit. Region 1 has no effect from the drug concentration, but the analysis of Regions 2 and 3 include P^* as the representative value of drug levels. Section 4 demonstrates numerically the effects of changing the drug concentration levels (including the impulse condition).

3.1.1 Region 1: Low Drug Levels

System (2.3) has three equilibrium points.

Disease-free equilibrium

The disease-free equilibrium is

$$(V_I, V_Y, V_N, T_S, T_I, T_Y) = (0, 0, 0, \frac{\lambda}{d_S}, 0, 0).$$

The basic reproductive number of Region 1, $R_{0,1}$, is computed using the next-generation method [36, 37] at the disease-free equilibrium. Using the same notation as [37], we find

$$F = \begin{pmatrix} 0 & 0 & 0 & 0 \\ 0 & 0 & 0 & 0 \\ r_I\overline{T}_S & 0 & 0 & 0 \\ 0 & r_Y\overline{T}_S & 0 & 0 \end{pmatrix}$$

$$V = \begin{pmatrix} d_V + r_I\overline{T}_S & 0 & -n_I\omega & 0 \\ 0 & d_V + r_Y\overline{T}_S & 0 & -n_I\omega \\ 0 & 0 & d_I & 0 \\ 0 & 0 & 0 & d_I \end{pmatrix},$$

where F is non-negative and V is a non-singular M-matrix. Then $R_{0,1}$ is the spectral radius of the FV^{-1} matrix. Thus

$$\begin{aligned} R_{0,1} &= \max\{R_{0,1,a}, R_{0,1,b}\} \\ &= max\Big\{\frac{r_I\lambda n_I\omega}{d_I(d_V d_S + r_I\lambda)}, \frac{r_Y\lambda n_I\omega}{d_I(d_V d_S + r_Y\lambda)}\Big\}. \end{aligned}$$

Note that $R_{0,1,a} > R_{0,1,b}$ since $r_I > r_Y$.

Theorem 3.1.1. *The disease-free equilibrium is locally asymptotically stable in Region 1 if $R_{0,1} < 1$ and unstable if $R_{0,1} > 1$.*

Proof. The Jacobian matrix for Region 1 is

$$J = \begin{bmatrix} -d_V - r_I T_S & 0 & 0 & -r_I V_I & n_I\omega & 0 \\ 0 & -d_V - r_Y T_S & 0 & -r_Y V_Y & 0 & n_I\omega \\ 0 & 0 & -d_V & 0 & n_I(1-\omega) & n_I(1-\omega) \\ -r_I T_S & -r_Y T_S & 0 & -r_I V_I - r_Y V_Y - d_S & 0 & 0 \\ r_I T_S & 0 & 0 & r_I V_I & -d_I & 0 \\ 0 & r_Y T_S & 0 & r_Y V_Y & 0 & -d_I \end{bmatrix}.$$

For the disease-free equilibrium, $\overline{V}_I = \overline{V}_Y = 0$ and $\overline{T}_S = \dfrac{\lambda}{d_S}$, so the characteristic polynomial is

$$\begin{aligned} 0 &= \det(J(\overline{V}_I, \overline{V}_Y, \overline{V}_N, \overline{T}_S, \overline{T}_I, \overline{T}_Y) - \mu I_6) \\ &= (-d_V - \mu)(-d_S - \mu)[\mu^2 + a_1\mu + b_1][\mu^2 + a_2\mu + b_2], \end{aligned} \tag{3.8}$$

where

$$\begin{aligned} a_1 &= d_V + r_I\overline{T}_S + d_I \\ b_1 &= d_I d_V + d_I r_Y \overline{T}_S + n_I\omega r_y \overline{T}_S \\ a_2 &= d_V + r_Y\overline{T}_S + d_I \\ b_2 &= d_I d_V + d_I r_I \overline{T}_S - n_I\omega r_I \overline{T}_S \\ &= \frac{d_I d_V d_S + r_I\lambda d_I}{d_S}(1 - R_{0,1,a}). \end{aligned}$$

We have $b_2 > 0$ if $R_{0,1,a} < 1$. By the Routh-Hurwitz conditions [38, 39], the Jacobian matrix has all eigenvalues with negative real part. Thus the disease-free equilibrium is locally asymptotically stable when $R_{0,1} < 1$ and unstable when $R_{0,1} > 1$. □

Endemic equilibria

The wild-type equilibrium is

$$(V_I, V_Y, V_N, T_S, T_I, T_Y) = (\overline{V}_I, 0, \overline{V}_N, \overline{T}_S, \overline{T}_I, 0),$$

where

$$\begin{aligned} \overline{V}_I &= \frac{d_S d_V + r_I\lambda}{r_I d_V}(R_{0,1,a} - 1) \\ \overline{V}_N &= \frac{n_I(1-\omega)(d_S d_V + r_I\lambda)}{r_I d_V(n_I\omega - d_I)}(R_{0,1,a} - 1) \\ \overline{T}_S &= \frac{\lambda d_V}{(d_S d_V + r_I\lambda)(R_{0,1,a} - 1) + d_S} \\ \overline{T}_I &= \frac{d_S d_V + r_I\lambda}{r_I(n_I\omega - d_I)}(R_{0,1,a} - 1). \end{aligned}$$

The mutant equilibrium is

$$(V_I, V_Y, V_N, T_S, T_I, T_Y) = (0, \overline{V}_Y, \overline{V}_N, \overline{T}_S, 0, \overline{T}_Y),$$

where

$$\begin{aligned}
\overline{V}_Y &= \frac{d_S d_V + r_Y \lambda}{r_Y d_V}(R_{0,1,b} - 1) \\
\overline{V}_N &= \frac{n_I(1-\omega)(d_S d_V + r_Y \lambda)}{r_Y d_V (n_I \omega - d_I)}(R_{0,1,b} - 1) \\
\overline{T}_S &= \frac{\lambda d_V}{(d_S d_V + r_Y \lambda)(R_{0,1,b} - 1) + d_S} \\
\overline{T}_Y &= \frac{d_S d_V + r_Y \lambda}{r_Y (n_I \omega - d_I)}(R_{0,1,b} - 1).
\end{aligned}$$

The wild-type equilibrium exists if $R_{0,1,a} > 1$, and the mutant equilibrium exists if $R_{0,1,b} > 1$.

Theorem 3.1.2. *When the endemic equilibria exist ($R_{0,1,a} > 1$ and/or $R_{0,1,b} > 1$), the wild-type equilibrium is locally asymptotically stable and the mutant equilibrium is unstable.*

Proof. For the wild-type equilibrium, $\overline{V}_Y = 0$, the characteristic polynomial is

$$\begin{aligned}
0 &= \det(J(\overline{V}_I, \overline{V}_Y, \overline{V}_N, \overline{T}_S, \overline{T}_I, \overline{T}_Y) - \mu I_6) \\
&= (d_V + \mu)[\mu^2 + a_1\mu + b_1][\mu^3 + a_2\mu^2 + b_2\mu + c_2],
\end{aligned}$$

where

$$\begin{aligned}
a_1 &= d_V + r_Y \overline{T}_S + d_I \\
b_1 &= \frac{d_I d_V (r_I - r_Y)}{r_I} \\
a_2 &= r_I \overline{V}_I + d_S + d_I + d_V + r_I \overline{T}_S \\
b_2 &= (d_V + r_I \overline{T}_S) d_S + (r_I \overline{V}_I + d_S) d_I + d_V r_I \overline{V}_I \\
c_2 &= (d_I d_V + r_I \overline{T}_S d_I - n_I \omega r_I \overline{T}_S)(r_I \overline{V}_I + d_S) - r_I \overline{T}_S (r_I \overline{V}_I d_I - r_I \overline{V}_I n_I \omega) \\
&= d_I (d_S d_V + r_I \lambda)(R_{0,1,a} - 1).
\end{aligned}$$

Since $r_I > r_Y$, we have $a_1, b_1 > 0$ meaning the quadratic equation $\mu^2 + a_1\mu + b_1$ has no roots with non-negative real parts. We have $a_2, b_2, c_2 > 0$ and $a_2 b_2 - c_2 > 0$ if $R_{0,1,a} > 1$. By the Routh-Hurwitz conditions [38, 39], the Jacobian matrix has all eigenvalues with negative real part if $R_{0,1} > 1$, meaning the wild-type equilibrium is locally asymptotically stable whenever it exists.

For the mutant equilibrium, $\overline{V}_I = 0$, the characteristic polynomial is

$$\begin{aligned}
0 &= \det(J(\overline{V}_I, \overline{V}_Y, \overline{V}_N, \overline{T}_S, \overline{T}_I, \overline{T}_Y) - \mu I_6) \\
&= (d_V + \mu)[\mu^2 + a_1\mu + b_1][\mu^3 + a_2\mu^2 + b_2\mu + c_2],
\end{aligned}$$

where

$$
\begin{aligned}
a_1 &= d_V + r_I\overline{T}_S + d_I \\
b_1 &= \frac{d_I d_V (r_Y - r_I)}{r_Y} \\
a_2 &= r_Y\overline{V}_Y + d_S + d_I + d_V + r_Y\overline{T}_S \\
b_2 &= (d_V + r_Y\overline{T}_S)d_S + (r_Y\overline{V}_Y + d_S)d_I + d_V r_Y\overline{V}_Y \\
c_2 &= (d_I d_V + r_Y\overline{T}_S d_I - n_Y\omega r_Y\overline{T}_S)(r_Y\overline{V}_Y + d_S) - r_Y\overline{T}_S(r_Y\overline{V}_Y d_I - r_Y\overline{V}_Y n_Y\omega) \\
&= (d_S d_V d_I + r_Y\lambda)(R_{0,1,b} - 1).
\end{aligned}
$$

Since the mutant equilibrium has the same characteristic polynomial as the wild-type equilibrium, except that r_I and $\overline{V}_I$ are interchanged with r_Y and $\overline{V}_Y$, we have $a_1 > 0$ and $b_1 < 0$ since $r_Y - r_I < 0$. By the Routh-Hurwitz conditions [38, 39], the Jacobian matrix has an eigenvalue with positive real part if $R_{0,1} > 1$, meaning the mutant equilibrium is unstable. □

We can also show that no interior equilibria exist for realistic parameters in Region 1. We assumed that $r_I > r_Y$ since since the mutant virus is less infectious.

Theorem 3.1.3. *For system (2.3), if $r_I \neq r_Y$, there are no interior equilibria.*

Proof. Let $r_I \neq r_Y$. For an interior equilibrium, we have $V_I \neq 0$ and $V_Y \neq 0$. Setting the right-hand side of system (2.3) to zero, we get, from the fifth and sixth equations of system (2.3),

$$T_I = \frac{r_I}{d_I} T_S V_I \tag{3.9}$$

$$T_Y = \frac{r_Y}{d_I} T_S V_Y. \tag{3.10}$$

Setting the first equation of system (2.3) equal to zero, and substituting T_I as in equation (3.9), we get

$$r_I T_S V_I \frac{n_I\omega - d_I}{d_I} - d_V V_I = 0.$$

Since $V_I \neq 0$, we have

$$T_S = \frac{d_V d_I}{r_I(n_I\omega - d_I)}. \tag{3.11}$$

Similarly, setting the second equation of system (2.3) equal to zero, and substituting T_Y as in equation (3.10), we get

$$T_S = \frac{d_V d_I}{r_Y(n_I\omega - d_I)}, \tag{3.12}$$

since $V_Y \neq 0$.
This implies that $r_I = r_Y$, which is a contradiction. □

In summary, if $R_{0,1} < 1$, the disease-free equilibrium is locally asymptotically stable in Region 1, and if $R_{0,1} > 1$, the wild-type equilibrium is locally asymptotically stable and the disease-free and mutant equilibria are unstable in Region 1. Also, in Region 1, there are no interior equilibria.

3.1.2 Region 2: Intermediate Drug Levels

In this case, the drug concentration level affects the outcome of the system. We denote the equilibrium solutions by $\overline{X}$ as those not affected by the drug dynamics (Region 1), and denote the equilibria by X^* as those that are affected by the drug dynamics (Region 2 and 3). System (2.4) has four equilibria. In all cases, we fix P^* constant such that $P_1 < P^* < P_2$, where P_1 and P_2 are the Region 1 and Region 2 thresholds, respectively.

Disease-free equilibrium

The disease-free equilibrium is

$$(V_I, V_Y, V_N, T_S, T_I, T_Y, T_{PN}, T_{PI}, T_{PY}, P) = (0, 0, 0, T_S^*, 0, 0, T_{PN}^*, 0, 0, P^*),$$

where

$$\begin{aligned} T_S^* &= \frac{\lambda}{d_S + r_P P^*} + \frac{m_P T_{PN}^*}{d_S + r_P P^*} \\ T_{PN}^* &= \frac{\lambda r_P P^*}{d_S(m_P + d_S) + d_S r_P P^*}. \end{aligned}$$

The basic reproductive number in Region 2, $R_{0,2}$, is computed as before using the next-generation method and is given by

$$R_{0,2} = \max\{R_{0,2,a}, R_{0,2,b}\},$$

where

$$\begin{aligned} R_{0,2,a} &= \frac{n_I \omega \big(r_Y T_S^* + r_Y T_{PN}^*\big)}{d_I(d_V + r_Y T_S^* + r_Y T_{PN}^*)} \\ R_{0,2,b} &= \frac{n_I \omega \big(m_P(r_I T_S^* + r_I T_{PN}^*) + d_I r_I T_S^*\big)}{d_I(d_I + r_P P^* + m_P)(r_I T_S^* + r_I T_{PN}^* + d_V)}. \end{aligned}$$

Theorem 3.1.4. *The disease-free equilibrium is locally asymptotically stable in Region 2 if $R_{0,2} < 1$ and unstable if $R_{0,2} > 1$.*

Proof. The Jacobian matrix for Region 2 is $J = [J_1|J_2]$, where

$$J_1 = \begin{bmatrix} -d_V - r_I T_S - r_I T_{PN} & 0 & 0 & -r_I V_I \\ 0 & -d_V - r_Y T_S - r_Y T_{PN} & 0 & -r_Y V_Y \\ 0 & 0 & -d_V & 0 \\ -r_I T_S & -r_Y T_S & 0 & -r_I V_I - r_Y V_Y - d_S - r_P P \\ r_I T_S & 0 & 0 & r_I V_I \\ 0 & r_Y T_S & 0 & r_Y V_Y \\ -r_I T_{PN} & -r_Y T_{PN} & 0 & r_P P \\ r_I T_{PN} & 0 & 0 & 0 \\ 0 & r_Y T_{PN} & 0 & 0 \\ 0 & 0 & 0 & 0 \end{bmatrix}$$

$$J_2 = \begin{bmatrix} n_I\omega & 0 & -r_I V_I & 0 & 0 & 0 \\ 0 & n_I\omega & -r_Y V_Y & 0 & n_I\omega & 0 \\ n_I(1-\omega) & n_I(1-\omega) & 0 & n_I & n_I(1-\omega) & 0 \\ 0 & 0 & m_P & 0 & 0 & -r_P T_S \\ -d_I - r_P P & 0 & 0 & m_P & 0 & -r_P T_I \\ 0 & -d_I - r_P P & 0 & 0 & m_P & -r_P T_Y \\ 0 & 0 & -m_P - r_Y V_Y - r_I V_I - d_S & 0 & 0 & r_P T_S \\ r_P P & 0 & r_I V_I & -m_P - d_I & 0 & r_P T_I \\ 0 & r_P P & r_Y V_Y & 0 & -m_P - d_I & r_P T_Y \\ 0 & 0 & 0 & 0 & 0 & -d_P \end{bmatrix}.$$

For the disease-free equilibrium, $V_I^* = V_Y^* = 0$, so the characteristic polynomial is

$$\begin{aligned} 0 &= \det(J(V_I^*, V_Y^*, V_N^*, T_S^*, T_I^*, T_Y^*, T_{PN}^*, T_{PI}^*, T_{PY}^*, P^*) - \mu I_{10}) \\ &= (d_V + \mu)(d_P + \mu)[\mu^3 + a_1\mu^2 + b_1\mu + c_1]f(\mu), \end{aligned}$$

where

$$\begin{aligned} a_1 &= m_P + d_I + d_V + r_I T_S^* + r_I T_{PN}^* + d_I + r_P P^* \\ b_1 &= (d_I + r_P P^*)(d_V + r_I T_S^* + r_I T_{PN}) + (m_P + d_I)(d_V + r_I T_S^* + r_I T_{PN}^* + d_I + r_P P^*) \\ &\quad - m_P r_P P^* - n_I \omega r_I T_S^* \\ c_1 &= d_I(r_I T_{PN}^* + r_I T_S^* + d_V)(d_I + r_P P^* + m_P)(1 - R_{0,2,b}) \end{aligned}$$

and where

$$f(\mu) = \det \begin{bmatrix} -d_V - r_Y T_S - r_Y T_{PN} & 0 & n_I\omega & 0 & n_I\omega \\ -r_Y T_S & -d_S - r_P P & 0 & m_P & 0 \\ r_Y T_S & 0 & -d_I - r_P P^* & 0 & m_P \\ -r_Y T_{PN} & r_P P & 0 & -m_P - d_S & 0 \\ r_Y T_{PN} & 0 & r_P P & 0 & -m_P - d_I \end{bmatrix}.$$

The third-order polynomial $\mu^3+a_1\mu^2+b_1\mu+c_1$ has $a_1, c_1 > 0$ and $a_1b_1-c_1 > 0$ if $R_{0,2,b} < 1$. Thus, by the Routh-Hurwitz conditions [38, 39], the third order polynomial has all eigenvalues with negative real part.

Computing the determinant of $f(\mu)$, we get

$$\det[f(\mu)] = [\mu^2 + a_2\mu + b_2][\mu^3 + a_3\mu^2 + b_3\mu + c_3],$$

where

$$\begin{aligned}
a_2 &= 2d_S + r_P P^* + m_P \\
b_2 &= d_S r_P P^* + d_S(m_P + d_S) \\
a_3 &= r_P P^* + 2d_I + d_V + r_Y T_S^* + r_Y T_{PN}^* + m_P \\
b_3 &= -m_P r_P P^* - n_I \omega r_Y (T_S^* + T_{PN}^*) + (r_P P^* + d_I)(d_V + r_Y T_S^* + r_Y T_{PN}^*) \\
&\quad + (m_P + d_I)(r_P P^* + d_I + d_V + r_Y T_S^* + r_Y T_{PN}^*) \\
c_3 &= (d_V + r_Y T_S^* + r_Y T_{PN}^*)[-m_P r_P P^* + (m_P + d_I)(d_I + r_P P^*)] - n_I \omega [r_Y T_S^*(m_P + d_I) \\
&\quad + m_P r_Y T_{PN}^* + r_Y T_S^* r_P P^* + r_Y T_{PN}^*(d_I + r_P P^*)] \\
&= d_I(r_Y T_{PN}^* + r_Y T_S^* + d_V)(d_I + r_P P^* + m_P)(1 - R_{0,2,a}).
\end{aligned}$$

We have $a_3, c_3 > 0$ and $a_3b_3 - c_3 > 0$ if $R_{0,2,b} < 1$. Hence, by the Routh-Hurwitz conditions [38, 39], the Jacobian matrix has all eigenvalues with negaitve real part meaning the disease-free equilibrium is locally asymptotically stable when $R_{0,2} < 1$ and unstable when $R_{0,2} > 1$. □

Endemic equilibria

The wild-type equilibrium is

$$(V_I, V_Y, V_N, T_S, T_I, T_Y, T_{PN}, T_{PI}, T_{PY}, P) = (V_I^*, 0, V_N^*, T_S^*, T_I^*, 0, T_{PN}^*, T_{PI}^*, 0, P^*),$$

where V_I^* is the positive root of the quadratic equation

$$\frac{\alpha_1}{\xi_1} V_I^{*2} + \frac{\beta_1}{\xi_1} V_I^* + \gamma_1 = 0,$$

for

$$\begin{aligned}
\xi_1 &= \frac{d_V m_P (r_P P^* + d_I)}{(r_P P^* + d_I)[(m_P - d_I)(r_P P^* + d_I) - r_P P^* + d_I]} \\
\alpha_1 &= r_I^2 (d_I + r_P P^*) \\
\beta_1 &= r_I (d_I + r_P P^*)(m_P + d_S - m_P r_P P^*) + r_I (r_I \lambda - d_V r_I \lambda) + (m_P + r_P P^*)(d_I + r_P P^*) \\
&\quad - r_I^2 \xi_1 r_P P^* \lambda \\
\gamma_1 &= r_I r_P P^* \lambda \left(\frac{1}{\xi_1} - m_P - d_S + r_P P^* + d_I \right) \\
&\quad + \frac{m_P + r_P P^*}{\xi_1} [r_I \lambda - d_V r_I \lambda + (d_I + r_P P^*)(m_P + d_S - m_P r_P P^*)]
\end{aligned}$$

and where

$$
\begin{aligned}
V_N^* &= \frac{n_I(1-\omega)T_I^* + n_I T_{PI}^*}{d_V} \\
T_S^* &= \frac{\lambda + m_P T_{PN}^*}{r_I V_I^* + d_S + r_P P^*} \\
T_I^* &= \frac{d_V V_I^* + r_I T_S^* V_I^* + r_I T_{PN}^* V_I^*}{n_I \omega} \\
T_{PN}^* &= \frac{r_P T_S^* P^*}{m_P + r_I V_I^* + d_S} \\
T_{PI}^* &= \frac{r_P P^* T_I^* + r_I T_{PN}^* V_I^*}{m_P + d_I}.
\end{aligned}
$$

The mutant equilibrium is

$$(V_I, V_Y, V_N, T_S, T_I, T_Y, T_{PN}, T_{PI}, T_{PY}, P) = (0, V_Y^*, V_N^*, T_S^*, 0, T_Y^*, T_{PN}^*, 0, T_{PY}^*, P^*),$$

where V_Y^* is the positive root of the quadratic equation

$$\frac{\alpha_2}{\xi_2} V_Y^{*2} + \frac{\beta_2}{\xi_2} V_Y^* + \gamma_2 = 0,$$

for

$$
\begin{aligned}
\xi_2 &= \frac{(d_I + r_P P^*)(m_P + d_I) + m_P r_P P^*}{n_I \omega (d_I + r_P P^* + m_P)(m_P + d_I)} \\
\alpha_2 &= r_Y \\
\beta_2 &= d_S + r_P P^* - \xi r_Y (m_P + d_I) \\
\gamma_2 &= -\xi d_V (m_P + d_I)(d_S + r_P P^*) - r_Y \lambda (m_P + d_I) + r_Y \lambda
\end{aligned}
$$

and where

$$
\begin{aligned}
V_N^* &= \frac{n_I(1-\omega)T_Y^* + n_I(1-\omega)T_{PY}^*}{d_V} \\
T_S^* &= \frac{\lambda + m_P T_{PN}^*}{r_Y V_Y^* + d_S + r_P P^*} \\
T_Y^* &= \frac{r_Y V_Y^* T_S^* + m_P T_{PY}^*}{d_I + r_P P^*} \\
T_{PN}^* &= \frac{r_P P^* T_S^*}{d_S + r_Y V_Y^* + m_P} \\
T_{PY}^* &= \frac{r_P T_Y^* P^* + r_Y T_{PN}^* V_Y^*}{m_P + d_I}.
\end{aligned}
$$

The interior equilibrium is

$$(V_I, V_Y, V_N, T_S, T_I, T_Y, T_{PN}, T_{PI}, T_{PY}, P) = (V_I^*, V_Y^*, V_N^*, T_S^*, T_I^*, T_Y^*, T_{PN}^*, T_{PI}^*, T_{PY}^*, P^*),$$

where V_Y^* is the positive root of the quadratic equation

$$\delta_1 V_Y^{*2} + \delta_2 V_Y^* + (\alpha_1 + \alpha_2) = 0,$$

for

$$\alpha_1 = r_Y \lambda \left[(n_I\omega - (d_I + r_P P^*) + \eta_1 r_P P^*) \Big(m_P + d_S + \frac{\eta_3 - \eta_2}{a - b} \Big) + r_P P^* \eta_1 (r_P P^* + 1)(d_I + r_P P^*) \right]$$

$$\alpha_2 = (\eta_1 + r_P P^* d_V - d_V(d_I + r_P P^*)) \left[\Big(\frac{\eta_3 - \eta_2}{a - b} + d_S + r_P P^* \Big) (m_P + \frac{\eta_3 - \eta_2}{a - b} + d_S) - r_P P^* m_P \right]$$

$$\delta_1 = r_Y^2 \left(\frac{2b}{b - a} \right)^2 (\eta_1 + r_P P^* d_V - d_V(d_I + r_P P^*))$$

$$\delta_2 = r_Y^2 \lambda \left(\frac{2a}{a - b} \right)^2 (\eta_1 r_P P^* - r_P P^* - d_I + n_I\omega))$$

$$\eta_1 = \frac{n_I\omega m_P + n_I\omega(d_I + r_P P^*)}{m + P + d_I + n_I\omega r_P P^*}$$

$$\eta_2 = \frac{r_Y}{\eta_1 r_P P^* d_V - d_V(d_I + r_P P^*)} \Big[r_P P^* (\eta_1 (r_P P^* + 1)(d_I + r_P P^*)) + (n_I\omega - (d_I + r_P P^*) + \eta_1 r_P P^*)(m_P + d_S) \Big]$$

$$\eta_3 = \frac{r_I(m_P + d_I)}{d_V(m_P + d_I) - r_P P^* d_V} \Big[r_P P^* \Big(\frac{r_P P^* + n_I\omega}{m_P + d_I} - (d_I + r_P P^*) \Big) + \Big(n_I\omega - (d_I + r_P P^*) + \frac{r_P P^*}{m_P + d_I} \Big) (m_P + d_S) \Big]$$

$$a = \frac{r_Y}{\eta_1 r_P P^* d_V - d_V(d_I + r_P P^*)} \Big[n_I\omega - d_I - r_P P^* - \eta_1 r_P P^* \Big]$$

$$b = \frac{r_I(m_P + d_I)}{r_P P^* d_V - d_V(m_P + d_I)} \Big[n_I\omega - d_I - r_P P^* + \frac{r_P P^*}{m_P + d_I} \Big],$$

and where

$$
\begin{aligned}
V_I^* &= \frac{n_I \omega T_I^*}{d_V + r_I T_S^* + r_I T_{PN}^*} \\
V_N^* &= \frac{n_I(1-\omega)(T_I^* + T_Y^* + T_{PY}^*) + n_I T_{PI}^*}{d_V} \\
T_S^* &= \frac{\lambda(m_P + r_Y V_Y^* + r_I V_I^* + d_S)}{(r_Y V_Y^* + r_I V_I^* + d_S + r_P P^*)(r_Y V_Y^* + r_I V_I^* + d_S) + m_P(r_Y V_Y^* + r_I V_I^* + d_S)} \\
T_I^* &= \frac{V_I^*(d_V + r_I T_S^* + r_I T_{PN}^*)}{n_I \omega} \\
T_Y^* &= \frac{r_Y V_Y^* T_S^* + m_P T_{PY}^*}{d_I + r_P P^*} \\
T_{PN}^* &= \frac{r_P P^* T_S^*}{m_P + r_Y V_Y^* + r_I V_I^* + d_S} \\
T_{PI}^* &= \frac{r_P P^* T_I + r_I T_{PN}^* V_I^*}{m_P + d_I} \\
T_{PY}^* &= \frac{r_P P^* V_Y^*(d_V + r_Y T_S^* + r_Y T_{PN}^*) + r_Y T_{PN}^* V_Y^*}{m_P + d_I + n_I \omega r_P P^*}.
\end{aligned}
$$

Theorem 3.1.5. *When the endemic equilibria exist and we have that $R_{0,2,a} > 1$ and $R_{0,2,b} > 1$, the wild-type and resistant strains will coexist in Region 2.*

Proof. For the wild-type equilibrium, $V_Y^* = 0$, the characteristic polynomial is

$$
\begin{aligned}
0 &= \det(J(V_I^*, V_Y^*, V_N^*, T_S^*, T_I^*, T_Y^*, T_{PN}^*, T_{PI}^*, T_{PY}^*, P^*) - \mu I_{10}) \\
&= (-d_V - \mu)(-d_P - \mu)[\mu^3 + a\mu^2 + b\mu + c] f(\mu),
\end{aligned}
$$

where

$$
f(\mu) = \det \begin{bmatrix}
-d_V - r_I T_S^* - r_I T_{PN}^* & -r_I V_I^* & n_I \omega & -r_I V_I^* & 0 \\
-r_I T_S^* & -r_I V_I^* - d_S - r_P P^* & 0 & m_P & 0 \\
r_I T_S^* & r_I V_I^* & -d_I - r_P P^* & 0 & m_P \\
-r_I T_{PN}^* & r_P P^* & 0 & -m_P - d_S - r_I V_I^* & 0 \\
r_I T_{PN}^* & 0 & r_P P^* & r_I V_I^* & -m_P - d_I
\end{bmatrix}
$$

and where

$$
\begin{aligned}
a &= 2d_I + r_P P^* + m_P + d_V + r_Y T_S^* + r_Y T_{PN}^* \\
b &= (d_V + r_Y T_S^* + r_Y T_{PN}^*)[(m_P + d_I) + (d_I + r_P P^*)] + (d_I + r_P P^*)(m_P + d_I) \\
&\quad - r_Y T_S^* n_I \omega + m_P r_P P^* - r_Y T_{PN}^* n_I \omega \\
c &= -n_I \omega r_Y T_S^*(m_P + d_I) + (d_V + r_Y T_S^* + r_Y T_{PN}^*)(m_P d_I + d_I^2 + d_I r_P P^*) - r_P P^* n_I \omega r_Y T_S^* \\
&\quad - r_Y T_{PN}^* n_I \omega m_P - r_Y T_{PN}^* n_I \omega (d_I + r_P P^*) \\
&= d_I(r_Y T_{PN}^* + r_Y T_S^* + d_V)(d_I + r_P P^* + m_P)(1 - R_{0,2,a}).
\end{aligned}
$$

We have $a > 0$ and $c < 0$ if $R_{0,2,a} > 1$. Hence, by the Routh-Hurwitz conditions [38, 39], the Jacobian matrix has an eigenvalue with a positive real part and thus the wild-type equilibrium is unstable.

For the mutant equilibrium, $V_I^* = 0$, the characteristic polynomial is

$$\begin{aligned} 0 &= \det(J(V_I^*, V_Y^*, V_N^*, T_S^*, T_I^*, T_Y^*, T_{PN}^*, T_{PI}^*, T_{PY}^*, P^*) - \mu I_{10}) \\ &= (-d_V - \mu)(-d_P - \mu)[\mu^3 + a\mu^2 + b\mu + c]f(\mu), \end{aligned}$$

where

$$f(\mu) = \det \begin{bmatrix} -d_V - r_I T_S - r_Y T_{PN} & -r_Y V_Y & n_I\omega & -r_Y V_Y & n_I\omega \\ -r_Y T_S & -r_Y V_Y - d_S - r_P P & 0 & m_P & 0 \\ r_Y T_S & r_Y V_Y & -d_I - r_P P & 0 & m_P \\ -r_Y T_{PN} & r_P P & 0 & m_P - d_S - r_Y V_Y & 0 \\ r_Y T_{PN} & 0 & r_P P & r_Y V_Y & -m_P - d_I \end{bmatrix}$$

and where

$$\begin{aligned} a &= 2d_I + r_P P^* + m_P + d_V + r_I T_S^* + r_I T_{PN}^* \\ b &= (d_V + r_I T_S^* + r_I T_{PN}^*)[(m_P + d_I) + (d_I + r_P P^*)] + (d_I + r_P P^*)(m_P + d_I) \\ &\quad - r_I T_S^* n_I \omega - m_P r_P P^* \\ c &= -n_I \omega r_I T_S^*(m_P + d_I) + (d_V + r_I T_S^* + r_I T_{PN}^*)(m_P + d_I)(d_I + r_P P^*) \\ &\quad - r_P P^* m_P (d_V + r_I T_S^* + r_I T_{PN}^*) - m_P n_I \omega r_I T_{PN}^* \\ &= d_I(r_I T_{PN}^* + r_I T_S^* + d_V)(d_I + r_P P^* + m_P)(1 - R_{0,2,b}). \end{aligned}$$

In this case, $a > 0$ and $c < 0$ if $R_{0,2,a} > 1$. It follows from the Routh-Hurwitz conditions [38, 39] that the wild-type equilibrium has an eigenvalue with a positive real part and is thus unstable.

Since the disease-free, wild-type and mutant equilibria are all locally unstable, this implies that the wild-type and resistant strains will co-exist. □

In summary, if $R_{0,2} < 1$, the disease-free equilibrium is locally asymptotically stable in Region 2, and if $R_{0,2} > 1$, the wild-type and resistant strains will co-exist in Region 2. However, it should be noted that it is not necessarily the interior orbit that trajectories approach. There may be other interior periodic orbits or more complex behaviour in which both strains coexist. Nevertheless, in this region, the mutant is not eliminated.

3.1.3 Region 3: High drug levels

If $r_P \geq r_{PP}$, system (2.5) has three equilibria: disease free (extinction of virus and infected cells), wild type (extinction of mutant) and mutant (extinction of wild type). In all three cases, there is a P^* such that $P^* > P_2$. If $r_P < r_{PP}$, then there is also an interior equilibrium, but we expect from the dose-effect curves that this will not be the case [40].

Disease-free equilibrium

The disease-free equilibrium is

$$(V_I, V_Y, V_N, T_S, T_I, T_Y, T_{PN}, T_{PI}, T_{PY}, T_{PPN}, T_{PPI}, T_{PPY}, P) = (0, 0, 0, T_S^*, 0, 0, T_{PN}^*, 0, 0, T_{PPN}^*, 0, 0, P^*),$$

where

$$\begin{aligned} T_S^* &= \frac{\lambda + m_P T_{PN}^*}{d_S + r_P P^*} \\ T_{PN}^* &= \frac{r_P P^* T_S^* + m_{PP} T_{PPN}^*}{m_P + d_S + r_{PP} P^*} \\ T_{PPN}^* &= \frac{r_{PP} P^* T_{PN}^*}{m_{PP} + d_S}. \end{aligned}$$

The basic reproductive number in Region 3, $R_{0,3}$, is computed as before using the next-generation method and is given by

$$R_{0,3} = \max\{R_{0,3,a}, R_{0,3,b}\} \tag{3.13}$$

where

$$R_{0,3,a} = \frac{n_I \omega \Big((d_I + r_P P^* + m_P)(m_{PP}(r_Y T_S^* + r_Y T_{PN}^* + r_Y T_{PPN}^*) + d_I(r_Y T_S^* + r_Y T_{PN}^*)) + r_Y T_S^* d_I r_{PP} P^* \Big)}{d_I(d_V + r_Y T_S^* + r_Y T_{PN}^* + r_Y T_{PPN}^*)\Big(d_I(d_I + r_P P^* + m_P + r_{PP} P^* + m_{PP}) + m_P m_{PP} + r_P P^* m_{PP} + r_P P^* r_{PP} P^* \Big)}$$

$$R_{0,3,b} = \frac{n_I \omega \Big((d_I + m_P)(m_P(r_I T_S^* + r_I T_{PN}^*) + d_I r_I T_S^*) + d_I r_{PP} P^* r_I T_S^* + m_P m_{PP} r_I T_{PPN}^* \Big)}{d_I(d_V + r_I T_S^* + r_I T_{PN}^* + r_I T_{PPN}^*)\Big(d_I(d_I + r_P P^* + m_P + r_{PP} P^* + m_{PP}) + m_P m_{PP} + r_P P^* m_{PP} + r_P P^* r_{PP} P^* \Big)}$$

The Jacobian matrix for Region 3 is $J = [J_1|J_2|J_3]$, where

$$J_1 = \begin{bmatrix} -d_V - r_I T_S - r_I T_{PN} - r_I T_{PPN} & 0 & 0 & -r_I V_I \\ 0 & -d_V - r_Y T_S - r_Y T_{PN} - r_Y T_{PPN} & 0 & -r_Y V_Y \\ 0 & 0 & -d_V & 0 \\ -r_I T_S & -r_Y T_S & 0 & -r_I V_I - r_Y V_Y - d_S - r_P P \\ r_I T_S & 0 & 0 & r_I V_I \\ 0 & r_Y T_S & 0 & r_Y V_Y \\ -r_I T_{PN} & -r_Y T_{PN} & 0 & r_P P \\ r_I T_{PN} & 0 & 0 & 0 \\ 0 & r_Y T_{PN} & 0 & 0 \\ -r_I T_{PPN} & -r_Y T_{PPN} & 0 & 0 \\ r_I T_{PPN} & 0 & 0 & 0 \\ 0 & r_Y T_{PPN} & 0 & 0 \\ 0 & 0 & 0 & 0 \end{bmatrix}$$

$$J_2 = \begin{bmatrix} n_I\omega & 0 & -r_I V_I & 0 \\ 0 & n_I\omega & -r_Y V_Y & 0 \\ n_I(1-\omega) & n_I(1-\omega) & 0 & n_I \\ 0 & 0 & m_P & 0 \\ -d_I - r_P P & 0 & 0 & m_P \\ 0 & -d_I - r_P P & 0 & 0 \\ 0 & 0 & -m_P - r_Y V_Y - r_I V_I - d_S - r_{PP} P & 0 \\ r_P P & 0 & r_I V_I & -m_P - d_I - r_{PP} P \\ 0 & r_P P & r_Y V_Y & 0 \\ 0 & 0 & r_{PP} P & 0 \\ 0 & 0 & 0 & r_{PP} P \\ 0 & 0 & 0 & 0 \\ 0 & 0 & 0 & 0 \end{bmatrix}$$

$$J_3 = \begin{bmatrix} 0 & -r_I V_I & 0 & 0 & 0 \\ n_I\omega & -r_Y V_Y & 0 & 0 & 0 \\ n_I(1-\omega) & 0 & n_I & n_I & 0 \\ 0 & 0 & 0 & 0 & -r_P T_S \\ 0 & 0 & 0 & 0 & -r_P T_I \\ m_P & 0 & 0 & 0 & -r_P T_Y \\ 0 & m_{PP} & 0 & 0 & r_P T_S - r_{PP} T_{PN} \\ 0 & 0 & m_{PP} & 0 & r_P T_I - r_{PP} T_{PI} \\ -m_P - d_I - r_{PP} P & 0 & 0 & m_{PP} & r_P T_Y - r_{PP} T_{PY} \\ 0 & -m_{PP} - r_I V_I - r_Y V_Y - d_S & 0 & 0 & r_{PP} T_{PN} \\ 0 & r_I V_I & -m_{PP} - d_I & 0 & r_{PP} T_{PI} \\ r_{PP} P & r_Y V_Y & 0 & -m_{PP} - d_I & r_{PP} T_{PY} \\ 0 & 0 & 0 & 0 & -d_P \end{bmatrix}.$$

The region of viral elimination

We now investigate the conditions under which the disease-free equilibrium becomes stable. We will consider a subset of Region 3, called Region 4, where P^* is sufficiently large so that the disease-free equilibrium is asymptotically stable. We shall refer to this subset of Region 3 as the region of viral elimination. Rearranging terms in T^*_{PN} from the disease-free equilibrium, we get

$$T^*_{PN} = \frac{\lambda r_P P^*(m_{PP} + ds)}{(d_S^2 + d_S r_{PP} P^* + d_S m_{PP})(d_S + r_P P^*) + d_S m_P (m_{PP} + d_S)}.$$

If we divide the numerator and the denominator by P^{*2} and take $P^* \to \infty$, we get

$$T^*_{PN} \to 0$$

in Region 4. Since $T^*_{PN} \to 0$ and $P^* \to \infty$, this implies that $T^*_S \to 0$. Rearranging terms in T^*_{PPN} from the disease-free equilibrium, we get

$$T^*_{PPN} = \frac{\lambda r_{PP} r_P P^{*2}}{(d_S^2 + d_S r_{PP} P^* + d_S m_{PP})(d_S + r_P P^*) + d_S m_P (m_{PP} + d_S)}.$$

Again, if we divide the numerator and the denominator by P^{*2} and take $P^* \to \infty$, we get

$$T^*_{PPN} \to \frac{\lambda}{d_S}.$$

Thus, in Region 4, when $P^* \to \infty$, the disease-free equilibrium has $T^*_S \to 0$, $T^*_{PN} \to 0$ and $T^*_{PPN} \to \dfrac{\lambda}{d_S}$.

The basic reproductive number for Region 4 is such that $R_{0,3} < 1$. When $P^* \to \infty$, we see that $R_{0,3}$ defined by (3.13) equals zero meaning in the limit of $P^* \to \infty$, the basic reproductive number certainly drops below unity.

Theorem 3.1.6. *The disease-free equilibrium is locally asymptotically stable when $P^* \to \infty$.*

Proof. Computing the Jacobian in Region 4 for the disease-free equilibrium, $V^*_I = V^*_Y = 0$, we get the characteristic polynomial

$$\begin{aligned} 0 &= \det\left(J(V^*_I, V^*_Y, V^*_N, T^*_S, T^*_I, T^*_Y, T^*_{PN}, T^*_{PI}, T^*_{PY}, T^*_{PPN}, T^*_{PPI}, T^*_{PPY}, P^*) - \mu I_{13}\right) \\ &= (-d_P - \mu)(-d_V - \mu)(\mu^7 + a_1\mu^6 + a_2\mu^3 + a_3\mu^4 + a_4\mu^3 + a_5\mu^2 + a_6\mu + a_7) f(\mu) \end{aligned}$$

where

$$f(\mu) = \det \begin{bmatrix} -d_V - r_Y T_{PPN} - \mu & n_I\omega & n_I\omega & 0 \\ 0 & -d_I - r_P P - \mu & m_P & 0 \\ 0 & r_P P & -m_P - r_{PP} P - d_I - \mu & m_{PP} \\ r_Y T_{PPN} & 0 & r_{PP} P & -m_{PP} - d_I - \mu \end{bmatrix}.$$

When taking $P^* \to \infty$, the seventh-order polynomial can be reduced to a third-order characteristic polynomial $\mu^3 + b_1\mu^2 + b_2\mu + b_3$, where

$$\begin{aligned} b_1 &= 2m_{PP} + d_S + d_I + d_V + r_I T^*_{PPN} \\ b_2 &= m_{pp}(d_S + d_V + r_I T^*_{PPN}) + (d_I + m_{PP})(d_V + r_I T^*_{PPN}) + d_S(d_I + m_{PP} + d_V + r_I T^*_{PPN}) \\ b_3 &= m_{PP} d_S (d_V + r_I T^*_{PPN}) + d_S (d_I + m_{PP})(d_V + r_I T^*_{PPN}). \end{aligned}$$

By the Routh-Hurwitz conditions [38, 39], the third order polynomial has all roots with negative real part if $b_1, b_3 > 0$ and $b_1 b_2 > b_3$. The Routh-Hurwitz conditions are always satisfied when $P^* \to \infty$, meaning the third order polynomial has all eigenvalues with negative real part.

Computing the determinant of $f(\mu)$ and taking $P^* \to \infty$, the fourth-order polynomial can be reduced to a second-order characteristic polynomial $\mu^2 + a\mu + b$, where

$$a = d_V + r_Y T^*_{PPN} + d_I$$
$$b = (d_V + r_Y T^*_{PPN}) d_I.$$

By the Routh-Hurwitz condition [38, 39], $f(\mu)$ has all roots with negative real part. Therefore, the disease-free equilibrium is locally asymptotically stable in Region 4 for $P^* \to \infty$. □

Note that elimination of free virus for this model is not equivalent to clearing the infection. See Discussion for more details.

It can also be shown that the wild-type equilibrium in Region 4 gives

$$V^*_I = -\Big(\frac{r_I\lambda + d_V d_S}{d_V r_I}\Big)$$
$$V^*_N = \frac{n_I(1-\omega)T^*_I + n_I(T^*_{PI} + T^*_{PPI})}{d_V}$$
$$T^*_S = \frac{\lambda + m_P T^*_{PN}}{r_I V^*_I + d_S + r_P P^*}$$
$$T^*_{PN} = \frac{r_P P^* T^*_S + m_{PP} T^*_{PPN}}{m_P + r_I V^*_I + d_S + r_{PP} P^*}$$
$$T^*_{PPN} = \frac{r_{PP} P^* T^*_{PN}}{m_{PP} + r_I V^*_I + d_S}$$
$$T^*_I = \frac{r_I V^*_I T^*_S + m_P T^*_{PI}}{d_I + r_P P^*}$$
$$T^*_{PI} = \frac{r_I V^*_I T^*_{PN} + r_P P^* T^*_I + m_{PP} T^*_{PPI}}{m_P + r_{PP} P^* + d_I}$$
$$T^*_{PPI} = \frac{r_I V^*_I T^*_{PPN} + r_{PP} P^* T^*_{PI}}{m_{PP} + d_I}$$

and the drug-resistant equilibrium in Region 4 gives

$$
\begin{aligned}
V_Y^* &= -\Big(\frac{r_Y\lambda(r_{PP}+d_S(r_P+r_{PP}))+d_Sd_Vr_{PP}}{r_Y^2\lambda(r_P+r_{PP})+d_Vr_Yr_{PP}}\Big)\\
V_N^* &= \frac{n_I(1-\omega)(T_Y^*+T_{PY}^*)+n_IT_{PPY}^*}{d_V}\\
T_S^* &= \frac{\lambda+m_PT_{PN}^*}{r_YV_Y^*+d_S+r_PP^*}\\
T_{PN}^* &= \frac{r_PP^*T_S^*+m_{PP}T_{PPN}^*}{m_P+r_YV_Y^*+d_S+r_{PP}P^*}\\
T_{PPN}^* &= \frac{r_{PP}P^*T_{PN}^*}{m_{PP}+r_YV_Y^*+d_S}\\
T_Y^* &= \frac{r_YV_Y^*T_S^*+m_PT_{PY}^*}{d_I+r_PP^*}\\
T_{PY}^* &= \frac{r_YV_Y^*T_{PN}^*+r_PP^*T_Y^*+m_{PP}T_{PPY}^*}{m_P+r_{PP}P^*+d_I}\\
T_{PPY}^* &= \frac{r_YV_Y^*T_{PPN}^*+r_{PP}P^*T_{PY}^*}{m_{PP}+d_I}.
\end{aligned}
$$

These are biologically meaningless in Region 4 since V_I^* and V_Y^* are negative.

In summary, if $P^* \to \infty$, the disease-free equilibrium is locally asymptotically stable and viral elimination is theoretically possible.

3.1.4 Summary of asymptotic behaviour

In summary for this section, we find that, at low drug levels (Region 1), resistance does not emerge and thus the wild-type strain dominates. In contrast, at intermediate drug levels (Region 2), drug resistance is guaranteed to emerge. Recall that we have defined intermediate drug levels as the regime in which the drugs significantly inhibit replication of the wild-type strain but have negligible effect on the drug-resistant strain.

For high drug levels (Regions 3), there exists a region (Region 4) where both populations of free virus will be driven to extinction. (We note that our model does not consider longer-lived reservoirs of virus, such as latent T cells, and thus elimination of free virus in our model is not equivalent to clearing infection.) Thus, if the drug level is very large, virus elimination is theoretically possible.

3.2 Equilibrium T cell counts

In this section, we examine the total uninfected T cell count at the stable equilibrium predicted in low, intermediate and high drug concentrations.

For low drug levels ($P < P_1$), we know from Section 3.1.1 that the wild-type

virus dominates. The total uninfected T cell count in Region 1 is

$$\overline{T}_S = \frac{d_I d_V}{r_I(n_I\omega - d_I)}.$$

Since n_I is large, $\overline{T}_S$ is small. Thus there are low levels of uninfected T cells in Region 1.

For intermediate drug levels ($P_1 < P < P_2$), we use the results of Section 3.1.2 to show the total uninfected T cell count for the interior equilibrium is

$$\begin{aligned} T_S^* + T_{PN}^* &= T_S^* + \frac{r_P P^* T_S^*}{m_P + d_S} \\ &= T_S^*\Big(1 + \frac{r_p P^*}{m_P + d_S}\Big) \\ &= T_S^*(1+\epsilon), \end{aligned}$$

where ϵ is small since m_P is large compared to P^* in Region 2. For realistic parameters in the intermediate drug levels (see Table 1), the total number of uninfected T cells is only slightly larger than for low drug levels.

For high drug levels ($P > P_2$), we examine the effect on the total uninfected T cell count as the dosing interval shrinks to zero, or as the doses increase to infinity, which we have defined as Region 4. The total number of uninfected T cells in Region 4 approaches

$$T_S^* + T_{PN}^* + T_{PPN}^* \to \frac{\lambda}{d_S},$$

where $T_S^* \to 0$, $T_{PN}^* \to 0$ and $T_{PPN}^* \to \dfrac{\lambda}{d_S}$ when $P^* \to \infty$ (described in Section 3.1.3). Thus the total number of uninfected T cells in Region 4 is identical to the disease-free state as $P^* \to \infty$. This implies that, if drug levels are sufficiently high, the number of infected T cells approaches that of the uninfected patient.

Note that we do not explicitly have the total number of uninfected T cells in Region 3. Based on numerical simulations shown in the inset of Figure 4C, the total uninfected T cell count is not as high as in Region 4.

4 Including impulses

We demonstrate the effects of varying the drug concentration levels by including an impulse (equation (2.7)). Adding this perturbation will cause drug concentration levels to fluctuate between regions. The endpoints of the impulsive periodic orbit are used in order to bound the orbit to stay within a region meaning the representative value P^* stays within a specific region. The endpoints are also used in order to show the effects of trajectories crossing multiple regions; this does not apply if P^* is constant.

4.1 Region thresholds

We demonstrate the various T cell, virus and drug behaviours given that the drug concentrations may move through all four regions. Based on the results of stability with P constant in Section 3, we expect that, when including the impulse condition and $P(t)$ is low, the wild-type strain of the virus should dominate. When $P(t)$ increases (attaining intermediate levels), the wild-type strain can co-exist with the mutant. When $P(t)$ becomes high, the mutant strain will dominate unless $P(t)$ is very high, where we expect viral elimination. Depending on the amount of time the drug spends in each region (if any), trajectories will likely oscillate, with either coexistence, one or the other strain gaining dominance, or the drugs eliminating both strains.

It was shown in Miron and Smith? [34], assuming perfect adherence, that the impulsive periodic orbit has endpoints

$$P(t_n^-) \to \frac{P^i e^{-d_P \tau}}{1 - e^{-d_P \tau}}$$

and

$$P(t_n^+) \to \frac{P^i}{1 - e^{-d_P \tau}},$$

as $n \to \infty$. Here P^i is the dosage, d_P is the rate at which the drug is cleared and $\tau = t_{k+1} - t_k$ is the (fixed) time between doses for perfect adherence.

It follows that trajectories will remain solely in Region 1 if

$$0 < P^i < P_1(1 - e^{-d_P \tau}).$$

Trajectories will remain solely in Region 2 if

$$P_1 e^{d_P \tau}(1 - e^{-d_P \tau}) < P^i < P_2(1 - e^{-d_P \tau}).$$

Finally, trajectories will remain solely in Region 3 if

$$P^i > P_2 e^{d_P \tau}(1 - e^{-d_P \tau}).$$

4.2 Numerical simulations

We now illustrate the dynamics of drug concentrations fluctuating between different regions. Figure 3 demonstrates the regions drug concentration trajectories will visit, for various combinations of dosing interval and dose. The curves plotted are

$$P^i = P_1(1 - e^{-d_P \tau})$$
$$P^i = P_1 e^{d_P \tau}(1 - e^{-d_P \tau})$$
$$P^i = P_2(1 - e^{-d_P \tau})$$
$$P^i = P_2 e^{d_P \tau}(1 - e^{-d_P \tau}).$$

The asterisk in Figure 3 is the FDA-approved dosage and dosing interval for the protease inhibitor ritonavir. The recommended dose lies in Region 3.

Figures 4 and 5 illustrate phase-plane plots of the populations of cells able to produce the wild-type or drug-resistant viral strains. Figure 4 illustrates the drug concentrations remaining in one specific region whereas Figure 5 illustrates the drug concentrations when two or more regions are crossed. In all cases, parameters and initial conditions are as in Table 2, with only the dosing interval τ and the dosage P^i varied. The insets in Figure 4 show the total number of uninfected T cells or T cells that only produce non-infectious virions. It should be noted that the results from Figure 4 are similar if P is fixed or if it's oscillating, since the endpoints of the periodic orbit remain solely within a region. Figure 5 occurs only if P oscillates between two or more regions.

In Region 1, the wild-type virus dominates. Initially, both strains of the virus can infect cells (initial increase in Figure 4A), but if the system stays in Region 1, the wild-type strain will out-compete the mutant strain. The end result is only wild-type-infected cells (Figure 4A) and low amounts of susceptible T cells (inset of Figure 4A).

If the drug forces the system to stay within Region 2, the mutant strain is the better competitor since it faces no evolutionary pressure, unlike the wild-type. The distance between Region 1 and Region 2 is so small that it is likely that the drug will never remain solely in Region 2. For Figure 4B, we increased the Region 2 threshold to $P_2 = 10^1$ in order to show numerically the effect of staying in Region 2. The end result is coexistence of the wild-type and mutant infected cells with high amounts of T cells able to produce resistant virus, and low amounts of uninfected T cells (inset of Figure 4B).

If a large enough amount of drug is taken to enter and remain solely in Region 3, there are higher numbers of mutant-infected cells than wild-type-infected cells (Figure 4C). There is also an increase in the number of mutant-infected T cells inhibited with high drug concentrations (inset of Figure 4C).

If P is very large such that the system reaches Region 4, there are a large number of uninfected T cells with high drug concentrations (inset of Figure 4D) and all the T cells able to produce infectious virions are eliminated (Figure 4D). Note that Figures 4A, 4C and 4D use the same parameters except the dosing interval and the dosage.

More than likely, the drug will allow the system to cross multiple regions. Figure 5 illustrates the dynamics when trajectories cross more than one region.

Figure 5A shows that, initially, both the wild-type and mutant virus infect susceptible T cells; the curve mimics that of remaining solely in Region 1. Once the drug fluctuates between Regions 1 and 2, the mutant strain is the better competitor in Region 2, but the wild-type strain is better in Region 1. This can be seen by the impulses shown in Figure 5A. The impulses are better shown by the sharp edges in the inset of Figure 5A where we have discontinuities in the derivatives. The end result is coexistence between strains but mostly all wild-type-infected T cells, meaning the system behaves similarly to Region 1. Again, we increase the Region 2 threshold to $P_2 = 10^1$ in order to show numerically the effect of staying below the Region 2 threshold since the distance between

the Region 2 and 3 thresholds is so small.

When the system fluctuates between Regions 2 and 3, we observe impulses in both the wild-type and mutant-infected T cells (Figure 5B). The end result is a large number of mutant-infected T cells. Here, again, we increase the distance between the Regions 1 and 2 thresholds in order to show the results of crossing between Regions 2 and 3. We have coexistence, but mostly the mutant strain dominates. The inset of Figure 5B shows the increase in wild-type-infected T cells unable to produce infectious virions.

When the drug forces the system to move between Regions 1, 2 and 3, we have near-viral elimination each time the system jumps into high levels of Region 3 (Figure 5C). The inset of Figure 5C shows how the trajectories enter Region 4 by causing the infected T cells to approach zero. Then an impulse occurs, after which the mutant and wild-type strains increase, causing fluctuations in the infected T cells and moving away from viral elimination. As a result, there is coexistence but many more T cells infected by the mutant strain.

In summary, if we include a fluctuation of drug levels, the mutant either dominates or coexists in all cases. Whenever Region 2 is entered, the mutant gains a rapid advantage.

4.3 Sensitivity to variations

Since parameters may fluctuate, we explore the sensitivity of R_0 to the parameter values using Latin Hypercube Sampling (LHS). LHS is a statistical sampling method that allows for an efficient analysis of parameter variations across simultaneous uncertainty ranges in each parameter [44, 45]; partial rank correlation coefficients rank the coefficients by the degree of influence each has on the outcome, regardless of whether that influence increases or decreases the effect.

Figures 6A, 7A, 8A and 9A show the partial rank correlation coefficient sensitivity analysis for 1000 runs. All relevant parameters are varied against R_0 throughout the ranges given in Table 2. In all regions, R_0 is the most sensitive to the death rate for the infected $CD4^+$ T cells, d_I; the effect of d_I on R_0 can also be seen in Figures 6B, 7B, 8B and 9B for Regions 1, 2, 3 and 4 respectively. In Regions 1, 2 and 3, R_0 is also sensitive to the number of infectious virions produced per day from an infected $CD4^+$ T cell, $n_I\omega$; the effect of $n_I\omega$ on R_0 can also be seen in Figures 6C, 7C and 8C for Regions 1, 2 and 3 respectively. In Region 3, R_0 is also sensitive to the infection rate of susceptible $CD4^+$ T cells with mutant virus, r_Y; the effect of r_Y on R_0 in Region 3 can also be seen in Figure 8D. In Region 4, R_0 is sensitive to the clearance rate of the drug from a highly inhibited cell, m_{PP}, and the drug dosage, P^*; the effect of m_{PP} and P^* on R_0 in Region 4 can also be seen in Figures 9C and 9D respectively. Figures 6, 7 and 8 B, C, and D run using a Monte Carlo simulation with parameters drawn using LHS. The LHS of all remaining parameters not seen in Figures 6, 7, 8 and 9 are approximately uniformly scattered. Varying $n_I\omega$ and d_I does not reduce R_0 below 1 in Regions 1 or 2. In Region 3 however, there are values for which $R_0 < 1$, corresponding to the region of viral elimination. As P^* gets

very large, varying the parameters does make R_0 increase beyond unity; R_0 is always below unity in Region 4. Note that the difference between variations in P^* and the impulse effects are that P^* varies in an orderly way, whereas the impulse occurs at a fixed, regular time. Thus if P^* varies slightly, it may not have a big affect on R_0 since the impulse may be the cause of the change.

5 Discussion

Drug therapy is crucial to the well-being and survival of HIV-infected patients. The strict drug regimens are often difficult to follow due to major side effects and pill fatigue. We have shown the different effects of having low, intermediate and high levels of drug concentration in a cell, and shown that, in all cases, entering Region 2 causes the mutant to gain rapid advantage.

Initially, we showed the effects on the wild-type and mutant virus populations when drug concentrations in a cell are constant at either low, intermediate or high levels. We conclude that, if the drug level is at an intermediate or high state, then drug resistance will emerge. We also showed that there is a theoretical region of free-virus elimination.

The number of uninfected T cells was also calculated in each region for a constant drug concentration. This is important because a higher number of uninfected T cells means a greater chance of controlling the virus and fighting off opportunistic infections. We showed that the total uninfected T cell count in Region 4 approaches that of the disease-free state. We also showed that Region 2 not only has low levels of uninfected T cells, it also has a large number of T cells able to produce the mutant strain. Similar results apply numerically when drug-concentration levels vary.

Numerical simulations showed the effects of varying the drug-concentration levels. This perturbation, included in the impulse, allows us to examine the effects of varying the drug-concentration levels either solely within a region or across multiple regions. Entering Region 2 depends on the drug dosage and the dosing interval. We have shown that T cells able to produce the mutant strain will dominate if trajectories enter Region 2. This will cause drug resistance and drug failure. It was also shown that crossing all 3 regions results in a high number of T cells able to produce the mutant strain. We have also shown that Region 1 has a high number of T cells able to produce the wild-type strain and a low number of T cells able to produce the mutant strain. Thus it is better for trajectories to remain in Region 1 than in Region 2 since the wild-type strain can be controlled by antiretroviral therapy.

The recommended dosage and dosing interval for one of the FDA-approved protease inhibitors, ritonavir, is shown in Figure 3. If taken with perfect adherence, the recommended dosage and dosing interval would remain in Region 3, causing the mutant strain to remain very low. However, if the drug is not administered at the recommended time (twice a day for ritonavir), then trajectories would fall into Region 2 (by moving to the right in Figure 3) where a rapid outbreak of mutant virus would occur. This can also be seen from Figure

4. The high amount of mutant-infected T cells inhibited with high drug levels in Region 3 (inset of Figure 4C) would rapidly become T cells that are able to produce infectious mutant virions when the drug level lowers and enters Region 2. Thus adherence is crucial to avoid the development of resistance.

Both a high dosage and small dosing interval are necessary in order to avoid drug resistance and theoretically attain viral elimination. Although drug toxicities may limit the extent to which this optimum can be approached, such a scenario is theoretically possible for protease inhibitors. One limitation is that the model does not include certain viral reservoirs such as latently infected cells or reproductive reservoirs. These reservoirs would cause the virus to persist even when in Region 4. Thus, elimination of free virus in our model is not equivalent to clearing the infection. A further limitation is that we restricted P^* to be constant in the analysis. Similar results can numerically be shown for varying drug levels. Future work would be to develop and compute stability analysis with varying drug levels in order to theoretically show the same results that are shown numerically in the Figures 4 and 5. Another limitation is that the system only includes protease inhibitors. In reality, most patients take triple drug cocktails including protease inhibitors and reverse transcriptase inhibitors, fusion inhibitors and/or integrase inhibitors. This would also change the dynamics of the system. Combination therapy can down-regulate the effectiveness of certain drugs, meaning their half-life and IC_{50} values could change. Future work would be to examine the effects of combination therapy using impulsive differential equations.

It should be noted that our model considers monotherapy for a single protease inhibitor (or, equivalently, an aggregate of multiple protease inhibitors with the same treatment cycle). Although monotherapy is not recommended, it is often used in the developing world, especially where economics make combination therapy impossible [24]. Monotherapy is sometimes used when other treatments have failed, or used after prolonged viral suppression. Bierman *et al.* [25] and Calza and Manfredi [26] showed that patients with prolonged viral suppression on highly active antiretroviral therapy (HAART) can successfully be treated with protease inhibitor monotherapy. Pillay *et al.* [27] showed that a boosted protease inhibitor monotherapy following a 24 week second-line induction was associated with an increase in low level viraemia, although generally in the absence of PI resistance. Furthermore, understanding monotherapy is a useful precursor for developing complex models of combination therapy.

It is theoretically possible to eliminate free virus in this system if the drug concentration level is very high. The total uninfected T cell count in Region 4 is similar to that of the disease-free state. It was shown numerically that the results for constant drug concentration are similar to varying drug concentrations. Thus high dosage and low interval time between doses can theoretically lead to an elimination of free virus and a disease-free uninfected T cell count.

Acknowledgements

REM is funded by an Ontario Graduate Scholarship. RJS? is supported by an NSERC Discovery Grant, an Early Researcher Award and funding from MITACS.

References

[1] Pillay, D., Bhaskaran, K., Jurriaans, S., Prins, M., Masquelier, B., Dabis, F., Gifford, R., Nielsen, C., Pedersen, C., Balotta, C., Rezza, G., Ortiz, M., de Mendoza, C., Kucherer, C., Poggensee, G., Gill, J., Porter K. 2006. The impact of transmitted drug resistance on the natural history of HIV infection and response to first-line therapy. *AIDS* **20**, 21-28.

[2] Janeway, C., Travers, P., Walport, M., Shlomchik, M. 2006. *Immunobiology: the immune system in health and disease, 6th edition.* GS: Garland Science, Taylor & Francis Group, pg. 461-510.

[3] Wheeler, W.H., Ziebell, R. A., Zabina, H., Pieniazek, D., Prejean, J., Bodnar, U.R., Mahle, K.C., Heneine, W., Johnson, J.A., Hall, H.I. 2010. Prevalence of transmitted drug resistance associated mutations and HIV-1 subtypes in new HIV-1 diagnoses, U.S.-2006. *AIDS* **24**(8), 1203-1212.

[4] Shiri, T., Welte, A. 2008. Transient antiretroviral therapy selecting for common HIV-1 mutations substantially accelerates the appearance of rare mutations. *Theor Biol Med Model.* **5**, 25.

[5] Shi, V., Tridane, A., Kuang, Y. 2008. A viral load-based cellular automata approach to modeling HIV dynamics and drug treatment. *J Theor Biol.* **253**(1), 24-35.

[6] Huang, Y., Wu, H., Acosta, E.P. 2010. Hierarchical Bayesian inference for HIV dynamic differential equation models incorporating multiple treatment factors. *Biom J.* **52**(4), 470-86.

[7] von Wyl, V., Cambiano, V., Jordan, M.R., Bertagnolio, S., Miners, A., Pillay, D., Lundgren, J., Phillips, A.N. 2012. Cost-Effectiveness of Tenofovir Instead of Zidovudine for Use in First-Line Antiretroviral Therapy in Settings without Virological Monitoring. *PLoS One* **7**(8).

[8] Wagner, B.G., Blower, S. 2012. Universal Access to HIV Treatment versus Universal 'Test and Treat': Transmission, Drug Resistance & Treatment Costs. *PLoS One* **7**(9).

[9] Heye, T.B., Tadesse, B.T., Yalew, A.W. 2012. Predictors of treatment failure and time to detection and switching in HIV-infected Ethiopian children receiving first line anti-retroviral therapy. *BMC Infect Dis.* **12**(1).

[10] Wu, J., Yan, P., Archibald, C. 2007. Modelling the evolution of drug resistance in the presence of antiviral drugs. *BMC Public Health.* **7**, 300.

[11] Rong, L., Gilchrist, M.A., Feng, Z., Perelson, A.S. 2007. Modeling within-host HIV-1 dynamics and the evolution of drug resistance: trade-offs between viral enzyme function and drug susceptibility. *J Theor Biol.* **247**(4), 804-18.

[12] Rong, L., Feng Z., Perelson, A.S. 2007. Emergence of HIV-1 drug resistance during antiretroviral treatment. *Bull Math Biol. 69*(6), 2027-60.

[13] Mohanty, U., Dixit, N.M. 2008. Mechanism-based model of the pharmacokinetics of enfuvirtide, an HIV fusion inhibitor. *J Theor Biol.* **251**(3), 541-51.

[14] Bhunu, C.P., Garira, W., Magombedze, G. 2009. Mathematical analysis of a two strain HIV/AIDS model with antiretroviral treatment. *Acta Biotheor.* **57**(3), 361-81.

[15] Smith?, R.J., Aggarwala, B.D. 2009. Can the viral reservoir of latently infected $CD4^+$ T cells be eradicated with antiretroviral HIV drugs? *Journal of Mathematical Biology* **59**(5), 697-715.

[16] Kitayimbwa, J.M., Mugisha, J.Y., Saenz, R.A. 2013. The role of backward mutations on the within-host dynamics of HIV-1. *J Math Biol.* **67**(5), 1111-1139.

[17] Rosenbloom, D.I., Hill, A.L., Rabi, S.A., Siliciano, R.F., Nowak, M.A. 2012. Antiretroviral dynamics determines HIV evolution and predicts therapy outcome. *Nat Med.* **18**(9), 1378-1385.

[18] Smith, R.J., Wahl, L.M. 2004. Distinct effects of protease and reverse transciptase inhibition in an immunological model of HIV-1 infection with impulsive drug effects. *Bull. Math. Biol.* **66**, 1259-1283.

[19] Smith, R.J., Wahl, L.M. 2005. Drug resistance in an immunological model of HIV-1 infection with impulsive drug effects. *Bulletin of Mathematical Biology* **67**, 783-813.

[20] Smith, R.J. 2006. Adherence to antiretroviral HIV drugs: how many doses can you miss before resistance emerges? *Proceedings of the Royal Society of London Series B: Biological Sciences* **273**(1586), 617-624.

[21] Krakovska, O., Wahl, L.M. 2007. Optimal drug treatment regimens for HIV depend on adherence. *Journal of Theoretical Biology* **246**(3), 499509.

[22] Lou, J., Smith?, R.J. 2011. Modelling the effects of adherence to the HIV fusion inhibitor enfuvirtide. *Journal of Theoretical Biology* **268**(1), 1-13.

[23] Lou, J., Lou, Y., Wu, J. 2011. Threshold virus dynamics with impulsive antiretroviral drug effects. *Journal of Mathematical Biology* **65**(4), 623-652.

[24] Okero, F.A., Aceng, E., Madraa, E., Namagala, E., Serutoke, J. 2003. Scaling up antiretroviral therapy: Experience in Uganda. Perspectives and practice in antiretroviral treatment. Case Study. World Health Organization and The Republic of Uganda.

[25] Bierman, W.F., van Agtmael, M.A., Nijhuis, M., Danner, S.A., Boucher, C.A. 2009. HIV monotherapy with ritonavir-boosted protease inhibitors: a systematic review. *AIDS* **23**(3), 279-91.

[26] Calza, L., Manfredi, R. 2012. Protease inhibitor monotherapy as maintenance regimen in patients with HIV infection. *Curr HIV Res.* **10**(8), 661-72.

[27] Pillay, D., Goodall, R., Gilks, C.F., Yirrell, D., Gibb, D., Spyer, M., Kaleebu, P., Munderi, P., Kityo, C., McCormick, A., Nkalubo, J., Lyagoba, F., Chirara, M., Hakim, J., DART. 2010. Virological findings from the SARA trial: boosted PI monotherapy as maintenance second-line ART in Africa. *J Int AIDS Soc.* **13**(Suppl 4), O20.

[28] Kepler, T.B., Perelson, A.S. 1998. Drug concentration heterogeneity facilitates the evolution of drug resistance. *Proc. Natl. Acad. Sci. USA* **95**, 11514-11519.

[29] Smith?, R.J., Schwartz, E.J. 2008. Predicting the potential impact of a cytotoxic T-lymphocyte HIV vaccine: how often should you vaccinate and how strong should the vaccine be? *Mathematical Biosciences* **212**, 180-187.

[30] Lakshmikantham, V., Bainov, D.D. & Simeonov, P.S. Theory of Impulsive Differential Equations. World Scientific, Singapore (1989).

[31] Bainov, D.D. & Simeonov, P.S. Systems with Impulsive Effect. Ellis Horwood Ltd, Chichester (1989).

[32] Bainov, D.D. & Simeonov, P.S. Impulsive differential equations: periodic solutions and applications. Longman Scientific and Technical, Burnt Mill (1993).

[33] Bainov, D.D. & Simeonov, P.S. Impulsive Differential Equations: Asymptotic Properties of the Solutions. World Scientific, Singapore (1995).

[34] Miron, R.M., Smith?, R.J. 2010. Modelling imperfect adherence to HIV induction therapy. *BMC Infectious Diseases* **10**(6).

[35] Ho, D.D. Neuwann, A.U., Perelson, A.S., Chen, W., Leonard, J.M., Markowitz, M. 1995. Rapid turnover of plasma visions and CD4 lymphocytes in HIV-1 infection. *Nature* **373**(6510), 123-126.

[36] Diekmann, O., Heesterbeek, J.A.P., Metz, J.A. 1990. On the definition and the computation of the basic reproduction ratio R0 in models for infectious diseases in heterogeneous populations. *J. Math. Biol.* **28**(4), 365.

[37] van den Driessche, P., Watmough, J. 2002. Reproduction numbers and subthreshold endemic equilibria for compartmental models of disease transmission. *Math. Biosci.* **180**, 29.

[38] Truccolo, W.A., Rangarajan, G., Chen, Y., Ding, M. 2003. Analysing stability of equilibrium points in neutral networks: a general approach. *Neutral Networks* **16**, 1453-1460.

[39] Allen, L.J.S. Introduction to Mathematical Biology. 2006. Pearson Education. pp. 150-151.

[40] Bilello, J.A., Bilello, P.A., Stellrecht, K., Leonard, J., Norbeck, D.W., Kempf, D.J., Robins, T., Drusano, G.L. 1996. Human Serum α_1 Acid Glycoprotein Reduces Uptake, Intracellular Concentration, and Antiviral Activity of A-80987, and Inhibitor of the Human Immunodeficiency Virus Type-1 Protease. *Antimicrobial Agents and Chemotherapy* **40**(6), 1491-1497.

[41] Perelson, A.S., Neumann, A.U. Markowitz, M., Leonard, J.M. Ho, D.D. 1996. HIV-1 dynamics in vivo: virion clearance rate, infected cell lifespan, and viral generation time. *Science* **271**, 1582-1585.

[42] Perelson, A.S., Kirschner, D.E., De Boer, R. 1993. Dynamics of HIV infection of $CD4^+$ T cells. *Mathematical Biosciences* **114**, 81-125.

[43] De Boer, R.J., Ribeiro, R.M., Perelson, A.S. 2010. Current Estimates for HIV-1 Production Imply Rapid Viral Clearance in Lymphoid Tissues. *PLoS Comput Biol* **6**(9), e1000906.

[44] Blower S.M., Dowlatabadi H. 1994. Sensitivity and uncertainty analysis of complex models of disease transmission: an HIV model, as an example. *International Statistical Review* **2**, 229-243.

[45] Stein, M. 1985. The use of LHS for variance reduction in simulations with many random parameters. *IBM Report RC11166* (#50265) 52385, mathematics, 46 pages.

Figure 1. The model. A. The model for Region 1. T_S, T_I and T_Y are the susceptible, infected with wild-type strain and infected with mutant strain T cells, respectively. V_I and V_Y are the wild-type and mutant strains, respectively. λ is the rate of new T cells produced. In Region 1, there is not enough drug to inhibit the T cells from creating either wild-type or mutant virus. B. The model for Region 2. T_{PN}, T_{PI} and T_{PY} are the susceptible, infected with wild-type strain and infected with mutant strain T cells, respectively, at intermediate drug levels. P is the drug concentration and m_P is the clearance rate. In Region 2, there is not enough drug in the T cells to inhibit the mutant strain from producing infectious virions, but the wild-type strain can be controlled, meaning it will only produce non-infectious virions, V_N. C. The model for Region 3. T_{PPN}, T_{PPI} and T_{PPY} are the susceptible, infected with wild-type strain and infected with mutant strain T cells, respectively, at high drug levels. In Region 3, there are sufficient levels of drug in the T cells to inhibit infectious viral budding of either strain.

Figure 2. Example of dose-effect curves for the wild-type (solid curve) and 10-fold resistance (dashed curve) virus strains. When drug concentrations are in Region 1, the amount of drug absorbed is insufficient to control either the wild-type or mutant strain. When the drug concentrations are in Region 2, drug absorbed can block the wild-type strain, but the resistant strain still emerges. When the drug concentration is in Region 3, both virus strains are controlled. This example is for the protease inhibitor ritonavir.

Figure 3. The possible combinations of regions that drug concentrations may traverse, for given dosages and dosing intervals. All parameters can be found in Table 1. This example is for the protease inhibitor ritonavir. The asterisk is the FDA-approved dosage and dosing interval for ritonavir. Note the log scale on the y-axis.

Figure 4. Infected T cell populations when trajectories of drug concentration remain solely within a region. Values of T_I and T_Y were estimated by numerical integration of system (2.3), (2.4) and (2.5). The inset shows the total number of uninfected T cells, and T cells unable to produce infectious virus. Note that the threshold for Region 2 is adjusted in Figure 4B as mentioned in Section 4. A. Region 1 ($\tau = 1$, $P^i = 10^{-4}$). In this case, there are no cells infected with the drug-resistant strain of the virus. T cells infected with the wild-type strain dominate, with all other T cells approaching zero. B. Region 2 ($\tau = 0.1$, $P^i = 0.5$). In this case both strains of the virus coexist. There are much higher levels of mutant virus than wild-type virus strains. C. Region 3, where the dosing intervals and dosages are not too extreme ($\tau = 0.1$, $P^i = 4$). In this case, there are large amounts of the drug-resistant strain, and there is a large population of infected T cells with the drug-resistant strain with high drug levels. D. Region 4, the region of viral elimination ($\tau = 0.0001$, $P^i = 30$). In this case, both strains of the virus are eliminated. Uninfected T cells with the drug-resistant strain with high drug levels dominate, with all other T cells approaching zero.

Figure 5. The behaviour when trajectories of drug concentrations cross multiple regions. All parameters except the dose and dosing interval are as for Figure 4. Note that the threshold for Region 2 is adjusted in Figures 5 and 5B as mentioned in Section 4. The main panels illustrate the dynamics between T cells able to produce wild-type and mutant virions. A. Regions 1 and 2 ($\tau = 1$, $P^i = 0.3$). In this case, both strains of the virus coexist. T cells able to produce the wild-type strain are significantly more numerous than T cells able to produce the mutant strain. The inset shows a closer look at the final time (shown as a solid circle on the main panels). B. Regions 2 and 3 ($\tau = 0.5$, $P^i = 0.6$). In this case, there is also coexistence, but the T cells able to produce the mutant strain dominate. The inset shows the high number of wild-type infected T cells unable to produce infectious virions. C. Regions 1, 2, 3 and 4 ($\tau = 1.5$, $P^i = 3$). In this case, both strains of the virus coexist, but the number of T cells able to produce the mutant strain is significantly higher. The inset shows that we do not have viral elimination. Note that the values chosen for the dosing interval and dosage allow trajectories to enter Region 4, but viral elimination does not occur since trajectories do not remain in Region 4.

Figure 6. Sensitivity analysis for Region 1. (a) Partial rank correlation coefficients for R_0 for all parameters. (b) The effect of the death rate for the infected $CD4^+$ T cells d_I on R_0. (c) The effect of the number of infectious virions produced per day from an infected $CD4^+$ T cell $n_I\omega$ on R_0.

Figure 7. Sensitivity analysis for Region 2. (a) Partial rank correlation coefficients for R_0 for all parameters. (b) The effect of the death rate for the infected $CD4^+$ T cells d_I on R_0. (c) The effect of the number of infectious virions produced per day from an infected $CD4^+$ T cell $n_I\omega$ on R_0.

Figure 8. Sensitivity analysis for Region 3. (a) Partial rank correlation coefficients for R_0 for all parameters. (b) The effect of the death rate for the infected $CD4^+$ T cells d_I on R_0. (c) The effect of the number of infectious virions produced per day from an infected $CD4^+$ T cell $n_I\omega$ on R_0. (d) The effect of the infection rate of susceptible $CD4^+$ T cells with mutant virus r_Y, on R_0.

Figure 9. Sensitivity analysis for Region 4. (a) Partial rank correlation coefficients for R_0 for all parameters. (b) The effect of the death rate for the infected $CD4^+$ T cells d_I on R_0. (c) The effect of the clearance rate of the drug from a highly inhibited cell m_{PP} on R_0. (d) The effect of the drug dosage P on R_0.

Table 1. Definition and units of parameters/state variables.

Parameter/state variable	Units	Description
n_I	day^{-1}	number of virions produced by a susceptible CD4$^+$ T cell
ω		proportion of infectious virions produced
r_I	day^{-1}	infection rate of CD4$^+$ T cells with wild-type virus
r_Y	day^{-1}	infection rate of CD4$^+$ T cells with mutant virus
d_V	day^{-1}	death rate for the virus
d_S	day^{-1}	death rate for the susceptible CD4$^+$ T cells
d_I	day^{-1}	death rate for the infected CD4$^+$ T cells
r_P	μM^{-1} day^{-1}	rate at which drug inhibits CD4$^+$ T cells when drug concentrations are intermediate
r_{PP}	μM^{-1} day^{-1}	rate at which drug inhibits CD4$^+$ T cells when drug concentrations are high
d_P	day^{-1}	drug clearance rate
λ	cells μL^{-1} day^{-1}	production rate of CD4$^+$ T cells
m_P	day^{-1}	clearance rate of the drug from an intermediate inhibited cell
m_{PP}	day^{-1}	clearance rate of the drug from a highly inhibited cell
P_1	μM	Region 1 threshold
P_2	μM	Region 2 threshold
τ	day	dosing interval
P^i	μM	drug dosage
V_I	virus μM^{-1}	wild-type virus
V_Y	virus μM^{-1}	mutant virus
V_N	virus μM^{-1}	non-infectious virus
T_S	cells μM^{-1}	susceptible CD4$^+$ T cells
T_I	cells μM^{-1}	CD4$^+$ T cells infected by the wild-type virus
T_Y	cells μM^{-1}	CD4$^+$ T cells infected by the mutant virus
T_{PN}	cells μM^{-1}	susceptible CD4$^+$ T cells with an intermediate level of drug
T_{PI}	cells μM^{-1}	CD4$^+$ T cells infected by the wild-type strain also with an intermediate level of drug

Table 2. Range of parameters.

Parameter/state variable	Range	Initial/sample value	References
$n_I\omega$	10^2–10^4	$10^5 \times 0.01$	[41, 18, 19]
r_I	0.001–0.1	0.01	[15, 18]
r_Y	0.0003–0.03	0.0032	[19]
d_V	1–5	3	[19, 42, 43]
d_S	0.002–0.2	0.02	[15, 18, 19, 42, 43]
d_I	0.05–1	0.5	[15, 18, 19, 42, 43]
r_P	30–50	40	[19]
r_{PP}	8–13	10.4	[19]
λ	100–250	180	[19]
m_P	1–4	$24\log(2)/6.2$	[19]
m_{PP}	1–4	$24\log(2)/6.2$	[19]
P^i	**R2: 10^{-2}–10^{-1} **R3: 10–40 **R4: 40–100	(varied)	
d_P		$24\log(2)/6.2$	[19]
P_1		10^{-3}	Section 2.2
P_2		10^{-2}	Section 2.2
τ		(varied)	
V_I		500	[19]
V_Y		5×10^{-5}	[19]
V_N		0	[19]
T_S		1000	[19]
T_I		0	[19]
T_Y		0	[19]
T_{PN}		0	[19]
T_{PI}		0	[19]
T_{PY}		0	[19]
T_{PPN}		0	[19]
T_{PPI}		0	[19]
T_{PPY}		0	[19]
P		0	[19]

** R2, R3 and R4 denote Region 2, Region 3 and Region 4.

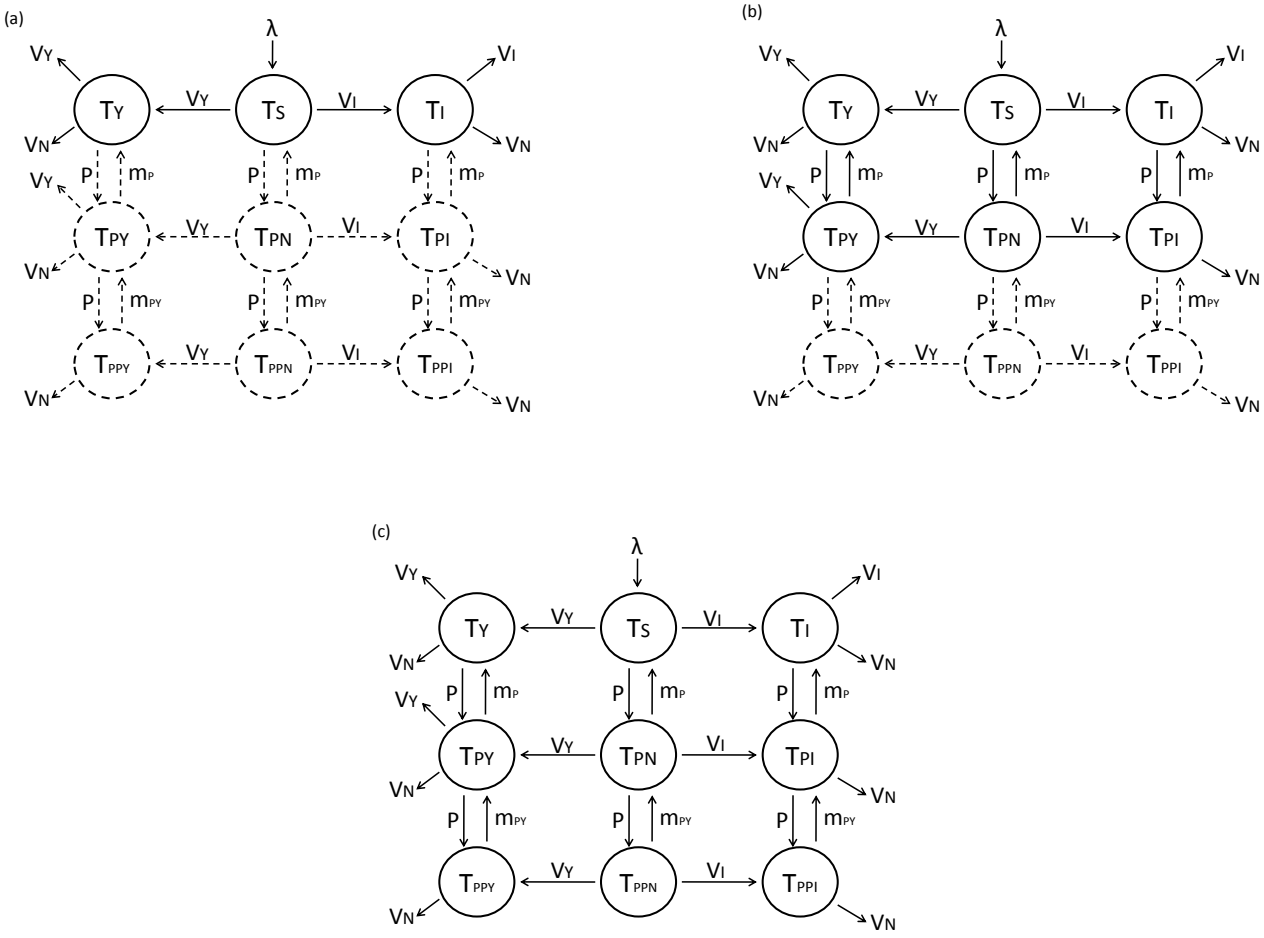

Figure 1:

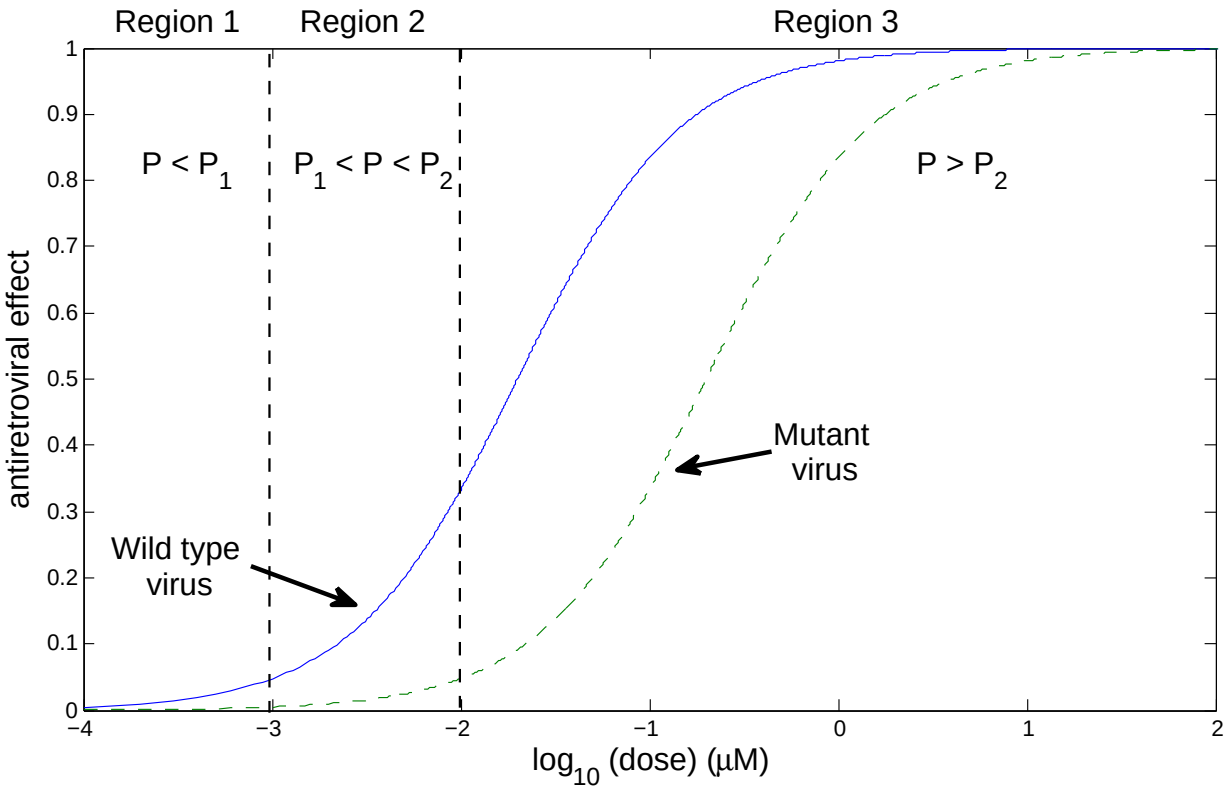
Region 1
Region 2
Region 3
P < P1
P1 < P < P2
P > P2
Mutant virus
Wild type virus
antiretroviral effect
log10 (dose) (μM)
0
0.1
0.2
0.3
0.4
0.5
0.6
0.7
0.8
0.9
1
−4
−3
−2
−1
0
1
2

Figure 2:

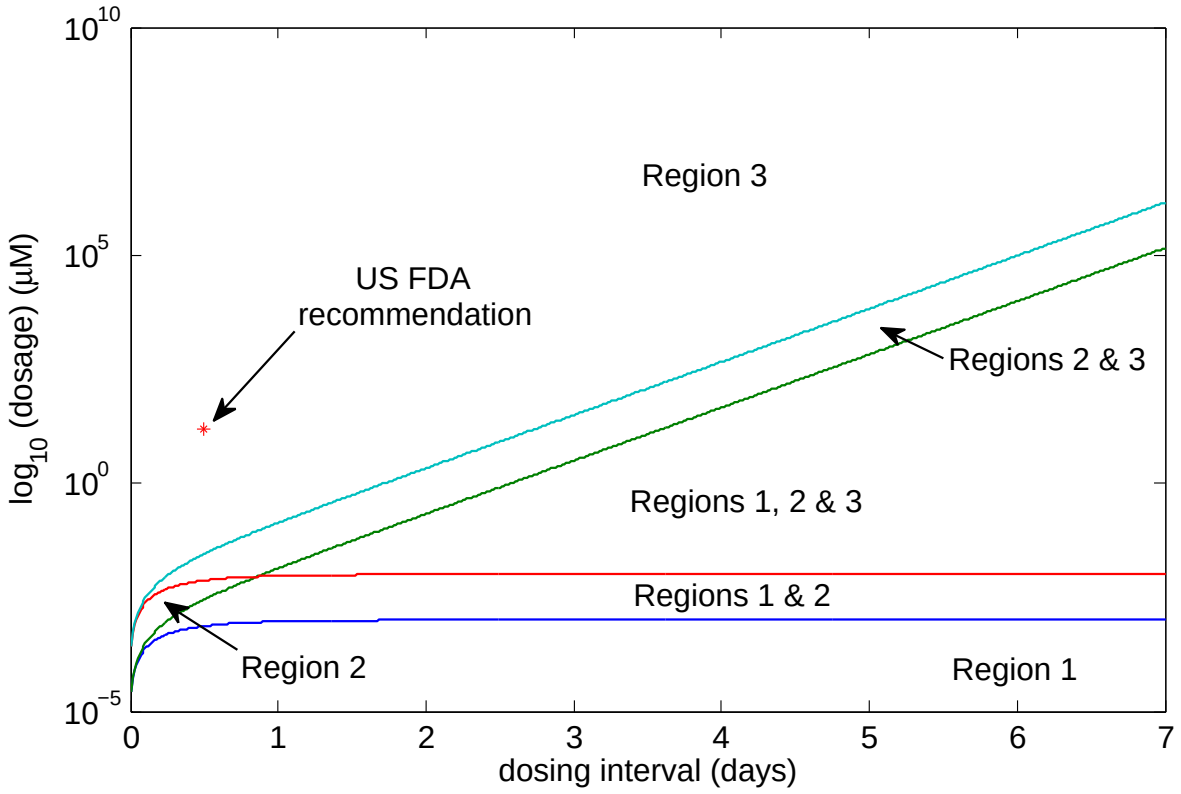
10^{10}
10^{5}
10^{0}
10^{-5}
$\log_{10}$ (dosage) (μM)
Region 3
US FDA
recommendation
Regions 2 & 3
Regions 1, 2 & 3
Regions 1 & 2
Region 2
Region 1
0
1
2
3
4
5
6
7
dosing interval (days)

Figure 3:

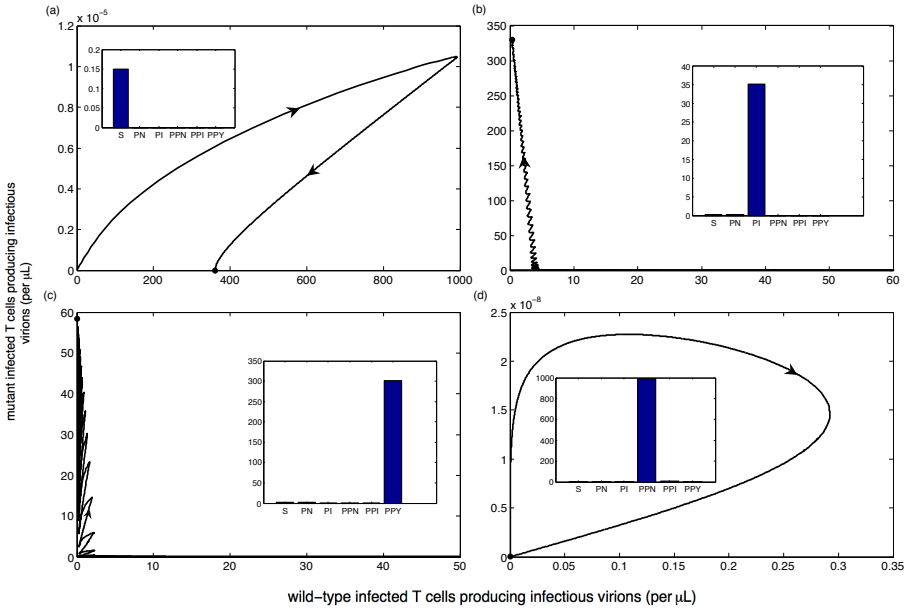
(a)
(b)
(c)
(d)
x 10^-5
x 10^-8
S PN PI PPN PPI PPY
mutant infected T cells producing infectious virions (per μL)
wild−type infected T cells producing infectious virions (per μL)

Figure 4:

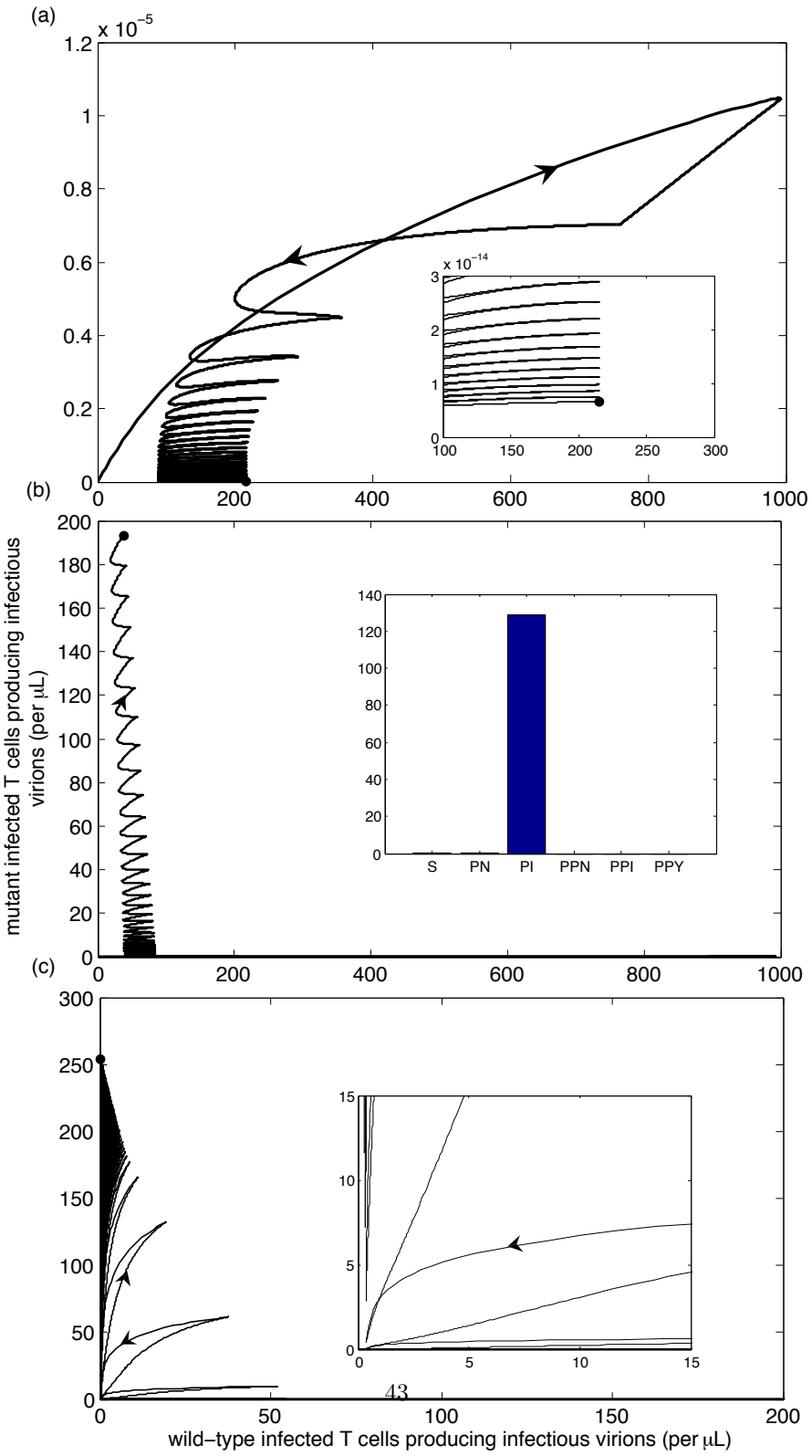
(a)
x 10^−5
1.2
1
0.8
0.6
0.4
0.2
0
0
200
400
600
800
1000
x 10^−14
3
2
1
0
100
150
200
250
300
(b)
mutant infected T cells producing infectious virions (per μL)
200
180
160
140
120
100
80
60
40
20
0
0
200
400
600
800
1000
140
120
100
80
60
40
20
0
S
PN
PI
PPN
PPI
PPY
(c)
300
250
200
150
100
50
0
0
50
100
150
200
15
10
5
0
0
5
10
15
wild−type infected T cells producing infectious virions (per μL)

Figure 5:

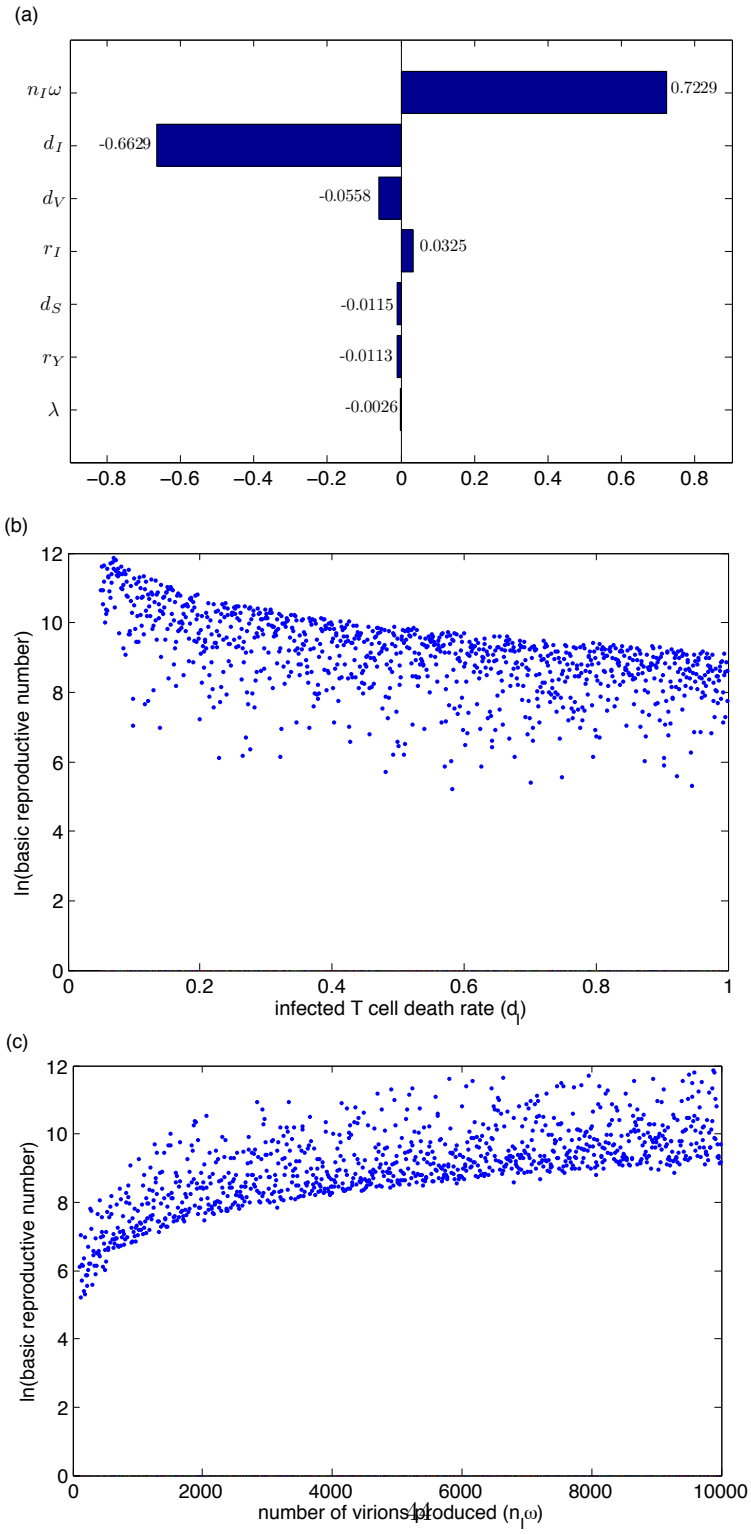
(a)
$n_I\omega$
d_I
d_V
r_I
d_S
r_Y
λ
0.7229
-0.6629
-0.0558
0.0325
-0.0115
-0.0113
-0.0026
−0.8 −0.6 −0.4 −0.2 0 0.2 0.4 0.6 0.8
(b)
ln(basic reproductive number)
infected T cell death rate (d_I)
0 0.2 0.4 0.6 0.8 1
0 2 4 6 8 10 12
(c)
ln(basic reproductive number)
number of virions produced ($n_I\omega$)
0 2000 4000 6000 8000 10000
0 2 4 6 8 10 12

Figure 6:

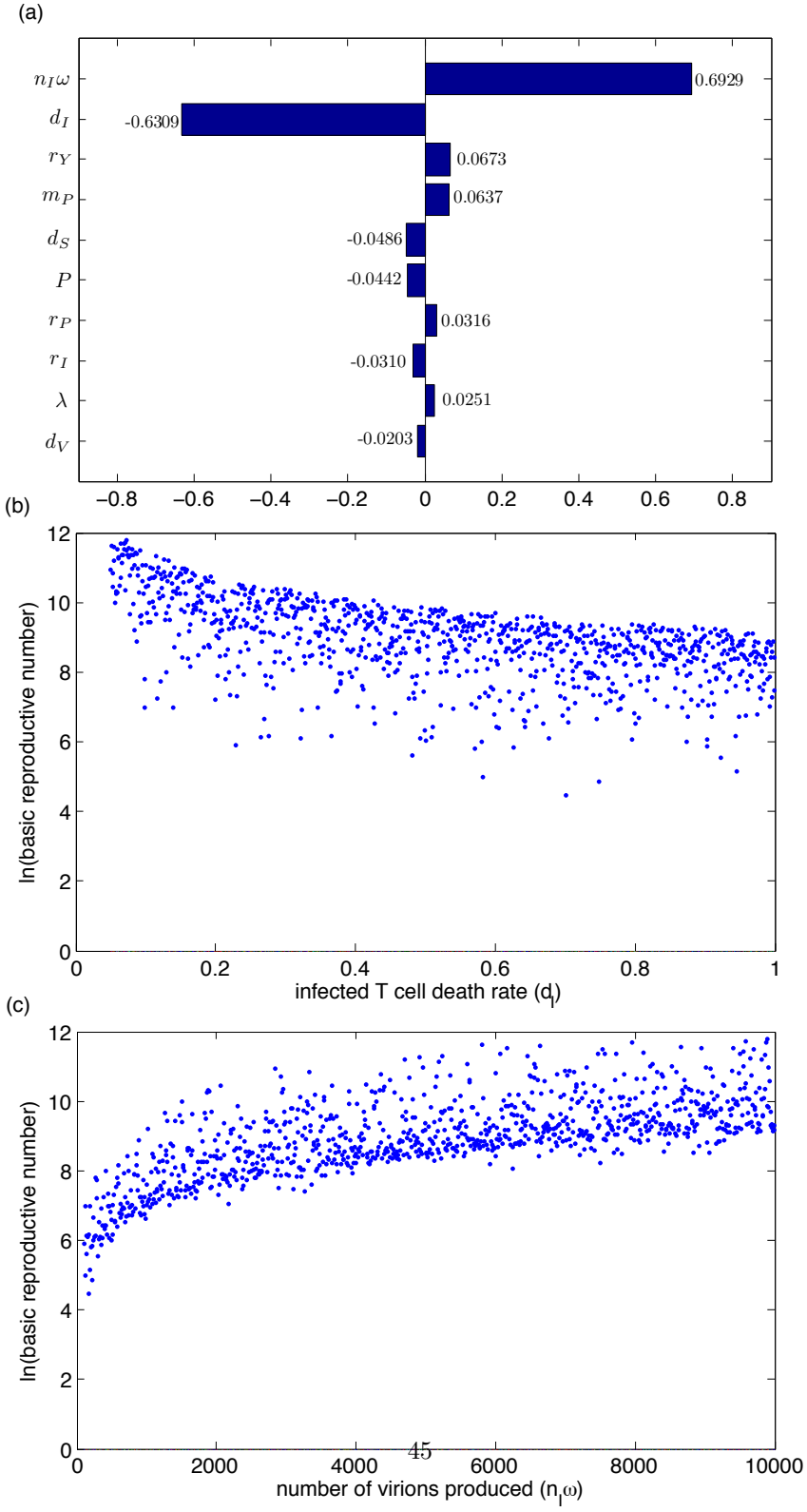
(a)
$n_I\omega$
d_I
r_Y
m_P
d_S
P
r_P
r_I
λ
d_V
0.6929
-0.6309
0.0673
0.0637
-0.0486
-0.0442
0.0316
-0.0310
0.0251
-0.0203
−0.8 −0.6 −0.4 −0.2 0 0.2 0.4 0.6 0.8
(b)
ln(basic reproductive number)
0 2 4 6 8 10 12
0 0.2 0.4 0.6 0.8 1
infected T cell death rate (d_I)
(c)
ln(basic reproductive number)
0 2 4 6 8 10 12
0 2000 4000 6000 8000 10000
number of virions produced ($n_I\omega$)

Figure 7:

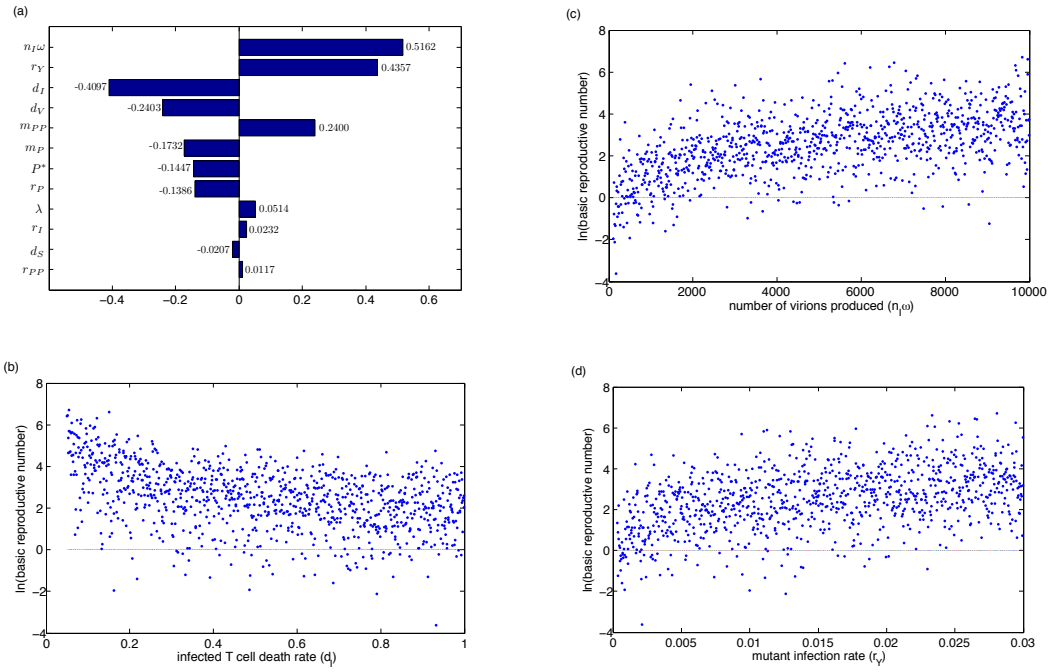
(a)
$n_I\omega$
r_V
d_I
d_V
m_{PP}
m_P
P^*
r_P
λ
r_I
d_S
r_{PP}
0.5162
0.4357
-0.4097
-0.2403
0.2400
-0.1732
-0.1447
-0.1386
0.0514
0.0232
-0.0207
0.0117
(c)
ln(basic reproductive number)
number of virions produced ($n_I\omega$)
(b)
ln(basic reproductive number)
infected T cell death rate (d_I)
(d)
ln(basic reproductive number)
mutant infection rate (r_V)

Figure 8:

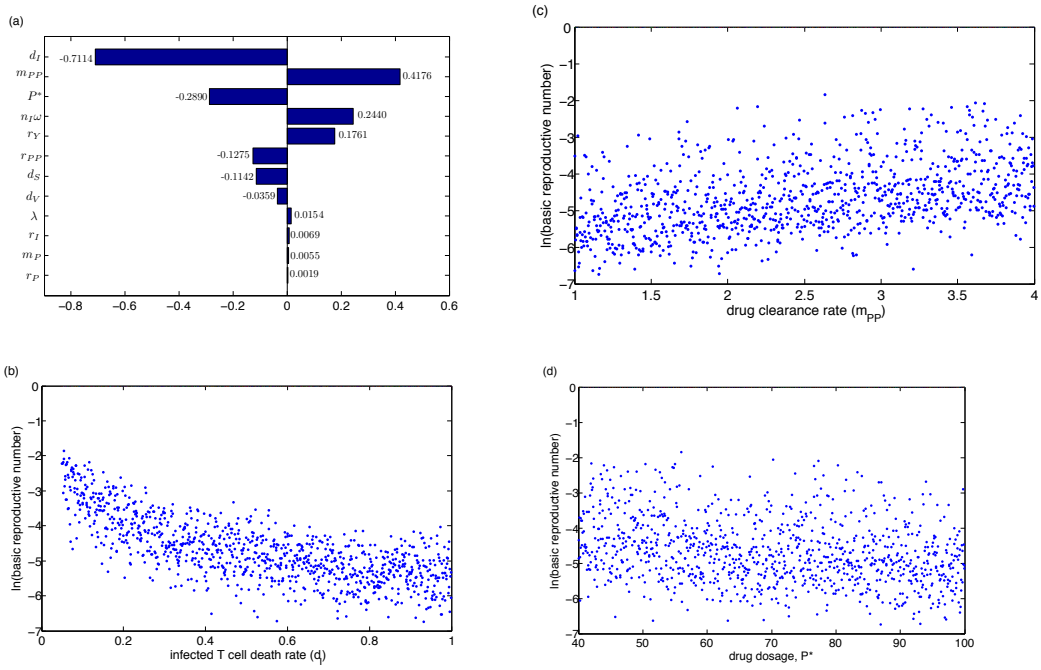
(a)
d_I
m_{PP}
P^*
$n_I\omega$
r_Y
r_{PP}
d_S
d_V
λ
r_I
m_P
r_P
-0.7114
0.4176
-0.2890
0.2440
0.1761
-0.1275
-0.1142
-0.0359
0.0154
0.0069
0.0055
0.0019
−0.8 −0.6 −0.4 −0.2 0 0.2 0.4 0.6
(c)
ln(basic reproductive number)
drug clearance rate (m_{PP})
1 1.5 2 2.5 3 3.5 4
(b)
ln(basic reproductive number)
infected T cell death rate (d_I)
0 0.2 0.4 0.6 0.8 1
(d)
ln(basic reproductive number)
drug dosage, P*
40 50 60 70 80 90 100

Figure 9:

Chapter 4

Two-dimensional impulsive differential system

Determining stability of nonlinear impulsive differential equations presents many challenges. There are a few ways we can determine the stability of a periodic orbit. If we have a two-dimensional autonomous system, we can use the theory presented in Section 2.7, where we can solve for the non-trivial Floquet multiplier and determine if this is greater or less than one in absolute value (unstable and stable, respectively). If the system is non-autonomous (or autonomous with dimension higher than two), we can find the variational equation presented in Section 2.6 and calculate the Floquet multipliers. Solving this variational system can also be challenging if the T-periodic solution is not explicitly known.

In this chapter, we analyze a two-dimensional model that is based on a reduced system of the models presented in Sections 3.1 and 3.2. With this two-dimensional model, we can find conditions for which stability of T-periodic solutions change. Each term in the reduced system is linear except for one nonlinear infection term. The importance of this nonlinear infection term has been studied with ordinary differential equations [23]-[29]. A common drawback of many within-host infectious-disease mod-

els is that they neglect the fact that a virion is lost when it infects a healthy cell (this nonlinear infection term) [23], [30]-[34]. There is debate about whether this term actually needs to be included in a system since it is very small, and some research states that it can be absorbed into the viral-clearance term [23]. However, this nonlinear infection term may play an important role for the dynamic behavior in certain individuals via the relationship between the $CD4^+$ T cell population and the viral load [24, 25]. It may also affect the probability of extinction of the initial viral load [24, 27] and the viral dynamics [28, 29]. It has also been found that viral clearance via drug therapy may explicitly depend on this nonlinear infection term, since the viral load is very small when a patient is under drug therapy [29].

In this chapter, we will look at how this nonlinear infection term affects stability in a simplified two-dimensional impulsive differential model that represents the dynamics between T cells and virus. We will analyze both, a linear and nonlinear two-dimensional impulsive differential system. We will first show how the models presented in Sections 3.1 and 3.2 can be reduced to a two-dimensional model. For the analysis of the two-dimensional impulsive system, we will first write a general system, consisting of all linear terms except the nonlinear infection term described above. We will also impose new impulsive conditions to account for drug therapy. With this general impulsive system, we will evaluate stability of the linear system (without the nonlinear infection term). We will also consider two subcases of the nonlinear general impulsive system and see how stability may differ when including or removing the nonlinear infection term.

4.1 The model without impulses

In this section, we analyze a reduced system of the model presented in Section 3.2. It should be noted that the reduced system of the model in Section 3.1 can be found in a similar fashion and yields the same results. We will first omit the non-infectious

virus, V_N, compartment since it is decoupled. The system without the non-infectious compartment is

$$\begin{aligned}
\frac{dV_I}{dt} &= n_I\omega T_I - d_V V_I - r_I T_S V_I - r_I T_{PN} V_I - r_I T_{PPN} V_I \\
\frac{dV_Y}{dt} &= n_I\omega (T_Y + T_{PY}) - d_V V_Y - r_Y T_S V_Y - r_Y T_{PN} V_Y - r_Y T_{PPN} V_Y \\
\frac{dT_S}{dt} &= \lambda - r_I T_S V_I - r_Y T_S V_Y - d_S T_S - \alpha_1 r_P P T_S + m_P T_{PN} \\
\frac{dT_I}{dt} &= r_I T_S V_I - d_I T_I - \alpha_1 r_P P T_I + m_P T_{PI} \\
\frac{dT_Y}{dt} &= r_Y T_S V_Y - d_I T_Y - \alpha_1 r_P P T_Y + m_P T_{PY} \\
\frac{dT_{PN}}{dt} &= \alpha_1 r_P P T_S - m_P T_{PN} - r_Y T_{PN} V_Y - r_I T_{PN} V_I - d_S T_{PN} - \alpha_2 r_{PP} P T_{PN} + m_{PP} T_{PPN} \\
\frac{dT_{PI}}{dt} &= r_I T_{PN} V_I + \alpha_1 r_P P T_I - m_P T_{PI} - \alpha_2 r_{PP} P T_{PI} + m_{PP} T_{PPI} - d_I T_{PI} \\
\frac{dT_{PY}}{dt} &= r_Y T_{PN} V_Y + \alpha_1 r_P P T_Y - m_P T_{PY} - \alpha_2 r_{PP} P T_{PY} + m_{PP} T_{PPY} - d_I T_{PY} \\
\frac{dT_{PPN}}{dt} &= \alpha_2 r_{PP} P T_{PN} - m_{PP} T_{PPN} - r_Y T_{PPN} V_Y - r_I T_{PPN} V_I - d_S T_{PPN} \\
\frac{dT_{PPI}}{dt} &= r_I T_{PPN} V_I + \alpha_2 r_{PP} P T_{PI} - m_{PP} T_{PPI} - d_I T_{PPI} \\
\frac{dT_{PPY}}{dt} &= r_Y T_{PPN} V_Y + \alpha_2 r_{PP} P T_{PY} - m_{PP} T_{PPY} - d_I T_{PPY}.
\end{aligned} \tag{4.1.1}$$

Let $C = T_S + T_I + T_Y + T_{PN} + T_{PI} + T_{PY} + T_{PPN} + T_{PPI} + T_{PPY}$ be the total number of CD4$^+$ T cells and $V = V_I + V_Y$ be the total virus population. Therefore, from model (4.1.1), we get

$$\frac{dC}{dt} = \lambda - d_S(T_S + T_{PN} + T_{PPN}) - d_I(T_I + T_Y + T_{PI} + T_{PY} + T_{PPI} + T_{PPY}).$$

We have that

$$d_S < d_I < d_V \tag{4.1.2}$$

(reference Section 3.2 [4]). We will consider the case when the death rate of the CD4$^+$

T cells is the same for susceptible and infected cells. Therefore

$$\frac{dC}{dt} \leq \lambda - d_S C.$$

We also have

$$\begin{aligned}\frac{dV}{dt} &= n_I\omega(T_I + T_Y + T_{PY}) - d_V(V_I + V_Y) - (r_I V_I + r_Y V_Y)(T_S + T_{PN} + T_{PPN}) \\ &\approx n_I\omega(T_I + T_Y + T_{PY}) - d_V(V_I + V_Y) - r_Y(T_S + T_{PN} + T_{PPN})V \\ &\approx n_I\omega C - d_V V - r_Y CV,\end{aligned}$$

since $r_I > r_Y$; i.e., the wild-type is the more infectious strain of the virus (reference Section 3.2 [4]).

System (4.1.1) can therefore be approximated by the two-dimensional system

$$\begin{aligned}\frac{dC}{dt} &= \lambda - d_S C \\ \frac{dV}{dt} &= n_I\omega C - d_V V - r_Y CV,\end{aligned} \tag{4.1.3}$$

where C is the total $CD4^+$ T cell count, V is the total virus population. We have that t is the time in days, n_I is the number of virions produced per day, ω is the proportion of infectious virions produced from an infected $CD4^+$ T cell, and r_Y is the infection rate of $CD4^+$ T cells with mutant virus. The constant λ is the rate at which new susceptible $CD4^+$ T cells are produced, while the death rates are denoted by d_V and d_S for the virus and susceptible $CD4^+$ T cells, respectively.

In this case, we are overestimating the number of T cells with our two-dimensional model during any stage of infection. The term $n_I\omega$ is the number of new infectious virions produced. This value is overestimated at the beginning stages of infection since most of the T cells are susceptible, and approximately accurate at the end stages of infection (AIDS) since most of the T cells are infected. The term $r_Y CV$ is the number of virus lost to every cell (each time a cell is infected). At the beginning stages of the infection, this term is approximately accurate since most of the T cells

are susceptible, but is overestimated at the end stages of infection since most cells are infected. Therefore, we assume that the change in virus is approximately equivalent to the 13-dimensional system throughout infection.

It should be noted that the virus population in the reduced system (4.1.3) does not affect the CD4$^+$ T cell population. If V does not impact C, then one loses a crucial aspect of the goal of this model. We will therefore generalize system (4.1.3) by including the effect of virus in two ways: 1. By a linear term (Section 4.1.1) and 2. By an impulse (Section 4.2.4).

4.1.1 General two-dimensional non-impulsive model

We now present the dynamics between the total CD4$^+$ T cell and virus populations by a general two-dimensional system based on the reduced system (4.1.3). We assume that the total CD4$^+$ T cell count, C, includes both the susceptible and infected T cells. We include only one aggregated virus population, V. Therefore the nonlinear system is

$$\frac{dC}{dt} = f(C,V) \qquad \frac{dV}{dt} = g(C,V) - rCV, \tag{4.1.4}$$

where r is the infection rate of the CD4$^+$ T cells with virus, $t \in \mathbb{R}$, $f : \mathbb{R}_+ \times \mathbb{R}_+ \to \mathbb{R}$, $g : \mathbb{R}_+ \times \mathbb{R}_+ \to \mathbb{R}$.

In order to view the effect of the nonlinear infection term, we assume that f and g are linear. Then, without loss of generality, we have that

$$f(C,V) = a_1C + a_2V + a_3$$
$$g(C,V) = b_1C + b_2V + b_3,$$

where a_1 is the death rate of the CD4$^+$ T cell population, so $a_1 < 0$; a_2 is the immunological response when virus is present. This implies that a_2 is the difference between the increased proliferation rate since virus is present and the infected T cells

death rate. Here we assume that the interaction between T cells and virus is only affected by the number of virions. Then a_2 can be positive or negative depending on whether the rate of proliferation is either greater or less than the death rate. We have that a_3 is a constant source of new $CD4^+$ T cells, so $a_3 > 0$; b_1 is the rate at which infectious virus is being produced from $CD4^+$ T cells, so $b_1 > 0$; b_2 is the virus death rate, so $b_2 < 0$; b_3 is a constant source of new virus, so $b_3 > 0$. The value for b_3 is approximately zero in practice, but is included for completeness. Therefore the following inequalities hold.

$$r, a_3, b_1, b_3 > 0, \quad a_1, b_2 < 0, \quad b_3 \approx 0. \tag{4.1.5}$$

We also have, from inequality (4.1.2), that

$$b_2 < a_1. \tag{4.1.6}$$

We include the effect of drugs indirectly via impulses.

4.2 The model with impulses

Drug dynamics are often modelled by an exponential decay between the time at which the drug is administered, and by an impulse when the drug is administered (reference Chapter 3 for examples, and [21]-[38]). We will instead consider that the effect of the drug reduces the virus by a proportion p when the drug is administered. We assume that the time it takes for the drug to be absorbed into the $CD4^+$ T cells is quick compared to the overall dynamics of the drug. Assuming a drug is taken at time τ_k, we have

$$\begin{aligned} \Delta C &= 0 \\ \Delta V &= -pV \end{aligned} \tag{4.2.1}$$

if $\tau_k = kT$, where T is the period and $0 \leq p < 1$.

4.2.1 Linear non-homogeneous impulsive differential system

We will first consider the general system (4.1.4) excluding the nonlinear term rCV. In this case, the system with drug is given by the ordinary differential system (4.1.4), coupled with the difference equation (4.2.1), and is denoted by the following

$$\begin{aligned} &\frac{dC}{dt} = a_1C + a_2V + a_3 \qquad \frac{dV}{dt} = b_1C + b_2V + b_3 \qquad t \neq kT \\ &\Delta C = 0 \qquad\qquad\qquad \Delta V = -pV \qquad\qquad\quad t = kT, \end{aligned} \tag{4.2.2}$$

for $t \in \mathbb{R}_+$ and $k \in \mathbb{Z}$.

Theorem 4.2.1 *Let the inequalities (4.1.5)-(4.1.6) hold. Then the linear equation (4.2.2) has a unique T-periodic solution with one impulse per period if*

1. *for $a_2 \neq 0$ and $\theta = (a_1 - b_2)^2 + 4b_1a_2 > 0$ we have*

$$p \neq \frac{2\sqrt{\theta}\left(e^{\lambda_1 T} + e^{\lambda_2 T} \pm \left(1 + e^{\lambda_1 T}e^{\lambda_2 T}\right)\right)}{\sqrt{\theta}\left(e^{\lambda_1 T} + e^{\lambda_2 T} \pm (2e^{\lambda_1 T}e^{\lambda_2 T})\right) - (a_1 - b_2)(e^{\lambda_1 T} - e^{\lambda_2 T})},$$

where

$$\lambda_{1,2} = \frac{1}{2}\left(a_1 + b_2 \pm \sqrt{\theta}\right);$$

2. *for $a_2 < 0$ and $\theta = 0$ we have*

$$p \neq \frac{e^{\delta_1 T} + e^{\delta_2 T} + e^{\delta_1 T}e^{\delta_2 T} - 4 \pm \left(e^{\delta_1 T} + e^{\delta_2 T}\right)}{\pm(e^{\delta_1 T}\xi_2 + e^{\delta_2 T}\xi_1) - (e^{\delta_1 T} + e^{\delta_2 T} + e^{\delta_1 T}e^{\delta_2 T})},$$

where

$$\delta_{1,2} = \frac{1}{2}\left(a_1 + b_2 \pm \sqrt{2}(a_1 - b_2)\right);$$

3. *for $a_2 < 0$ and $\theta < 0$ we have*

$$p \neq \frac{-\omega e^{-\frac{1}{2}(a_1+b_2)T} \pm \omega\cos\left(\frac{\omega}{2}T\right) - e^{\frac{1}{2}(a_1+b_2)T}\left(\omega^2\cos^2\left(\frac{\omega}{2}T\right) - ((a_1 - b_2)^2 + 4b_1a_2)\sin^2\left(\frac{\omega}{2}T\right)\right)}{\pm\omega\left(\omega\cos\left(\frac{\omega}{2}T\right) - (a_1 - b_2)\sin\left(\frac{\omega}{2}T\right)\right) - e^{\frac{1}{2}(a_1+b_2)T}\left(\omega^2\cos^2\left(\frac{\omega}{2}T\right) - ((a_1 - b_2)^2 + 4b_1a_2)\sin^2\left(\frac{\omega}{2}T\right)\right)},$$

where

$$\omega^2 = |(a_1 - b_2)^2 + 4b_1a_2|.$$

Proof: The homogenous equation of (4.2.2) is given by

$$\begin{aligned} \frac{dx}{dt} &= Ax \qquad t \neq \tau_k \\ \Delta x &= Bx \qquad t = \tau_k, \end{aligned} \tag{4.2.3}$$

where

$$A = \begin{bmatrix} a_1 & a_2 \\ b_1 & b_2 \end{bmatrix} \qquad B = \begin{bmatrix} 0 & 0 \\ 0 & -p \end{bmatrix} \qquad x = \begin{bmatrix} C \\ V \end{bmatrix}$$

The eigenvalues $\lambda_{1,2}$ of the matrix A are determined from the characteristic equation

$$\lambda^2 - \lambda(a_1 + b_2) + a_1 b_2 - b_1 a_2 = 0, \tag{4.2.4}$$

and the fundamental matrix $\Phi(t)$ of the homogeneous equation $\frac{d\Phi}{dt} = A\Phi$ is determined from the eigenvalues

$$\lambda_{1,2} = \frac{1}{2}\left(a_1 + b_2 \pm \sqrt{(a_1 - b_2)^2 + 4b_1 a_2}\right), \tag{4.2.5}$$

in the following cases.

Case 1. If $a_2 \neq 0$ and $\theta = (a_1 - b_2)^2 + 4b_1 a_2 > 0$ then the roots of (4.2.4) are real and distinct with

$$\Phi(t) = \frac{1}{\lambda_1 - \lambda_2} \begin{bmatrix} \frac{1}{2}\left(e^{\lambda_1 t}(a_1 - b_2 + \sqrt{\theta}) + e^{\lambda_2 t}(b_2 - a_1 + \sqrt{\theta})\right) & a_2(e^{\lambda_1 t} - e^{\lambda_2 t}) \\ b_1(e^{\lambda_1 t} - e^{\lambda_2 t}) & \frac{1}{2}\left(e^{\lambda_1 t}(b_2 - a_1 + \sqrt{\theta}) + e^{\lambda_2 t}(a_1 - b_2 + \sqrt{\theta})\right) \end{bmatrix}.$$

Case 2. If $a_2 < 0$ and $\theta = 0$ then $\lambda_1 = \lambda_2 = \dfrac{a_1 + b_2}{2}$ and

$$\Phi(t) = \begin{bmatrix} \xi_1 e^{\delta_1 t} + \xi_2 e^{\delta_2 t} & \xi_3\left(e^{\delta_1 t} - e^{\delta_2 t}\right) \\ \xi_4\left(e^{\delta_1 t} - e^{\delta_2 t}\right) & \xi_2 e^{\delta_1 t} + \xi_1 e^{\delta_2 t} \end{bmatrix},$$

where

$$\xi_1 = \frac{1}{2} + \frac{\sqrt{2}}{4}$$
$$\xi_2 = \frac{1}{2} - \frac{\sqrt{2}}{4}$$
$$\xi_3 = \frac{\sqrt{2}|a_2|}{2(a_1 - b_2)}$$
$$\xi_4 = \frac{\sqrt{2}(a_1 - b_2)}{8|a_2|}$$
$$\delta_1 = \frac{1}{2}\left(a_1 + b_2 + \sqrt{2}(a_1 - b_2)\right)$$
$$\delta_2 = \frac{1}{2}\left(a_1 + b_2 - \sqrt{2}(a_1 - b_2)\right).$$

Case 3. If $a_2 < 0$ and $\theta < 0$ then $\lambda_1 = \lambda_2^* = \frac{1}{2}(a_1 + b_2 + i\omega)$, where $\omega^2 = |(a_1 - b_2)^2 + 4b_1a_2|$, and

$$\Phi(t) = \frac{e^{\frac{1}{2}(a_1+b_2)t}}{\omega}\begin{bmatrix} (a_1 - b_2)\sin\left(\frac{\omega}{2}t\right) + \omega\cos\left(\frac{\omega}{2}t\right) & 2a_2\sin\left(\frac{\omega}{2}t\right) \\ 2b_1\sin\left(\frac{\omega}{2}t\right) & (b_2 - a_1)\sin\left(\frac{\omega}{2}t\right) + \omega\cos\left(\frac{\omega}{2}t\right) \end{bmatrix}.$$

We will evaluate each case separately.

Case 1. Let

$$E = \begin{bmatrix} 1 & 0 \\ 0 & 1 \end{bmatrix}.$$

A fundamental matrix of the linear homogeneous system (4.2.3) is

$$\tilde{X}(T) = (E + B)e^{AT}$$
$$= \frac{1}{\lambda_1 - \lambda_2}\begin{bmatrix} \frac{1}{2}\left(e^{\lambda_1 T}(a_1 - b_2 + \sqrt{\theta}) + e^{\lambda_2 T}(b_2 - a_1 + \sqrt{\theta})\right) & a_2(e^{\lambda_1 T} - e^{\lambda_2 T}) \\ b_1(1-p)(e^{\lambda_1 T} - e^{\lambda_2 T}) & \frac{1-p}{2}\left(e^{\lambda_1 T}(b_2 - a_1 + \sqrt{\theta}) + e^{\lambda_2 T}(a_1 - b_2 + \sqrt{\theta})\right) \end{bmatrix}.$$

In order to calculate the multipliers μ_i for $i = 1, 2$ of (4.2.3), we have to calculate the eigenvalues of the matrix $M = \tilde{X}(T)\tilde{X}^{-1}(0)$ (reference Chapter 2; Remark 2.4.2). Since $\tilde{X}^{-1}(0)$ is the identity matrix, we have $M = \tilde{X}(T)$.

The Floquet multipliers satisfy the characteristic equation

$$\mu^2 - \mu\left(\frac{1}{2(\lambda_1-\lambda_2)}\left(p(a_1-b_2)(e^{\lambda_1 T}-e^{\lambda_2 T})+\sqrt{\theta}(2-p)(e^{\lambda_1 T}+e^{\lambda_2 T})\right)\right)+(1-p)e^{(\lambda_1+\lambda_2)T}=0.$$

Therefore the Floquet multipliers μ_j $(j=1,2)$ are

$$\mu_{1,2}=\frac{1}{2}\left(\eta\pm\sqrt{\eta^2-\Phi}\right), \tag{4.2.6}$$

where

$$\eta=\frac{1}{2(\lambda_1-\lambda_2)}\left(p(a_1-b_2)(e^{\lambda_1 T}-e^{\lambda_2 T})+\sqrt{\theta}(2-p)(e^{\lambda_1 T}+e^{\lambda_2 T})\right)$$
$$\Phi=4(1-p)e^{(\lambda_1+\lambda_2)T}.$$

Both $\eta,\Phi>0$ since $\lambda_1>\lambda_2$. The multipliers are distinct from 1 if $|\mu_j|\neq 1$, or

$$p\neq\frac{2\sqrt{\theta}\left(e^{\lambda_1 T}+e^{\lambda_2 T}\pm\left(1+e^{\lambda_1 T}e^{\lambda_2 T}\right)\right)}{\sqrt{\theta}\left(e^{\lambda_1 T}+e^{\lambda_2 T}\pm(2e^{\lambda_1 T}e^{\lambda_2 T})\right)-(a_1-b_2)(e^{\lambda_1 T}-e^{\lambda_2 T})},$$

and so the homogenous equation (4.2.3) has no non-trivial T-periodic solutions. Thus the non-homogeneous equation (4.2.2) has a unique T-periodic solution $\tilde{x}(t)$ (reference Chapter 2; Theorem 2.5.1). The T-periodic solution to the linear impulsive system (4.2.2) is given by

$$\tilde{x}(t)=X(t)[E-X(T)]^{-1}\int_0^T X(T)X^{-1}(s)g(s)ds+\int_0^t X(t)X^{-1}(s)g(s)ds \tag{4.2.7}$$

where $X(T)=M$ is the monodromy matrix of (4.2.3) and $g(t)=\begin{bmatrix} a_3 \\ b_3 \end{bmatrix}$.

Case 2. A fundamental matrix of the linear homogeneous system (4.2.3) is

$$\tilde{X}(T)=(E+B)e^{AT}$$
$$=\begin{bmatrix} \xi_1 e^{\delta_1 T}+\xi_2 e^{\delta_2 T} & \xi_3\left(e^{\delta_1 T}-e^{\delta_2 T}\right) \\ \xi_4(1-p)\left(e^{\delta_1 T}-e^{\delta_2 T}\right) & (1-p)\left(\xi_2 e^{\delta_1 T}+\xi_1 e^{\delta_2 T}\right)\end{bmatrix}.$$

The multipliers μ_i for $i = 1, 2$ of (4.2.3) are calculated in the same way as Case 1. We have that $X^{-1}(0)$ is the identity matrix, and so $M = \tilde{X}(T)$.

The Floquet multipliers satisfy the characteristic equation

$$\mu^2 - \mu\left(e^{\delta_1 T}(\xi_1 + (1-p)\xi_2) + e^{\delta_2 T}(\xi_2 + (1-p)\xi_1)\right) + \frac{1}{4}(1-p)\left(\left(e^{\delta_1 T}\right)^2 + \left(e^{\delta_2 T}\right)^2 + e^{\delta_1 T}e^{\delta_2 T}\right) = 0.$$

Therefore, the Floquet multipliers μ_j $(j = 1, 2)$ are

$$\mu_{1,2} = \frac{1}{2}\left(\eta \pm \sqrt{\eta^2 - \Phi}\right), \tag{4.2.8}$$

where

$$\eta = e^{\delta_1 T}(\xi_1 + (1-p)\xi_2) + e^{\delta_2 T}(\xi_2 + (1-p)\xi_1)$$
$$\Phi = (1-p)\left(\left(e^{\delta_1 T}\right)^2 + \left(e^{\delta_2 T}\right)^2 + e^{\delta_1 T}e^{\delta_2 T}\right).$$

Both $\eta, \Phi > 0$ since $\xi_1, \xi_2 > 0$. We have that the multipliers are distinct from 1 if

$$p \neq \frac{e^{\delta_1 T} + e^{\delta_2 T} + e^{\delta_1 T}e^{\delta_2 T} - 4 \pm \left(e^{\delta_1 T} + e^{\delta_2 T}\right)}{\pm(e^{\delta_1 T}\xi_2 + e^{\delta_2 T}\xi_1) - (e^{\delta_1 T} + e^{\delta_2 T} + e^{\delta_1 T}e^{\delta_2 T})},$$

and so the homogenous equation (4.2.3) has no non-trivial T-periodic solutions. Thus the non-homogeneous equation (4.2.2) has a unique T-periodic solution $\tilde{x}(t)$ given by equation (4.2.7).

Case 3. A fundamental matrix of the linear homogeneous system (4.2.3) is

$$\tilde{X}(T) = (E + B)e^{AT}$$
$$= \frac{e^{\frac{1}{2}(a_1+b_2)T}}{\omega}\begin{bmatrix} (a_1 - b_2)\sin\left(\frac{\omega}{2}T\right) + \omega\cos\left(\frac{\omega}{2}T\right) & 2a_2\sin\left(\frac{\omega}{2}T\right) \\ 2b_1(1-p)\sin\left(\frac{\omega}{2}T\right) & (1-p)\left((b_2 - a_1)\sin\left(\frac{\omega}{2}T\right) + \omega\cos\left(\frac{\omega}{2}T\right)\right) \end{bmatrix}.$$

The multipliers μ_i for $i = 1, 2$ of (4.2.3) are calculated in the same way as Case 1. We have that $X^{-1}(0)$ is the identity matrix, and so $M = \tilde{X}(T)$.

The Floquet multipliers satisfy the characteristic equation

$$\mu^2 - \frac{e^{\frac{1}{2}(a_1+b_2)T}}{\omega}\mu\left((a_1-b_2)\sin\left(\frac{\omega}{2}T\right)+\omega\cos\left(\frac{\omega}{2}T\right)+(1-p)\left(-(a_1-b_2)\sin\left(\frac{\omega}{2}T\right)+\omega\cos\left(\frac{\omega}{2}T\right)\right)\right)$$
$$+\frac{(1-p)e^{(a_1+b_2)T}}{\omega^2}\left(\omega^2\cos^2\left(\frac{\omega}{2}T\right)-\left((a_1-b_2)^2+4b_1a_2\right)\sin^2\left(\frac{\omega}{2}T\right)\right)=0.$$

Therefore the Floquet multipliers μ_j $(j=1,2)$ are

$$\mu_{1,2}=\frac{1}{2}\left(\eta\pm\sqrt{\eta^2-\Phi}\right), \tag{4.2.9}$$

where

$$\eta=\frac{e^{\frac{1}{2}(a_1+b_2)T}}{\omega}\left(p(a_1-b_2)\sin\left(\frac{\omega}{2}T\right)+(1-p)\omega\cos\left(\frac{\omega}{2}T\right)\right)$$
$$\Phi=4\frac{(1-p)e^{(a_1+b_2)T}}{\omega^2}\left(\omega^2\cos^2\left(\frac{\omega}{2}T\right)-\left((a_1-b_2)^2+4b_1a_2\right)\sin^2\left(\frac{\omega}{2}T\right)\right).$$

Both $\eta,\Phi>0$ since $a_1-b_2>0$ and $(a_1-b_2)^2+4b_1a_2<0$. We have that the multipliers are distinct from 1 if

$$p\neq\frac{-\omega e^{-\frac{1}{2}(a_1+b_2)T}\pm\omega\cos\left(\frac{\omega}{2}T\right)-e^{\frac{1}{2}(a_1+b_2)T}\left(\omega^2\cos^2\left(\frac{\omega}{2}T\right)-((a_1-b_2)^2+4b_1a_2)\sin^2\left(\frac{\omega}{2}T\right)\right)}{\pm\omega\left(\omega\cos\left(\frac{\omega}{2}T\right)-(a_1-b_2)\sin\left(\frac{\omega}{2}T\right)\right)-e^{\frac{1}{2}(a_1+b_2)T}\left(\omega^2\cos^2\left(\frac{\omega}{2}T\right)-((a_1-b_2)^2+4b_1a_2)\sin^2\left(\frac{\omega}{2}T\right)\right)},$$

and so the homogenous equation (4.2.3) has no non-trivial T-periodic solutions. Thus the non-homogeneous equation (4.2.2) has a unique T-periodic solution $\tilde{x}(t)$ given by equation (4.2.7).

∎

Theorem 4.2.2 *Under the conditions of Theorem 4.2.1, the unique T-periodic orbit is exponentially stable if*

1. *$a_2\neq 0$, $\theta=(a_1-b_2)^2+4b_1a_2>0$ and either*

   (1.1) we have, if $\eta^2-\Phi\geq 0$, that

$$\frac{-2(\lambda_1-\lambda_2)-2\sqrt{\theta}(e^{\lambda_1T}+e^{\lambda_2T})}{(a_1-b_2)(e^{\lambda_1T}-e^{\lambda_2T})-\sqrt{\theta}(e^{\lambda_1T}+e^{\lambda_2T})}<p<\frac{2(\lambda_1-\lambda_2)-2\sqrt{\theta}(e^{\lambda_1T}+e^{\lambda_2T})}{(a_1-b_2)(e^{\lambda_1T}-e^{\lambda_2T})-\sqrt{\theta}(e^{\lambda_1T}+e^{\lambda_2T})},$$

(1.2) or we have, if $\eta^2 - \Phi < 0$, *that*

$$p > 1 - e^{-\lambda_1 T} e^{-\lambda_2 T},$$

where

$$\begin{aligned}
\eta &= \frac{1}{2(\lambda_1 - \lambda_2)} \left(p(a_1 - b_2)(e^{\lambda_1 T} - e^{\lambda_2 T}) + \sqrt{\theta}(2-p)(e^{\lambda_1 T} + e^{\lambda_2 T}) \right) \\
\Phi &= 4(1-p)e^{(\lambda_1 + \lambda_2)T} \\
\lambda_{1,2} &= \frac{1}{2} \left(a_1 + b_2 \pm \sqrt{\theta} \right);
\end{aligned}$$

2. $a_2 < 0$, $\theta = 0$ *and either*

(2.1) we have, if $\eta^2 - \Phi \geq 0$, *that*

$$\frac{1 - (e^{\delta_1 T} + e^{\delta_2 T})(\xi_1 + \xi_2)}{\xi_2 e^{\delta_1 T} + \xi_1 e^{\delta_2 T}} < p < \frac{1 + (e^{\delta_1 T} + e^{\delta_2 T})(\xi_1 + \xi_2)}{\xi_2 e^{\delta_1 T} + \xi_1 e^{\delta_2 T}},$$

(2.2) or we have, if $\eta^2 - \Phi < 0$, *that*

$$p > 1 - \left(\frac{4}{(e^{\delta_1 T})^2 + (e^{\delta_2 T})^2 + e^{\delta_1 T} e^{\delta_2 T}} \right),$$

where

$$\begin{aligned}
\eta &= e^{\delta_1 T}(\xi_1 + (1-p)\xi_2) + e^{\delta_2 T}(\xi_2 + (1-p)\xi_1) \\
\Phi &= (1-p) \left(\left(e^{\delta_1 T}\right)^2 + \left(e^{\delta_2 T}\right)^2 + e^{\delta_1 T} e^{\delta_2 T} \right) \\
\delta_{1,2} &= \frac{1}{2} \left(a_1 + b_2 \pm \sqrt{2}(a_1 - b_2) \right);
\end{aligned}$$

3. $a_2 < 0$, $\theta < 0$ *and either*

(3.1) we have, if $\eta^2 - \Phi \geq 0$, *that*

$$\frac{-\omega \left(e^{-\frac{1}{2}(a_1+b_2)T} + \cos\left(\frac{\omega}{2}T\right) \right)}{(a_1 - b_2)\sin\left(\frac{\omega}{2}T\right) - \omega\cos\left(\frac{\omega}{2}T\right)} < p < \frac{\omega \left(e^{-\frac{1}{2}(a_1+b_2)T} - \cos\left(\frac{\omega}{2}T\right) \right)}{(a_1 - b_2)\sin\left(\frac{\omega}{2}T\right) - \omega\cos\left(\frac{\omega}{2}T\right)},$$

(3.2) or we have, if $\eta^2 - \Phi < 0$*, that*

$$p > 1 - \left(\frac{\omega^2}{e^{(a_1+b_2)T}\left(\omega^2 \cos^2\left(\frac{\omega}{2}T\right) - ((a_1-b_2)^2 + 4b_1a_2)\sin^2\left(\frac{\omega}{2}T\right)\right)} \right),$$

where

$$\eta = \frac{e^{\frac{1}{2}(a_1+b_2)T}}{\omega}\left((a_1-b_2)\sin\left(\frac{\omega}{2}T\right) + \omega\cos\left(\frac{\omega}{2}T\right) + (1-p)\left(-(a_1-b_2)\sin\left(\frac{\omega}{2}T\right) + \omega\cos\left(\frac{\omega}{2}T\right)\right)\right)$$

$$\Phi = 4\frac{(1-p)e^{(a_1+b_2)T}}{\omega^2}\left(\omega^2\cos^2\left(\frac{\omega}{2}T\right) - \left((a_1-b_2)^2 + 4b_1a_2\right)\sin^2\left(\frac{\omega}{2}T\right)\right)$$

$$\omega^2 = |(a_1-b_2)^2 + 4b_1a_2|.$$

Proof: The proof of Theorem 4.2.2 requires the Floquet multipliers given by equations (4.2.6), (4.2.8) and (4.2.9) for Cases 1, 2 and 3, respectively. We reference Chapter 2; Remark 2.5.2 for exponential stability of the T-periodic solution.

Case 1. For the stability of the non-homogenous linear system (4.2.2), we have

(1.1) If $\eta^2 - \Phi > 0$, then $\mu_1 > \mu_2$, and the multipliers are by modulus smaller than 1 if $|\mu_1| < 1$. We have

$$\begin{aligned} |\mu_1| &= \frac{1}{2}|\eta + \sqrt{\eta^2 - \Phi}| \\ &< \frac{1}{2}|\eta + \sqrt{\eta^2}| \\ &= \frac{1}{2}|\eta + \eta| \\ &= |\eta|. \end{aligned}$$

Therefore $|\mu_1| < 1$ if $|\eta| < 1$ which implies that the T-periodic solution $\tilde{x}(t)$ of the non-homogeneous equation (4.2.2) is exponentially stable. Therefore

$$\frac{-2(\lambda_1-\lambda_2) - 2\sqrt{\theta}(e^{\lambda_1 T} + e^{\lambda_2 T})}{(a_1-b_2)(e^{\lambda_1 T} - e^{\lambda_2 T}) - \sqrt{\theta}(e^{\lambda_1 T} + e^{\lambda_2 T})} < p < \frac{2(\lambda_1-\lambda_2) - 2\sqrt{\theta}(e^{\lambda_1 T} + e^{\lambda_2 T})}{(a_1-b_2)(e^{\lambda_1 T} - e^{\lambda_2 T}) - \sqrt{\theta}(e^{\lambda_1 T} + e^{\lambda_2 T})}.$$

Note: When $\eta^2 - \Phi = 0$, we have $\mu_{1,2} = \frac{1}{2}\eta$. Therefore we have

$$\begin{aligned} |\mu_1| &= \frac{1}{2}|\eta| \\ &< |\eta|. \end{aligned}$$

This is the same criteria as before (when $\eta^2 - \Phi > 0$) meaning the T-periodic solution is exponentially stable for $\eta^2 - \Phi \geq 0$ if $|\eta| < 1$.

(1.2) If $\eta^2 - \Phi < 0$, then $\mu_{1,2} = \frac{1}{2}\left(\eta \pm i\sqrt{\Phi - \eta^2}\right)$. The multipliers are by modulus smaller than 1 if $|\mu_{1,2}| < 1$. We have

$$\begin{aligned} |\mu_{1,2}| &= \frac{1}{2}\sqrt{\eta^2 + (\Phi - \eta^2)} \\ &= \frac{1}{2}\sqrt{\Phi}. \end{aligned}$$

Therefore $|\mu_{1,2}| < 1$ if $\frac{1}{2}\sqrt{\Phi} < 1$, which implies that the T-periodic solution $\tilde{x}(t)$ of the non-homogeneous equation (4.2.2) is exponentially stable. Therefore

$$p > 1 - e^{-\lambda_1 T}e^{-\lambda_2 T}.$$

Case 2. For the stability of the non-homogenous linear system (4.2.2), we have similar conditions as in Case 1.

(2.1) If $\eta^2 - \Phi \geq 0$, then $\mu_1 > \mu_2$. The multipliers are by modulus smaller than 1 if $|\eta| < 1$, which implies that the T-periodic solution $\tilde{x}(t)$ of the non-homogeneous equation (4.2.2) is exponentially stable. Therefore

$$\frac{1 - (e^{\delta_1 T} + e^{\delta_2 T})(\xi_1 + \xi_2)}{\xi_2 e^{\delta_1 T} + \xi_1 e^{\delta_2 T}} < p < \frac{1 + (e^{\delta_1 T} + e^{\delta_2 T})(\xi_1 + \xi_2)}{\xi_2 e^{\delta_1 T} + \xi_1 e^{\delta_2 T}}.$$

(2.2) If $\eta^2 - \Phi < 0$, then $\mu_{1,2} = \frac{1}{2}\left(\eta \pm i\sqrt{\Phi - \eta^2}\right)$. The multipliers are by modulus smaller than 1 if $\frac{1}{2}\sqrt{\Phi} < 1$, which implies that T-periodic solution $\tilde{x}(t)$ of the non-homogeneous equation (4.2.2) is exponentially stable. Therefore

$$p > 1 - \left(\frac{4}{(e^{\delta_1 T})^2 + (e^{\delta_2 T})^2 + e^{\delta_1 T}e^{\delta_2 T}}\right).$$

Case 3. For the stability of the non-homogenous linear system (4.2.2), we have similar conditions as in Case 1.

(3.1) If $\eta^2 - \Phi \geq 0$, then $\mu_1 > \mu_2$. The multipliers are by modulus smaller than 1 if $|\eta| < 1$, which implies that the T-periodic solution $\tilde{x}(t)$ of the non-homogeneous equation (4.2.2) is exponentially stable. Therefore

$$\frac{-\omega\left(e^{-\frac{1}{2}(a_1+b_2)T} + \cos\left(\frac{\omega}{2}T\right)\right)}{(a_1-b_2)\sin\left(\frac{\omega}{2}T\right) - \omega\cos\left(\frac{\omega}{2}T\right)} < p < \frac{\omega\left(e^{-\frac{1}{2}(a_1+b_2)T} - \cos\left(\frac{\omega}{2}T\right)\right)}{(a_1-b_2)\sin\left(\frac{\omega}{2}T\right) - \omega\cos\left(\frac{\omega}{2}T\right)}.$$

(3.2) If $\eta^2 - \Phi < 0$, then $\mu_{1,2} = \frac{1}{2}\left(\eta \pm i\sqrt{\Phi - \eta^2}\right)$. The multipliers are by modulus smaller than 1 if $\frac{1}{2}\sqrt{\Phi} < 1$, which implies that the T-periodic solution $\tilde{x}(t)$ of the non-homogeneous equation (4.2.2) is exponentially stable. Therefore

$$p > 1 - \left(\frac{\omega^2}{e^{(a_1+b_2)T}\left(\omega^2\cos^2\left(\frac{\omega}{2}T\right) - ((a_1-b_2)^2 + 4b_1a_2)\sin^2\left(\frac{\omega}{2}T\right)\right)}\right).$$

∎

Remark. The existence, uniqueness and stability of T-periodic solutions for the case when $a_2 = 0$ will be examined in Section 4.2.3.

Positivity of the unique T-periodic solution can be shown numerically. We set all the parameters equal to those described in Section 3.2 except for a_2 and p since changing these parameters affect stability in the general linear system (4.2.2) (see Table 1).

In this section, we fix $p = 0.5$ and see the effect of changing a_2. Different values of a_2 give ranges for p in which we have stability.

Table 4.1: Parameter values and initial conditions.

Parameter	Units	Description	Sample value/Initial condition
a_1	day^{-1}	death rate of $CD4^+$ T cells	-0.02
a_2	day^{-1}	immune response rate	varied
a_3	cells day^{-1}	constant source of new $CD4^+$ T cells	180
b_1	day^{-1}	rate of infectious virus being produced	1000
b_2	day^{-1}	virus death rate	-3
b_3	virus day^{-1}	constant source of new virus	0.000001
p	day^{-1}	proportion of virus reduced when drug is administered	varied
C	population μM^{-1}	$CD4^+$ T cell population	300
V	population μM^{-1}	Virus population	500

The values chosen for a_2 in Figures 4.1 and 4.2 show the trajectories of the T-periodic solution when in Case 1, Figure 4.3 is for Case 2 and Figure 4.4 is for Case 3.

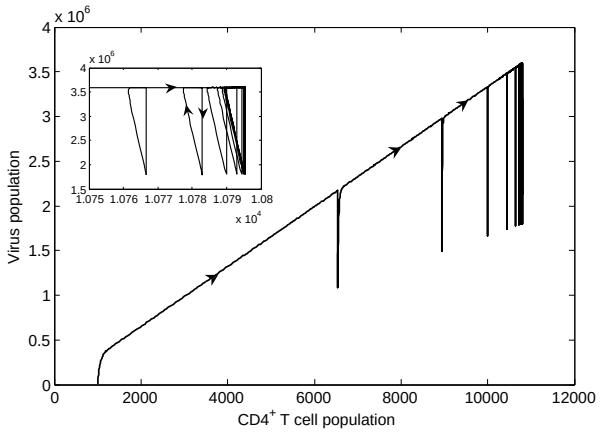

Figure 4.1: The behaviour of the CD4$^+$ T cell and virus populations when $a_2 = 0.0001$ and $p = 0.5$ (all other parameters are fixed at their sample value in Table 1). In this case, condition (1.2) for stability in Theorem 4.2.2 is satisfied and we have a stable positive T-periodic solution. The inset shows a close up of the periodic orbit.

Figure 4.1 shows the case when $a_2 > 0$ in the linear system (4.2.2) and the stability condition (1.2) in Theorem 4.2.2 is satisfied ($a_2 = 0.0001$). In this case, we have a positive, stable T-periodic solution for $p = 0.5$.

The value $a_2 = 0.0032$ used in Figure 4.2 shows an unstable impulsive periodic orbit for $p = 0.5$. In this case, the values from Table 1 do not satisfy condition (1.1) in Theorem 4.2.2.

For the parameters described in Table 1, Figures 4.3 and 4.4 show the case when $a_2 < 0$ in the linear system (4.2.2) and the stability conditions in Theorem 4.2.2 are satisfied. Figure 4.3 shows the case when $a_2 < 0$ in the linear system (4.2.2) and the stability condition (2.2) in Theorem 4.2.2 is satisfied ($a_2 = -0.00222$). Figure 4.4 shows the case when $a_2 < 0$ in the linear system (4.2.2) and both stability conditions

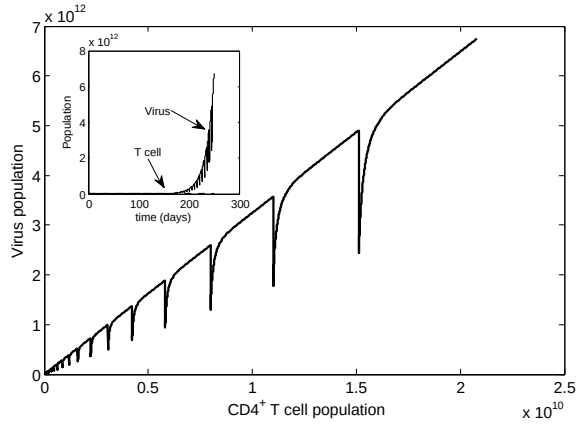

Figure 4.2: The behaviour of the CD4$^+$ T cell and virus populations when $a_2 = 0.0032$ and $p = 0.5$ (all other parameters are fixed at their sample value in Table 1). In this case, condition (1.1) for stability in Theorem 4.2.2 is not satisfied and we have an unstable impulsive periodic orbit. The inset shows the time dynamics for the populations.

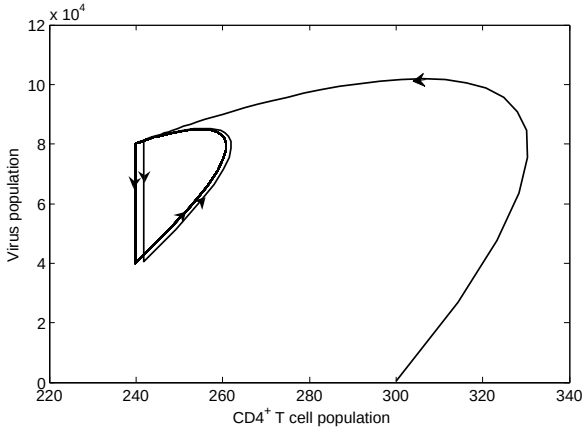

Figure 4.3: The behaviour of the CD4$^+$ T cell and virus populations when $a_2 = -0.0022$ and $p = 0.5$ (all other parameters are fixed at their sample value in Table 1). In this case, condition (2.2) for stability in Theorem 4.2.2 is satisfied and we have a stable positive T-periodic solution.

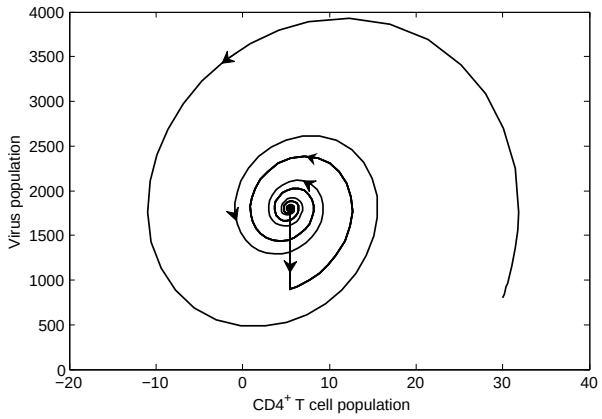

Figure 4.4: The behaviour of the CD4$^+$ T cell and virus populations when $a_2 = -0.1$ and $p = 0.5$ (all other parameters are fixed at their sample value in Table 1). In this case, conditions (3.1) and (3.2) for stability in Theorem 4.2.2 are satisfied and we have a stable positive T-periodic solution.

(3.1) and (3.2) in Theorem 4.2.2 are satisfied ($a_2 = -0.1$).

4.2.2 Nonlinear impulsive differential system

If we include the nonlinear term, the system with drug is given by the ordinary differential system (4.1.4) coupled with the difference equation (4.2.1), and is denoted by the following

$$\begin{aligned} &\frac{dC}{dt} = a_1 C + a_2 V + a_3 \qquad \frac{dV}{dt} = b_1 C + b_2 V + b_3 - rCV \qquad t \neq kT \\ &\Delta C = 0 \qquad\qquad\qquad \Delta V = -pV \qquad\qquad\qquad t = kT, \end{aligned} \tag{4.2.10}$$

for $t \in \mathbb{R}_+$ and $k \in \mathbb{N}$.

Proving existence and uniqueness of T-periodic solutions for the nonlinear impulsive system (4.2.10) is challenging (reference Section 2.6). In this general case, it is not possible to compute stability analytically.

In the general impulsive system case, finding stability condition for the T-periodic solution of the nonlinear impulsive system (4.2.10) is extremely complicated. Finding

the variational equation to system (4.2.10) is possible (reference Section 2.6), but solving the variational equation without knowing the explicit solution to the impulsive orbit is not possible.

However, we can numerically show, for specific parameter values, the existence and stability of positive T-periodic solutions for the general system (4.2.10). Again we use the parameters in Table 1 to show how stability changes. In this case, we vary both a_2 and the parameter r.

The values chosen for a_2 in Figures 4.5 and 4.6 show the trajectories of the T-periodic solution of the nonlinear system (4.2.10) when the positive T-periodic solution of the linear system (4.2.2) is stable in Case 1. Figures 4.7 and 4.8 show the trajectories of the T-periodic solution of the nonlinear system (4.2.10) when the positive T-periodic solution of the linear system (4.2.2) is stable in Case 3. Figures 4.9, 4.10 and 4.11 show the trajectories of the T-periodic solution of the nonlinear system (4.2.10) when the positive T-periodic solution of the linear system (4.2.2) is unstable in Case 1.

We will first look at the case when the stability conditions are satisfied for the positive T-periodic solution of the linear system (4.2.2) when $a_2 > 0$ (see Figure 4.1). Figures 4.5 and 4.6 show the cases when $a_2 > 0$ in the nonlinear system (4.2.10) and the stability conditions for positive the T-periodic solution in the linear case are satisfied. We choose the same value for a_2 as in the linear case. The only difference is varying the parameter r. Changing r does not seem to destroy stability. The value of r seems to only affect the number of virus.

We will now look at the case when the stability conditions are satisfied for the positive T-periodic solution of the linear system (4.2.2) when $a_2 < 0$ (see Figure 4.4). Figures 4.7 and 4.8 show the cases when $a_2 < 0$ in the nonlinear system (4.2.10) and the stability conditions for the positive T-periodic solution in the linear case are satisfied. We see the same type of behaviour as before. The numerical simulations show that the parameter r does not seem to destroy stability.

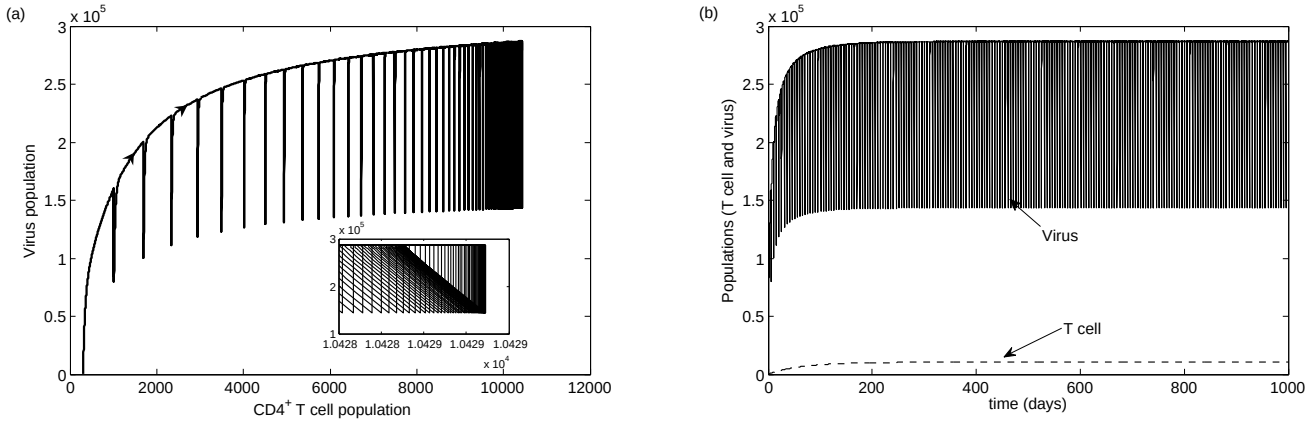

Figure 4.5: The behaviour of the $CD4^+$ T cell and virus populations when $a_2 = 0.0001$, $p = 0.5$ and $r = 0.0032$ (all other parameters are fixed at their sample value in Table 1). In this case, stability conditions in the linear system (Theorem 4.2.2; Case 1) are satisfied. We still have a stable positive T-periodic solution in the nonlinear system. (a) $CD4^+$ T cell population versus virus population; inset: close up of periodic solution. (b) Time dynamics versus populations.

We now investigate the effect of the parameter r when the positive T-periodic solution of the general linear system (4.2.2) is unstable (see Figure 4.2). We can observe that if we choose $a_2 > 0$ such that the stability conditions for the positive T-periodic solution of the linear system are not satisfied (Figure 4.2), there are values of the parameter r such that the T-periodic solution for the nonlinear system is stable (see Figures 4.9 and 4.10). Note that all the parameter values used to generate Figures 4.2 (linear), 4.9 and 4.10 (nonlinear) are the same except for the parameter r that is varied in Figures 4.9 and 4.10. Therefore we can numerically observe that the nonlinear infection term does seem to affect stability. We see that the value of r also seems to affect the T cell population. Figure 4.11 show the case when the positive T-periodic solution of the nonlinear system is unstable (see Figure 4.11). In this case, we choose a value of r that is small and change the value of b_1 in order to discern

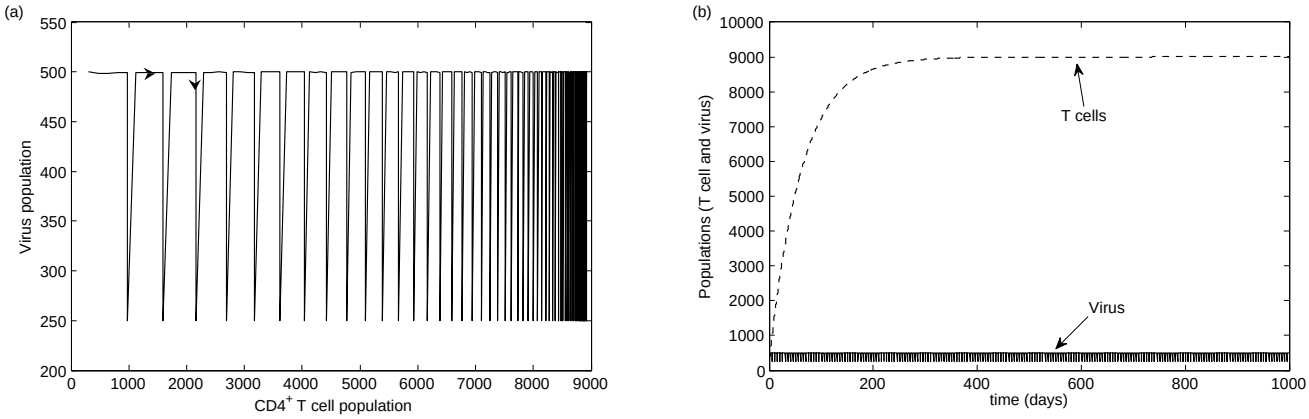

Figure 4.6: The behaviour of the CD4$^+$ T cell and virus populations when $a_2 = 0.0001$, $p = 0.5$ and $r = 2$ (all other parameters are fixed at their sample value in Table 1). In this case, stability conditions in the linear system (Theorem 4.2.2; Case 1) are satisfied. We still have a stable positive T-periodic solution in the nonlinear system. (a) CD4$^+$ T cell population versus virus population. (b) Time dynamics versus populations.

the effect of an unstable T-periodic orbit. The change in the parameter b_1 allows for more realistic values of r when running the simulations in order to obtain an unstable T-periodic solution.

We can also numerically solve for the T-periodic solution in order to obtain the Floquet multipliers of the general nonlinear system (4.2.10). In this case, we use the parameters values in Table 1, except we set $b_1 = 100$ (same value used in Figure 4.11 for instability). By solving for the Floquet multipliers numerically, we can obtain a region in which the T-periodic solution is stable (when the largest multiplier is less than one). Figure (4.12) shows that if the parameter r is bigger than 0.0011, the T-periodic solution of the system (4.2.10) is stable. We also showed from Figure 4.11 that if $r = 10^{-10}$, the T-periodic solution of the system (4.2.10) is unstable. Therefore r is a bifurcation parameter. We must note that even though r does change the stability

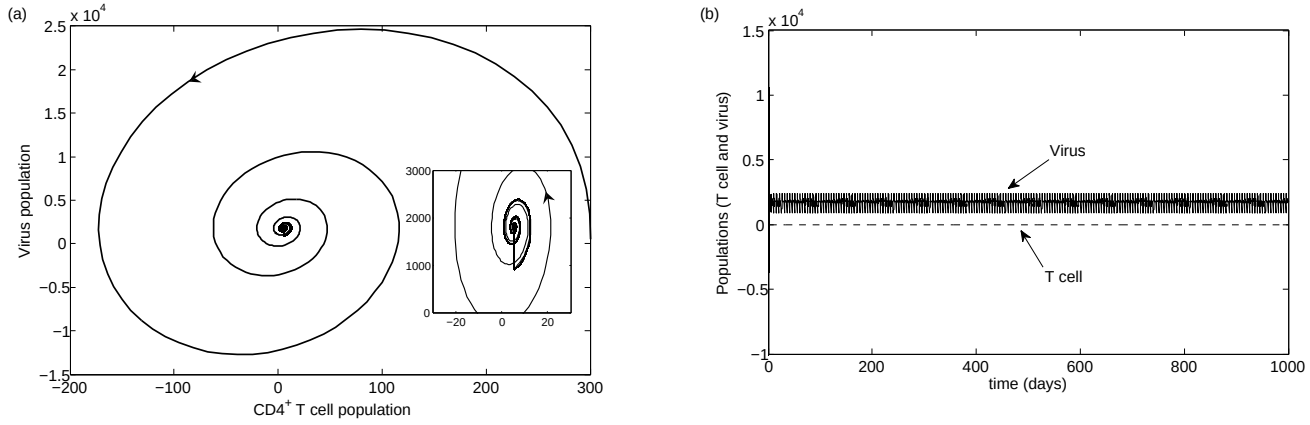

Figure 4.7: The behaviour of the $CD4^+$ T cell and virus populations when $a_2 = -0.1$, $p = 0.5$ and $r = 0.0032$ (all other parameters are fixed at their sample value in Table 1). In this case, stability conditions in the linear system (Theorem 4.2.2; Case 3) are satisfied. We still have a stable positive T-periodic solution in the nonlinear system. (a) $CD4^+$ T cell population versus virus population; inset: close up of periodic solution. (b) Time dynamics versus populations.

of the T-periodic solution, $r = 0.0011$ is not necessarily the bifurcation point. In order to numerically solve for the Floquet multipliers, we must have the solution of the T-periodic solution. A T-periodic solution can only be obtained numerically if the solution is stable. Therefore, we can only guarantee that, for r greater than 0.0011, that the T-periodic solution is stable. Since the value of $r = 10^{-10}$ shows an unstable T-periodic solution, we can assume that, between $10^{-10} < r \leq 0.0011$, a bifurcation occurs.

We will now show analytically, under specific conditions (see the next sections), the existence and sometimes uniqueness of T-periodic solutions, and how stability can change under certain conditions when the nonlinear infection term is included.

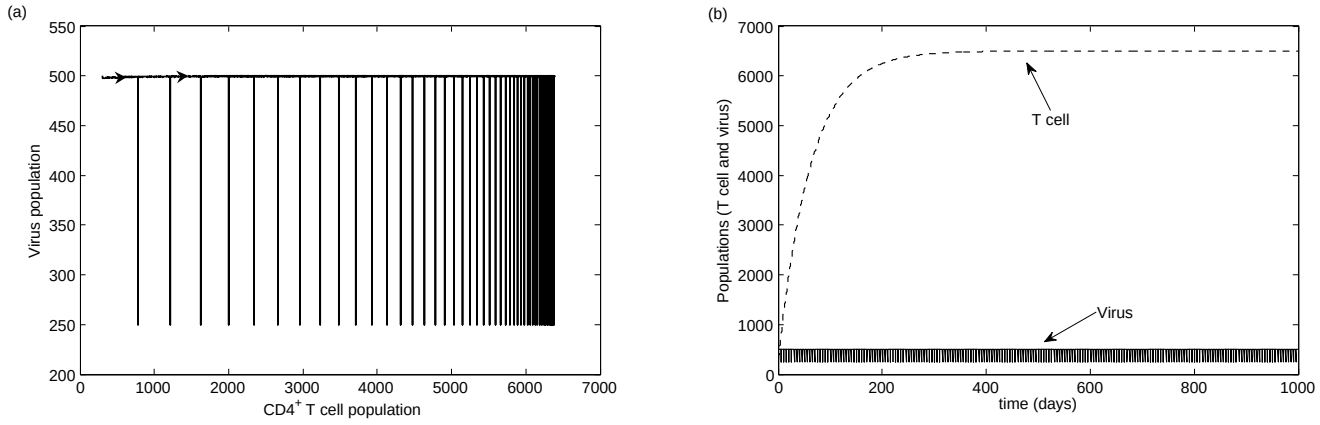

Figure 4.8: The behaviour of the CD4$^+$ T cell and virus populations when $a_2 = -0.1$, $p = 0.5$ and $r = 2$ (all other parameters are fixed at their sample value in Table 1). In this case, stability conditions in the linear system (Theorem 4.2.2; Case 3) are satisfied. We still have a stable positive T-periodic solution in the nonlinear system. (a) CD4$^+$ T cell population versus virus population. (b) Time dynamics versus populations.

4.2.3 Impulsive system without an immune response

We will consider a subcase of the general system (4.1.4). If we set $a_2 = 0$ and $b_3 = 0$ in equations (4.1.4), the ordinary differential equations are exactly the same as the reduced system (4.1.3).

Linear non-homogeneous impulsive system

We will consider the case from (4.1.4) where $a_2 = 0$. Variations in b_3 do not affect stability since it is a non-homogeneous term; it will only change the T-periodic solution. In this case, the results for stability when $b_3 = 0$ will be the same as for $b_3 \neq 0$. We get the following impulsive differential system

$$\begin{aligned} &\frac{dC}{dt} = a_1 C + a_3 \qquad \frac{dV}{dt} = b_1 C + b_2 V + b_3 \qquad t \neq kT \\ &\Delta C = 0 \qquad\qquad \Delta V = -pV \qquad\qquad t = kT, \end{aligned} \tag{4.2.11}$$

for $t \in \mathbb{R}_+$ and $k \in \mathbb{N}$.

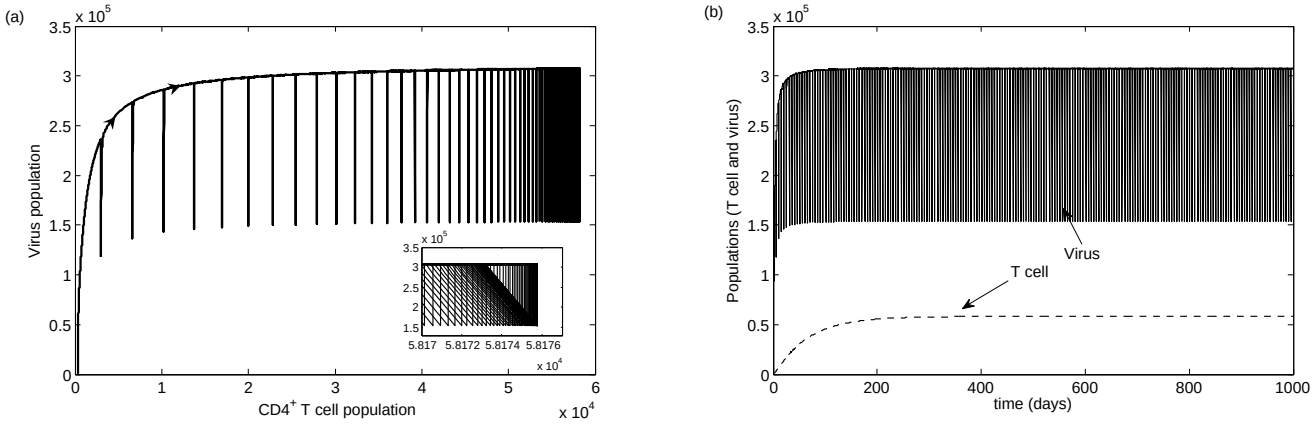

Figure 4.9: The behaviour of the $CD4^+$ T cell and virus populations when $a_2 = 0.0032$, $p = 0.5$ and $r = 0.0032$ (all other parameters are fixed at their sample value in Table 1). In this case, stability conditions in the linear system (Theorem 4.2.2; Case 1) are not satisfied, but we do have a stable positive T-periodic solution in the nonlinear system. (a) $CD4^+$ T cell population versus virus population; inset: close up of periodic solution. (b) Time dynamics versus populations.

Theorem 4.2.3 *Let the inequalities (4.1.5)-(4.1.6) hold. Then model (4.2.11) has a unique positive T-periodic solution with one impulse per period, and this T-periodic orbit is exponentially stable.*

Proof: Introduce the notation $C(0+), V(0+), C(T+)$ and $V(T+)$ as the solution after the impulse effect at times 0 and T, respectively. We will construct a periodic solution $(\tilde{C}(t), \tilde{V}(t))$ to equation (4.2.11) by explicitly solving the boundary value problem $C(0+) = C(T+)$, $V(0+) = V(T+)$, which can be shown to have at most one solution. So, for $0 < t < T$, a T-periodic solution has the form

$$x(t) = X(t, 0+)x_0 + \int_0^t X(t, s)g(s)ds, \tag{4.2.12}$$

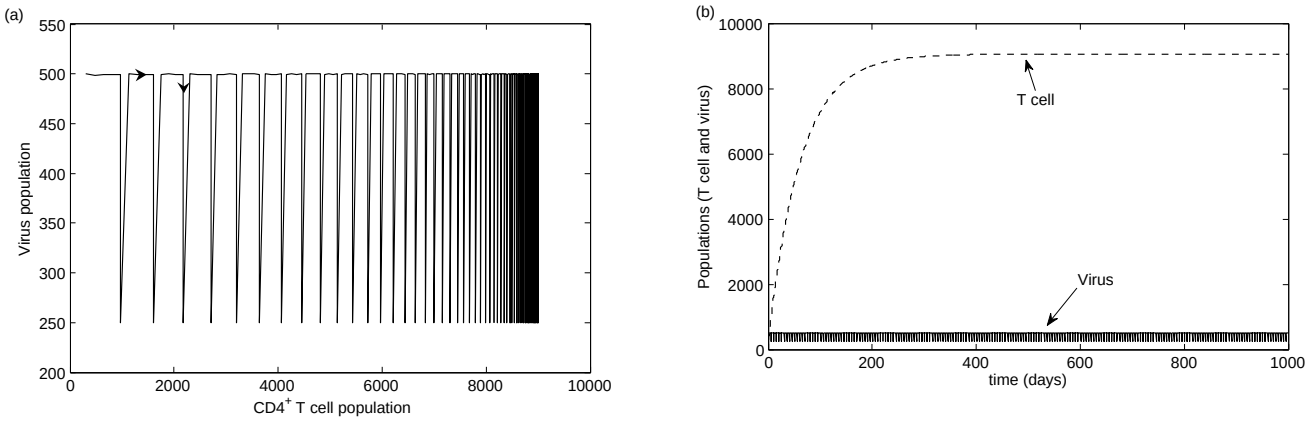

Figure 4.10: The behaviour of the CD4$^+$ T cell and virus populations when $a_2 = 0.0032$, $p = 0.5$ and $r = 2$ (all other parameters are fixed at their sample value in Table 1). In this case, stability conditions in the linear system (Theorem 4.2.2; Case 1) are not satisfied, but we do have a stable positive T-periodic solution in the nonlinear system. (a) CD4$^+$ T cell population versus virus population. (b) Time dynamics versus populations.

where $X(t,s)$ is the Cauchy matrix of the homogenous impulsive equation (reference Chapter 2; Section 2.3). In this case, we have

$$\tilde{C}(t) = e^{a_1 t}\left(C(0+) + a_3\int_0^t e^{-a_1 s}ds\right)$$
$$\tilde{V}(t) = e^{b_2 t}\left(V(0+) + \int_0^t e^{b_2 s}\left(b_1\tilde{C}(s) + b_3\right)ds\right).$$

Since $C(0+) = C(T+)$ and $V(0+) = V(T+)$, we have

$$C(0+) = -\frac{a_3}{a_1}$$
$$V(0+) = \frac{1}{1-(1-p)e^{b_2 T}}\left(\frac{1-p}{|b_2|}\left(b_3 + \frac{b_1 a_3}{|a_1|}\right)(1-e^{b_2 T})\right).$$

Therefore we have

$$\begin{aligned}\tilde{C}(t) &= -\frac{a_3}{a_1}\\ \tilde{V}(t) &= e^{b_2 t}V(0+) + \frac{1}{b_3}\left(b_3 + \frac{b_1 a_3}{|a_1|}\right)(1-e^{b_2 t}).\end{aligned} \tag{4.2.13}$$

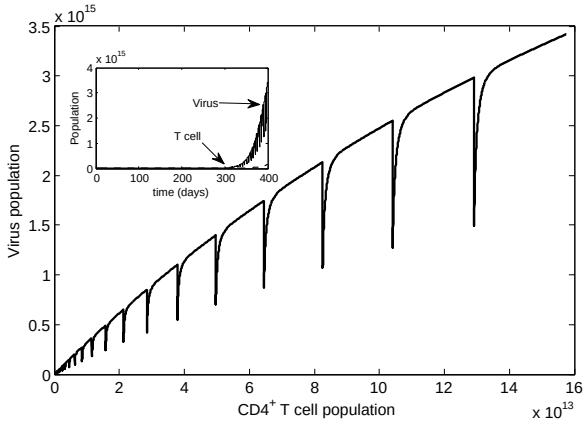

Figure 4.11: The behaviour of the CD4$^+$ T cell and virus populations when $a_2 = 0.0032$, $p = 0.5$, $r = 10^{-10}$ and $b_1 = 100$ (all other parameters are fixed at their sample value in Table 1). In this case, stability conditions in the linear system (Theorem 4.2.2; Case 1) are not satisfied, and T-periodic solution in the nonlinear system is also unstable. The inset shows the time dynamics for the populations.

This T-periodic orbit is positive since $a_1, b_2 < 0$.

The homogenous equation of (4.2.11) is given by

$$\begin{aligned} \frac{dx}{dt} &= Ax \qquad t \neq \tau_k \\ \Delta x &= Bx \qquad t = \tau_k, \end{aligned} \tag{4.2.14}$$

where

$$A = \begin{bmatrix} a_1 & 0 \\ b_1 & b_2 \end{bmatrix} \qquad B = \begin{bmatrix} 0 & 0 \\ 0 & -p \end{bmatrix} \qquad x = \begin{bmatrix} C \\ V \end{bmatrix}.$$

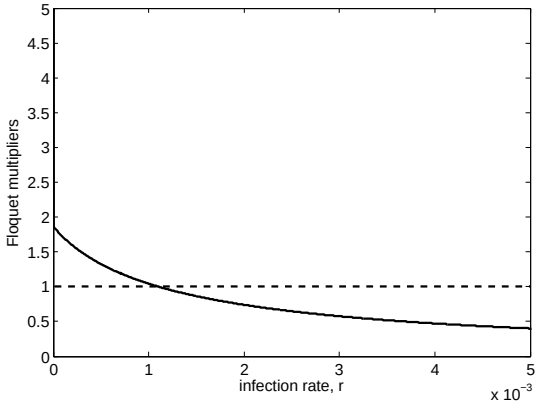

Figure 4.12: The relationship between the infection term, r, and the stability of the general nonlinear system (4.2.10). All parameters are fixed at their sample value in Table 1, except $p = 0.5$, $b_1 = 100$ and $a_2 = 0.0032$. In this case, for $r > 0.0011$, the Floquet multipliers of the nonlinear system (4.2.10) are such that the T-periodic solution is stable.

A fundamental matrix of (4.2.14) is

$$\begin{aligned}\tilde{X}(T+) &= (E+B)e^{AT} \\ &= \begin{bmatrix} 1 & 0 \\ 0 & 1-p \end{bmatrix} \begin{bmatrix} e^{a_1 T} & 0 \\ \dfrac{b_1}{a_1 - b_2}(e^{a_1 T} - e^{b_2 T}) & e^{b_2 T} \end{bmatrix} \\ &= \begin{bmatrix} e^{a_1 T} & 0 \\ \frac{b_1(1-p)}{a_1 - b_2}(e^{a_1 T} - e^{b_2 T}) & (1-p)e^{b_2 T} \end{bmatrix}.\end{aligned}$$

The multipliers μ_i for $i = 1, 2$ of (4.2.14) are given by the eigenvalues of the matrix $M = \tilde{X}(T+)\tilde{X}^{-1}(0+)$ (reference Chapter 2; Remark 2.4.2) where $\tilde{X}^{-1}(0+)$ is the identity matrix in this case. Therefore we have $M = \tilde{X}(T+)$.

The Floquet multipliers μ_j $(j = 1, 2)$ are given by

$$\mu_1 = e^{a_1 T}$$

$$\mu_2 = (1-p)e^{b_2 T}.$$

Since all the multipliers are distinct from 1, the homogenous equation (4.2.14) has no non-trivial T-periodic solutions. Thus the non-homogeneous equation (4.2.11) has a unique T-periodic solution $\tilde{x}(t)$ (reference Chapter 2; Theorem 2.5.1) given by equation (4.2.13).

Also, since all the multipliers μ_j of the homogeneous equation (4.2.14) are by modulus smaller than 1 (since $a_1, b_2 < 0$), then the T-periodic solution $\tilde{x}(t)$ of the non-homogeneous equation (4.2.11) is exponentially stable (reference Chapter 2; Remark 2.5.2).

∎

In this case, since $a_2 = 0$ and $r = 0$, we always have a stable T-periodic solution. Figure 4.13 shows, for parameters values in Table 1, that there is a stable T-periodic orbit.

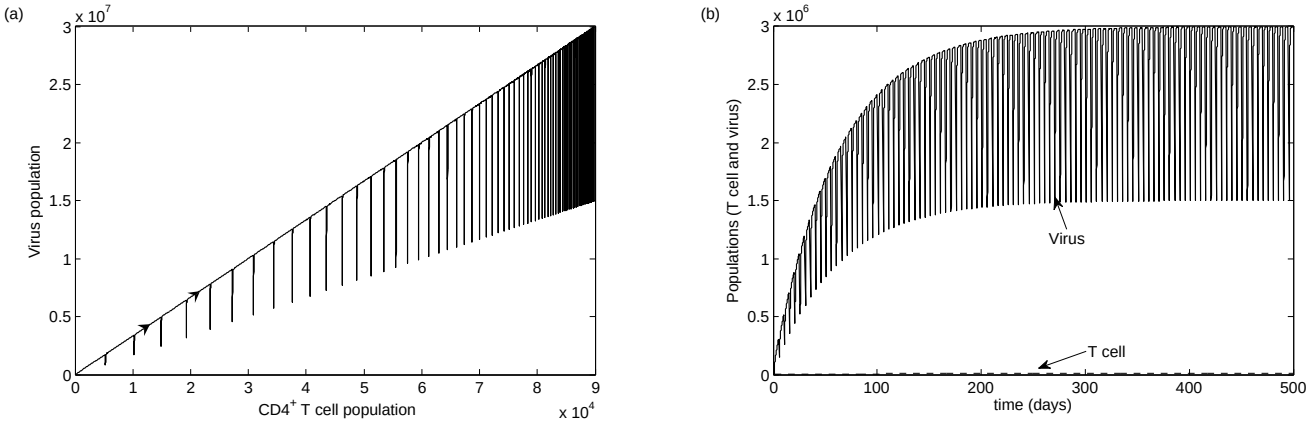

Figure 4.13: The behaviour of the CD4$^+$ T cell and virus populations when $a_2 = 0$ and $r = 0$ (all other parameters are fixed at their sample value in Table 1). In this case, we have a stable positive T-periodic solution. (a) CD4$^+$ T cell population versus virus population. (b) Time dynamics versus populations.

Nonlinear impulsive system

If we include in equation (4.2.11) the nonlinear term found in equations (4.1.4), the reduced system with drug is given by

$$\begin{aligned} \frac{dC}{dt} &= a_1C + a_3 \qquad & \frac{dV}{dt} &= b_1C + b_2V + b_3 - rCV \qquad & t \neq kT \\ \Delta C &= 0 & \Delta V &= -pV & t = kT, \end{aligned} \tag{4.2.15}$$

for $t \in \mathbb{R}_+$ and $k \in \mathbb{N}$.

Theorem 4.2.4 *Let the inequalities (4.1.5)-(4.1.6) hold. Then model (4.2.15) has a unique positive T-periodic solution with one impulse per period. The impulsive periodic orbit is exponentially stable.*

Proof: We will construct a periodic solution $(\tilde{C}(t), \tilde{V}(t))$ to equation (4.2.15) by explicitly solving the boundary value problem $C(0+) = C(T+)$, $V(0+) = V(T+)$, which can be shown to have at most one solution. The solution to the T-periodic orbit is given by equation (4.2.12). So, for $0 < t < T$, the T-periodic solution satisfies

$$\tilde{C}(t) = e^{a_1 t}\left(C(0+) + a_3\int_0^t e^{-a_1 s}ds\right).$$

Since $C(0+) = C(T+)$, we have

$$C(0+) = -\frac{a_3}{a_1}.$$

From the V equation in model (4.2.15), we can write the Cauchy matrix for the corresponding homogeneous equation

$$\begin{aligned} \frac{dV}{dt} &= (b_2 - r\tilde{C}(t))V \qquad & t \neq \tau_k \\ \Delta V &= -pV & t = \tau_k \end{aligned} \tag{4.2.16}$$

as the function

$$X(t) = \exp\Big[\int_0^t (b_2 - r\tilde{C}(z))dz\Big] \qquad 0 < t < T. \tag{4.2.17}$$

Then

$$X(T+) = (1-p)\exp\Big[\int_0^T (b_2 - r\tilde{C}(z))dz\Big]. \tag{4.2.18}$$

We have that

$$\tilde{V}(t) = X(t)\left(V(0+) + \int_0^t X^{-1}(s)g(s)ds\right). \tag{4.2.19}$$

Therefore the T-periodic solution for $0 < t < T$ is given by

$$\begin{aligned}
\tilde{C}(t) &= -\frac{a_3}{a_1} \\
\tilde{V}(t) &= e^{\left(b_2 + r\frac{a_3}{a_1}\right)t}V(0+) + \left(b_3 - \frac{b_1 a_3}{a_1}\right)\left(\frac{e^{\left(b_2+r\frac{a_3}{a_1}\right)t} - 1}{b_2 + r\frac{a_3}{a_1}}\right),
\end{aligned}$$

where

$$V(0+) = \frac{\left(b_3 - \frac{b_1 a_3}{a_1}\right)\left(\frac{e^{\left(b_2+r\frac{a_3}{a_1}\right)T} - 1}{b_2 + r\frac{a_3}{a_1}}\right)}{1 - (1-p)e^{\left(b_2+r\frac{a_3}{a_1}\right)T}}.$$

This is a positive T-periodic orbit since $0 \le p < 1$ and $a_1, b_2 < 0$.

We now apply impulsive Floquet theory to the nonlinear system (4.2.15) to establish exponential stability of the periodic orbit (reference Section 2.6). For the nonlinear equations (4.2.15), we associate with the solution $\phi(t) = (\tilde{C}(t), \tilde{V}(t))$ with moment of impulse effect τ_k, the variational equation

$$\begin{aligned}
\frac{dz}{dt} &= \frac{\partial f}{\partial x}(t, \phi(t))z \qquad && t \neq \tau_k \\
\Delta z &= L_k z && t = \tau_k,
\end{aligned} \tag{4.2.20}$$

where

$$f_k = f(\tau_k^-, \phi(\tau_k^-)) \qquad f_k^+ = f(\tau_k^+, \phi(\tau_k^+)) \qquad L_k = \frac{\partial I_k}{\partial x}(\phi(\tau_k^-)).$$

We have that

$$\frac{\partial f}{\partial x} = \begin{bmatrix} a_1 & 0 \\ b_1 - r\tilde{V}(t) & b_2 - r\tilde{C}(t) \end{bmatrix} \qquad \frac{\partial I_k}{\partial x} = \begin{bmatrix} 0 & 0 \\ 0 & -p \end{bmatrix} \qquad f_k = \begin{bmatrix} a_3 + a_1\tilde{C}(\tau_k) \\ b_1\tilde{C}(\tau_k) + b_2\tilde{V}(\tau_k) + b_3 - r\tilde{C}(\tau_k)\tilde{V}(\tau_k) \end{bmatrix}$$

In this case, the variational equation is reduced to

$$\begin{aligned} \frac{dz}{dt} &= \begin{bmatrix} a_1 & 0 \\ b_1 - r\tilde{V}(t) & b_2 - r\tilde{C}(t) \end{bmatrix} z \qquad && t \neq \tau_k \\ \Delta z &= \begin{bmatrix} 0 & 0 \\ 0 & -p \end{bmatrix} z && t = \tau_k. \end{aligned} \tag{4.2.21}$$

This is a linear homogenous impulsive system. Since $\dfrac{\partial f}{\partial x}(t, \phi(t))$ is a lower triangular matrix and $\tilde{C}(t)$ is constant, the exponents of the Floquet multipliers are the diagonal entries of $\dfrac{\partial f}{\partial x}(t, \phi(t))$. Since $E - L_k$ is a diagonal matrix, the Floquet multipliers are scaled accordingly. Therefore the Floquet multipliers are given by

$$\begin{aligned} \mu_1 &= e^{a_1 T} \\ \mu_2 &= (1-p)e^{(b_2 + r\frac{a_3}{a_1})T}. \end{aligned}$$

Since the multipliers are such that $|\mu_i| < 1$ for $i = 1, 2$ (since $a_1, b_2 < 0$), we have that the variational equation is exponentially stable. This implies that the T-periodic solution $\phi(t) = (\tilde{C}(t), \tilde{V}(t))$ of the nonlinear system (4.2.15) is also exponentially stable (reference Chapter 2; Remark 2.6.1).

∎

Using the parameter values in Table 1, Figures 4.14 and 4.15 show that changing the nonlinear infection rate r does not change stability.

For Figure 4.14, we set r such that the positive T-periodic solution of the general nonlinear system (4.2.10) was stable. In this case, the positive T-periodic solution of the nonlinear reduced system (4.2.15) is also stable. For Figure 4.15, we set r

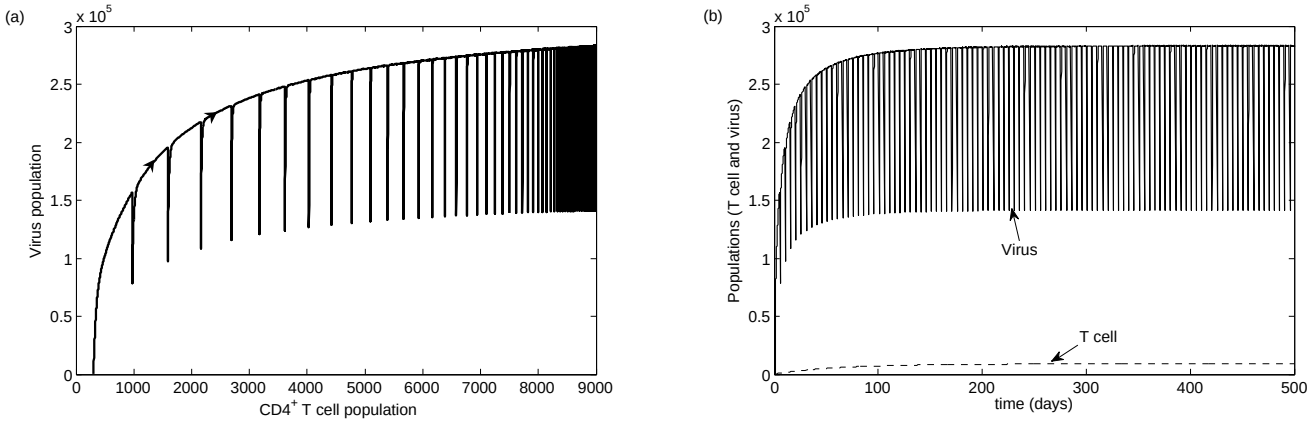

Figure 4.14: The behaviour of the $CD4^+$ T cell and virus populations when $a_2 = 0$ and $r = 0.0032$ (all other parameters are fixed at their sample value in Table 1). In this case, we have a stable positive T-periodic solution. (a) $CD4^+$ T cell population versus virus population. (b) Time dynamics versus populations.

such that the positive T-periodic solution of the general nonlinear system (4.2.10) was unstable. In this case, the positive T-periodic solution of the nonlinear reduced system (4.2.15) is stable.

4.2.4 Impulsive system with an immune response as an impulse

Since biologically we know that the T cells are affected by the presence of virus, we will now consider a system where $a_2 = 0$ but that the effect of the virus is included in an impulse. We have

$$\Delta C = \theta V \qquad \text{if } t = \tau_k. \tag{4.2.22}$$

This means that when a drug is taken, the number of T cells will increase (or decrease depending on the sign of θ) when virus is present. This change is similar to that of

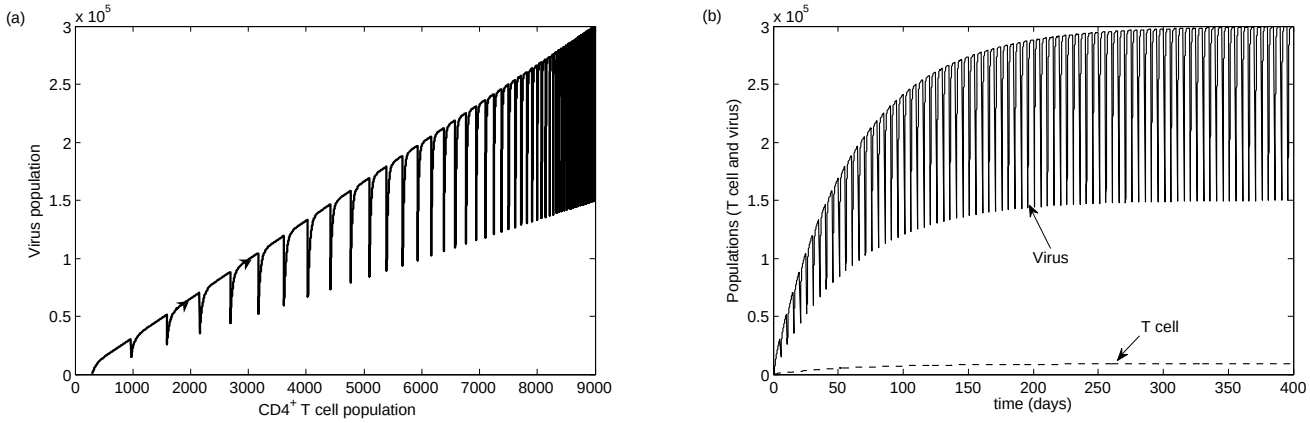

Figure 4.15: The behaviour of the $CD4^+$ T cell and virus populations when $a_2 = 0$, $r = 10^{-10}$ and $b_1 = 100$ (all other parameters are fixed at their sample value in Table 1). In this case, we have a stable positive T-periodic solution. (a) $CD4^+$ T cell population versus virus population. (b) Time dynamics versus populations.

a_2. The difference between the models with either a_2 or θ as the immune response is that the change in T cells is instantaneous when the immune response is an impulse. Biologically, an impulse condition for the immune response is not as realistic as the continuous case, but the inclusion of an immune response rate in this form will allow for analytical results on the effect of the nonlinear infection term.

Linear non-homogeneous impulsive system

We will consider the case from (4.1.4) with $a_2 = 0$. When a drug is taken, the T cells undergo an impulse as described in (4.2.22). We get the following impulsive differential system

$$\begin{aligned} &\frac{dC}{dt} = a_1 C + a_3 \qquad \frac{dV}{dt} = b_1 C + b_2 V + b_3 \qquad t \neq kT \\ &\Delta C = \theta V \qquad\qquad \Delta V = -pV \qquad\qquad t = kT, \end{aligned} \tag{4.2.23}$$

for $t \in \mathbb{R}_+$ and $k \in \mathbb{N}$.

Theorem 4.2.5 *Let the inequalities (4.1.5)-(4.1.6) hold. Then model (4.2.23) has a unique positive T-periodic solution with one impulse per period if*

$$\theta \neq \frac{(a_1 - b_2)\left(\pm 1 - e^{a_1 T} - (1-p)e^{b_2 T}\right)(1 \pm e^{a_1 T}))}{b_1(e^{a_1 T} - e^{b_2 T})}$$

and

$$\frac{a_3(1-p)(1-e^{a_1 T})}{a_1 V(0+)} < \theta < \frac{(1-(1-p)e^{b_2 T})(1-e^{a_1 T})(a_1 - b_2)}{b_1(e^{a_1 T} - e^{b_2 T})}.$$

Proof: We will construct a periodic solution $(\tilde{C}(t), \tilde{V}(t))$ to equation (4.2.23) by explicitly solving the boundary value problem $C(0+) = C(T+)$, $V(0+) = V(T+)$, which can be shown to have at most one solution. The solution to the T-periodic orbit is given by equation (4.2.12). So, for $0 < t < T$, we have

$$\tilde{C}(t) = e^{a_1 t}\left(C(0+) + a_3 \int_0^t e^{-a_1 s} ds\right)$$
$$\tilde{V}(t) = e^{b_2 t}\left(V(0+) + \int_0^t e^{-b_2 s}\left(b_1 \tilde{C}(s) + b_3\right) ds\right).$$

Since $C(0+) = C(T+)$ and $V(0+) = V(T+)$, we have

$$C(0+) = \frac{1}{1 - e^{a_1 T}}\left(\frac{\theta}{1-p} V(T+) - \frac{a_3}{a_1}(1 - e^{a_1 T})\right)$$
$$V(0+) = \frac{e^{b_2 T}(1-p)}{1-(1-p)e^{b_2 T}}\left(b_1 \int_0^T \tilde{C}(s) e^{-b_2 s} ds - \frac{b_3}{b_2}(e^{-b_2 T} - 1)\right).$$

Therefore we have

$$\tilde{C}(t) = -\frac{a_3}{a_1} + \frac{\theta e^{a_1 t}}{(1-p)(1-e^{a_1 T})} V(0+)$$
$$\tilde{V}(t) = e^{b_2 t}\left(V(0+) + \frac{\theta b_1}{(1-p)(1-e^{a_1 T})(a_1 - b_2)}(e^{a_1 t} - e^{b_2 t})\right) - \frac{1}{b_2}\left(b_3 + \frac{b_1 a_3}{|a_1|}\right)(1 - e^{b_2 t}), \tag{4.2.24}$$

where

$$V(0+) = \frac{(1-(1-p)e^{b_2 T})(1-p)(1-e^{a_1 T})(a_1 - b_2)}{(1-(1-p)e^{b_2 T})(1-p)(1-e^{a_1 T})(a_1 - b_2) - e^{b_2 T} b_1 \theta (1-p)(e^{(a_1 - b_2)T} - 1)}$$
$$\times \left(\frac{(1-e^{b_2 T})(1-p)}{1-(1-p)e^{b_2 T}}\left(\frac{b_1 a_3 + |a_1| b_3}{a_1 b_2}\right)\right).$$

Therefore $V(0+) > 0$ if

$$(1-(1-p)e^{b_2T})(1-p)(1-e^{a_1T})(a_1-b_2) > e^{b_2T}b_1\theta(1-p)(e^{(a_1-b_2)T}-1)$$

or

$$\theta < \frac{(1-(1-p)e^{b_2T})(1-e^{a_1T})(a_1-b_2)}{b_1(e^{a_1T}-e^{b_2T})}. \tag{4.2.25}$$

We have that $C(0+) > 0$ when

$$\frac{\theta}{(1-p)(1-e^{a_1T})}V(0+) - \frac{a_3}{a_1} > 0,$$

or when

$$\theta > \frac{a_3(1-p)(1-e^{a_1T})}{a_1V(0+)}. \tag{4.2.26}$$

When the conditions on $C(0+)$ and $V(0+)$ are satisfied, we have a positive T-periodic solution.

The homogenous equation of (4.2.23) is given by

$$\begin{aligned} \frac{dx}{dt} &= Ax \qquad t \neq \tau_k \\ \Delta x &= Bx \qquad t = \tau_k, \end{aligned} \tag{4.2.27}$$

where

$$A = \begin{bmatrix} a_1 & 0 \\ b_1 & b_2 \end{bmatrix} \qquad B = \begin{bmatrix} 0 & \theta \\ 0 & -p \end{bmatrix} \qquad x = \begin{bmatrix} C \\ V \end{bmatrix}.$$

A fundamental matrix of (4.2.27) is

$$\begin{aligned} \tilde{X}(T+) &= (E+B)e^{AT} \\ &= \begin{bmatrix} e^{a_1T} + \frac{b_1\theta}{a_1-b_2}(e^{a_1T}-e^{b_2T}) & \theta e^{b_2T} \\ \frac{b_1(1-p)}{a_1-b_1}(e^{a_1T}-e^{b_1T}) & (1-p)e^{b_2T} \end{bmatrix}. \end{aligned}$$

We calculate the multipliers μ_i for $i = 1, 2$ of (4.2.27) by calculating the eigenvalues of the matrix $M = \tilde{X}(T+)\tilde{X}^{-1}(0+)$ (reference Chapter 2; Remark 2.4.2) where $\tilde{X}^{-1}(0+)$ is the identity matrix in this case. Therefore we have $M = \tilde{X}(T+)$.

The Floquet multipliers satisfy the characteristic equation

$$\mu^2 - \mu\left(e^{a_1T} + (1-p)e^{b_2T} + \frac{b_1\theta}{a_1 - b_2}(e^{a_1T} - e^{b_2T})\right) + (1-p)e^{(a_1+b_2)T} = 0. \quad (4.2.28)$$

Therefore the Floquet multipliers μ_j $(j = 1, 2)$ are

$$\mu_{1,2} = \frac{1}{2}\Bigg(e^{a_1T} + (1-p)e^{b_2T} + \frac{b_1\theta}{a_1 - b_2}(e^{a_1T} - e^{b_2T}) \quad (4.2.29)$$

$$\pm \sqrt{\left(e^{a_1T} - (1-p)e^{b_2T} + \frac{b_1\theta}{a_1 - b_2}(e^{a_1T} - e^{b_2T})\right)^2 + \frac{4b_1(1-p)e^{b_2T}\theta}{a_1 - b_2}(e^{a_1T} - e^{b_2T})}\Bigg). \quad (4.2.30)$$

The multipliers are distinct from 1 in absolute value if

$$e^{a_1T} + (1-p)e^{b_2T}(1 - e^{a_1T}) + \frac{b_1\theta}{a_1 - b_2}(e^{a_1T} - e^{b_2T}) \neq 1, \quad (4.2.31)$$

or if

$$e^{a_1T} + (1-p)e^{b_2T}(1 + e^{a_1T}) + \frac{b_1\theta}{a_1 - b_2}(e^{a_1T} - e^{b_2T}) \neq -1, \quad (4.2.32)$$

and so in this case, the homogenous equation (4.2.27) has no non-trivial T-periodic solutions. Thus the non-homogeneous equation (4.2.23) has a unique T-periodic solution $\tilde{x}(t)$ (reference Chapter 2; Theorem 2.5.1) given by equation (4.2.24). ∎

We can also demonstrate numerically the positivity and uniqueness of T-periodic solutions with the values in Table 1. In this case we have $a_2 = 0$ and $r = 0$ and we vary θ and T. Figure 4.16 shows the relationship between the time between doses and the immune response rate. The values of T and θ such that uniqueness is not satisfied (equations (4.2.31) and (4.2.32)) is represented by the dashed lines, whereas

the solid and dotted lines represent the inequalities that need to be satisfied in order to maintain positivity of solutions (The solid line represents equation (4.2.25) and the dotted line represents equation (4.2.26)). We have that a bigger immune response requires a larger period in order to maintain positivity. Note that certain positive values for θ do not preserve positivity of T-periodic solutions.

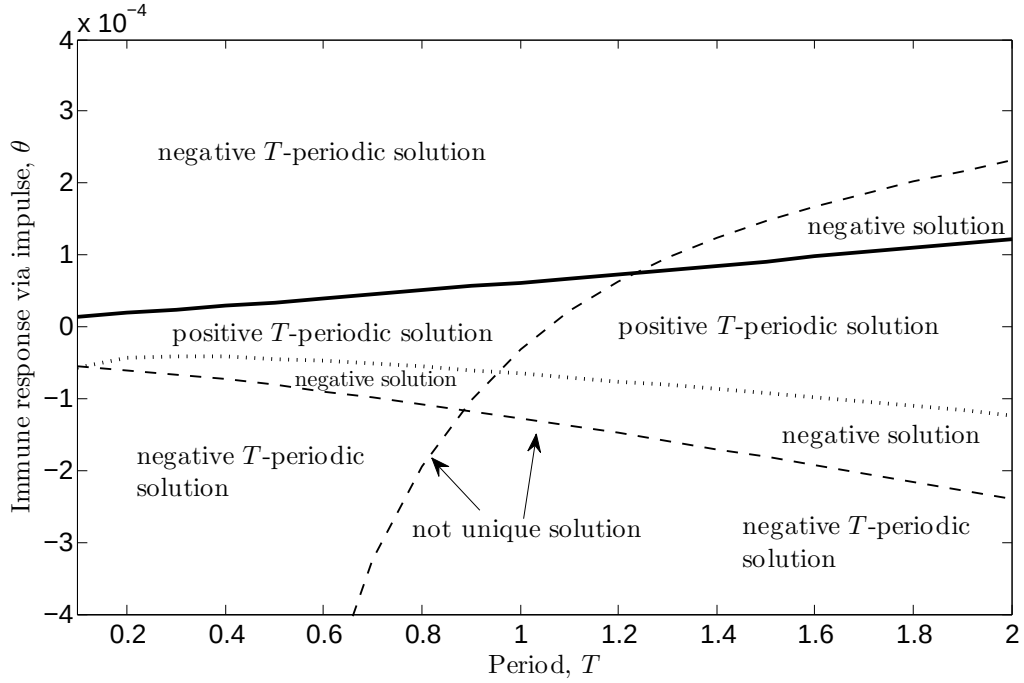

Figure 4.16: Regions in which we have a unique positive T-periodic solution. All parameters are described in Table 4.1. The dashed lines represent the equalities that need to be satisfied for uniqueness of solutions (equations (4.2.31) and (4.2.32)), whereas the solid and dotted lines represent the inequalities that need to be satisfied in order to maintain positivity of solutions, equations (4.2.25) and (4.2.26) respectively.

Theorem 4.2.6 *Under the conditions of Theorem 4.2.5, the unique positive T-periodic orbit is exponentially stable if*

1. $\theta > 0$ *and*

$$\left| e^{a_1 T} + (1-p)e^{b_2 T} + \frac{b_1 \theta}{a_1 - b_2}(e^{a_1 T} - e^{b_2 T}) \right| < 1;$$

2. $\theta < 0$,

$$|\theta| < \frac{(a_1 - b_2)\left(e^{a_1 T} - (1-p)e^{b_2 T} + \frac{b_1\theta}{a_1 - b_2}(e^{a_1 T} - e^{b_2 T})\right)^2}{4b_1(1-p)e^{b_2 T}(e^{a_1 T} - e^{b_2 T})},$$

and

$$\left| e^{a_1 T} + \frac{b_1\theta}{a_1 - b_2}(e^{a_1 T} - e^{b_2 T}) \right| < 1;$$

3. $\theta < 0$,

$$|\theta| = \frac{(a_1 - b_2)\left(e^{a_1 T} - (1-p)e^{b_2 T} + \frac{b_1\theta}{a_1 - b_2}(e^{a_1 T} - e^{b_2 T})\right)^2}{4b_1(1-p)e^{b_2 T}(e^{a_1 T} - e^{b_2 T})},$$

and

$$\frac{1}{2}\left| e^{a_1 T} + (1-p)e^{b_2 T} + \frac{b_1\theta}{a_1 - b_2}(e^{a_1 T} - e^{b_2 T}) \right| < 1;$$

4. $\theta < 0$,

$$|\theta| > \frac{(a_1 - b_2)\left(e^{a_1 T} - (1-p)e^{b_2 T} + \frac{b_1\theta}{a_1 - b_2}(e^{a_1 T} - e^{b_2 T})\right)^2}{4b_1(1-p)e^{b_2 T}(e^{a_1 T} - e^{b_2 T})},$$

and

$$\frac{1}{2}\sqrt{\frac{4b_1(1-p)e^{b_2 T}|\theta|}{a_1 - b_2}(e^{a_1 T} - e^{b_2 T})} < 1.$$

Proof: The proof of Theorem 4.2.6 requires that we know the Floquet multipliers. They are given by equation (4.2.29). We use Chapter 2; Remark 2.5.2 for exponential stability. The multipliers of the characteristic equation (4.2.28) are as follows.

(i) If $\theta > 0$, the multipliers $(\mu_1 > \mu_2)$ are distinct real numbers since $a_1 - b_2 > 0$ and $e^{a_1 T} - e^{b_2 T} > 0$.

(ii) If $\theta < 0$, we have three cases.

(ii.1) If

$$\left(e^{a_1T}-(1-p)e^{b_2T}+\frac{b_1\theta}{a_1-b_2}(e^{a_1T}-e^{b_2T})\right)^2>\frac{4b_1(1-p)e^{b_2T}|\theta|}{a_1-b_2}(e^{a_1T}-e^{b_2T}),$$

then we have two distinct real numbers with $\mu_1>\mu_2$.

(ii.2) If

$$\left(e^{a_1T}-(1-p)e^{b_2T}+\frac{b_1\theta}{a_1-b_2}(e^{a_1T}-e^{b_2T})\right)^2=\frac{4b_1(1-p)e^{b_2T}|\theta|}{a_1-b_2}(e^{a_1T}-e^{b_2T}),$$

then we have one multiplier

$$\mu=\frac{1}{2}\left(e^{a_1T}+(1-p)e^{b_2T}+\frac{b_1\theta}{a_1-b_2}(e^{a_1T}-e^{b_2T})\right).$$

(ii.3) If

$$\left(e^{a_1T}-(1-p)e^{b_2T}+\frac{b_1\theta}{a_1-b_2}(e^{a_1T}-e^{b_2T})\right)^2<\frac{4b_1(1-p)e^{b_2T}|\theta|}{a_1-b_2}(e^{a_1T}-e^{b_2T}),$$

then we have complex numbers where

$$\mu_{1,2}=\frac{1}{2}\Bigg(e^{a_1T}+(1-p)e^{b_2T}+\frac{b_1\theta}{a_1-b_2}(e^{a_1T}-e^{b_2T})$$
$$\pm i\sqrt{\frac{4b_1(1-p)e^{b_2T}|\theta|}{a_1-b_2}(e^{a_1T}-e^{b_2T})-\left(e^{a_1T}-(1-p)e^{b_2T}+\frac{b_1\theta}{a_1-b_2}(e^{a_1T}-e^{b_2T})\right)^2}\Bigg).$$

For the stability of the non-homogeneous linear system (4.2.23), we have the following cases.

1. If $\theta>0$, we have that the multipliers are by modulus smaller than 1 if $|\mu_1|<1$.

   Therefore

$$|\mu_1|<\frac{1}{2}\left|e^{a_1T}+(1-p)e^{b_2T}+\frac{b_1\theta}{a_1-b_2}(e^{a_1T}-e^{b_2T})+\sqrt{\left(e^{a_1T}+(1-p)e^{b_2T}+\frac{b_1\theta}{a_1-b_2}(e^{a_1T}-e^{b_2T})\right)^2}\right|$$
$$=\left|e^{a_1T}+(1-p)e^{b_2T}+\frac{b_1\theta}{a_1-b_2}(e^{a_1T}-e^{b_2T})\right|$$
$$\equiv\mu_1^*.$$

Hence if $\mu_1^* < 1$, all the multipliers μ_j of the homogeneous equation (4.2.27) are by modulus smaller than 1, and the T-periodic solution $\tilde{x}(t)$ of the non-homogeneous equation (4.2.23) is exponentially stable.

2. $\theta < 0$ and we have case (ii.1), we have that the multipliers are by modulus smaller than 1 if $|\mu_1| < 1$. Therefore

$$\begin{aligned}|\mu_1| &< \frac{1}{2}\left|e^{a_1T} + (1-p)e^{b_2T} + \frac{b_1\theta}{a_1-b_2}(e^{a_1T}-e^{b_2T}) + \sqrt{\left(e^{a_1T} - (1-p)e^{b_2T} + \frac{b_1\theta}{a_1-b_2}(e^{a_1T}-e^{b_2T})\right)^2}\right| \\ &= \left|e^{a_1T} + \frac{b_1\theta}{a_1-b_2}(e^{a_1T}-e^{b_2T})\right| \\ &\equiv \mu_2^*.\end{aligned}$$

Hence if $\mu_1^* < 1$, all the multipliers μ_j of the homogeneous equation (4.2.27) are by modulus smaller than 1, and the T-periodic solution $\tilde{x}(t)$ of the non-homogeneous equation (4.2.23) is exponentially stable.

3. If $\theta < 0$ and we have case (ii.2), then

$$\begin{aligned}|\mu| &= \frac{1}{2}\left|e^{a_1T} + (1-p)e^{b_2T} + \frac{b_1\theta}{a_1-b_2}(e^{a_1T}-e^{b_2T})\right| \\ &\equiv \mu_3^*.\end{aligned}$$

Hence if $\mu_3^* < 1$, all the multipliers μ_j of the homogeneous equation (4.2.27) are by modulus smaller than 1, and the T-periodic solution $\tilde{x}(t)$ of the non-homogeneous equation (4.2.23) is exponentially stable.

4. If $\theta < 0$ and we have case (ii.3), then

$$\begin{aligned}|\mu_{1,2}| &= \frac{1}{2}\sqrt{\frac{4b_1(1-p)e^{b_2T}|\theta|}{a_1-b_2}(e^{a_1T}-e^{b_2T})} \\ &\equiv \mu_4^*.\end{aligned}$$

Hence if $\mu_4^* < 1$, all the multipliers μ_j of the homogeneous equation (4.2.27) are by modulus smaller than 1, and the T-periodic solution $\tilde{x}(t)$ of the non-homogeneous equation (4.2.23) is exponentially stable.

∎

We can also numerically illustrate these results with the values in Table 1. In this case we have $a_2 = 0$ and $r = 0$ and we vary θ. The value $p = 0.8$ is fixed, but it should be noted that slight changes in p ($0 \leq p < 1$) do not change stability. Figures 4.17 and 4.18 show the T-periodic solution when the condition for stability in Theorem 4.2.6 of the T-periodic solution of the linear system (4.2.23) is satisfied.

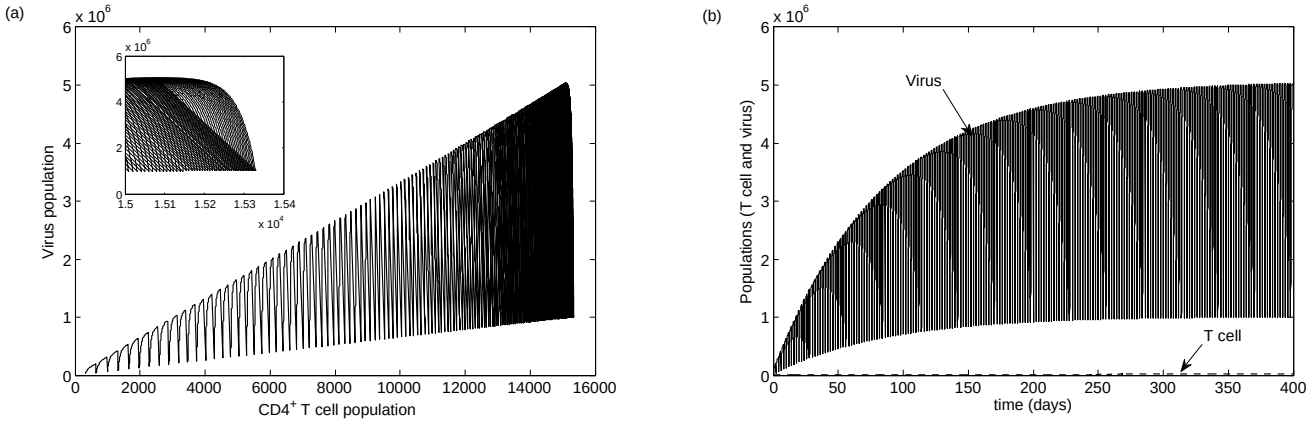

Figure 4.17: The behaviour of the CD4$^+$ T cell and virus populations when $a_2 = 0$, $p = 0.8$ and $\theta = 0.00005$ (all other parameters are fixed at their sample value in Table 1). In this case, the conditions for positivity and stability in Theorems 4.2.5 and 4.2.6, respectively, are satisfied and we have a stable positive T-periodic solution. (a) CD4$^+$ T cell population versus virus population; inset: close up of periodic solution. (b) Time dynamics versus populations.

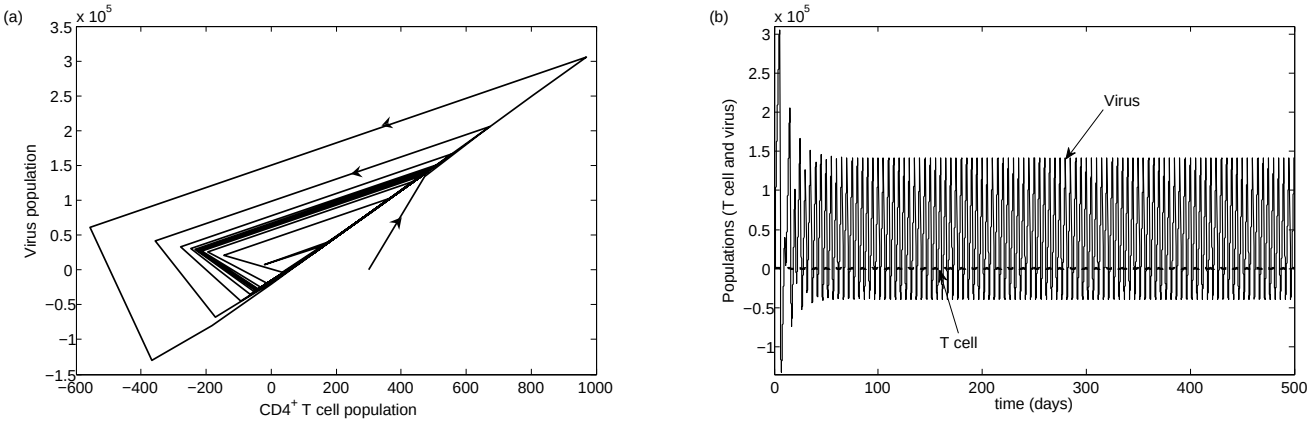

Figure 4.18: The behaviour of the $CD4^+$ T cell and virus populations when $a_2 = 0$, $p = 0.8$ and $\theta = -0.005$ (all other parameters are fixed at their sample value in Table 1). In this case, the condition for stability in Theorem 4.2.6 is satisfied and we have a stable T-periodic solution. Note that the condition for positivity is not satisfied (Theorem 4.2.5). (a) $CD4^+$ T cell population versus virus population. (b) Time dynamics versus populations.

Figure 4.17 shows a positive, stable T-periodic solution since both the positivity and stability conditions in Theorems 4.2.5 and 4.2.6, respectively, are satisfied, whereas in Figure (4.18), the stability conditions in Theorem 4.2.6 are satisfied but the positivity conditions in Theorem 4.2.5 are violated. For the latter case, we have a stable T-periodic solution, but it is not positive. Figures 4.19 and 4.20 show the T-periodic solution when the condition for stability is not satisfied. In this case, we have an unstable T-periodic solution.

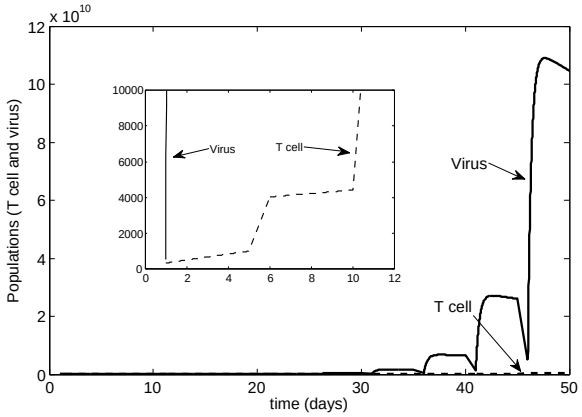

Figure 4.19: The behaviour of the CD4$^+$ T cell and virus populations when $a_2 = 0$, $p = 0.8$ and $\theta = 0.01$ (all other parameters are fixed at their sample value in Table 1). In this case, the conditions for stability in Theorem 4.2.6 are not satisfied and we have an unstable T-periodic solution. The inset shows a close up of the time dynamics for the populations.

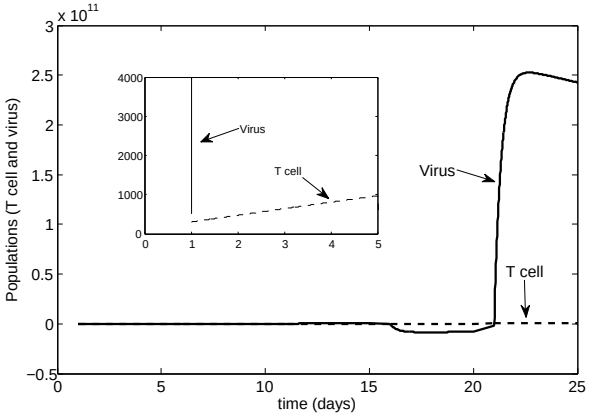

Figure 4.20: The behaviour of the CD4$^+$ T cell and virus populations when $a_2 = 0$, $p = 0.8$ and $\theta = -0.1$ (all other parameters are fixed at their sample value in Table 1). In this case, the conditions for stability in Theorem 4.2.6 are not satisfied and we have an unstable T-periodic solution. The inset shows a closer up of the time dynamics for the populations.

Nonlinear impulsive system

If we include in equation (4.2.23) the nonlinear term found in equation (4.1.4), the reduced system including the impulse in C (equation (4.2.22)) is given by

$$\begin{aligned} \frac{dC}{dt} &= a_1C + a_3 \qquad & \frac{dV}{dt} &= b_1C + b_2V + b_3 - rCV \qquad & t &\neq kT \\ \Delta C &= \theta V & \Delta V &= -pV & t &= kT, \end{aligned} \tag{4.2.33}$$

for $t \in \mathbb{R}_+$ and $k \in \mathbb{N}$.

Theorem 4.2.7 *Let the inequalities (4.1.5)-(4.1.6) hold. Then model (4.2.33) has a positive T-periodic solution $(\tilde{C}(t), \tilde{V}(t))$ with one impulse per period, provided there is a positive solution $\tilde{C}(0+)$ of the equation*

$$C(0+) = \frac{\theta}{(1-p)(1-e^{a_1T})}\left(\int_0^T f(s; C(0+))ds - \frac{a_3(1-p)(1-e^{a_1T})}{a_1\theta}\left(\frac{1}{1-p}\exp\left[-\left(b_2 + \frac{a_3r}{a_1}\right)T + \frac{r}{a_1}(e^{a_1T}-1)\left(C(0+) + \frac{a_3}{a_1}\right)\right] - 1\right)\right),$$

where

$$f(s; C(0+)) = \exp\left[-\left(b_2 + \frac{ra_3}{a_1}\right)s + \left(\frac{rC(0+)}{a_1} + \frac{ra_3}{a_1^2}\right)(e^{a_1s}-1)\right]\left(b_1\left(e^{a_1s}C(0+) - \frac{a_3}{a_1}(1-e^{a_1s})\right) + b_3\right),$$

with $\theta \neq 0$ and $r\tilde{V}(t) < b_1$.

Proof: We will construct a periodic solution $(\tilde{C}(t), \tilde{V}(t))$ to equation (4.2.33) by explicitly solving the boundary value problem $C(0+) = C(T+)$, $V(0+) = V(T+)$. The solution to the T-periodic orbit is given by equation (4.2.12). Let $r\tilde{V}(t) < b_1$. So for $0 < t < T$, we have

$$\tilde{C}(t) = e^{a_1t}\left(C(0+) + a_3\int_0^t e^{-a_1s}ds\right)$$

$$\tilde{V}(t) = \exp\left[b_2t - r\int_0^t \tilde{C}(s)ds\right]\left(V(0+) + \int_0^t \exp\left[-b_2s + r\int_0^s \tilde{C}(w)dw\right]\left(b_1\tilde{C}(s) + b_3\right)ds\right).$$

Since $C(0+) = C(T+)$ and $V(0+) = V(T+)$, we have

$$C(0+) = \frac{e^{a_1 T}\int_0^T e^{-a_1 s}a_3 ds + \dfrac{\theta}{1-p}V(0+)}{1-e^{a_1 T}}$$
$$V(0+) = \frac{\int_0^T \exp\left[-b_2 T + r\int_0^s \tilde{C}(w)dw\right]\left(b_1\tilde{C}(s)+b_3\right)ds}{\frac{1}{1-p}\exp\left[-b_2 T + r\int_0^T \tilde{C}(w)dw\right]-1}.$$

Solving, we have that $C(0+)$ satisfies the implicit equation

$$C(0+) = \frac{\theta}{(1-p)(1-e^{a_1 T})}\left(\int_0^T f(s;C(0+))ds - \frac{a_3(1-p)(1-e^{a_1 T})}{a_1\theta}\left(\frac{1}{1-p}\exp\left[-\left(b_2+\frac{a_3 r}{a_1}\right)T + \frac{r}{a_1}(e^{a_1 T}-1)\left(C(0+)+\frac{a_3}{a_1}\right)\right]-1\right)\right), \tag{4.2.34}$$

where

$$f(s;C(0+)) = \exp\left[-\left(b_2+\frac{ra_3}{a_1}\right)s + \left(\frac{rC(0+)}{a_1}+\frac{ra_3}{a_1^2}\right)(e^{a_1 s}-1)\right]\left(b_1\left(e^{a_1 s}C(0+) - \frac{a_3}{a_1}(1-e^{a_1 s})\right)+b_3\right).$$

Therefore if $C(0+) > 0$, then $V(0+) > 0$, and so the T-periodic solution is positive.

∎

Theorem 4.2.8 *Under the conditions of Theorem 4.2.7, the positive impulsive periodic orbit is exponentially stable if*

1. $\theta > 0$ *and*

$$\left|e^{a_1 T} + z_2^1(T+) + \frac{\theta}{1-p}(z_2^2(T+) - z_2^1(T+))\right| < 1;$$

2. $\theta < 0$,

$$\left(e^{a_1 T} - z_2^1(T+) + \frac{\theta}{1-p}\left(z_2^2(T+) - z_2^1(T+)\right)\right)^2 > \frac{2|\theta| z_2^1(T+)}{1-p}\left(z_2^2(T+) - z_2^1(T+)\right),$$

and

$$\frac{1}{2}\left|e^{a_1T}+z_2^1(T+)+\frac{\theta}{1-p}\left(z_2^2(T+)-z_2^1(T+)\right)\right.$$
$$\left.+\sqrt{\left(e^{a_1T}-z_2^1(T+)+\frac{\theta}{1-p}\left(z_2^2(T+)-z_2^1(T+)\right)\right)^2+\frac{2\theta z_2^1(T+)}{1-p}\left(z_2^2(T+)-z_2^1(T+)\right)}\right|<1;$$

3. $\theta<0$,

$$\left(e^{a_1T}-z_2^1(T+)+\frac{\theta}{1-p}\left(z_2^2(T+)-z_2^1(T+)\right)\right)^2=\frac{2|\theta|z_2^1(T+)}{1-p}\left(z_2^2(T+)-z_2^1(T+)\right),$$

and

$$\frac{1}{2}\left|e^{a_1T}+z_2^1(T+)+\frac{\theta}{1-p}(z_2^2(T+)-z_2^1(T+))\right|<1;$$

4. $\theta<0$,

$$\left(e^{a_1T}-z_2^1(T+)+\frac{\theta}{1-p}\left(z_2^2(T+)-z_2^1(T+)\right)\right)^2<\frac{2|\theta|z_2^1(T+)}{1-p}\left(z_2^2(T+)-z_2^1(T+)\right),$$

and

$$\frac{1}{2}\sqrt{\frac{2|\theta|z_2^1(T+)}{1-p}\left(z_2^2(T+)-z_2^1(T+)\right)}<1,$$

where

$$z_2^1(T+)=(1-p)\exp\left[\int_0^T(b_2-r\tilde{C}(s))ds\right]$$
$$z_2^2(T+)=(1-p)\exp\left[\int_0^T(b_2-r\tilde{C}(s))ds\right]\left(1+\int_0^T\exp\left[-\int_0^s(b_2-r\tilde{C}(w))dw\right]e^{a_1s}\left(b_1-r\tilde{V}(s)\right)ds\right).$$

Proof: We now apply impulsive Floquet theory to the nonlinear system (4.2.33) to establish exponential stability of the periodic orbit (reference Section 2.6). For the nonlinear equations (4.2.33), we associate with the solution $\phi(t)=(\tilde{C}(t),\tilde{V}(t))$ with moment of impulse effect τ_k, the variational equation

$$\begin{aligned}\frac{dz}{dt}&=\begin{bmatrix}a_1 & 0\\ b_1-r\tilde{V}(t) & b_2-r\tilde{C}(t)\end{bmatrix}z \qquad t\neq\tau_k\\ \Delta z&=\begin{bmatrix}0 & \theta\\ 0 & -p\end{bmatrix}z \qquad t=\tau_k.\end{aligned}\tag{4.2.35}$$

(see equation (4.2.20)). This is a linear homogenous impulsive system. A fundamental solution for the system is $\tilde{X}(t) = \begin{bmatrix} v_1(t) & v_2(t) \end{bmatrix}$ where

$$v_1(t) = \begin{bmatrix} z_1^1(t) \\ z_2^1(t) \end{bmatrix} \qquad v_2(t) = \begin{bmatrix} z_1^2(t) \\ z_2^2(t) \end{bmatrix}$$

are independent solutions to the variational equation (4.2.35). We have, if $z_1^1(t) \equiv 0$, that

$$\begin{aligned} z_1^1(0+) &= 0 \\ z_1^1(T+) &= \theta z_2^1(T) = \frac{\theta}{1-p} z_2^1(T+), \end{aligned}$$

and we have that

$$\begin{aligned} \frac{dz_2^1}{dt} &= \left(b_2 - r\tilde{C}(t)\right) z_2^1 \qquad && t \neq \tau_k \\ \Delta z_2^1 &= -p z_2^1 && t = \tau_k, \end{aligned} \tag{4.2.36}$$

where this homogeneous equation has a Cauchy matrix given by the same function as (4.2.17). Then a solution to (4.2.36) for $0 < t < T$ is given by

$$z_2^1(t) = z_2^1(0+) \exp\left[\int_0^T (b_2 - r\tilde{C}(s))ds\right],$$

where

$$\begin{aligned} z_2^1(0+) &= 1 \\ z_2^1(T+) &= (1-p) \exp\left[\int_0^T (b_2 - r\tilde{C}(s))ds\right]. \end{aligned}$$

Therefore a solution to system (4.2.35) is

$$\begin{aligned} v_1(0+) &= \begin{bmatrix} 0 \\ 1 \end{bmatrix} \\ v_1(T+) &= \begin{bmatrix} \frac{\theta}{1-p} z_2^1(T+) \\ z_2^1(T+) \end{bmatrix}. \end{aligned}$$

Now if $z_1^2 \neq 0$, then we have a solution given by

$$z_1^2(t) = e^{a_1 t},$$

where

$$\begin{aligned} z_1^2(0+) &= 1 \\ z_1^2(T+) &= e^{a_1 T} + \theta z_2^2(T) \\ &= e^{a_1 T} + \frac{\theta}{1-p} z_2^2(T+). \end{aligned}$$

We thus have

$$\begin{aligned} \frac{dz_2^2}{dt} &= (b_1 - r\tilde{V}(t))e^{a_1 t} + (b_2 - r\tilde{C}(t))z_2^2 \qquad t \neq \tau_k \\ \Delta z_2^2 &= -pz_2^2 \qquad\qquad\qquad\qquad\qquad\qquad t = \tau_k. \end{aligned} \tag{4.2.37}$$

This is a linear, non-homogenous equation. The Cauchy matrix for the corresponding homogenous equation

$$\begin{aligned} \frac{dz_2^2}{dt} &= (b_2 - r\tilde{C}(t))z_2^2 \qquad t \neq \tau_k \\ \Delta z_2^2 &= -pz_2^2 \qquad\qquad\qquad\qquad t = \tau_k \end{aligned} \tag{4.2.38}$$

is given by the same function as (4.2.17). Therefore we have, for $0 < t < T$, a solution given by

$$z_2^2(t) = \exp\left[\int_0^t (b_2 - r\tilde{C}(s))ds\right]\left(z_2^2(0+) + \int_0^t \exp\left[-\int_0^t (b_2 - r\tilde{C}(s))ds\right](b_1 - r\tilde{V}(s))e^{a_1 s}ds\right), \tag{4.2.39}$$

where

$$\begin{aligned} &z_2^2(0+) = 1 \\ &z_2^2(T+) = (1-p)\exp\left[\int_0^T (b_2 - r\tilde{C}(s))ds\right]\left(1 + \int_0^T \exp\left[-\int_0^T (b_2 - r\tilde{C}(s))ds\right](b_1 - r\tilde{V}(s))e^{a_1 s}ds\right) \end{aligned}$$

We have that $z_2^2 > 0$ since $r\tilde{V}(t) < b_1$. Therefore a solution to system (4.2.35) is

$$v_2(0+) = \begin{bmatrix} 1 \\ 1 \end{bmatrix}$$

$$v_2(T+) = \begin{bmatrix} e^{a_1 T} + \frac{\theta}{1-p} z_2^2(T+) \\ z_2^2(T+) \end{bmatrix}.$$

In order to calculate the multipliers μ_i for $i = 1, 2$ of (4.2.35), we calculate the eigenvalues of the matrix $M = \tilde{X}(T+)\tilde{X}^{-1}(0+)$ (reference Chapter 2; Remark 2.4.2). We have

$$\tilde{X}(T+) = \begin{bmatrix} \frac{\theta}{1-p} z_2^1(T+) & e^{a_1 T} + \frac{\theta}{1-p} z_2^2(T+) \\ z_2^1(T+) & z_2^2(T+) \end{bmatrix} \qquad \tilde{X}^{-1}(0+) = \begin{bmatrix} -1 & 1 \\ 1 & 0 \end{bmatrix}.$$

Therefore

$$\begin{aligned} M &= \tilde{X}(T+)\tilde{X}^{-1}(0+) \\ &= \begin{bmatrix} e^{a_1 T} + \frac{\theta}{1-p}\left(z_2^2(T+) - z_2^1(T+)\right) & \frac{\theta}{1-p} z_2^1(T+) \\ z_2^2(T+) - z_2^1(T+) & z_2^1(T+) \end{bmatrix}. \end{aligned}$$

The Floquet multipliers satisfy the characteristic equation

$$\mu^2 - \mu\left(e^{a_1 T} + z_2^1(T+) + \frac{\theta}{1-p}\left(z_2^2(T+) - z_2^1(T+)\right)\right) + z_2^1(T+)e^{a_1 T} = 0.$$

Therefore the Floquet multipliers μ_j $(j = 1, 2)$ are

$$\begin{aligned} \mu_{1,2} = \frac{1}{2}\Bigg(& e^{a_1 T} + z_2^1(T+) + \frac{\theta}{1-p}\left(z_2^2(T+) - z_2^1(T+)\right) \\ & \pm \sqrt{\left(e^{a_1 T} - z_2^1(T+) + \frac{\theta}{1-p}\left(z_2^2(T+) - z_2^1(T+)\right)\right)^2 + \frac{2\theta z_2^1(T+)}{1-p}\left(z_2^2(T+) - z_2^1(T+)\right)} \Bigg). \end{aligned}$$

We have several cases similar to the ones presented in the linear system (4.2.23).

(i) If $\theta > 0$, the multipliers are two distinct real numbers since $z_2^2(T+) - z_2^1(T+) > 0$ where $\mu_1 > \mu_2$.

(ii) If $\theta < 0$, we have three cases.

(ii.1) If

$$\left(e^{a_1 T} - z_2^1(T+) + \frac{\theta}{1-p}\left(z_2^2(T+) - z_2^1(T+)\right)\right)^2 > \frac{2|\theta| z_2^1(T+)}{1-p}\left(z_2^2(T+) - z_2^1(T+)\right),$$

then we have two real distinct numbers with $\mu_1 > \mu_2$.

(ii.2) If

$$\left(e^{a_1 T} - z_2^1(T+) + \frac{\theta}{1-p}\left(z_2^2(T+) - z_2^1(T+)\right)\right)^2 = \frac{2|\theta| z_2^1(T+)}{1-p}\left(z_2^2(T+) - z_2^1(T+)\right),$$

then we have one multiplier

$$\mu = \frac{1}{2}\left(e^{a_1 T} + z_2^1(T+) + \frac{\theta}{1-p}\left(z_2^2(T+) - z_2^1(T+)\right)\right).$$

(ii.3) If

$$\left(e^{a_1 T} - z_2^1(T+) + \frac{\theta}{1-p}\left(z_2^2(T+) - z_2^1(T+)\right)\right)^2 < \frac{2|\theta| z_2^1(T+)}{1-p}\left(z_2^2(T+) - z_2^1(T+)\right),$$

then we have complex numbers, where

$$\mu_{1,2} = \frac{1}{2}\Bigg(e^{a_1 T} + z_2^1(T+) + \frac{\theta}{1-p}\left(z_2^2(T+) - z_2^1(T+)\right) \pm i\sqrt{\frac{2|\theta||z_2^1(T+)|}{1-p}\left|z_2^2(T+) - z_2^1(T+)\right| - \left(e^{a_1 T} - z_2^1(T+) + \frac{\theta}{1-p}\left(z_2^2(T+) - z_2^1(T+)\right)\right)^2}\Bigg).$$

For the stability of the non-homogeneous nonlinear system (4.2.33), we have the following cases.

1. If $\theta > 0$, we have that the multipliers are by modulus smaller than 1 if $|\mu_1| < 1$.

   Therefore

$$\begin{aligned}|\mu_1| &< \frac{1}{2}\left|e^{a_1 T} + z_2^1(T+) + \frac{\theta}{1-p}\left(z_2^2(T+) - z_2^1(T+)\right) + \sqrt{\left(e^{a_1 T} + z_2^1(T+) + \frac{\theta}{1-p}\left(z_2^2(T+) - z_2^1(T+)\right)\right)^2}\right| \\ &< \left|e^{a_1 T} + z_2^1(T+) + \frac{\theta}{1-p}\left(z_2^2(T+) - z_2^1(T+)\right)\right| \\ &\equiv \mu_1^*.\end{aligned}$$

Hence if $\mu_1^* < 1$, all the multipliers μ_j of the homogeneous equation (4.2.27) are by modulus smaller than 1, and the T-periodic solution $\tilde{x}(t)$ of the non-homogeneous equation (4.2.23) is exponentially stable (reference Chapter 2; Remark 2.5.2).

2. If $\theta < 0$ and we have case (ii.1), we have that the multipliers are by modulus smaller than 1 if $|\mu_1| < 1$. In this case it can not be simplified since the $z_2^1(T+)$ and $z_2^2(T+)$ contain θ. So if $|\mu_1| < 1$, all the multipliers μ_j of the homogeneous equation (4.2.27) are by modulus smaller than 1, and the T-periodic solution $\tilde{x}(t)$ of the non-homogeneous equation (4.2.23) is exponentially stable (reference Chapter 2; Remark 2.5.2).

3. If $\theta < 0$ and we have case (ii.2), then

$$\begin{aligned} |\mu| &= \frac{1}{2}\left| e^{a_1 T} + z_2^1(T+) + \frac{\theta}{1-p}\left(z_2^2(T+) - z_2^1(T+)\right)\right| \\ &\equiv \mu_2^*. \end{aligned}$$

Hence if $\mu_2^* < 1$, all the multipliers μ_j of the homogeneous equation (4.2.27) are by modulus smaller than 1, and the T-periodic solution $\tilde{x}(t)$ of the non-homogeneous equation (4.2.23) is exponentially stable (reference Chapter 2; Remark 2.5.2).

4. If $\theta < 0$ and we have case (ii.3), then

$$\begin{aligned} |\mu_{1,2}| &= \frac{1}{2}\sqrt{\frac{2|\theta| z_2^1(T+)}{1-p}\left(z_2^2(T+) - z_2^1(T+)\right)} \\ &\equiv \mu_3^*. \end{aligned}$$

Hence if $\mu_3^* < 1$, all the multipliers μ_j of the homogeneous equation (4.2.27) are by modulus smaller than 1, and the T-periodic solution $\tilde{x}(t)$ of the non-homogeneous equation (4.2.23) is exponentially stable (reference Chapter 2; Remark 2.5.2).

We can also numerically illustrate these results with the values in Table 1. In this case we set $a_2 = 0$ and we vary θ and r. We again fix $p = 0.8$ to see the changes when varying θ and r. In this case, Figures 4.21–4.24 and 4.26 all show a stable T-periodic solution, whereas Figure 4.25 shows an unstable T-periodic solution.

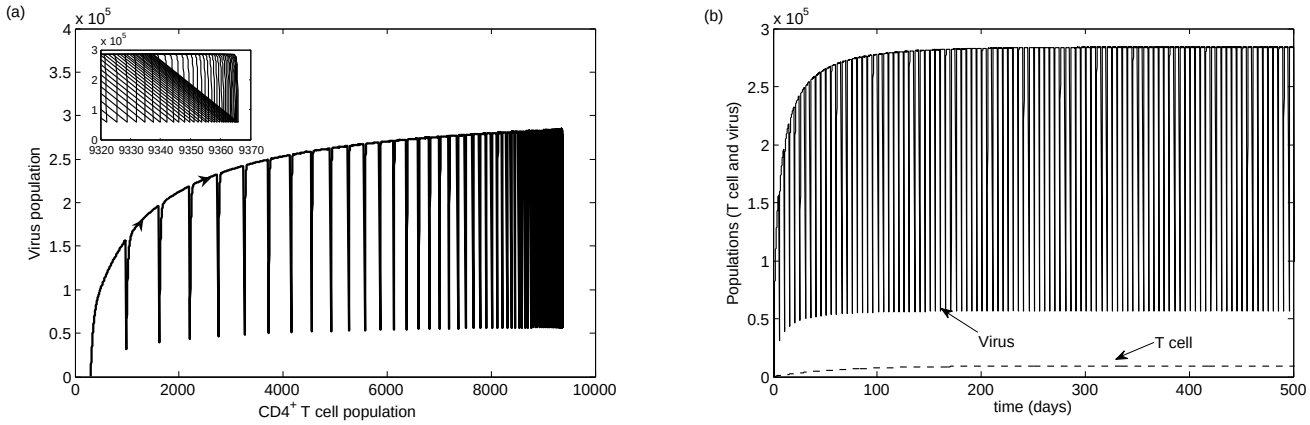

Figure 4.21: The behaviour of the CD4$^+$ T cell and virus populations when $a_2 = 0$, $r = 0.0032$ and $\theta = 0.0001$ (all other parameters are fixed at their sample value in Table 1). In this case, the conditions for stability in Theorem 4.2.8 are satisfied and we have a stable positive T-periodic solution. (a) CD4$^+$ T cell population versus virus population; inset: close up of periodic solution. (b) Time dynamics versus populations.

When the T-periodic solution of the linear system (4.2.23) is stable, the T-periodic solution of the nonlinear system (4.2.33) is also stable (Figures 4.21 and 4.22). When the T-periodic solution of the linear system (4.2.23) is unstable, the nonlinear system (4.2.33) has a T-periodic solution that is stable (Figures 4.23 and 4.24). When the T-periodic solution of the linear system (4.2.23) is unstable and $\theta < 0$, the stability of the T-periodic solutions of the nonlinear system (4.2.33) changes

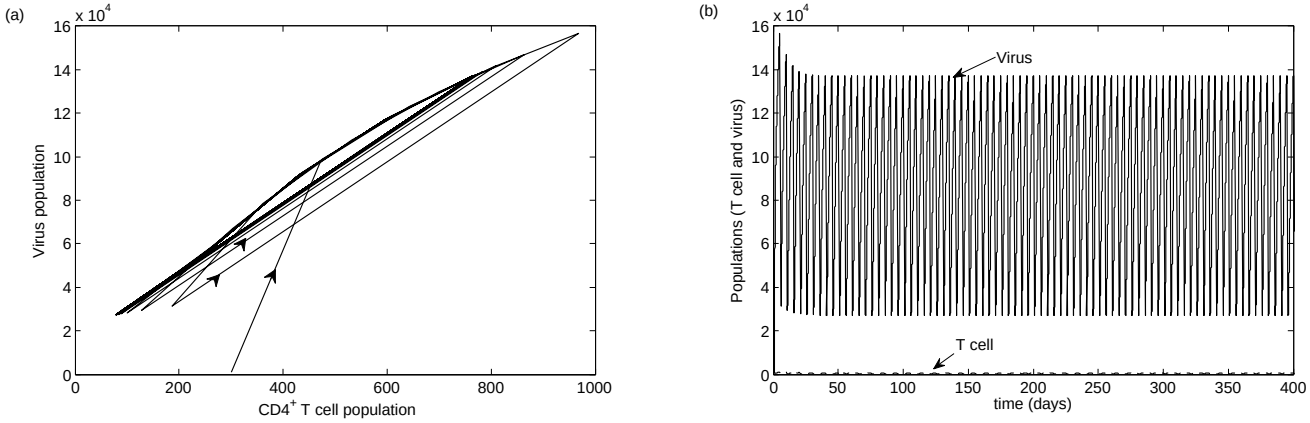

Figure 4.22: The behaviour of the CD4$^+$ T cell and virus populations when $a_2 = 0$, $r = 0.0032$ and $\theta = -0.005$ (all other parameters are fixed at their sample value in Table 1). In this case, the conditions for stability in Theorem 4.2.8 are satisfied and we have a stable positive T-periodic solution. (a) CD4$^+$ T cell population versus virus population. (b) Time dynamics versus populations.

based on r (Figures 4.25 and 4.26).

4.3 Summary

In summary, the general linear impulsive system (4.2.2) has a unique T-periodic solution that is exponentially stable under the conditions presented in Theorems 4.2.1 and 4.2.2, respectively. For the general nonlinear impulsive system (4.2.10), we can numerically show that, for the parameters in Table 1, a T-periodic solution exists and that stability can change based on the value of the nonlinear parameter r. Hence the nonlinear term changes a T-periodic solution from unstable to stable, but not vice versa. Therefore the nonlinear term seems to enlarge the region of stability.

We also showed that varying the immune response rate (a_2) in the general linear system (4.2.2) changes the stability. We considered the following two subcases of the

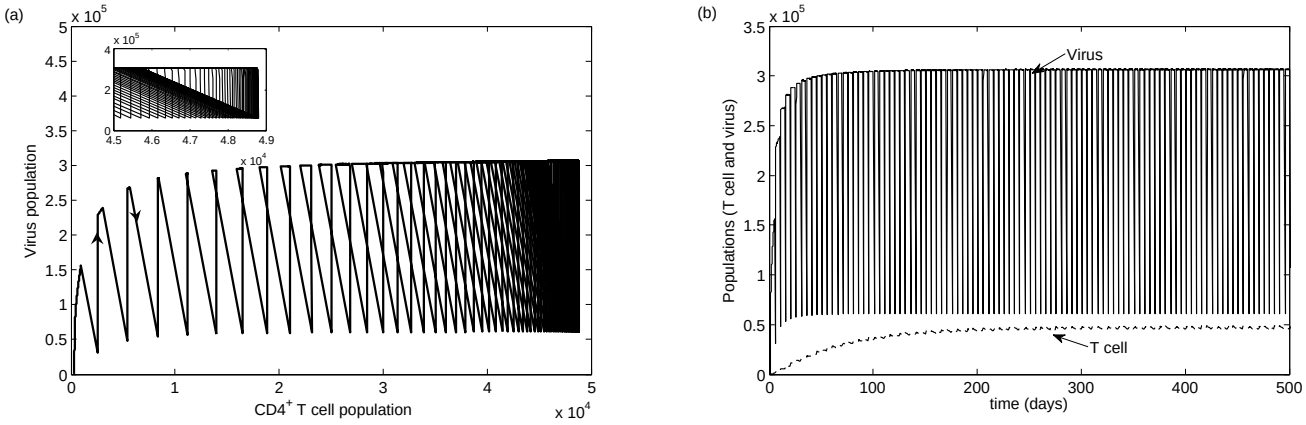

Figure 4.23: The behaviour of the $CD4^+$ T cell and virus populations when $a_2 = 0$, $r = 0.0032$ and $\theta = 0.01$ (all other parameters are fixed at their sample value in Table 1). In this case, the conditions for stability in Theorem 4.2.8 are satisfied and we have a stable positive T-periodic solution. (a) $CD4^+$ T cell population versus virus population; inset: close up of periodic solution. (b) Time dynamics versus populations.

general impulsive system (4.2.10) in order to view the effect of the nonlinear infection term and the immune response rate:

Case 1. We set the immune response rate to zero in the general differential equations (4.1.4) ($a_2 = 0$).

Case 2. We set the immune response rate to zero in the general differential equations (4.1.4) ($a_2 = 0$), but include an immune response by an impulse.

If we set $a_2 = 0$ in the general impulsive system (4.2.10) (Case 1), both the linear and nonlinear impulsive systems have a unique positive T-periodic solution that is exponentially stable. Therefore we proved that, without an immune response, the

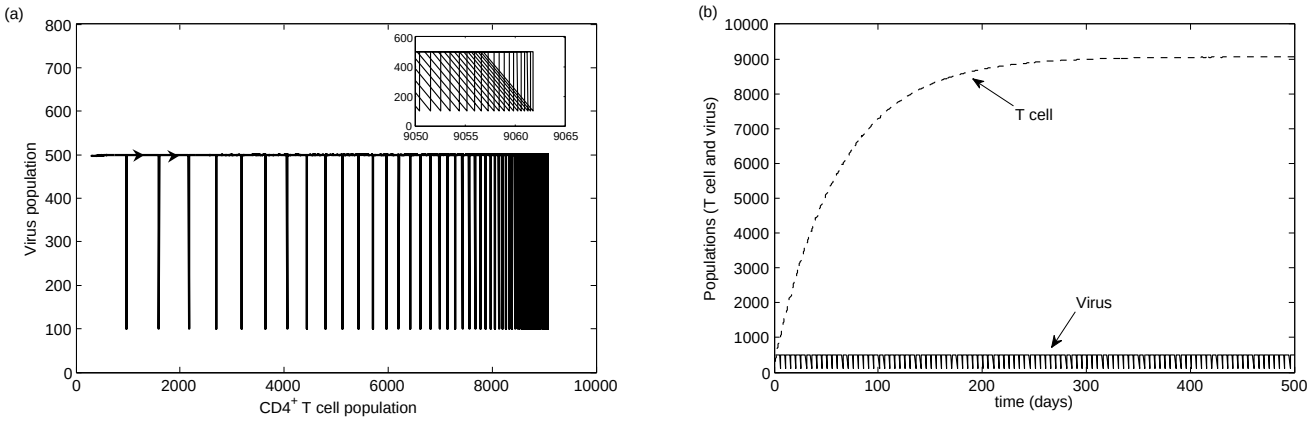

Figure 4.24: The behaviour of the CD4$^+$ T cell and virus populations when $a_2 = 0$, $r = 2$ and $\theta = 0.01$ (all other parameters are fixed at their sample value in Table 1). In this case, the conditions for stability in Theorem 4.2.8 are satisfied and we have a stable positive T-periodic solution. (a) CD4$^+$ T cell population versus virus population; inset: close up of periodic solution. (b) Time dynamics versus populations.

nonlinear term has no effect on stability.

If we set $a_2 = 0$ in the general impulsive system (4.2.10), but we include an immune response represented by an impulse (equation (4.2.22)) (Case 2), a positive T-periodic solution exists in both the linear and nonlinear cases. We also proved that for certain conditions on θ (the impulsive immune response rate), the T-periodic solution is exponentially stable in both the linear and nonlinear impulsive systems. We numerically show that the nonlinear term can change an unstable periodic orbit in the linear system to a stable one in the nonlinear system. This implies that, if an immune response is included, the nonlinear term and the immune response may affect stability.

The effect of this nonlinear infection term has been previously studied in ordinary differential equations for infectious disease systems. Though often the term

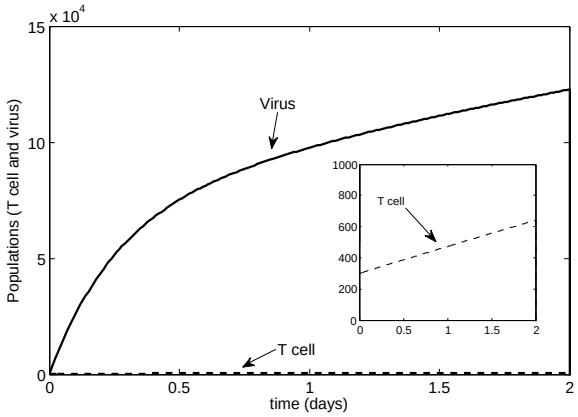

Figure 4.25: The behaviour of the CD4$^+$ T cell and virus populations when $a_2 = 0$, $r = 0.0032$ and $\theta = -0.1$ (all other parameters are fixed at their sample value in Table 1). In this case, the conditions for stability in Theorem 4.2.8 are not satisfied and we have an unstable T-periodic solution. The inset shows the initial increase in the T cell population.

is neglected, it has been found that viral clearance via drug therapy may explicitly depend on this nonlinear infection term since the viral load is low [29]. The work previously done used ordinary differential systems to view the effect of the nonlinear infection term when viral load was low. We were able to explicitly show that when drug therapy is included, the nonlinear infection term does have an effect on the stability of T-periodic solutions. We only look at the effect of the nonlinear infection term on a two-dimensional system, where every other term in the model is linear. In practice, infectious disease systems are often of higher dimensions than two (for example, including susceptible and infected T cells would be more realistic meaning a three-dimensional system). Solving for higher-dimensional systems is challenging and often not possible when nonlinear terms are included. Since the nonlinear infection term plays a role in stability for a two-dimensional system, we certainly have arguments to show that it would also play a role in the stability for higher-dimensional systems. The analysis of the two-dimensional system gives us an indication that the

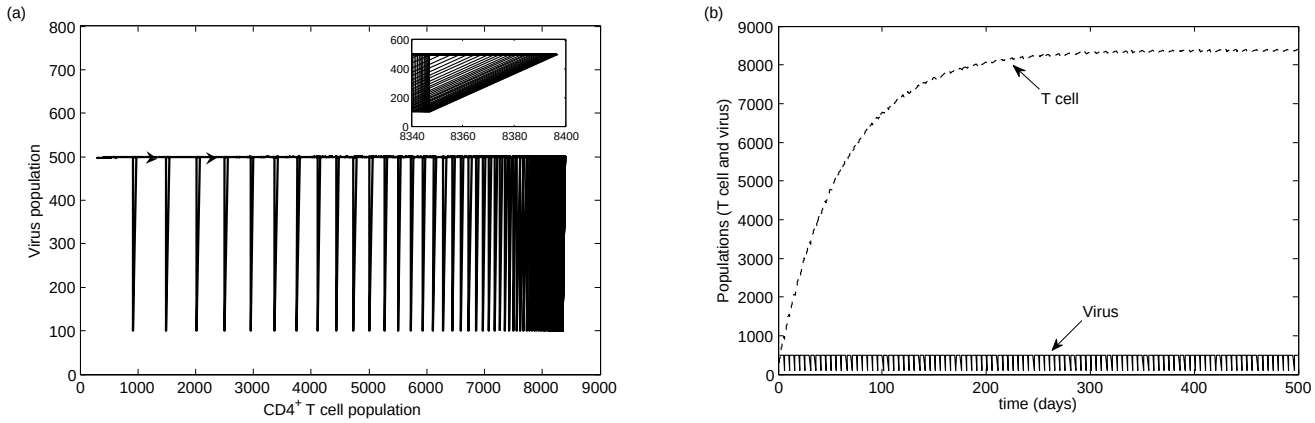

Figure 4.26: The behaviour of the $CD4^+$ T cell and virus populations when $a_2 = 0$, $r = 2$ and $\theta = -0.1$ (all other parameters are fixed at their sample value in Table 1). In this case, the conditions for stability in Theorem 4.2.8 are satisfied and we have a stable positive T-periodic solution. (a) $CD4^+$ T cell population versus virus population; inset: close up of periodic solution. (b) Time dynamics versus populations.

nonlinear infection term does play an important role in the stability of T-periodic solutions.

Chapter 5

Application of impulsive differential equations to Rift Valley Fever

Given the right circumstance, an emerging infectious disease has the potential to devastate newly infected host populations [39]. Emerging diseases are infections that have expanded their host or geographic range [39]. The emergence of these diseases is mitigated by a number of factors, many of which are driven by anthropogenic change including ecosystem modification, international travel, technology and health policy [39]. Modification of existing ecosystems or the encroachments of human ecosystem fronts create new interfaces for many zoonotic pathogens to interact with and infect humans [40]. HIV, malaria and dengue are all examples of diseases that have proliferated globally as a result of changing human demographics and behaviour such as massive population growth, large-scale migration and urbanization [39]. Host-parasite dynamics are intimately tied to climatic conditions, and there is growing concern that the extreme weather events associated with global climate change may further exasperate the incidence and spread of emerging pathogens [41, 42]. This is especially

true for diseases with water-breeding vectors such as mosquitoes [39, 41, 42, 43].

Following the emergence and increased virulence of West Nile virus (WNV) in North America, much attention has been focused on the potential of other mosquito-borne pathogens to expand their natural ranges [39, 42, 44, 45, 46]. Of the many potential mosquito-borne pathogens able to invade North America like WNV, one particular concern is Rift Valley Fever (RVF), an arthropod-borne viral zoonosis that has seen an expansion in its geographic range and virulence since its formal identification in Kenya's Rift Valley in 1931 [44, 45, 46, 47]. Incidence of RVF is believed to have a particularly strong connection to climate variation and has been linked with El Niño-southern oscillation (ENSO) events or incidents of localized heavy rainfall [41, 43, 47, 48]. Prior to 1977, incidents of RVF had primarily been concentrated in sub-Saharan Africa and were mainly a concern of the agricultural industry; infection was typically fatal in young domestic ruminants and initiated fetal death in pregnant animals, while cases were typically mild in humans [45, 46, 47, 49]. In 1977, RVF's potential to spread beyond its endemic range in sub-Saharan Africa was confirmed when it appeared without apparent precedent in Egypt; unlike previously documented outbreaks, human infection was significant, with over 200 000 cases, 600 of which were fatal [44, 47, 48, 49]. Since then, RVF has become endemic in previously unexposed areas of Western and Eastern Africa; it has even reached the Arabian Peninsula as of the early 21st century [50]. When considering RVF's success at establishing its endemicity in novel environments, and given the wide variety of arthropods capable of acting as its vectors, it is no surprise that there is much interest in its potential to spread elsewhere [46, 47, 51].

RVF is an arthropod-borne viral zoonosis, meaning that it is transmitted between humans and animals by an arthropod vector [47, 49, 50]. RVF can infect a fairly wide range of vertebrate hosts and has an even wider range of insect vectors, most of which are mosquitoes [46, 47, 49, 50]. RVF's success at establishing its endemicity in novel environments is due in part to its flexibility in both hosts and vectors [52].

For more information on the etiology of the virus, the vectors that transmit the virus, the viable hosts and the epidemiology of the virus, see Appendix H.

5.1 A multi-season transmission model for Rift Valley Fever: Invasion analysis in North America

For a vector-borne emerging infectious disease to become endemic in a new location, there must be a sufficient number of susceptible hosts and competent vectors [53]. Due to RVF's large range of viable hosts and vectors, its potential to establish itself elsewhere is especially high compared to other vector-borne diseases. Gaff *et al.* [54] modelled RVF's transmission using an ordinary differential equation model for two populations of mosquito species — those that can transmit vertically and those that cannot — and one population of domestic livestock animals with disease-dependent mortality. They analyzed the model to find the stability of the disease-free equilibrium and tested which model parameters affect the stability most significantly.

It is important to note that Rift Valley Fever is a vector-borne disease transmitted to domestic livestock and humans. We altered the Gaff *et al.* [54] model in order to incorporate a human population. The effect of the human population is of great interest to public health agencies, and so incorporating a human population in the model can give us important and meaningful results. We also include fetal death caused by RVF infection in the domestic livestock population, which is not included in [54]. Gaff *et al.* [54] used standard incidence for the interaction terms in their model. We know that human and livestock populations are unlikely to be well-mixed (meaning that each infected individual does not have an equal chance of infecting every susceptible individual), so we also use standard incidence for transmission. But all other terms, including the interactions between mosquitoes and hosts, are mass-action because the mosquito and host populations are assumed to be well-mixed.

We assume that the number of bites per day per mosquito are proportional to the fraction of bites on a susceptible host. The spread of RVF is much more likely between mosquitoes and hosts than between hosts because the interaction between host and mosquito populations is higher in a given area than host to host interaction. The model is composed of eleven ordinary differential equations describing the interaction between mosquito, human and livestock populations when the Rift Valley Fever virus is present.

We use mathematical modelling in order to investigate the effect of decreasing the mosquito survival time. Gaff *et al.* [54] showed that, by changing the values for contact rates and death rates associated with cattle, for any given contact rate, there is a low level of endemic prevalence, meaning the disease could persist if introduced in an isolated system. We instead look at changing the survival time of mosquitoes since the reduction can be done by spraying and has been proven to be a good way of eradicating vector-bourne diseases such as malaria [55, 56, 57, 58].

The manuscript is split into two categories: a one-season model and a multiple-season model. The one-season model only includes the ordinary differential equations with no impulse effect. The equilibrium points and stability are found, as well as the basic reproductive number. We address the following research questions: 1. Can Rift Valley Fever invade North America? 2. If the virus does invade, is it likely to be eradicated? 3. What are the effects of multiple seasons on a persistent outbreak? The third research question is answered by including between-season effects as impulses. The multiple-season model is composed of the ordinary differential equations, coupled with difference equations that describe the effects on the human, livestock and mosquito populations after a winter season. The effects of seasonal changes is an important research question in North America, since the mosquito population is highly affected by winter, and this is included in the model by imposing impulses.

Numerical simulations show that, in order to eradicate the disease, we must decrease the survival time of mosquitoes below 8.67 days. Thus, mechanisms such

as aggressive spraying could contain an outbreak, if the mosquito population is sufficiently controlled. Otherwise, Rift Valley Fever is likely to establish itself as a recurring seasonal outbreak. Sensitivity analysis explored the relationship between the basic reproductive number and the parameter values using Latin Hypercube Sampling. We show that the basic reproductive number is most sensitive to the mosquito death rate, meaning that changing the survival time has a big impact on lowering the basic reproductive number below one. Simulation details, errata and extra comments for the manuscript can be found in Appendix I.

The contribution by each author is as follows. The third author wrote the initial draft of the introduction. The first and second authors developed and analysed an early version of the model. The first author developed and analysed the current model, performed numerical simulations and wrote the manuscript. The fourth author designed the project and edited the manuscript.

This paper is in press in the journal Mathematical Population Studies [5];
Miron, R.E., Giordano, G.A., Kealey, A.D., Smith?, R.J. 2014. A multi-season transmission model for Rift Valley Fever: Invasion analysis in North America. *Mathematical Population Studies* (in press).

Multi-season transmission for Rift Valley Fever in North America

Rachelle E. Miron[1], Gaël A. Giordano[1], Alison D. Kealey[2], Robert J. Smith?[3]

1. Department of Mathematics

The University of Ottawa

585 King Edward Ave

Ottawa ON K1N 6N5, Canada

2. Department of Community Health and Epidemiology

Queen's University

Jeffery Hall, University Ave

Kingston ON K7L 3N6, Canada

3. Department of Mathematics and Faculty of Medicine

The University of Ottawa

585 King Edward Ave

Ottawa ON K1N 6N5, Canada

(to whom correspondence should be addressed)

Abstract

Rift Valley Fever is a vector-borne disease transmitted to humans and domestic livestock that is primarily found in West Africa. Its similarities to West Nile Virus suggest that establishment in the developed world may be possible. Rift Valley Fever has the potential to invade North America, where seasons play a role in disease persistence. The values for the basic reproductive number show that, in order to eradicate the disease, the survival time of mosquitoes must decrease below 8.67 days. Mechanisms such as aggressive spraying that decreases the mosquito population can contain an outbreak. Otherwise, Rift Valley Fever is likely to establish itself as a recurring seasonal outbreak. Rift Valley Fever poses a potential threat to North America that would require aggressive interventions in order to prevent a recurring seasonal outbreak.

Keywords: Rift Valley Fever, mathematical model, impulsive differential equations, spraying, seasons

1 Introduction

The emergence of West Nile Virus in North America has drawn attention to the possibility for other mosquito-borne pathogens to expand their natural ranges (Morse, 1995; Patz et al., 2005; Favier et al., 2006; Moutailler et al., 2008; Turell et al., 2008a). West Nile virus (WNV) first appeared in the United States in 1999, causing acute illness in 62 individuals, 7 of whom died (Roche, 2002). Outbreaks of encephalitis caused by WNV have occurred in the late summer and early autumn months yearly in New York City since 1999 (Karpati et al., 2004). By the end of 2002, West Nile virus activity had been reported in all but four continential U.S. states, with more than $3,500$ human cases reported (Mostashari et al., 2003).

Of the many potential mosquito-borne pathogens able to invade North America like WNV, one particular concern is Rift Valley Fever (RVF), an arthropod-borne viral zoonosis, which has seen an expansion in its geographic range and virulence since its formal identification in Kenya's Rift Valley

in 1931 (House et al., 1992; Favier et al., 2006; Moutailler et al., 2008; Turell et al., 2008a). Incidence of RVF is believed to have a particularly strong connection to climate variation and has been linked with El Niño–southern oscillation events or incidents of localized heavy rainfall (House et al., 1992; Traoré-Lamizana et al., 2001; Porphyre et al., 2005; Despommiers et al., 2007; Anyamba et al., 2009). Prior to 1977, incidents of RVF had primarily been concentrated in sub-Saharan Africa and were mainly a concern of the agricultural industry. Infection was fatal in young domestic ruminants and initiated abortion in pregnant animals, while cases were mild in humans (Meegan, 1980; House et al., 1992; Moutailler et al., 2008; Turell et al., 2008a). In 1977, RVF's potential to spread beyond its endemic range in sub-Saharan Africa was confirmed when it appeared without apparent precedent in Egypt. Unlike previously documented outbreaks, human infection exceeded 200,000 cases, 600 of which were fatal (Meegan, 1980; House et al., 1992; Traoré-Lamizana et al., 2001; Favier et al., 2006; Gaff et al., 2007). Since then, RVF has become endemic in previously unexposed areas of Western and Eastern Africa. It reached the Arabian Peninsula in the early 21st century (Gerdes, 2004). RVF's success at establishing its endemicity in novel environments, with a wide variety of arthropods capable of acting as its vectors, constitutes a serious threat (House et al., 1992; Turell et al., 2008a,b).

Rift Valley Fever is an arthropod-borne viral zoonosis: it is transmitted between humans and animals by an arthropod vector (House et al., 1992; Meegan, 1980; Gerdes, 2004). RVF can infect a fairly wide range of vertebrate hosts and has an even wider range of insect vectors: over 40 species of mosquitoes from eight different genera have been isolated in the field (Meegan, 1980; House et al., 1992; Gerdes, 2004; Turell et al., 2008a,b). RVF's success at establishing its endemicity in novel environments is due in part to its flexibility in both hosts and vectors (Balkhy and Memish, 2003). Mosquitoes belonging to the Aedes species are an important vector, as they may vertically transmit infection to their young through transovarial transmission, enabling the maintenance of RVF during inter-epizootic periods (House et al., 1992; Traoré-Lamizana et al., 2001; Bowman

et al., 2005). Culex species and those belonging to Eretmapodites are believed to be strongly involved with epizootic outbreaks (House et al., 1992; Traoré-Lamizana et al., 2001; Bowman et al., 2005). Both the Aedes and Culex species are known to transmit West Nile Virus. RVF can also be transmitted through aerosol exposure from handling infected carcasses. Laboratory workers, veterinarians, and individuals involved with meat processing are particularly vulnerable to this form of infection (House et al., 1992; Traoré-Lamizana et al., 2001; Moutailler et al., 2008; Turell et al., 2008a,b).

RVF has a very wide range of viable vertebrate hosts, as might be expected, considering the diversity of its vectors (Balkhy and Memish, 2003). RVF's most significant host species are domestic ruminants such as sheep and cattle (House et al., 1992; Balkhy and Memish, 2003; Turell et al., 2008a,b). Newborn lambs and goats are most susceptible to disease, followed by calves and sheep. Moderate disease occurs in adult cattle, sheep, goats, humans, water buffalo, and rats. Humans and ruminants are capable of developing enough viremia to infect mosquitoes. Camels, horses, pigs, cats, dogs, guinea pigs, rabbits, hedgehogs, and monkeys are susceptible, but do not necessarily display clinical disease. Birds, with the exception of pigeons and chickens, and reptiles are believed to be resistant to infection (House et al., 1992; Gerdes, 2004). Balkhy and Memish (2003) showed that fatality in adult cattle and sheep can be as high as 30%, while young animals may experience 100% fatality. Gerdes (2004) showed that the disease is most significant in young animals, particularly lambs and goats, which may experience 70–100% mortality. Newborn animals experience 100% fatality and most epidemics are defined by high incidences of abortion (Gerdes, 2004). Prior to the Egyptian outbreak in 1977, the disease in humans had mostly been asymptomatic or mild, often manifesting as influenza-like symptoms. Complications such as encephalitis may occur and less than 1% of cases may present hemorrhagic fever (House et al., 1992; Balkhy and Memish, 2003; Gerdes, 2004; Turell et al., 2008a).

In order for a vector-borne emerging infectious disease to become endemic in a new location,

there must be enough susceptible hosts and vectors (House et al., 1992). Due to RVF's large range of viable hosts and vectors, its potential to establish itself is high compared to other vector-borne diseases. Gaff et al. (2007) modeled RVF transmission using ordinary differential equations for two populations of mosquito species — those that can transmit vertically and those that cannot — and one population of domestic livestock animals with disease-dependent mortality. They found the stability of the disease-free equilibrium and identified parameters affecting the stability. They showed that, for any given contact rate, there is a low level of endemic prevalence, which implies that the disease could persist if introduced into an isolated system.

Bicout and Sabatier (2004) and Zell (2004) demonstrated that the incidence of many vector-borne infectious diseases shows seasonality, and extreme weather events are often accompanied by additional outbreaks. Favier et al. (2006) assessed the possibility of endemicity without wild animals providing a permanent virus reservoir. Using a deterministic model, endemicity without a permanent virus reservoir is impossible in a single site except when there is a strictly periodic rainfall pattern, but is possible when there are herd movements and sufficient inter-site variability in rainfall, which drives mosquito emergence.

2 The Model

We use a compartmental model derived from Gaff et al. (2007) with three populations: the human, domestic livestock, and mosquito populations (Figure 1). The model has four different classes: the S classes are susceptible individuals, the E classes are infected but non-infectious individuals, the I classes are infectious individuals, and the R classes are recovered and immune individuals. When initially infected, the individual is non-infectious for a while; only individuals in class I can infect the susceptible populations. Once recovered from the disease, the individual has lifelong immunity.

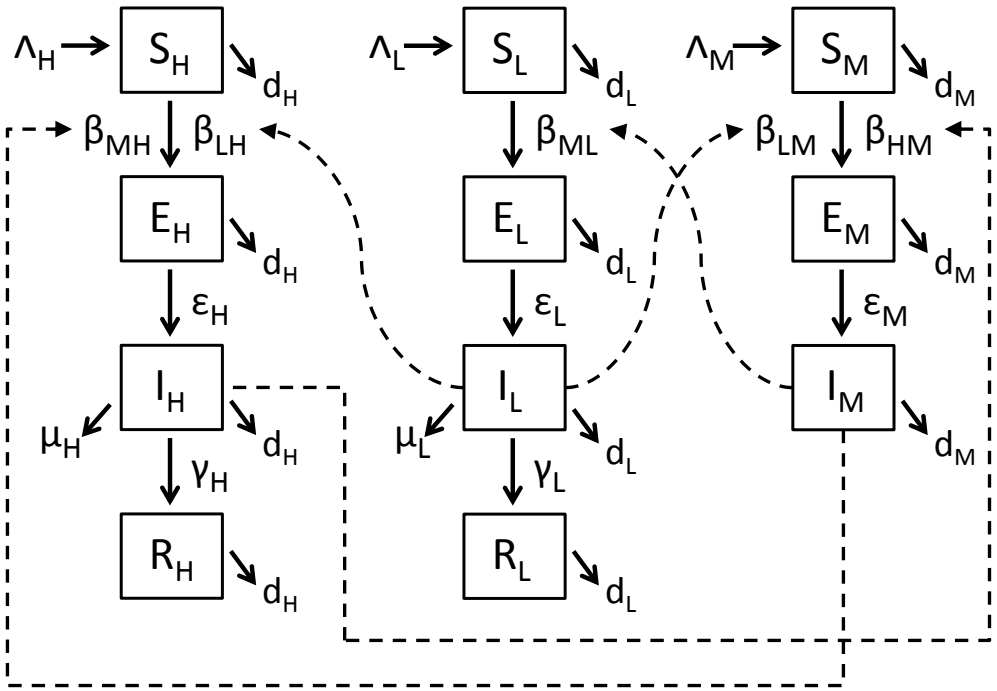

Figure 1: The model. The index "H" refers to human, "L" to livestock, and "M" to mosquitoes. S_H, S_L, and S_M are the susceptible populations, E_H, E_L, and E_M are the exposed populations, I_H, I_L, and I_M are the infected populations, and R_H and R_L are the recovered populations (mosquitoes do not recover from the disease). Other parameters are listed in Table 2.

The human population is described by

$$\begin{cases} S'_H(t) = \Lambda_H - d_H S_H(t) - \beta_{LH}\dfrac{S_H(t)I_L(t)}{N_L(t)} - \beta_{MH}S_H(t)I_M(t) \\ E'_H(t) = \beta_{LH}\dfrac{S_H(t)I_L(t)}{N_L(t)} + \beta_{MH}S_H(t)I_M(t) - d_H E_H(t) - \epsilon_H E_H(t) \\ I'_H(t) = \epsilon_H E_H(t) - d_H I_H(t) - \mu_H I_H(t) - \gamma_H I_H(t) \\ R'_H(t) = \gamma_H I_H(t) - d_H R_H(t)\,, \end{cases} \tag{1}$$

where $N_L(t) = S_L(t) + E_L(t) + I_L(t) + R_L(t)$.

The domestic livestock population is described by

$$\begin{cases} S'_L(t) = \Lambda_L - d_L S_L(t) - \beta_{ML} S_L(t) I_M(t) \\ E'_L(t) = \beta_{ML} S_L(t) I_M(t) - d_L E_L(t) - \epsilon_L E_L(t) \\ I'_L(t) = \epsilon_L E_L(t) - d_L I_L(t) - \mu_L I_L(t) - \gamma_L I_L(t) \\ R'_L(t) = \gamma_L I_L(t) - d_L R_L(t)\,. \end{cases} \tag{2}$$

The Aedes mosquito population is described by

$$\begin{cases} S'_M(t) = \Lambda_M - d_M S_M(t) - \beta_{LM} S_M(t) I_L(t) - \beta_{HM} S_M(t) I_H(t) \\ E'_M(t) = \beta_{LM} S_M(t) I_L(t) + \beta_{HM} S_M(t) I_H(t) - d_M E_M(t) - \epsilon_M E_M(t) \\ I'_M(t) = \epsilon_M E_M(t) - d_M I_M(t)\,. \end{cases} \tag{3}$$

Each population has infection rate β_j ($j = H, L, M$). The natural death rates are d_j, the disease-induced death rates μ_j, the rates at which a non-infectious individual becomes infectious ϵ_j, and the recovery rates γ_j. The mosquito population contains no R class, because mosquitoes never clear the infection once they are infected. A summary of the parameters and units are given in Table 1.

The birth rates in the system are constant sources of susceptible individuals Λ_i for $i = H, L, M$; in the absence of disease, the susceptible populations converge to the disease-free equilibrium at an exponential rate. We also include fetal death caused by RVF infection in the domestic livestock population, which is not included in Gaff et al. (2007). Human and livestock populations are unlikely to be well-mixed (meaning that each infected individual has equal chance of infecting every susceptible individual), so we use standard incidence for transmission. All other terms, including the interactions between mosquitoes and hosts, are mass-action because the mosquito and host populations are assumed to be well-mixed. The spread of RVF is much more likely between mosquitoes

Table 1: Definition of parameters.

Parameter	Units	Definition
Λ_H	population $\times$ days^{-1}	Human birth rate
Λ_L	population $\times$ days^{-1}	Immigration of livestock
Λ_M	population $\times$ days^{-1}	Mosquito birth rate
$1/d_H$	days	Human survival time
$1/d_L$	days	Livestock survival time
$1/d_M$	days	Mosquito survival time
μ_H	days^{-1}	Disease death rate for humans
μ_L	days^{-1}	Disease death rate for livestock
β_{MH}	(days $\times$ population)$^{-1}$	Infection rate from mosquitoes to humans
β_{LH}	(days $\times$ population)$^{-1}$	Infection rate from livestock to humans
β_{ML}	(days $\times$ population)$^{-1}$	Infection rate from mosquitoes to livestock
β_{LM}	(days $\times$ population)$^{-1}$	Infection rate from livestock to mosquitoes
β_{HM}	(days $\times$ population)$^{-1}$	Infection rate from humans to mosquitoes
$1/\epsilon_H$	days	Human incubation time
$1/\epsilon_L$	days	Livestock incubation time
$1/\epsilon_M$	days	Mosquito incubation time
$1/\gamma_H$	days	Human recovery time
$1/\gamma_L$	days	Livestock recovery time

and hosts than between hosts because the interaction between host and mosquito populations is higher in a given area than host to host interaction.

3 Asymptotic behavior: one-season model

The model has two equilibria: the disease-free equilibrium and the endemic equilibrium (developed in the Appendix). For the endemic equilibrium, several solutions could exist, resulting in a backward bifurcation. If this is the case, then lowering the basic reproductive number below 1 may no longer be sufficient for control (Li et al., 2011). This presents a serious complication when a disease is already endemic because the outcome depends on initial conditions. In the case of RVF, we only consider sufficiently small perturbations away from the disease-free equilibrium because the disease is present in North America. This contrasts with the situation in Africa, where the disease is already established, so more rigorous control efforts would be required.

The Jacobian matrix is computed at the disease-free equilibrium (expressed in the Appendix). For fixed parameters and state variables, the stability changes as the mosquito death rate d_M varies. For the values used in Table 2, the Routh-Hurwitz conditions are satisfied for the characteristic equation

$$f(\alpha) = \alpha^6 + c_1\alpha^5 + c_2\alpha^4 + c_3\alpha^3 + c_4\alpha^2 + c_5\alpha + c_6\,, \tag{4}$$

when $0.15 < d_M < 0.68$. The disease-free equilibrium is locally stable in this region.

Table 2: Range of parameters.

Parameter	Sample Value	Range	Units	References
Λ_H	$1000 \times d_H$	$1000 \times d_H$	people days^{-1}	(Bowman et al., 2005)
Λ_L	0.1	0.01–0.5	livestock days^{-1}	Assumed
Λ_M	$10000 \times (1/14)$	200–1000	mosquitoes days^{-1}	(Gaff et al., 2007)
$1/d_H$	80×365	70–90	days	(Bowman et al., 2005)
$1/d_L$	20×365	10–25	days	(Gaff et al., 2007)
$1/d_M$	varies	3–60	days	(Gaff et al., 2007)
μ_H	0.01	0.01–0.1	days^{-1}	(Directors of Health Promotion and Education, 2013)
μ_L	1/25	1/10–1/40	days^{-1}	(Gaff et al., 2007)
β_{MH}	0.2762/1000	0.2762/10000–0.2762/100	days^{-1}	(Bowman et al., 2005)
β_{LH}	10^{-5}	10^{-5}–10^{-3}	days^{-1}	(Xue et al., 2012)
β_{ML}	β_{MH}	β_{MH}	days^{-1}	(Gaff et al., 2007)
β_{LM}	$\beta_{ML}/8$	$\beta_{ML}/8$	days^{-1}	(Gaff et al., 2007)
β_{HM}	$\beta_{MH}/10$	$\beta_{MH}/10$	days^{-1}	(Xue et al., 2012)
$1/\epsilon_H$	5	4–6	days	(Bowman et al., 2005), (CDC, 2003)
$1/\epsilon_L$	2	1–3	days	(Gaff et al., 2007),(CDC, 2003)
$1/\epsilon_M$	6	4–8	days	(Gaff et al., 2007)
$1/\gamma_H$	5	2–7	days	(Bowman et al., 2005),(CDC, 2003)
$1/\gamma_L$	3	1–5	days	(Gaff et al., 2007)

We calculated R_0, the average number of secondary infections that any single infected individual will cause by using the next-generation method (van den Driessche and Watmough, 2002). The solution (developed in the Appendix) to the characteristic polynomial gives a cubic equation with one real solution and two complex conjugates. The value for R_0 is the largest modulus of our eigenvalues (Greenhalgh, 1996).

4 Multiple-season model

4.1 Impulse conditions

In most of northern America, the mosquito population drops during the winter months. This fact is taken into account though impulsive differential equations (Lakshmikantham et al., 1989; Bainov and Simeonov, 1989, 1993, 1995). At impulse times t_k:

$$\Delta x = x(t_k^+) - x(t_k^-) = f(t_k, x(t_k^-))\,, \tag{5}$$

where $f(t, x)$ maps the solution before the impulse, $x(t_k^-)$, to $x(t_k^+)$. We reset the mosquito, human, and domestic livestock populations at the beginning of each summer.

We consider two seasons: the summer season, when the mosquitoes will infect hosts, and the winter season, when the mosquitoes die from the cold weather. During the winter, there is no vector to spread the disease; the domestic livestock and human populations increase, as abortions no longer occur.

The mosquitoes decrease to zero with the cold, but reappear at the beginning of summer. The Aedes mosquito has very few offspring surviving through the winter (Dohm et al., 2002). We assume that all adult mosquitoes die during winter.

At time t_k,

$$\begin{cases} \Delta S_H = r_1 S_H^- + p_1(E_H^- + I_H^- + R_H^-) \\ \Delta E_H = -E_H^- \\ \Delta I_H = -I_H^- \\ \Delta R_H = E_H^- + I_H^- - p_1(E_H^- + I_H^- + R_H^-)\,, \end{cases} \tag{6}$$

where S_H, E_H, I_H, and R_H are the susceptible, exposed, infected, and recovered human populations. The susceptible population increases by a fraction r_1. Because the infection period is short, by the end of winter, the total infected population has recovered so that $I_H = 0$. A fraction p_1 of the recovered offspring is susceptible.

At time t_k,

$$\begin{cases} \Delta S_L = r_2 S_L^- + c + p_2(E_L^- + I_L^- + R_L^-) \\ \Delta E_L = -E_L^- \\ \Delta I_L = -I_L^- \\ \Delta R_L = E_L^- + I_L^- - p_2(E_L^- + I_L^- + R_L^-)\,, \end{cases} \tag{7}$$

where S_L, E_L, I_L, and R_L are the susceptible, exposed, infected, and recovered domestic livestock populations. Because infection causes death in livestock, the susceptible livestock increases at a fixed amount c, reflecting the purchase of livestock for breeding.

The opposite happens with the mosquito population. By the end of winter season 1, few mosquitoes remain. At time t_k,

$$\begin{cases} \Delta S_M = -r_3 S_M^- + p_3 I_M^- \\ \Delta E_M = -E_M^- \\ \Delta I_M = -(r_3 + p_3) I_M^-\,, \end{cases} \tag{8}$$

where S_M and I_M are the susceptible and infected mosquito populations; r_3 is the total decrease in the mosquito population; and p_3 is the proportion of mosquitoes who are born with no infection

from an original infected mosquito. The total number of exposed mosquitoes who have offspring is zero, because a mosquito only stays in the exposed class for a short period of time.

The basic reproductive number for the one-season model has similar properties to that of the extended model. In the one-season model, R_0 larger than 1 causes an outbreak of RVF in the human and livestock populations. The dynamics in the first season of the extended model are the same for subsequent seasons. The reset initial conditions for the second season do not change the equilibrium points for this season and, because R_0 is greater than 1, we have an outbreak in the second season.

5 Simulations

5.1 One-season model

We calculated the effects on the human and domestic livestock populations by having infected mosquitoes enter North America. The initial site of infection is a small, fictitious coastal city. All the values used in the simulations are shown in Table 1. Each farmer buys one cow every 10 days, so $\Lambda_L = 0.1$. We take β_{HM} 10 times smaller than β_{MH}, because the infection rate from human to mosquito is smaller than from mosquito to human. The infection rate from livestock to mosquito is likewise smaller than mosquito to livestock. Mosquitoes infect humans and livestock at the same rate.

Using the values in Table 2, Figure 2 shows the effect of decreasing the survival time of mosquitoes. As the survival time of mosquitoes is decreased (due to mosquito spraying), R_0 is reduced below 1.

For Figure 3, we choose the mosquito survival time to be such that $R_0 < 1$, which caused no outbreaks within the year and led to eradication of the disease. For Figure 4, we choose the mosquito survival time to be such that $R_0 > 1$, which caused a disease outbreak at the beginning

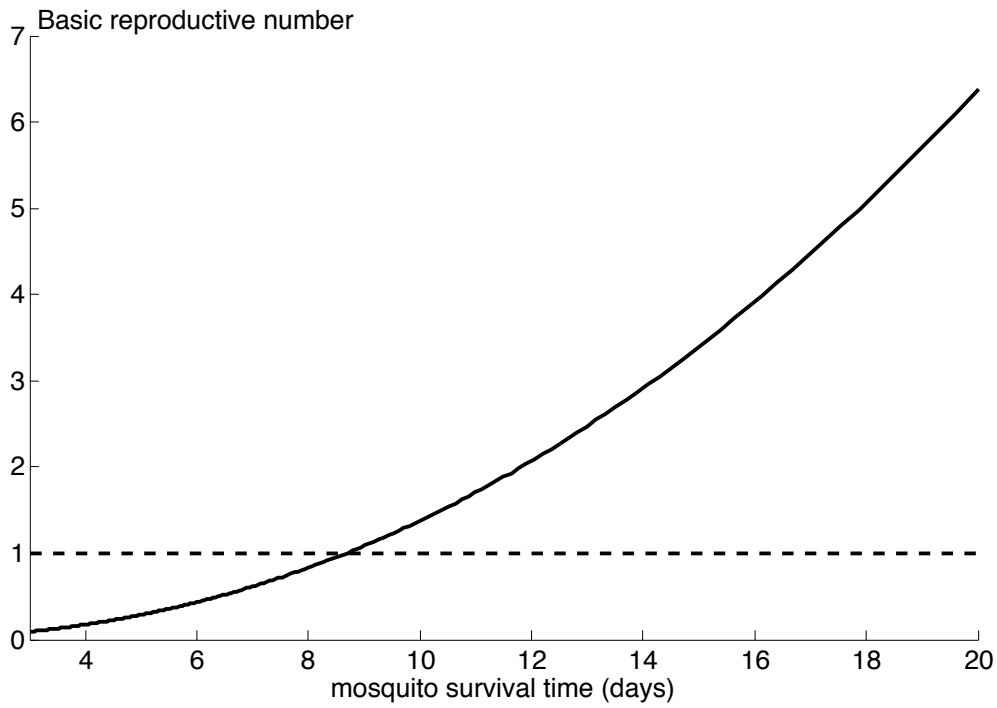

Figure 2: The effects of mosquito survival time on the basic reproductive number, R_0. R_0 drops below 1 if the mosquito survival time is sufficiently small. All other parameters are set to their median values listed in Table 2.

of the year, but the disease was still eradicated after the outbreak.

For $R_0 < 1$, the mosquito population in Figure 3c decreases. Because mosquitoes do not recover from the disease, and the mosquito survival time is such that $R_0 < 1$, we take the death rate to be large enough so that the mosquitoes do not have enough time to infect the human and domestic livestock populations in order to have an outbreak. Because infection between humans and livestock is nonexistent, it suggests that the disease-free equilibrium is stable and RVF does not become endemic.

For a small value of d_M resulting in $R_0 > 1$, the disease causes a decrease in the susceptible human and domestic livestock populations, which follows an increase in the recovered human and

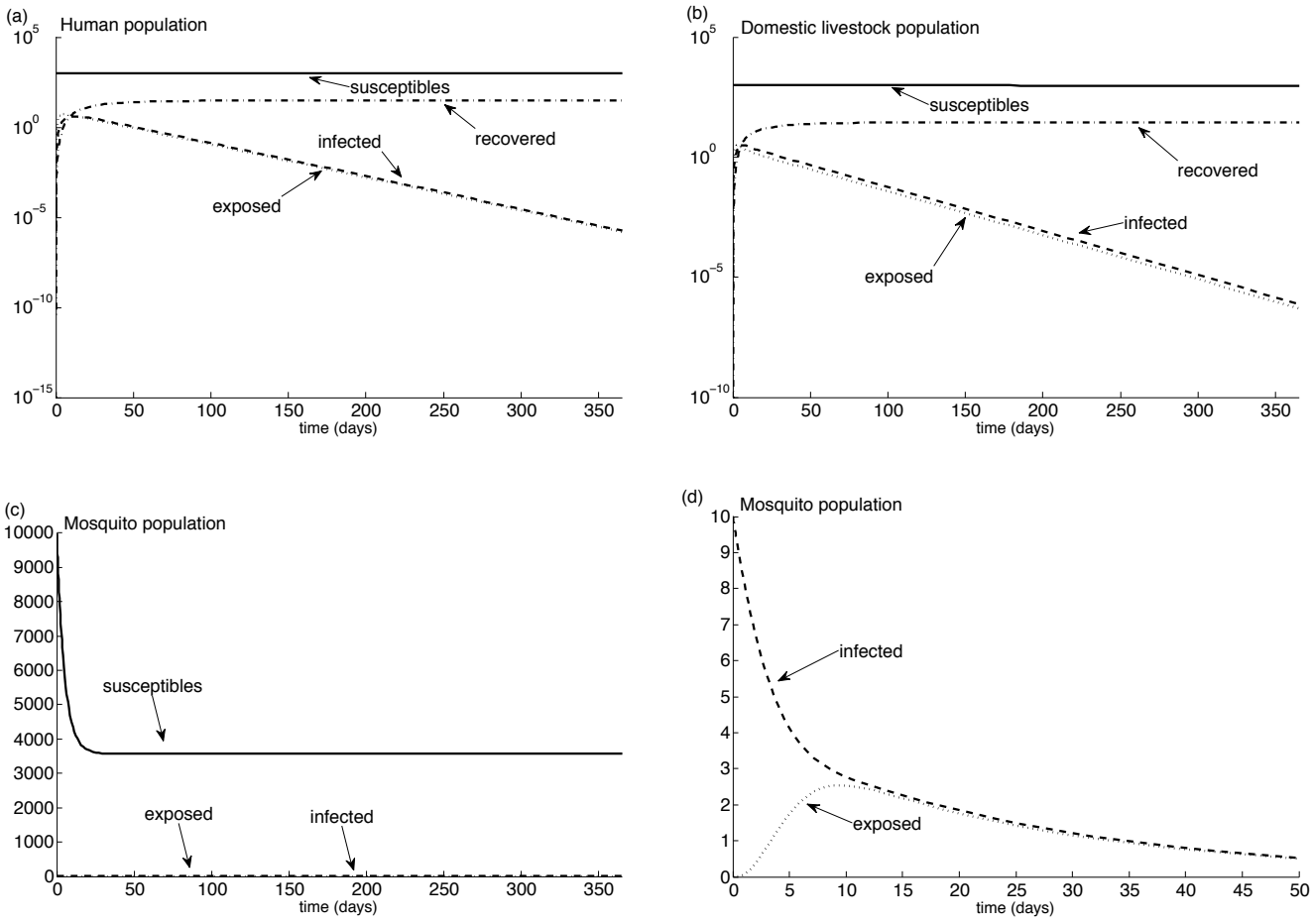

Figure 3: The behavior of (a) the human population, (b) the domestic livestock population, and (c) the mosquito population when the mosquito survival time is such that $R_0 < 1$ for one season (assuming winter does not change the dynamics of populations). The solid lines represent the susceptible populations, the dotted lines the exposed populations, the dashed lines the infected populations, and the dash-dot lines are the recovered populations. (d) The initial behavior of the mosquito population when $R_0 < 1$.

domestic livestock populations, because both populations have lifelong immunity (Figures 4a and 4b). The infection does not completely eradicate the virus, which suggests that the endemic equilibrium is stable.

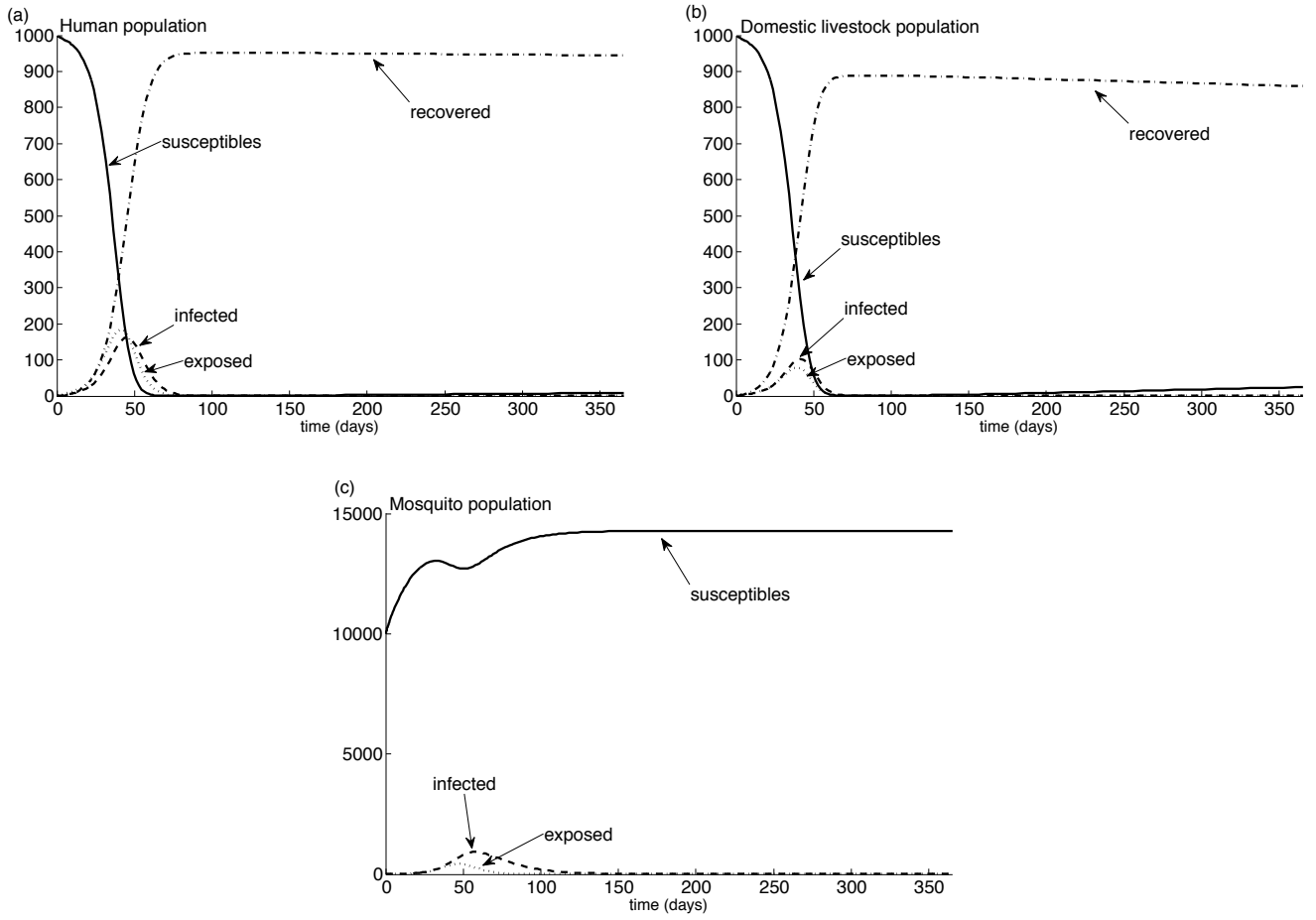

Figure 4: The behavior of (a) the human population, (b) the domestic livestock population and (c) the mosquito population when the mosquito survival time is such that $R_0 > 1$ for one season (assuming winter does not change the dynamics of populations). The solid lines represent the susceptible populations, the dotted lines the exposed populations, the dashed lines the infected populations, and the dash-dot lines are the recovered populations.

5.2 Multiple-season model

We allow 2% of the second generation of susceptible mosquitoes to survive the winter. Meanwhile, the susceptible human population increases by 10%, the infected population decreases to zero, and 10% of the recovered population becomes susceptible. The domestic livestock population grows at

the same rate as the human population. The susceptible population increases by 40% during the winter months, so 40% of the recovered population becomes susceptible. The domestic livestock increases by 10% to account for the buying of livestock due to deaths in the previous season.

Figure 5 shows the effects of choosing the mosquito survival time to be such that $R_0 < 1$, which causes no outbreaks within five years and leads to eradication of the disease. Figure 6 shows the effects of choosing the mosquito survival time to be such that $R_0 > 1$, which causes a disease outbreak every year in the human and domestic livestock populations.

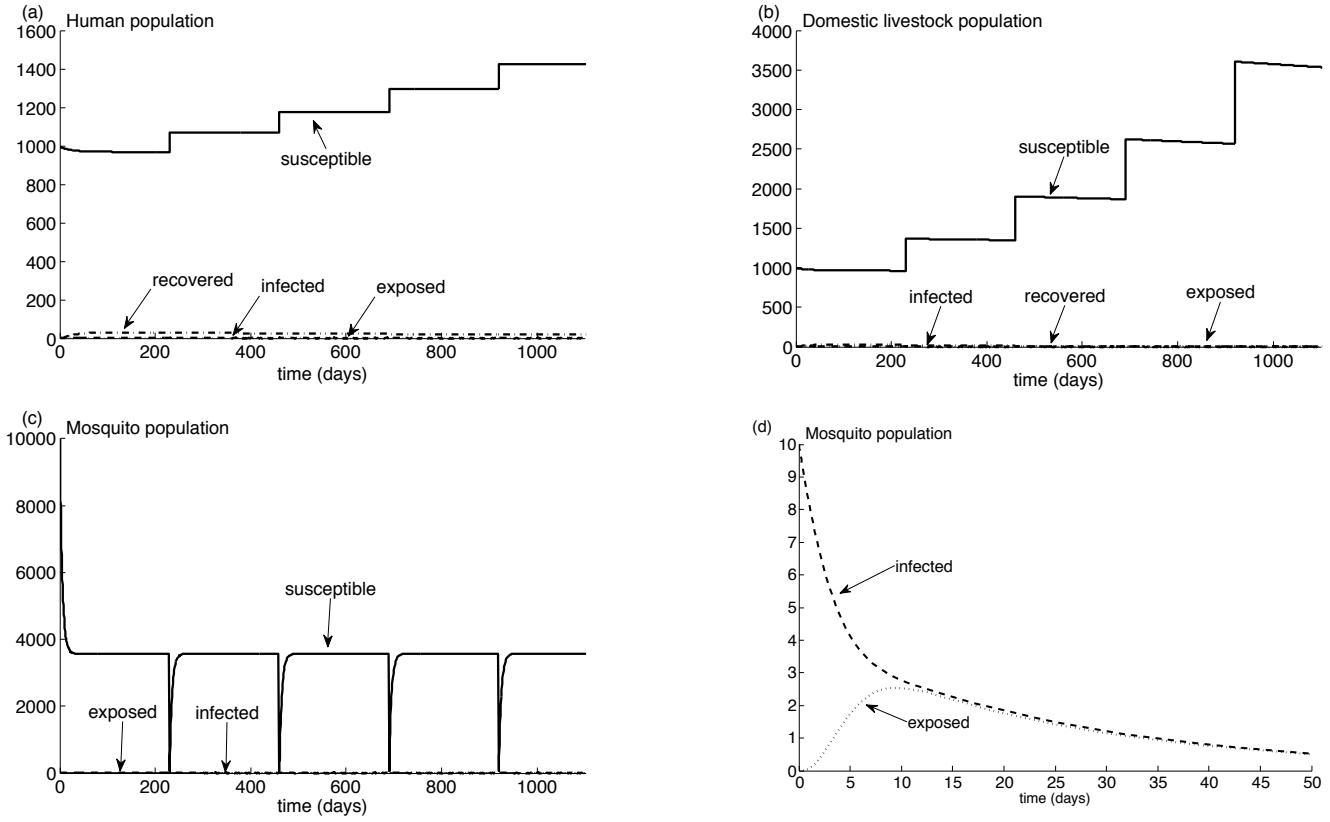

Figure 5: The behavior of (a) the human population, (b) the domestic livestock population, and (c) the mosquito population when the mosquito survival time is such that $R_0 < 1$ for multiple seasons. The solid lines represent the susceptible populations, the dotted lines the exposed populations, the dashed lines the infected populations, and the dash-dot lines the recovered populations. (d) The initial behavior of the mosquito population when $R_0 < 1$.

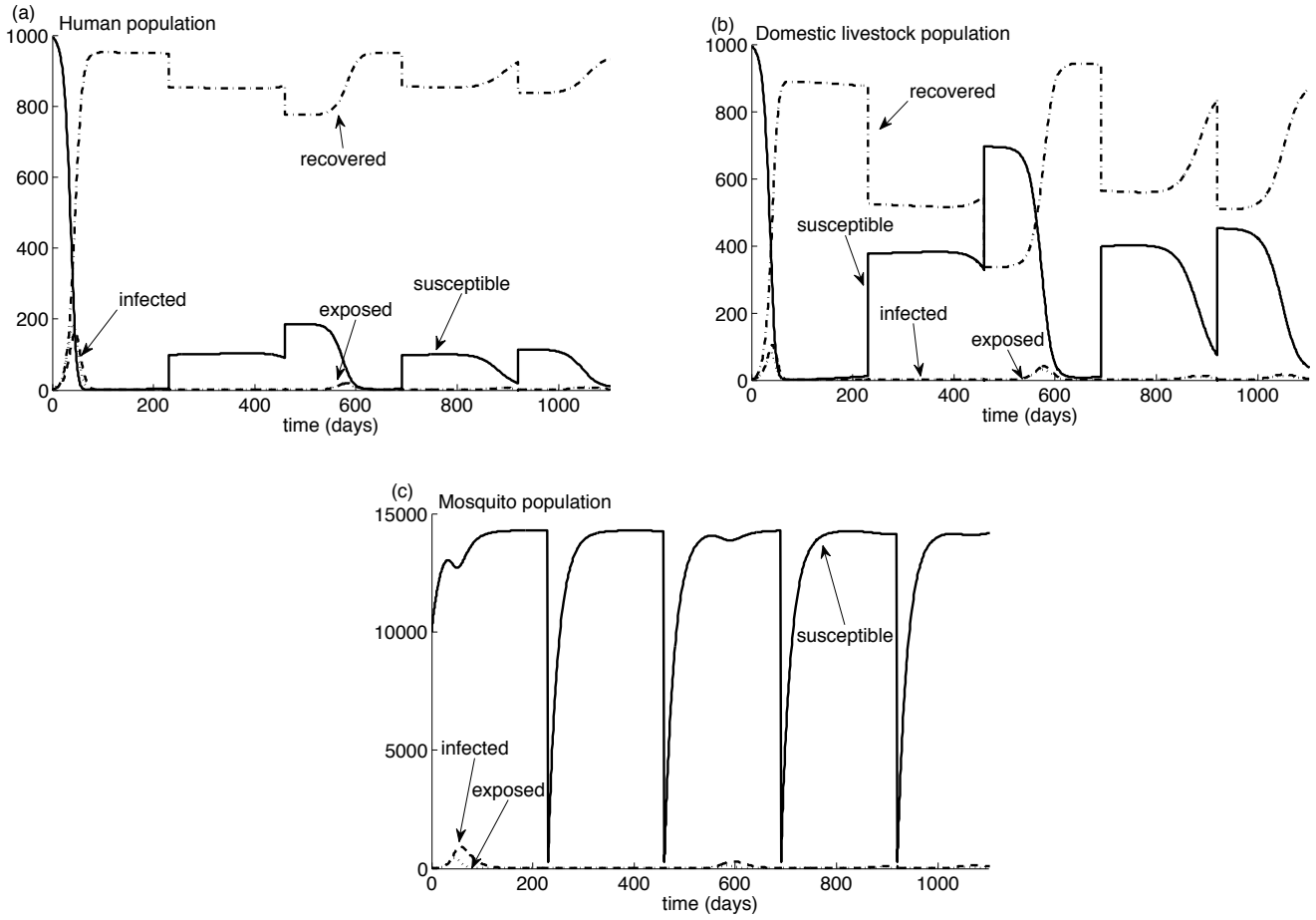

Figure 6: The behavior of (a) the human population, (b) the domestic livestock population, and (c) the mosquito population when the mosquito survival time is such that $R_0 > 1$ for multiple seasons. The solid lines represent the susceptible populations, the dotted lines the exposed populations, the dashed lines the infected populations, and the dash-dot lines the recovered populations.

Figure 5c shows the effects of impulses on the mosquito population by decreasing 98% of all the susceptible mosquitoes during the winter seasons when $R_0 < 1$. For both the human and domestic livestock populations, the disease-free equilibrium is stable (Figures 5a and 5b). The only difference is a change in the susceptible populations due to the discontinuous increase in populations during the winter months.

For $R_0 > 1$, outbreaks occur every year. The first outbreak is larger than subsequent years,

but the infected populations remain endemic. Infection persists in the mosquito population even though 98% of the infected are removed from the model due to winter (Figure 6c).

5.3 Sensitivity

Latin Hypercube Sampling (LHS) is a statistical sampling that allows for an efficient analysis of parameter variations across simultaneous uncertainty ranges in each parameter; partial rank correlation coefficients rank the coefficients by the degree of influence each has on the outcome, regardless of whether that influence increases or decreases the effect. LHS is most efficient if the outcome variable is a monotonic function of each of the input parameters (Blower and Dowlatabadi, 1994). Stein (1985) showed that, for many simulations, LHS is the most efficient design, even if the outcome variable is not monotonic. Figure 7a shows the partial rank correlation coefficient sensitivity for all parameters for 1000 runs. R_0 is most sensitive to the mosquito death rate d_M, as Figure 7b shows.

6 Conclusion

An outbreak of Rift Valley Fever in North America is theoretically possible. A very small number of infected mosquitoes is enough to establish the virus in North America. As seen with West Nile Virus, a disease can establish itself with a mosquito as a vector, and humans and livestock as hosts. The virulence of West Nile Virus in North America demonstrates the potential of other mosquito-borne pathogens.

We showed that reducing the survival time of mosquitoes below approximately 8.67 days would be sufficient to control an imported outbreak of Rift Valley Fever. This could be achieved through spraying insecticides. Insecticide control of mosquitoes has been effective in reducing malaria worldwide between the 1940s and 1960s (Trigg and Kondrachine, 1998; Mabaso et al., 2004; Macintyre et

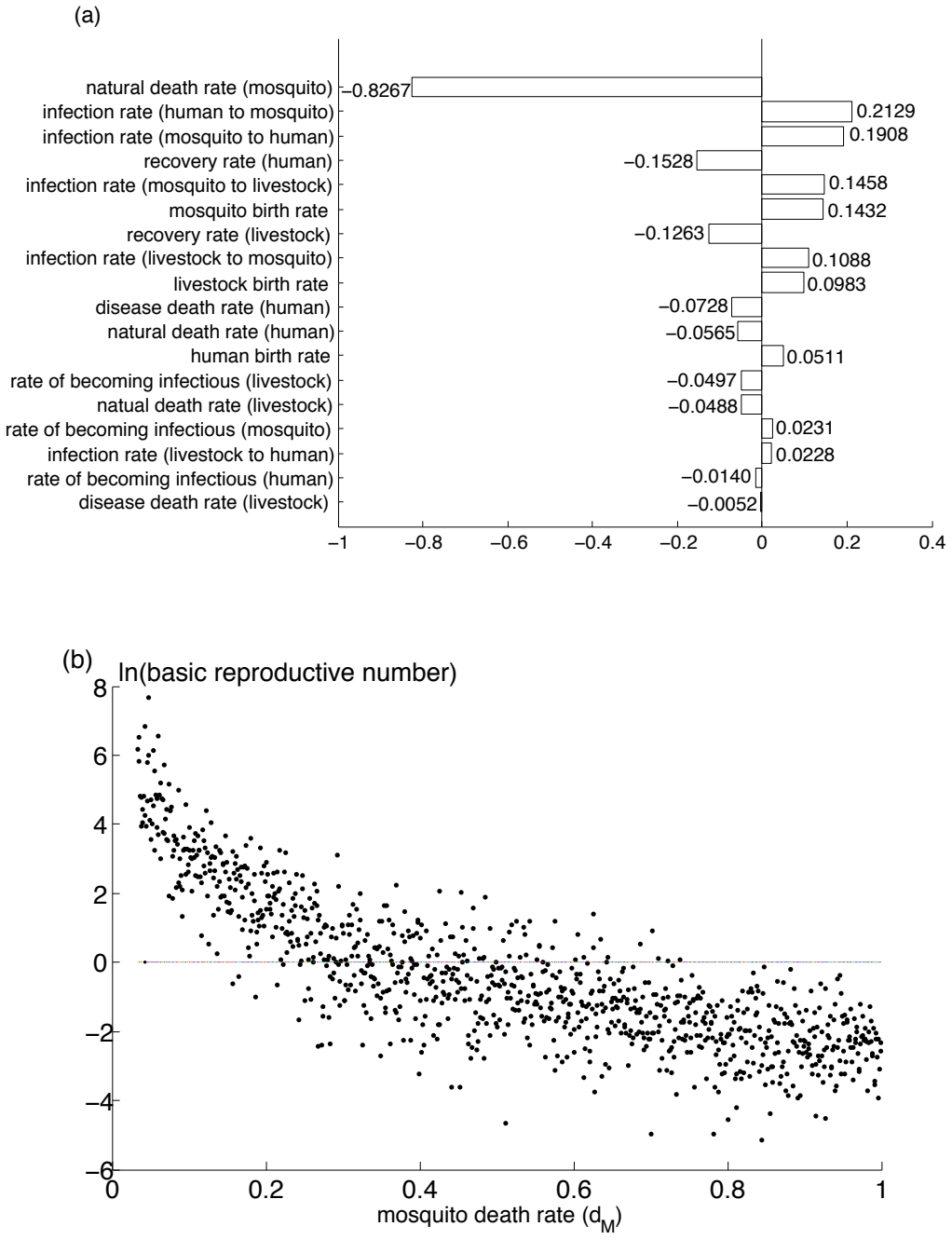

Figure 7: (a) Partial rank correlation coefficient sensitivity analysis on R_0 for all parameters. (b) The effect of the disease death rate d_M on R_0 using Monte Carlo simulations with parameters drawn using Latin Hypercube Sampling.

al., 2006; Al-arydah and Smith?, 2011). Female mosquitoes live between two weeks and a month, depending on warmth and moisture (CDC, 2012); reducing this duration to less than 8.67 days results in disease eradication.

The multiple season model shows the same results. If RVF can enter North America, an outbreak is likely to occur unless it can be controlled quickly. Furthermore, if RVF invades North America once, it is likely to break out again each year. The sufficient condition given in Section A.2 to have eigenvalues with negative real part (ensuring that the disease-free equilibrium is stable) is $d_M > 0.15$, where d_M is the mosquito death rate. This threshold is different from the one found using R_0 ($d_M > 0.115$). The difference is due to the condition used in Section A.2, which is sufficient but not necessary in order to have all eigenvalues negative. A sufficient and necessary threshold could be calculated from the Routh-Hurwitz conditions if fewer parameters were involved.

While the behavior of the system is consistent with expectations, most parameters have little effect on R_0. Density-independence and mass-action terms limit the model to small populations. We used initial values corresponding to a small coastal population in North America instead of the entire North American population. We ignored the presence of cities.

Our results suggest that countries in the developed world face ongoing threats of disease introduction. As global travel increases the movement of humans, livestock, and vectors around the world, the potential for new outbreaks is heightened. We must be ready to face these challenges.

Acknowledgements

The authors are grateful to Jing Li for technical discussions. RM is funded by an Ontario Graduate Scholarship. Robert J. Smith? is supported by an NSERC Discovery Grant, an Early Researcher Award, and funding from MITACS. The question mark in "Smith?" is part of the author's name.

A Appendix

A.1 Equilibria

The model has two equilibria. The disease-free equilibrium is $(S_H^*, E_H^*, I_H^*, R_H^*, S_L^*, E_L^*, I_L^*, R_L^*, S_M^*, E_M^*, I_M^*)$ $= \left(\frac{\Lambda_H}{d_H}, 0, 0, 0, \frac{\Lambda_L}{d_L}, 0, 0, 0, \frac{\Lambda_M}{d_M}, 0, 0\right)$. The endemic equilibrium is

$$(S_H^*, E_H^*, I_H^*, R_H^*, S_L^*, E_L^*, I_L^*, R_L^*, S_M^*, E_M^*, I_M^*)\,, \tag{9}$$

where I_M^* is the solution to

$$\rho I_M^3 + \eta I_M^2 + \delta I_M + \omega = 0 \tag{10}$$

with

$$\xi_1 = \frac{\beta_{LM}\epsilon_L\beta_{ML}\Lambda_L}{(d_L + \mu_L + \gamma_L)(d_L + \epsilon_L)} \tag{11}$$

$$\xi_2 = \frac{\beta_{HM}\epsilon_L\Lambda_L}{(d_H + \mu_H + \gamma_H)(d_H + \epsilon_H)} \tag{12}$$

and

$$\rho = d_M(d_M+\epsilon_M)\big(\xi_1\beta_{MH}\beta_{ML}+\beta_{ML}^2 d_M\beta_{MH}+\xi_2\beta_{MH}\beta_{ML}^2\big) \tag{13}$$

$$\begin{aligned}\eta = {} & d_M^2(d_M+\epsilon_M)\beta_{ML}(\xi_1+\beta_{ML}+2d_L\beta_{MH}) \\ & + d_M(d_M+\epsilon_M)\beta_{ML}(\xi_1\xi_2+\xi_2\beta_{MH}d_L+\xi_1 d_H)+\xi_1^2 d_M(d_M+\epsilon_M) \\ & - \big(\beta_{ML}\epsilon_L\Lambda_L - d_L d_M(d_M+\epsilon_M)\big)(\xi_1\beta_{MH}+\xi_2\beta_{MH}\beta_{ML})\end{aligned} \tag{14}$$

$$\begin{aligned}\delta = {} & d_M^2 d_L(d_M+\epsilon_M)\big(\xi_1+2\beta_{ML}+d_L\beta_{MH}\big) \\ & - \big(\beta_{ML}\epsilon_L\Lambda_L - d_L d_M(d_M+\epsilon_M)\big)(\xi_1\xi_2+\xi_2\beta_{MH}d_L+\xi_1 d_H) \\ & - \beta_{MH}d_L\epsilon_M\Lambda_M(\xi_1+\xi_2\beta_{ML})-\xi_1^2\epsilon_M\Lambda_M\end{aligned} \tag{15}$$

$$\omega = d_M^2 d_L^2(d_M+\epsilon_M)-\xi_1 d_H d_L\epsilon_M\Lambda_M-\xi_2\beta_{MH}d_L^2\epsilon_M\Lambda_M-\xi_1\xi_2 d_L\epsilon_M\Lambda_M\,, \tag{16}$$

where

$$S_H^* = \frac{\Lambda_H}{d_H + \beta_{MH} I_M^* + \beta_{LH} I_L^*} \tag{17}$$

$$E_H^* = \frac{\beta_{MH} S_H^* I_M^* + \beta_{LH} S_H^* I_L^* / N_L^*}{d_H + \epsilon_H} \tag{18}$$

$$I_H^* = \frac{\epsilon_H E_H^*}{d_H + \mu_H + \gamma_H} \tag{19}$$

$$R_H^* = \frac{\gamma_H I_H^*}{d_H} \tag{20}$$

$$S_L^* = \frac{\Lambda_L}{d_L + \beta_{ML} I_M^*} \tag{21}$$

$$E_L^* = \frac{\beta_{ML} S_L^* I_M^*}{d_L + \epsilon_L} \tag{22}$$

$$I_L^* = \frac{\epsilon_L E_L^*}{d_L + \mu_L + \gamma_L} \tag{23}$$

$$R_L^* = \frac{\gamma_L I_L^*}{d_L} \tag{24}$$

$$S_M^* = \frac{\Lambda_M}{d_M + \beta_{HM} I_H^* + \beta_{LM} I_L^*} \tag{25}$$

$$E_M^* = \frac{\beta_{HM} S_M^* I_H^* + \beta_{LM} S_M^* I_L^*}{d_M + \epsilon_M} \tag{26}$$

and where I_M^* is the solution to Eq. (10).

A.2 Stability of the disease-free equilibrium

The Jacobian matrix evaluated at the disease-free equilibrium is $J_{DFE} = (J^{(1)}_{DFE}|J^{(2)}_{DFE})$, where

$$J^{(1)}_{DFE} = \begin{pmatrix} -d_H & 0 & 0 & 0 & 0 & 0 \\ 0 & -d_H - \epsilon_H & 0 & 0 & 0 & 0 \\ 0 & \epsilon_H & -d_H - \mu_H - \gamma_H & 0 & 0 & 0 \\ 0 & 0 & \gamma_H & -d_H & 0 & 0 \\ 0 & 0 & 0 & 0 & -d_L & 0 \\ 0 & 0 & 0 & 0 & 0 & -d_L - \epsilon_L \\ 0 & 0 & 0 & 0 & 0 & \epsilon_L \\ 0 & 0 & 0 & 0 & 0 & 0 \\ 0 & 0 & -\beta_{HM} S^*_M & 0 & 0 & 0 \\ 0 & 0 & \beta_{HM} S^*_M & 0 & 0 & 0 \\ 0 & 0 & 0 & 0 & 0 & 0 \end{pmatrix} \tag{27}$$

$$J^{(2)}_{DFE} = \begin{pmatrix} -\beta_{LH}S^*_H/S^*_L & 0 & 0 & 0 & -\beta_{MH}S^*_H \\ \beta_{LH}S^*_H/S^*_L & 0 & 0 & 0 & \beta_{MH}S^*_H \\ 0 & 0 & 0 & 0 & 0 \\ 0 & 0 & 0 & 0 & 0 \\ 0 & 0 & 0 & 0 & -\beta_{ML}S^*_L \\ 0 & 0 & 0 & 0 & \beta_{ML}S^*_L \\ -d_L - \mu_L - \gamma_L & 0 & 0 & 0 & 0 \\ \gamma_L & -d_L & 0 & 0 & 0 \\ -\beta_{LM}S^*_M & 0 & -d_M & 0 & 0 \\ \beta_{LM}S^*_M & 0 & 0 & -d_M - \epsilon_M & 0 \\ 0 & 0 & 0 & \epsilon_M & -d_M \end{pmatrix}. \tag{28}$$

The matrix has the characteristic equation

$$0 = \det(J_{DFE}(S^*_H, E^*_H, I^*_H, R^*_H, S^*_L, E^*_L, I^*_L, R^*_L, S^*_M, E^*_M, I^*_M) - \alpha I_{11}) \tag{29}$$

$$= (-d_H - \alpha)^2(-d_L - \alpha)^2(-d_M - \alpha)f(\alpha) \tag{30}$$

where $f(\alpha)$ is the determinant of $(M_1|M_2)$ where

$$M_1 = \begin{pmatrix} -d_H - \epsilon_H - \alpha & 0 & 0 \\ \epsilon_H & -d_H - \mu_H - \gamma_H - \alpha & 0 \\ 0 & 0 & -d_L - \epsilon_L - \alpha \\ 0 & 0 & \epsilon_L \\ 0 & \beta_{HM}\dfrac{\Lambda_M}{d_M} & 0 \\ 0 & 0 & 0 \end{pmatrix} \tag{31}$$

$$M_2 = \begin{pmatrix} \beta_{LH}\dfrac{\Lambda_H d_L}{d_H \Lambda_L} & 0 & \beta_{MH}\dfrac{\Lambda_H}{d_H} \\ 0 & 0 & 0 \\ 0 & 0 & \beta_{ML}\dfrac{\Lambda_L}{d_L} \\ -d_L - \mu_L - \gamma_L - \alpha & 0 & 0 \\ \beta_{LM}\dfrac{\Lambda_M}{d_M} & -d_M - \epsilon_M - \alpha & 0 \\ 0 & \epsilon_M & -d_M - \alpha \end{pmatrix} \tag{32}$$

and S_H^*, S_L^*, and S_M^* are the disease-free equilibrium values. Solving for $f(\alpha)$, we have

$$f(\alpha) = \alpha^6 + c_1\alpha^5 + c_2\alpha^4 + c_3\alpha^3 + c_4\alpha^2 + c_5\alpha + c_6 \tag{33}$$

where

$$c_1 = 2d_H + \mu_H + \gamma_H + \epsilon_H + 2d_L + \epsilon_L + \mu_L + \gamma_L \tag{34}$$

$$\begin{aligned} c_2 = {} & (d_H + \epsilon_H + \gamma_H)(d_H + \epsilon_H) + (2d_H + \epsilon_H + \mu_H + \gamma_H)(2d_L + \epsilon_L + \mu_L + \gamma_L) \\ & + (2d_H + \epsilon_H + \mu_H + \gamma_H)(2d_M + \epsilon_M) + (d_L + \epsilon_L)(d_L + \mu_L + \gamma_L) \\ & + (2d_L + \epsilon_L + \mu_L + \gamma_L)(2d_M + \epsilon_M) + d_M(d_M + \epsilon_M) \end{aligned} \tag{35}$$

$$\begin{aligned} c_3 = {} & (d_H + \mu_H + \gamma_H)(d_H + \epsilon_H)(2d_L + \epsilon_L + \mu_L + \gamma_L) \\ & + (d_H + \mu_H + \gamma_H)(d_H + \epsilon_H)(2d_M + \epsilon_M) \\ & + (d_L + \epsilon_L)(d_L + \mu_L + \gamma_L)(2d_H + \mu_H + \epsilon_H + \gamma_H) \\ & + (2d_L + \mu_L + \epsilon_L + \gamma_L)(2d_M + \epsilon_M)(2d_H + \mu_H + \epsilon_H + \gamma_H) \\ & + d_M(d_M + \epsilon_M)(2d_H + \mu_H + \epsilon_H + \gamma_H) \\ & + (d_L + \epsilon_L)(2d_M + \epsilon_M)(d_L + \mu_L + \gamma_L) \\ & + d_M(d_M + \epsilon_M)(2d_L + \epsilon_L + \mu_L + \gamma_L) \end{aligned} \tag{36}$$

$$\begin{aligned} c_4 = {} & (d_H + \mu_H + \gamma_H)(d_H + \epsilon_H)(d_L + \epsilon_L)(d_L + \mu_L + \gamma_L) \\ & + (d_H + \epsilon_H)(d_H + \mu_H + \gamma_H)(2d_M + \epsilon_M)(2d_L + \epsilon_L + \mu_L + \gamma_L) \\ & + d_M(d_M + \epsilon_M)(d_H + \epsilon_H)(d_H + \mu_H + \gamma_H) \\ & + (d_L + \epsilon_L)(2d_M + \epsilon_M)(d_L + \mu_L + \gamma_L)(2d_H + \mu_H + \epsilon_H + \gamma_H) \\ & + d_M(d_M + \epsilon_M)(2d_H + \mu_H + \epsilon_H + \gamma_H)(2d_L + \mu_L + \epsilon_L + \gamma_L) \\ & + d_M(d_M + \epsilon_M)(d_L + \epsilon_L)(d_L + \mu_L + \gamma_L) - \epsilon_H\epsilon_M\beta_{HM}\beta_{MH}\frac{\Lambda_M}{d_M}\frac{\Lambda_H}{d_H} \\ & - \epsilon_L\epsilon_M\beta_{LM}\beta_{ML}\frac{\Lambda_L}{d_L}\frac{\Lambda_M}{d_M} \end{aligned} \tag{37}$$

$$
\begin{aligned}
c_5 = {} & (d_H + \mu_H + \gamma_H)(d_H + \epsilon_H)(d_L + \epsilon_L)(2d_M + \epsilon_M)(d_L + \mu_L + \gamma_L) \\
& + d_M(d_M + \epsilon_M)(d_H + \mu_H + \gamma_H)(d_H + \epsilon_H)(2d_L + \epsilon_L + \mu_L + \gamma_L) \\
& + d_M(d_M + \epsilon_M)(d_L + \mu_L + \gamma_L)(d_L + \epsilon_L)(2d_H + \epsilon_H + \mu_H + \gamma_H) \\
& - \epsilon_H \epsilon_M \beta_{HM} \beta_{MH} \frac{\Lambda_M}{d_M} \frac{\Lambda_H}{d_H}(2d_L + \epsilon_L + \mu_L + \gamma_L) \\
& - \epsilon_L \epsilon_M \beta_{LM} \beta_{ML} \frac{\Lambda_L}{d_L} \frac{\Lambda_M}{d_M}(2d_H + \epsilon_H + \mu_H + \gamma_H)
\end{aligned} \tag{38}
$$

and

$$
\begin{aligned}
c_6 = {} & d_m(d_M + \epsilon_M)(d_H + \mu_H + \gamma_H)(d_H + \epsilon_H)(d_L + \mu_L + \gamma_L)(d_L + \epsilon_L) \\
& - \epsilon_L \epsilon_M \beta_{LM} \beta_{ML} \frac{\Lambda_L}{d_L} \frac{\Lambda_M}{d_M}(d_H + \mu_H + \gamma_H)(d_H + \epsilon_H) \\
& - \epsilon_H \epsilon_M \beta_{MH} \beta_{HM} \frac{\Lambda_H}{d_H} \frac{\Lambda_M}{d_M}(d_L + \mu_L + \gamma_L)(d_L + \epsilon_L) \\
& - \epsilon_H \epsilon_L \epsilon_M \beta_{LH} \beta_{ML} \beta_{HM} \frac{\Lambda_M}{d_M} \frac{\Lambda_H}{d_H} \,.
\end{aligned} \tag{39}
$$

Necessary and sufficient conditions for all the zeros of $f(\alpha)$ to have negative real parts are that c_4, c_5, and c_6 be bigger than zero (because c_1, c_2, and c_3 are strictly positive), and

$$
a_1 a_2 a_3 + a_1 a_5 > a_3^3 + a_1^2 a_4 \tag{40}
$$

$$
\begin{aligned}
& a_1 a_6 a_2 (2a_1 a_5 - a_3^2) + a_1^2 a_6 (a_4 a_3 - a_1 a_6) + a_1 a_5 (a_4 a_5 - 3a_3 a_6) + a_6 a_3^3 \\
& + a_5^2 a_1 a_4 > a_1^2 a_5 a_4^2 + a_5 (a_3 a_4 - a_5 a_2)(a_3 - a_1 a_2) \,.
\end{aligned} \tag{41}
$$

If these Routh-Hurwitz conditions are satisfied, the disease-free equilibrium is stable (Truccolo et al., 2003; Allen, 2006). For the values used in Table 2, c_4, c_5, and c_6 vary depending on parameter values and the state variables S_H^*, S_L^*, and S_M^*. By fixing the state variables, the values for d_M (mosquito death rate) can be varied in order to change c_4, c_5, and c_6 from positive to negative. The

stability changes depending on the mosquito survival time. Numerically, c_4, c_5, and c_6 are positive when $d_M > 0.15$ (Figure 8), and the two inequalities are satisfied when $0 < d_M < 0.68$. The disease-free equilibrium is stable if $0.15 < d_M < 0.68$.

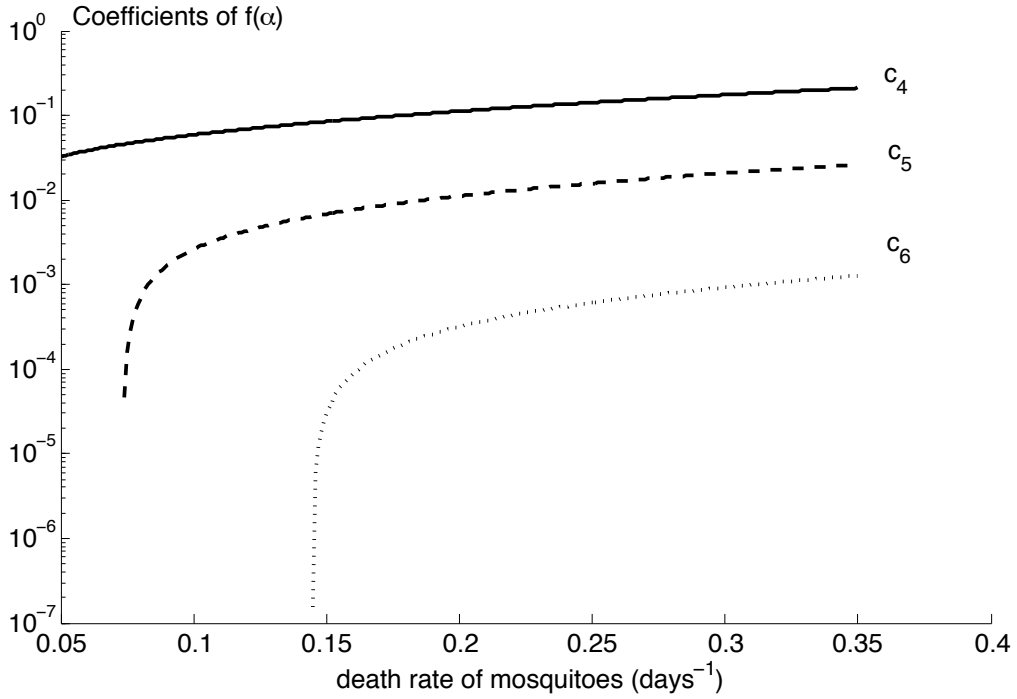

Figure 8: Sign change for certain parameters in $f(\alpha)$. When c_6 becomes negative (at around 0.15), both c_4 and c_5 are still positive. The values of c_4 and c_5 only become negative after c_6 has already fallen below zero.

A.3 Basic Reproductive Number

The model has six infected populations, E_H, I_H, E_L, I_L, E_M, and I_M. The vector $\mathcal{F}$ representing new infections and the vector $\mathcal{V}$ representing transfers between compartments are given by

$$\mathcal{F} = \begin{pmatrix} \beta_{LH}\frac{S_H^* I_L^*}{N_L^*} + \beta_{MH} S_H^* I_M^* \\ 0 \\ \beta_{ML} S_L^* I_M^* \\ 0 \\ \beta_{LM} S_M^* I_L^* + \beta_{HM} S_M^* I_H^* \\ 0 \end{pmatrix} \tag{42}$$

$$\mathcal{V} = \begin{pmatrix} (d_H + \epsilon_H) E_H^* \\ (d_H + \mu_H + \gamma_H) I_H^* - \epsilon_H E_H^* \\ (d_L + \epsilon_L) E_L^* \\ (d_L + \mu_L + \gamma_L) I_L^* - \epsilon_L E_L^* \\ (d_M + \epsilon_M) E_M^* \\ d_M I_M^* - \epsilon_M E_M^* \end{pmatrix}. \tag{43}$$

The matrices F and V are

$$F = \begin{pmatrix} 0 & 0 & 0 & \beta_{LH}S_H^*/S_L^* & 0 & \beta_{MH}S_H^* \\ 0 & 0 & 0 & 0 & 0 & 0 \\ 0 & 0 & 0 & 0 & 0 & \beta_{ML}S_L^* \\ 0 & 0 & 0 & 0 & 0 & 0 \\ 0 & \beta_{HM}S_M^* & 0 & \beta_{LM}S_M^* & 0 & 0 \\ 0 & 0 & 0 & 0 & 0 & 0 \end{pmatrix} \tag{44}$$

$$V = \begin{pmatrix} d_H + \epsilon_H & 0 & 0 & 0 & 0 & 0 \\ -\epsilon_H & d_H + \mu_H + \gamma_H & 0 & 0 & 0 & 0 \\ 0 & 0 & d_L + \epsilon_L & 0 & 0 & 0 \\ 0 & 0 & -\epsilon_L & d_L + \mu_L + \gamma_L & 0 & 0 \\ 0 & 0 & 0 & 0 & d_M + \epsilon_M & 0 \\ 0 & 0 & 0 & 0 & -\epsilon_M & d_M \end{pmatrix}, \tag{45}$$

where S_H^*, S_L^*, and S_M^* are the disease-free equilibrium values. Next, $FV^{-1} = (FV_{(1)}^{-1}|FV_{(2)}^{-1})$ was

calculated, and the eigenvalue with the largest modulus is the value of R_0. We have

$$FV_{(1)}^{-1} = \begin{pmatrix} 0 & 0 & \frac{\beta_{LH} S_H^* \epsilon_L}{S_L^*(d_L+\mu_L+\gamma_L)(d_L+\epsilon_L)} \\ 0 & 0 & 0 \\ 0 & 0 & 0 \\ 0 & 0 & 0 \\ \frac{\beta_{HM} S_M^* \epsilon_H}{(d_H+\epsilon_H)(d_H+\mu_H+\gamma_H)} & \frac{\beta_{HM} S_M^*}{d_H+\mu_H+\gamma_H} & \frac{\beta_{LM} S_M^* \epsilon_L}{(d_L+\epsilon_L)(d_L+\mu_L+\gamma_L)} \\ 0 & 0 & 0 \end{pmatrix} \tag{46}$$

$$FV_{(2)}^{-1} = \begin{pmatrix} \frac{\beta_{LH} S_H^*}{S_L^*(d_L+\mu_L+\gamma_L)} & \frac{\beta_{MH} S_H^* \epsilon_M}{d_M(d_M+\epsilon_M)} & \frac{\beta_{MH} S_H^*}{d_M} \\ 0 & 0 & 0 \\ 0 & \frac{\beta_{ML} S_L^* \epsilon_M}{d_M(d_M+\epsilon_M)} & \frac{\beta_{ML} S_L^*}{d_M} \\ 0 & 0 & 0 \\ \frac{\beta_{LM} S_M^*}{d_L+\mu_L+\gamma_L} & 0 & 0 \\ 0 & 0 & 0 \end{pmatrix}. \tag{47}$$

The characteristic polynomial is

$$\det(FV^{-1} - \alpha I_6) = \alpha^3 g(\alpha) \tag{48}$$

where $g(\alpha)$ is the determinant of

$$\begin{pmatrix} -\alpha & \frac{\beta_{LH} S_H^* \epsilon_L}{S_L^*(d_L+\mu_L+\gamma_L)(d_L+\epsilon_L)} & \frac{\beta_{MH} S_H^* \epsilon_M}{d_M(d_M+\epsilon_M)} \\ 0 & -\alpha & \frac{\beta_{ML} S_L^* \epsilon_M}{d_M(d_M+\epsilon_M)} \\ \frac{\beta_{HM} S_M^* \epsilon_H}{(d_H+\epsilon_H)(d_H+\mu_H+\gamma_H)} & \frac{\beta_{LM} S_M^* \epsilon_L}{(d_L+\epsilon_L)(d_L+\mu_L+\gamma_L)} & -\alpha \end{pmatrix}. \tag{49}$$

Solving for α, we have:

$$-\alpha^3 + A\alpha + B = 0 \tag{50}$$

where

$$\begin{aligned} A = & \frac{\beta_{LM} S_M^* \epsilon_L}{(d_L + \epsilon_L)(d_L + \mu_L + \gamma_L)} \frac{\beta_{ML} S_L^* \epsilon_M}{d_M (d_M + \epsilon_M)} \\ & + \frac{\beta_{HM} S_M^* \epsilon_H}{(d_H + \epsilon_H)(d_H + \mu_H + \gamma_H)} \frac{\beta_{MH} S_H^* \epsilon_M}{d_M (d_M + \epsilon_M)} \end{aligned} \tag{51}$$

$$B = \frac{\beta_{HM} S_M^* \epsilon_H}{(d_H + \epsilon_H)(d_H + \mu_H + \gamma_H)} \frac{\beta_{LH} S_H^* \epsilon_L}{(d_L + \mu_L + \gamma_L)(d_L + \epsilon_L)} \frac{\beta_{ML} \epsilon_M}{d_M (d_M + \epsilon_M)} . \tag{52}$$

Because A and B are positive, the equation $\alpha^3 = A\alpha + B$ has a real solution (Figure 9).

Eq. (50) has solutions

$$\alpha_1 = \frac{1}{6} \xi^{\frac{1}{3}} + 2A \xi^{-\frac{1}{3}} \tag{53}$$

$$\alpha_2 = \frac{1}{6} \Big(-\frac{1}{2} + i \frac{3^{\frac{1}{2}}}{2} \Big) \xi^{\frac{1}{3}} + 2A \Big(-\frac{1}{2} - i \frac{3^{\frac{1}{2}}}{2} \Big) \xi^{-\frac{1}{3}} \tag{54}$$

$$\alpha_3 = \frac{1}{6} \Big(-\frac{1}{2} - i \frac{3^{\frac{1}{2}}}{2} \Big) \xi^{\frac{1}{3}} + 2A \Big(-\frac{1}{2} + i \frac{3^{\frac{1}{2}}}{2} \Big) \xi^{-\frac{1}{3}} \tag{55}$$

where

$$\xi = 108B + 12 \left(81B^2 - 12A^3 \right)^{\frac{1}{2}} . \tag{56}$$

The value for R_0 is the largest modulus of the eigenvalues α_i (Greenhalgh, 1996).

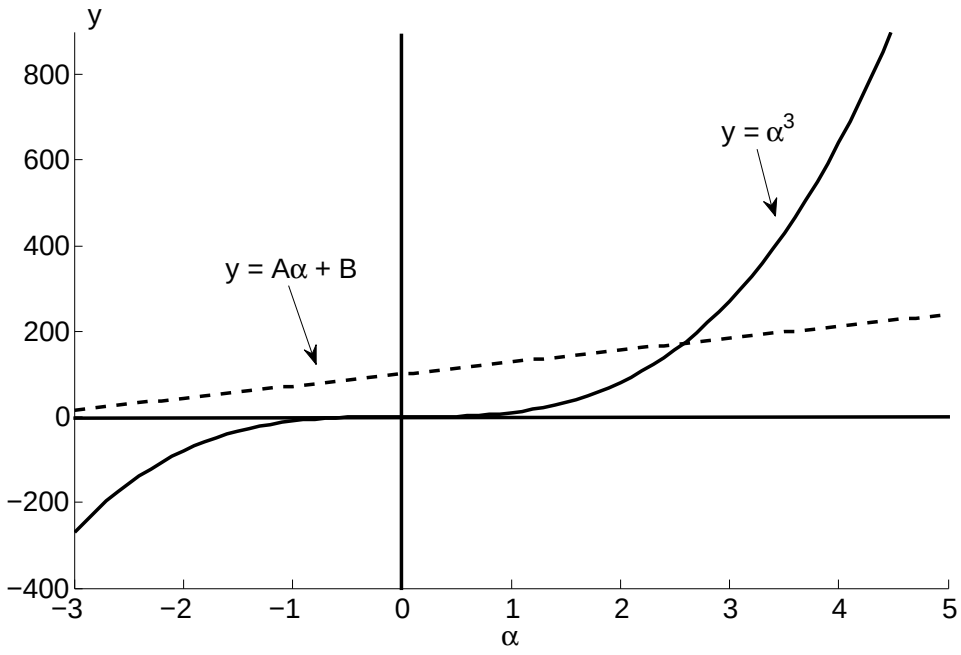

Figure 9: Intersection of the line $y = A\alpha + B$ with the cubic polynomial $y = \alpha^3$ when A and B are positive.

Case 1. If $81B^2 - 12A^3 > 0$, with $M = \frac{1}{6}\xi^{\frac{1}{3}}$ and $N = 2A\xi^{-\frac{1}{3}}$, then

$$\alpha_1 = M + N \tag{57}$$

$$\alpha_{2,3} = -\frac{1}{2}(M+N) \pm \frac{3^{\frac{1}{2}}}{2} i(M-N) \tag{58}$$

and the modulus of each eigenvalue is

$$|\alpha_1| = \left((M+N)^2\right)^{\frac{1}{2}} \tag{59}$$

$$= \left(M^2 + 2MN + N^2\right)^{\frac{1}{2}} \tag{60}$$

and

$$|\alpha_{2,3}| = \left(\frac{1}{4}(M+N)^2 + \frac{3}{4}(M-N)^2\right)^{\frac{1}{2}} \tag{61}$$

$$= \frac{1}{2}\left(4N^2 - 4MN + 4M^2\right)^{\frac{1}{2}} \tag{62}$$

$$= \left(M^2 - 2MN + N^2\right)^{\frac{1}{2}} \tag{63}$$

where $|\alpha_1| > |\alpha_{2,3}|$. $R_0^{(1)} = |\alpha_1|$, where $R_0^{(1)}$ is the basic reproductive number if $81B^2 - 12A^3$ is positive.

Case 2. If $81B^2 - 12A^3 < 0$ then $|\alpha_1| = |\alpha_{2,3}|$. $R_0^{(2)} = |\alpha_1|$, where $R_0^{(2)}$ is the basic reproductive number if $81B^2 - 12A^3$ is negative. We use the fact that $|\alpha_1| = (\alpha_1\bar{\alpha}_1)^{\frac{1}{2}}$ and polar coordinates to find the modulus. Because $r = ((108B)^2 + 12^2|81B^2 - 12A^3|)^{\frac{1}{2}}$ and $\cos\theta = \dfrac{108B}{r}$,

$$\alpha_1 = \frac{1}{6}r^{\frac{1}{3}}\exp\left(\frac{i\theta}{3}\right) + 2Ar^{-\frac{1}{3}}\exp\left(-\frac{i\theta}{3}\right) \tag{64}$$

$$\bar{\alpha}_1 = \frac{1}{6}r^{\frac{1}{3}}\exp\left(-\frac{i\theta}{3}\right) + 2Ar^{-\frac{1}{3}}\exp\left(i\frac{\theta}{3}\right) \tag{65}$$

and so

$$R_0^{(2)} = |\alpha_1| \tag{66}$$

$$= \frac{1}{36} r^{\frac{1}{3}} + \frac{A}{3} \cos \frac{2\theta}{3} + 4A^2 r^{-\frac{2}{3}} \,. \tag{67}$$

We have

$$R_0 = |\alpha_1| \,. \tag{68}$$

A.4 The effects of reducing winter to an impulse

The seasonal changes occurring after an introduction of RVF to North America reduce the dynamics of the human, livestock, and mosquito populations in the winter months to a single impulse. We compare this seasonal-jump model to a continuous ODE model for both the summer and winter months with impulses only at the end of each season.

In a continuous model for the winter with $S_M = E_M = I_M = \Lambda_M = 0$ at the end of winter, the susceptible, exposed, and infected mosquitoes tend to zero exponentially fast. Figure 10 shows the dynamics of the continuous winter season for the susceptible mosquito population.

At the end of summer, the susceptible mosquito population is at S_M^-. Throughout the winter, the mosquito population decreases exponentially. At the end of the winter season, $S_M^{\text{ends}} = S_M^- \exp(-rT)$, where T is the duration of winter. A proportion p_3 of offspring of the infected mosquitoes hatch at the end of winter which increases the total population of mosquitoes before the next summer season to $S_M^+ = S_M^- \exp(-rT) + p_3 I_M$. If $r_3 = 1 - \exp(-rT)$, the two models give the same results for the mosquito population. The same results apply to the human and livestock populations.

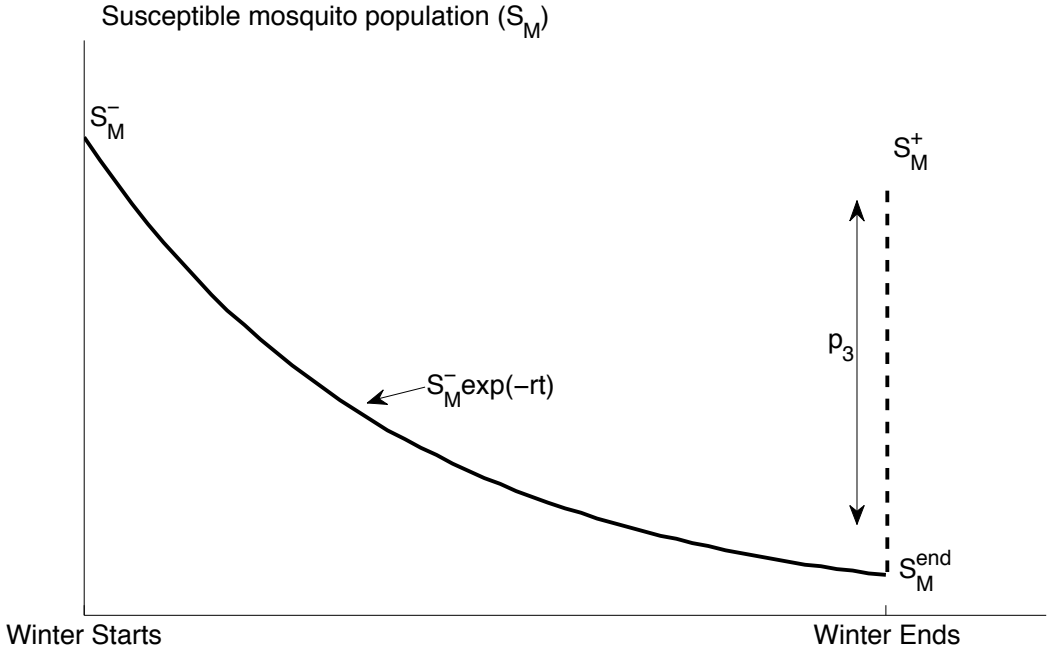

Figure 10: Comparison between full-time model and seasonal-jump model. The curve $S_M = S_M^- \exp(-rt)$ reflects the dynamics of the susceptible mosquito population during the winter months. At the end of the winter (S_M^{end}), the mosquito population increases by p_3. S_M^- is the value before the impulse for the seasonal-jump model and S_M^+ is the value after the impulse .

References

Al-Arydah, M. and Smith?, R. (2011). Controlling malaria with indoor residual spraying in spatially heterogeneous environments. *Mathematical Biosciences and Engineering, 8*(4), 889–914.

Allen, L.J.S. Introduction to Mathematical Biology. (2006). Zug: Pearson Education.

Anyamba, A., Chretien, J.P., Smalla, J., et al. (2009). Prediction of a Rift Valley Fever outbreak PNAS. *Proceedings of the National Academy of Science, 106*: 955–959.

Bainov, D.D. and Simeonov, P.S. (1989). *Systems with Impulsive Effect*. Chichester: Ellis Horwood.

Bainov, D.D. and Simeonov, P.S. (1993). *Impulsive differential equations: periodic solutions and applications.* Burnt Mill: Longman Scientific and Technical.

Bainov, D.D. and Simeonov, P.S. (1995). *Impulsive Differential Equations: Asymptotic Properties of the Solutions.* Singapore: World Scientific.

Balkhy, H.H. and Memish, Z.A. (2003). Rift Valley Fever: an uninvited zoonosis in the Arabian peninsula. *International Journal of Antimicrobial Agents, 21*: 153–157.

Bicout, D.J. and Sabatier, P. (2004). Mapping Rift Valley Fever Vectors and Prevalence Using Rainfall Variations. *Vector-borne and Zoonotic diseases, 4*(1): 33-42.

Blower S.M. and Dowlatabadi H. (1994). Sensitivity and uncertainty analysis of complex models of disease transmission: an HIV model, as an example. *International Statistical Review, 2*: 229–243.

Bowman, C., Gumel, A., van den Driessche, P., et al. (2005). A mathematical model for assessing control strategies against West Nile Virus. *Bulletin of Mathematical Biology, 67*: 1107–1133.

Centers for Disease Control and Prevention (2003). Rift Valley Fever Information Sheet. `http://www.cdc.gov/ncidod/dvrd/spb/mnpages/dispages/rvf.htm`

Centers for Disease Control and Prevention. (2012). Malaria. `http://www.cdc.gov/malaria/about/biology/mosquitoes/`

Despommiers, D., Ellis, B.R., and Wilcox, B.A. (2007). The Role of Ecotones in Emerging Infectious Diseases. *EcoHealth, 3*: 281–289.

Directors of Health Promotion and Education. (2013). Rift Valley Fever. `https://dhpe.site-ym.com/`

Dohm D.J., Sardelis M.R., and Turell M.J. (2002). Experimental vertical transmission of West Nile Virus by Culex pipiens (Diptera: Culicidae). *Journal of Medical Entomology, 39*(4), 640–644.

van den Driessche, P. and Watmough, J. (2002). Reproduction numbers and sub-threshold endemic equilibria for compartmental models of disease transmission. *Mathematical Biosciences, 180*: 29–48.

Favier, C., Chalvet-Monfray, K., Sabatier, P., Lancelot, R., et al. (2006). Rift Valley Fever in West Africa: the role of space in endemicity. *Tropical Medicine and International Health, 12*: 1878–1888.

Gaff H.D., Hartley, D.M., and Leahy, N.P., (2007). An Epidemiological Model of Rift Valley Fever. *Electronic Journal of Differential Equations, 2007*: 1–12.

Gerdes, G.H. (2004). Rift Valley Fever. *Revue scientifique et technique de l'office international des epizooties, 23*: 613–623.

Greenhalgh D. (1996). Effects of Heterogeneity on the Spread of HIV/AIDS Among Intravenous Drug Users in Shooting Galleries. *Mathematical Biosciences, 136*: 141–186.

House, J.A., Turell, M.J., and Mebus, C.A. (1992). Rift Valley Fever: present status and risk to the Western Hemisphere. *Annals New York Academy of Sciences, 653*: 233–242.

Karpati, A.M., Perrin M.C., Matte, T., et al. (2004). Pesticide Spraying for West Nile Virus Control and Emergency Department Asthma Visits in New York City, 2000. *Environmental Health Perspectives, 112*(11), 1183–1187.

Lakshmikantham, V., Bainov, D.D., and Simeonov, P.S. (1989). *Theory of Impulsive Differential Equations.* Singapore: World Scientific.

Li J., Blakeley, D., and Smith?, R.J. (2011). The Failure of R_0. *Computational and Mathematical Methods in Medicine, 2011*: Article ID 527610.

Mabaso, M.L., Sharp, B., and Lengeler, C. (2004). Historical review of malarial control in southern Africa with emphasis on the use of indoor residual house-spraying. *Tropical Medicine and International Health, 9*: 846–856.

Macintyre, K., Keating, J., Okbaldt, Y.B., et al. (2006). Rolling out insecticide treated nets in Eritrea: Examining the determinants of possession and use in malarious zones during the rainy season. *Tropical Medicine and International Health, 11*: 824–833.

Meegan, J.M. (1980). The Rift Valley Fever epizootic in Egypt 1977–78 1. Description of the epizootic and virological studies. *Transactions of the Royal Society of Tropical Medicine and Hygiene, 73*: 618–623.

Morse, S.S. (1995). Factors in the Emergence of Infectious Diseases. *Emerging Infectious Diseases, 1*: 7–15.

Mostashari, F., Kulldorff, M., Hartman, J.J., et al. (2003). Dead Bird Clusters as an Early Warning System for West Nile Virus Activity. *Emerging Infectious Diseases, 9*(6), 641646.

Moutailler, S., Krida, G., Schaffner, F., et al. (2008). Potential Vectors of Rift Valley Fever Virus in the Mediterranean Region. *Vector-Borne and Zoonotic Diseases, 8*: 749–753.

Murray, J.D. (1991). *Mathematical Biology* (Second Edition). New York: Springer-Verlag.

Patz, J.A., Campbell-Lendrum, D., Holloway, and T., Foley, J.A. (2005). Impact of regional climate change on human health. *Nature, 438*: 310–317.

Porphyre, T., Bicout, D.J., and Sabatier, P. (2005). Modelling the abundance of mosquito vectors versus flooding dynamics. *Ecological Modelling, 183*: 173–181.

Roche, J.P. (2002). The New York Academy of Medicine Print Media Coverage of Risk-Risk Tradeoffs Associated with West Nile Encephalitis and Pesticide Spraying. *Journal of Urban Health: Bulletin of the New York Academy of Medicine, 79*(4).

Stein, M. (1985). The use of LHS for variance reduction in simulations with many random parameters. *IBM Report RC11166* Yorktown Heights: Tech Report IBM Research Center.

Traoré-Lamizana, M., Fontenille, D., Diallo, M., et al. 2001. Arbovirus surveillance from 1990–1995 in the Barkedji Area (Ferlo) of Senegal, a Possible Natural Focus of Rift Valley Fever Virus. (2001). *Journal of Medical Entomology, 38*: 480–491.

Trigg, P.I. and Kondrachine, A.V. (1998). Commentary: Malaria control in the 1990s. *Bulletin of the World Health Organization, 76*: 11–16.

Truccolo, W.A., Rangarajan, G., Chen, Y., and Ding, M. (2003). Analysing stability of equilibrium points in neutral networks: a general approach. *Neutral Networks, 16*: 1453–1460.

Turell, M.J., Dohm, D.J., Mores, et al. (2008). Potential for North American Mosquitoes to Transmit Rift Valley Fever Virus. *Journal of the American Mosquito Control Association, 24*: 502–507.

Turell, M.J., Linthicum, K.J., Patrican, et al. (2008). Vector Competence of Selected African Mosquito (Diptera: Culicidae) Species for Rift Valley Fever Virus. *Journal of Medical Entomology, 45*: 102–108.

Xue, L., Scott, M., and Scoglio, C. (2012). A Network-Based Meta-Population Approach to Model Rift Valley Fever Epidemics. *Journal of Theoretical Biology 306*(7): 129–144

Zell, R. (2004). Global climate change and the emergence/re-emergence of infectious diseases. *International Journal of Medical Microbiology, 293*(37), 16–26.

Chapter 6

Discussion, conclusion and future work

6.1 Discussion

Impulsive differential equations are becoming a more popular way of describing biological systems. Three different applications of impulsive differential systems were developed and analyzed. Each system was related to the spread of infectious diseases, and each looked at the long-term outcomes either at an immunological or epidemiological level. Two of the applications were viewed at an immunological level for HIV and the third application was at an epidemiological level for the spread of Rift Valley Fever. Impulsive differential equations allowed us to analyze the HIV models by including drug therapy as an impulse. The development and analysis of such models allowed us to make predictions about finite drug treatment and drug resistance. The inclusion of an impulsive differential equation in the Rift Valley Fever model allowed us to incorporate seasonal changes in the populations. In North America, winter highly affects the mosquito populations, and so including a winter term and decrease in the mosquito population is crucial to show more realistic results.

In each application, the long-term behaviours were analysed either by solving the impulsive differential equations or by looking at stability of the system. We first looked at a protease-inhibitor-sparing HIV drug regimen on a finite time scale (Section 3.1). We define a new way of determining the Region 2 threshold. Smith? [16] defined the Region 2 threshold based on the point of inflection on the transformed IC_{50} graph. This method is not precise and the cutoff is arbitrary. We define the Region 2 threshold by determining the time taken for resistance levels to reach a minimum in order to ensure that resistance cannot emerge when patients are not taking a drug holiday. Since the time taken for resistance levels to reach a minimum is time-dependant, it relies on initial conditions. Since we assume that initial conditions are small for the drug-resistant-virus population, the local minimum values will only be slightly affected by the initial conditions. We then found the endpoints of our impulsive periodic orbit. (We use the endpoints since drugs decay exponentially, and thus the solution between impulses is monotonic.) These endpoints allowed us to calculate the number of drug holidays a patient may take while on a triple-drug cocktail of antiretroviral drugs without allowing drug resistance to emerge.

The second application looks at the stability analysis for a protease inhibitor HIV drug system for fixed drug concentration levels (Section 3.2). An impulse is included to describe the drug dynamics. The stability analysis describes the interaction between wild-type and resistant viruses at either a low, intermediate or high drug level. Including the impulse allows the drug concentration level to vary either solely within a region or cross between multiple regions. This behaviour is more likely to occur, and numerical simulations show the effects of drug levels crossing between regions. We consider many time scales within this system. The virus life cycle is fast compared to the T cell life cycle. The mutation rate of the virus and the drug absorption rates are also on different time scales. The differences in the time scales are investigated in Chapter 4.

A third application examines the differences between a one-season and multiple-

season Rift Valley Fever model (Chapter 5). Stability conditions were computed for the one-season model. The basic reproductive number, R_0, was computed and stability analysis was performed for the disease-free equilibrium. Figure 2 shows that $R_0 < 1$ if the mosquito survival time is below approximately 8.67 days. When solving for stability of the disease-free equilibrium, we have a stable equilibrium point if $1/d_M < 7.67$ days. The discrepancy appears to be caused by a backward bifurcation. The value of R_0 can be misleading if a backward bifurcation occurs. If we have sufficiently large initial conditions, this could cause an outbreak of the disease even if $R_0 < 1$. In our case, since we are introducing a completely new disease into North America, the initial conditions are very small, and so the backward bifurcation will not have an effect on our results.

Impulses were then used to describe a multiple-season model where outbreaks occurred every season, depending on certain thresholds. We should note that, in the ordinary differential equations, the growth rate is independent of the population size; in the impulse conditions, the growth is proportional to the population size. Since we are considering two different systems (ordinary differential equations and difference equations), these do not need to be consistent. The ordinary differential equations need to equilibrate (the reason why we make the growth rate independent). The impulses are only used to mimic winter, and so they are simply used to jump across the winter season.

Stability analysis was done using the system of ordinary differential equations. Since the models are nonlinear and contain many equations, solving for stability of the T-periodic solutions of the impulsive system is highly complicated. Therefore, from the HIV models, we developed a general two-dimensional system of impulsive differential equations in order to explicitly solve for T-periodic solutions, and examined stability when certain parameters change (Chapter 4). We reduce the HIV systems presented in Chapter 3 to an almost linear model where only one term is nonlinear. This nonlinear infection term has been studied in ordinary differential equations, and

there is debate about whether this term needs to be included in a system since it is very small and studies have assumed that it could be absorbed in to the viral-clearance term. The reduced system excludes the effect of the virus on the $CD4^+$ T cell population. When virus is present and detected, the proliferation rate of T cells increase. Also, when a virus enters a cell, the death rate of the T cells changes. In order to have a model describing the interaction between $CD4^+$ T cells and virus, this interaction term is crucial. Therefore, we include the effect of the virus on the T cell population in the general model as a linear term. We also included the effect of the virus on the T cell population via an impulse. We looked at the effect of the nonlinear infection term in our two-dimensional impulsive system. We were able to solve for the linear system, and find conditions for stability that depend on the immune response rate and the impulse condition. We were also numerically able to show that including the nonlinear infection term may change stability (when it was unstable in the linear system, including the nonlinear infection term made the T-periodic solution stable). We thus analyzed two subcases. These subcases showed the effects of the nonlinear infection term when an immune response rate is either not included or is included via an impulse. Again we can show how the T-periodic solution is stabilized when the nonlinear term is included when it was unstable in the linear case. This seemed to lead to the conclusions that the nonlinear infection term does affect stability by creating a larger area of stability. This system was a two-dimensional system, and so more work needs to be done to see the effect of this term on higher dimensional systems. Another biological limitation to the two-dimensional model is that positivity of solutions does not preserve under certain cases. However, since we are comparing the linear to the nonlinear system, this limitation applies equally to both systems. In this case, the effect of the nonlinear infection term is not caused by this limitation. The two-dimensional system gives us an indication that excluding the nonlinear infection term might change the results of the entire system when including impulses.

The use of impulsive differential equations is potentially unlimited. There are

many real-world events that could be further analyzed by including an impulse. The analysis of such systems can become very difficult if the impulses are state-dependent, but the results found for fixed impulse effect can be of great insight. Impulsive differential equations are becoming a more popular way of modelling biological events, but a lot more work needs to be done on the subject.

6.2 Conclusion

The use of impulsive differential equations provides great insight into the behaviour of systems. We predict long-term behaviour for three different biological systems, and show how stability of T-periodic solutions change based on different factors for a two-dimensional impulsive system. The first biological system described induction-maintenance therapy, and was used to investigate the effects of imperfect adherence during the inductive phase. By solving for the endpoints of the impulsive system, we showed that induction therapy with partial adherence is tolerable, but the outcome depends on the drug cocktail. The second biological system described the interaction between T cells, HIV-1 and protease inhibitors. By computing the stability analysis of the system with fixed drug concentration levels, a region was found where free virus elimination is theoretically possible. These same results were numerically seen when varying the drug concentration levels within a given region. Numerical simulations also demonstrate the effects of crossing between regions. We also include a reduced two-dimensional HIV model used to view the effects of stability on T-periodic solutions. The two-dimensional model shows that the nonlinear infection term that is often omitted in disease modelling with ordinary differential equations can change stability of the T-periodic solutions. The third biological system investigated the effects of decreasing the mosquito survival time in a Rift Valley Fever–infected population. Stability was calculated for a one-season model, and the analysis of a multiple season model was conducted by including impulsive differential equations. Rift Val-

ley Fever poses a potential threat to North America that would require aggressive interventions in order to prevent a recurring seasonal outbreak. The analysis of each of the impulsive differential systems aids in solving real biological questions.

6.3 Future work

The use of impulsive differential equations can be extended to an extremely wide variety of biological settings. In particular, many disease models including treatment therapy are being modelled using impulsive differential equations.

6.3.1 Stability for systems with periodic drug regimens

Stability analysis and linearization in ordinary differential equations is widely used in mathematical biology to predict long-term behaviours. Since impulsive differential systems have periodic solutions, linearization does not necessarily imply results about stability. However, it is interesting to note that, for the system described in Section 3.2 (where the drug dynamics is the only equation that included an impulse), the behaviour of stability between regions for a fixed drug level is similar to the behaviour when the drug level varied within a given region. Future work would be to analyze the periodic solution of the system in Section 3.2 by looking at the variational equation (similar technique as in Chapter 4). In this case, the disease-free periodic orbits would be similar to the equilibrium points found in the article. The endemic periodic orbits would be more challenging; since the impulse only occurs for the drug equation, and this equation can be decoupled, we can easily solve for this. By plugging this solution into the other equations, a periodic solution could be found, and analysis using the variational equation may be possible.

6.3.2 Finite drug therapies

We analyzed the effects of imperfect adherence to triple-drug cocktails excluding protease inhibitors. Future work could investigate the effects of imperfect adherence to triple-drug cocktails involving protease inhibitors while on induction-maintenance therapy. This would change the dynamics between T cells, virus and drugs. The drug would now affect both the rate at which the virus enters the cell, and the number of infectious virions budding from an infected cell. The analysis could be done in a similar manner when considering the drug dynamics; the only difference would be the effects between impulses that would be seen in the ordinary differential equations. Furthermore, all previous mathematical models of adherence considered therapy without an endpoint. Since induction therapy only occurs for a finite time, we had to consider the viral load when induction therapy ends. Future work could be to apply these procedures to a variety of different drug therapies with finite endpoints, such as drug therapy for tuberculosis, chlamydia and gonorrhea.

6.3.3 HIV drug treatment

We analyzed the immunological behaviour of T cells, HIV-1 and protease inhibitors. In reality, most patients take triple-drug cocktails including protease inhibitors and reverse transcriptase inhibitors, fusion inhibitors and/or integrase inhibitors which would change the dynamics of the system. Future work would be to show the dynamics of patients on combination therapy. The analysis of such a system would be similar to that done in Section 3.2, but as mentioned in Section 6.3.2, the ordinary differential equations would include more nonlinear terms since we would include multiple ways to control the virus.

Another problem that arises in specific systems is the dual-layered system of impulses where we have major and minor impulses. For example, we could have an HIV patient taking a double-drug cocktail for 3 months, and then for one month

taking a triple-drug cocktail, and then the next 3 months the same double-drug cocktail as before and so on. In this case, we have minor impulses (time between changing cocktails) and we have major impulses (the increase which occurs from changing from a double to a triple-drug cocktail, or the decrease that occurs from changing from a triple to a double-drug cocktail). Future work could be to develop a general mathematical theory for dual-layered impulsive systems.

6.3.4 Rift Valley Fever

We analyzed the effect of decreasing the mosquito survival time using an impulsive differential system in order to eradicate Rift Valley Fever if it were to invade North America. Future work could be to examine the effects of discontinuous spraying on the mosquito population using another impulsive differential equation. As with West Nile virus and malaria, pesticides, adulticides, insecticides and larvicides are beneficial and could be modelled for Rift Valley Fever using impulses. Optimal length of spraying could also be analyzed.

We could also look at solving the impulsive differential system. We could look at a reduced system of the RVF model by grouping the mosquito population into only one equation. This would imply that all mosquitoes are infected, but it would allow us to solve the impulsive differential system in a similar way as in Chapter 4. With this reduction and solving the mosquito equation, this would turn our nonlinear model into an almost linear model, where the analysis may be simplified, and results for the stability of the impulsive differential system may be possible.

6.3.5 Multiple disease modelling and drug therapy

The possibility of having multiple infections at a given time is common, since the immune system is compromised. The immune system is at a greater disadvantage being infected with multiple diseases than with just one. Future work could be to

combine multiple diseases to see the effects of drug therapy, and whether the efficacy of the drug decreases when the immune system is compromised. Likely combination of diseases to consider would be the Human papilloma virus (HPV) and HIV, HIV and tuberculosis, and HIV and any hepatitis (A, B or C).

Appendix A

Human Immunodeficiency Virus

A.1 Immunology and Microbiology

Infection with HIV leads to an immune response similar to that of any other virus. The problem is that the infection will not prevent ongoing replication of the virus for various reasons. There are two main strains of HIV; most AIDS cases are caused by the more virulent HIV-1, whereas HIV-2 is endemic in West Africa, and is now spreading in India [12]. HIV-1 was spread to humans by chimpanzees *Pan troglodytes*, whereas HIV-2 infected humans from the sooty mangabey *Cercocebus atys* [12]. New strains of HIV are still being discovered. On August 2^{nd}, 2009, a research team of the University of Rouen, France announced there was a new strain of HIV discovered in one HIV positive patient living in Cameroon, Africa [13]. This new strain appears to be closely related to a form of simian virus recently discovered in wild gorillas [13].

During primary infection, HIV largely infects the immune $CD4^+$ T cells, which are necessary for an immune response. Cytotoxic T lymphocytes (CTLs) play an important role in the immune response to HIV during acute state of infection. Leviyang [59] introduced a model of CTL attack during the acute stage. Leviyang showed that early mutation events can have significant impact on HIV genealogies. Simonov *et al.*

[60] modelled the adaptive regulatory T cell dynamics in early HIV infection. They constructed a delay differential equation model to examine the possible existence of two distinct regulatory T cell populations and their respective effects in limiting viral load. They observed oscillatory and steady state behaviours, which give insight into the importance of downregulation of $CD4^+$ cells by normal regulatory T cells on viral load. Antibodies are formed when an HIV-negative person is infected, and are the main method of identifying HIV-positive patients. If tested during the primary stages, an individual may be misdiagnosed, since it takes approximately 3-4 weeks in order for antibodies to be produced [12]. An example where misdiagnosis causes the infection to spread was that of an HIV-negative individual receiving a transplant, and then being identified as HIV-positive. The donor was initially tested and shown HIV negative. It turned out the donor had died within 3-4 weeks of getting the infection, meaning the antibodies for HIV had not produced, resulting in a false negative [61].

The uninfected $CD4^+$ T cell count is approximately 1200 cells μl^{-1}, but after an initial infection it drops to approximately 800 cells μl^{-1}. Once an individual reaches 200 cells μl^{-1}, they are considered an AIDS patient [12]. Once you have AIDS, the period of clinical latency ends, and opportunistic infections begin to appear. A patient with AIDS lives, on average, for 1-2 years without treatment [12]. In very few cases, genetic variation in either virus or host result in slower disease progression. Genetic variation in HLA type of the host modifies the disease outcome: HLA-B57 and HLA-B27 are associated with better prognosis and HLA-B35 with more rapid disease progression [62]. Homozygosity of HLA also leads to a more rapid progression since T cell response to infection is less diverse [62]. There are people who are infected with HIV yet remain disease free and virus negative. Some people are resistant to the virus because they have a mutation in a cell-surface chemokine receptor that is used as a co-receptor for viral entry. Lacerda *et al.* [63] developed a mutation-selection model of T cell epitope evolution that allows HLA genotype of the host cell to influence the evolutionary process. With a Markov model, they identified amino acid positions that

appear to evolve under immune pressure in the presence of specific potential epitopes on host immune cells.

As mentioned above, HIV can enter a host via body fluids. HIV is an enveloped retrovirus that contains two copies of an RNA genome. These are reverse transcribed into DNA in the infected cell, and then integrated into the host chromosome [12]. The RNA transcripts produced from the integrated viral DNA serve both as mRNA to direct the synthesis of the viral proteins and later as the RNA genomes of new viral particles [12]. New virions escape from the cell by budding from the plasma membrane, each in a membrane envelope.

In order for the virus to enter the cell, specific receptors must bind. HIV enters a cell by binding two glycoproteins, gp120 and gp41, and by binding with a co-receptor [64]. The glycoprotein gp120 binds with high affinity to the cell-surface molecule $CD4^+$, which means gp120 binds to $CD4^+$ T cells, dendritic cells and macrophages. There are two chemokine co-receptors for HIV that allow the virus to enter the cell. The two chemokine receptors are CCR5 (expressed on dendritic cells, macrophages and $CD4^+$ T cells) and CXCR4 (expressed on activated T cells) [64]. After binding gp120 and its co-receptor, gp41 causes fusion of the viral envelope and the plasma membrane of the cell, allowing the viral genome and associated viral proteins to enter the cytoplasm [64]. Depending on when the infection occurs, different chemokine co-receptors are activated. During primary infection, CCR5 binds with the CC chemokines CCL3, CCL4 and CCL5 as a co-receptor [12]. These do not require high levels of $CD4^+$ on the cells they infect (this happens during sexual contact since it is the primary response). When infecting only T cells, CXCR4 binds to the chemokine CXCL12 co-receptor [12]. These require high levels of $CD4^+$ on the cells they infect.

There are two different ways HIV can infect an individual. The first way is by contact with mucosal epithelia. HIV can enter a host by coming into contact with epithelial cell lining in the vagina, penis, cervix and anus; each of these areas have several layers of epithelial cells [12]. When coming into contact, intraepithelial

dendritic cells initiate infection by binding HIV and transporting it to the lymphoid tissue, where it is transferred to $CD4^+$ T cells. HIV attaches to dendritic cells by the binding of viral gp120 to a dendritic cell-surface molecule DC-SIGN [12]. This mediates the internalization of HIV into a mildly acidic endosomal compartment, which protects the virus during the passage of dendritic cells to lymphoid tissue [12]. The second way HIV can enter a host is by the intestinal tracks such as the rectum and the endocervix which are covered by a single layer of epithelial cells. These epithelial cells express CCR5, and the binding of CCR5 to $CD4^+$ T cells occurs early in infection [12]. Later in infection, the viral phenotype switches and uses CXCR4 co-receptors, which creates a decline in the $CD4^+$ T cell count, and increases progression to AIDS [12].

Once the virus binds gp120 and gp41 and its co-receptors, the viral genome and the reverse transcriptase protein are integrated into the cell. The reverse transcriptase protein transcribes the viral RNA into a complementary DNA copy (cDNA) [12]. The viral cDNA (known as a provirus) is then integrated into the host cell genome by the viral integrase, which also enters the cell with the viral RNA. In activated $CD4^+$ T cells, virus replication is initiated by transcription of the provirus. HIV can establish a latent infection in which the provirus remains inactive [12]. This occurs in memory T cells and in dormant macrophages.

The HIV genome consists of nine genes edged by long terminal repeat sequences (LTR), which are required for the integration of the provirus into host cell DNA, and contain binding sites for gene regulatory proteins that control the expression of the viral genes [65]. HIV has three major genes: gag, pol and env [65]. It also has six other smaller genes encoding proteins that affect viral replication and infectivity [65]. Gag gene encodes the structural proteins of the viral core, pol encodes the enzymes involved in viral replication and integration, and env encodes the viral envelope glycoprotein. The gag and pol mRNAs are translated to give polyproteins-long peptide chains that are then cleaved by the viral protease into individual functional proteins.

The product of the env gene, gp160, has to be cleaved by a host cell protease into gp120 and gp41, which are then assembled as trimers into the viral envelope [65].

The main reservoir of HIV is in the lymphoid tissue in which infected $CD4^+$ T cells, monocytes, macrophages and dendritic cells are found [12]. Infected memory $CD4^+$ T cells have a very long half life of about 44 months [12]. HIV generates an adaptive immune response that contains the virus, but will very rarely eliminate it. Infectious virus is low in the peripheral blood in the primary stages of an infected individual, during which the virus is replicated persistently in lymphoid tissues. During this period, $CD4^+$ T cell counts gradually decline, although antibodies and CD8 cytotoxic T cells directed against the virus remain at high levels [12]. The $CD4^+$ T cells in an infected HIV patient decline in three ways. First, there is evidence for direct killing of infected cells; second, there is increased susceptibility to the induction of apoptosis in infected cells; third, there is killing of infected $CD4^+$ T cells by CD8 cytotoxic lymphocytes that recognize viral peptides [12]. Eventually, the levels of antibodies and cytotoxic T lymphocytes also decline, and there is a progressive increase in infectious HIV in the blood. When the $CD4^+$ T cell count drops below 200 cells μl^{-1}, the chance of infection by opportunistic microbes increases [66]. This causes no activation of the TH1 or TH2 responses, and eventually leads to the individual's death.

HIV has a rapid replication rate of about 10^9 to 10^{10} new virions every day coupled with a mutation rate of approximately 3×10^{-5} per nucleotide base cycle of replication, which leads to the generation of many variants of HIV in a single infected patient in the course of a day [12]. Since HIV is highly variable, it rapidly develops resistance to antiretroviral drugs. New antiretroviral drugs are continuously being tested, all of which hope increase the number of healthy T cells, and help increase the number of years HIV/AIDS patients can live.

A.2 Drug Therapy

Many mathematical models have been developed to describe drug resistance [68]-[73]. Some more recent models are Mohanty and Dixit [74] who presented a model showing the dynamics between a fusion inhibitor and target cells, Bhunu *et al.* [75] who presented a two-strain nonlinear HIV model with antiretroviral treatment, and Rosenbloom *et al.* [76] who presented a model that incorporates drug properties, fitness, differences between susceptible and resistant strains, mutation and adherence in order to explain the differences between adherence and likelihood of drug resistance. However, such models have focused on the emergence of drug resistance during continuous therapy [76]-[80].

Since the mutation rate of HIV is so fast, some reverse transcriptase inhibitors require only one or two mutations in order for HIV to build resistance towards the drug, whereas protease inhibitors such as ritonavir need 7–9 mutations, meaning these will take much longer for the virus to be resistant towards it [67]. Also, the reverse transciptase inhibitor zidovudine (AZT) — the first drug created — needs only 3–4 point mutations in the viral genome to become resistant, which only takes a few months [67].

A more recent tool to model drug dynamics is that of impulsive differential equations. Smith and Wahl [21] used impulsive differential equations to model the interaction between cell/virus dynamics and reverse transcriptase inhibitors, integrase inhibitors and fusion inhibitors. Smith and Wahl [22] also used impulsive differential equations to model drug resistance by considering immunological behaviour for HIV dynamics, including the effects of reverse transcriptase inhibitors and other drugs that prevent cellular infection. Smith [16] answered the question of determining how many doses may be skipped before HIV treatment response is adversely affected by the emergence of drug-resistance using impulsive differential equations. Krakovska and Wahl [35] developed a model that predicts optimal treatment regimens, and used

this model, coupled with impulsive differential equations, to investigate the effects of adherence. Lou and Smith? [37] developed a mathematical model that describes the binding of the virus to T cells in the presence of the fusion inhibitor enfuvirtide using impulsive differential equations. Lou et al. [38] used impulsive differential equations to develop a rigorous approach to analyze the threshold behaviours of nonlinear virus dynamics with impulsive drug effects and to examine the feasibility of virus clearance.

Drug treatment decreases the half life of the virus. Since $CD4^+$ memory T cells carry integrated provirus and are very long-lasting reservoirs of the infection, these cells are resistant to HIV drug therapy. This is one of the many reasons the immune system cannot completely eliminate HIV. The infection of HIV from mother to child is easily preventable by simply taking the drug zidovudine or nevirapine [12]. The nevirapine prophylactic regimen is particularly easy to use, with a single dose given to the woman at the onset of labour, and one dose of syrup administered to the baby within 72 hours of delivery, reducing transmission by around 40% [81].

The use of antiretroviral drugs among uninfected individuals has also been analyzed. Cremin *et al.* [82] examined whether antiretroviral drugs can reduce HIV acquisition among uninfected individuals (as pre-exposure prophylaxis) and reduce onward transmission among infected individuals. They developed a mathematical model of a hyperendemic setting with relatively low levels of condom use. They estimated the prevention impact and cost of various pre-exposure prophylaxis interventions. They showed that it is more efficient to provide antiretroviral therapy to more infected individuals earlier rather than providing pre-exposure prophylaxis to uninfected individuals. They showed that antiretrovial therapy alone cannot reduce HIV incidence to very low levels and pre-exposure prophylaxis can be used cost-effectively in addition to earlier antiretroviral therapy.

A.3 Increased Incidence of HIV

One of the problems with antiretroviral therapy is that it inflicts major side effects, which deter patients from taking their drugs. The use of antiretroviral drugs reduces the viral load in a patient, which in turn reduces the chance of spreading the disease. Imperfect adherence creates an increase in drug resistance. Studies have shown that patients must have 95% adherence to drug therapy in order to prevent biological resistance [15]. They also show that 40–60% of patients are less than 90% adherent to their drugs, and adherence decreases over time [15]. In order to determine regimens for partial adherence, a number of mathematical models have attempted to quantify how drug concentration levels in the body of an HIV patient affect viral replication [16, 35], [83]-[88]. Wahl and Nowak [83] considered two types of treatment failure: failure to eliminate the wild-type virus, and the emergence of drug-resistant virus. They determined the conditions under which resistance dominates as a result of imperfect adherence. Phillips *et al.* [84] gained insight into the consequences for development of resistance as a result of different drug-use patterns. Tchetgen *et al.* [85] extended previously developed models of antiretroviral therapy to include screening for adherence, and showed that new HIV infections in the population would likely increase unless screening accuracy is extremely high.

Research on HIV is continuously being funded in order to eliminate the disease, but may be controversial. In January 2008, a paper was published saying that if you were a seropositive individual not suffering from any other STDs and following a drug therapy with perfect adherence, then you would not and could not transmit HIV [89]. It fails to mention that certain antiretroviral drugs are unable to enter the male and female reproductive systems. Since the disease is spread by sexual intercourse, this causes major problems. The use of antiretroviral drugs will lower the number of virus particles in the peripheral blood and in the genital tract, but will not eliminate HIV [90, 91]. This paper caused a lot of controversy because uninformed

HIV-positive individuals may believe they can practice unsafe sex with no chance of infecting others [92]. Boily *et al.* [93] investigated the various effects of antiretroviral therapy on risk behaviours and sexually transmitted infections. They developed a mathematical model of bacterial sexually transmitted diseases and treated/untreated HIV/AIDS infection for an open homosexual population. They assumed that susceptible and healthy HIV-positive individuals do not increase risk behaviour as a result of antiretroviral therapy over time, but individuals with AIDS who are successfully treated can resume activity. Over 10 years, they showed that 0-55% of new bacterial sexually transmitted infections could be attributed to the widescale use of antiretroviral therapy as a result of more modest increases (0-25%) in risky sex occurring at the population level rather than at the individual level.

Another major factor limiting the prevention dividend of HIV treatment is that more than 60% of people living with HIV are unaware of their HIV status [6]. This limits access to treatment and care services and hampers prevention efforts. According to the US CDC (Centres for Disease Control), there are approximately 25% of people in the US who are HIV positive, but unaware of their status, since there are few side effects once initially infected with HIV [94]. Smith? and Aggarwala [95] compared the number of infected HIV individuals in the United States with the number of HIV-positive individuals their mathematical model predicts, and showed that the number of people living with HIV, but not AIDS, in the United States is more than four times larger than the current estimate.

A.4 Worldwide Issues

Women's rights have always been a worldwide issue. Certain progress has been made, but these issues still continue today. The proportion of women living with HIV has remained stable at 50% globally, although women are more affected in sub-Saharan Africa (59% of all people living in Sub-saharan Africa with HIV) and the Caribbean

(53%) [6, 96]. There are ten million people infected with HIV from the ages 15-34, where 78% are women and girls [96]. Marriage is actually a risk factor for HIV [97]. A study in 2004 compared several underlying HIV risk factors, and explored the counterintuitive finding that married adolescent girls in urban centers in Kenya and Zambia have higher rates of HIV infection than do sexually active unmarried girls [97]. Some countries allow men to be polygamous. In Senegal, for example, nearly 47% of marriages are multiple [98]. Also, the spread of HIV in truck drivers across Africa is high due to intercourse with sex workers [99, 100]. It also increases the spread of sexually transmitted diseases such as chlamydia and gonorrhea, which are known to severely increase the chance of transmission of HIV to a seronegative individual [101, 102, 103].

Rape is also a factor that is included in the increased numbers of HIV. Men, women and children all over the world can become victims of rape. Power, maturity and lack of knowledge are but a few reasons rape occurs. Lack of knowledge can be seen in some cases in South Africa where men rape female children with the mistaken belief that sex with a virgin will cure the HIV-infected person [104]. Sexual violence against children, including the raping of infants, has increased 400% over the past decade [11]. A girl born in South Africa has a greater chance of being raped in her lifetime than learning how to read [11]. The University of South Africa reports that 1 million women and children are raped in South Africa each year [105]. It may take decades to change a society's beliefs, but this is certainly required to prevent women and children from continuously being infected.

Discrimination occurs in many communities, the gay community being one of the most affected. HIV in the Western world started as a gay disease, or as the media called it, "the gay plague" [106, 107]. Male-to-female heterosexual transmission of HIV is two to eight times more efficient compared to female-to-male, with a male-to-female per contact infectivity estimated to be 0.0009, whereas receptive anal intercourse results in an estimated per-contact infectivity of 0.0082 [108]. The

reason for the increased rate of infection from penile-anal sex compared to penile-vaginal sex may be due to the differences in the architecture of the rectum/colon and vagina/cervix. The rectum/colon is lined with simple columnar epithelial cells that are involved in transportation and adsorption of molecules, secretion, and protection [108]. Since the easiest way for the virus to enter a body is by the anus, gay men are at higher risk for contacting HIV. Herek and Glunt [106] explain how, in the early years of infection, the stigma of only gay people having HIV increased the spread of the disease, since heterosexuals were not educated enough to know that HIV could be spread by vaginal-penile intercourse. In 2003, Parker and Aggleton [109] describe the stigma and issues that arise from the gay community, and how these problems are still in the society years after the initial infection of HIV. Unless these issues can be resolved, it will always be difficult to not only accept the gay community, but also to eradicate HIV since, without knowledge of any disease, the general population may think they are not prone to catching HIV. Some ways to prevent the spread of HIV through the gay community have been with bath houses and the use of condoms, which are houses geared towards men having sex with men, and trying focusing on safe sex.

Another major cause of the spread of HIV is the lack of education. The World Health Organization (WHO) states that levels of knowledge of safe sex and HIV remain low in many countries, even in countries with high incidence and growth of HIV [110]. In 24 sub-Saharan countries (including Cameroon, Côte d'Ivoire, Kenya, Nigeria, Senegal and Uganda), two-thirds or more of young women (aged 15–24 years) lacked comprehensive knowledge of HIV transmission [110]. There have been various responses to the pandemic, led by Uganda, which has had the greatest success in combating the disease, in part by a formalized information, education and communication strategy [111, 112]. Joshi *et al.* [113] formulated a mathematical model to show the positive effects of information and education campaigns on the HIV epidemic in Uganda. According to a major survey carried out in the Philippines in 2003 by the

WHO, more than 90% of respondents still believed that HIV could be transmitted by sharing a meal with an HIV-positive person [110]. Kassa and Ouhinou [114] constructed a mathematical model for human disease epidemics that takes into account the human learning behaviour and self-protective measures. Their model assumed that people start reacting against contracting a disease with self-protective measures whenever they are informed about the disease and when the burden of the disease is in a recognizable stage. They showed that increasing the average effectiveness of self-protective measures is more important than increasing the proportion of individuals in a population into which awareness is created in order to decrease the prevalence of a disease. The lack of education causes societies to grow without prior knowledge of important factors, and could have major impacts on the population as a whole. For example in 2006, the South African president, was put on trial for raping a young woman. When the president was told the woman had HIV, he reported that it didn't matter since he had showered after intercourse [115]. Many of these issues could be avoided by sufficient education about the disease, but it is sometimes almost impossible to transmit this information to a society with rooted beliefs. Another way of contracting HIV is by oral sex, which many people believe is not possible. It may be a low risk factor, but HIV can spread by oral sex with a population-attributable risk percentage of 0.1% [116]. It is important for individuals all over the world to understand the ways HIV can spread, and understand the consequences involved in becoming infected. As many as one in three HIV-positive people continue unprotected sexual practices after learning that they are HIV infected [117]. It was also proven that the intervention to reduce risk of HIV transmission (educating people on HIV) resulted in significantly less unprotected intercourse and greater condom use at follow-up [118]. Transmission-risk behaviours with non-HIV-positive sexual partners and estimated HIV transmission rates over a one-year horizon were also significantly lower for the behavioural risk-reduction intervention group [117]. Mukandavir and Garira [119] created a model showing the effects of education campaigns and the role

of sex workers on the spread of HIV/AIDS among heterosexuals. Their model considered the movement of individuals from high to low sexual activity groups as a result of public health education campaigns. They showed that sex workers enlarges the epidemic threshold, and that public health educational campaigns reduces the basic reproductive number.

A.5 New and Ongoing Strategies for Prevention

New HIV prevention strategies are being developed. A new HIV prevention strategy is vaginal microbicides, which is a cream or gel applied inside the vagina that prevents the spread of HIV and prevents pregnancy. A study was done in South Africa showing that, if developed, 82% of men preferred a vaginal microbicide to a condom [120]. The downside is that the microbicides do not have as high an efficacy as using a condom. A condom is 87% effective for the prevention of HIV [121], so if a less effective microbicide is introduced in a country, it may decrease the use of condoms, which could in turn increase the spread of HIV. An option would be to use both the condom and the microbicide in order to achieve the best prevention results. Smith *et al.* [122] presented a mathematical model to view the effects of introducing vaginal microbicides to female sex workers, and to see which factor, microbicide efficacy or microbicide use, is more important to maximize in order to reduce the risk of female sex workers acquiring HIV. Risk equations were developed and Monte Carlo simulations were performed to show that microbicide usage and efficacy are both important factors in reducing the risk of acquiring HIV, but that usage has a higher impact.

Another strategy for reducing the spread of HIV targets men with male circumcision. Clinical trials in Kenya, South Africa and Uganda indicate that voluntary medical male circumcision reduces the risk of female-to-male sexual transmission by about 60% [6, 123, 124]. Verguet [125] presented a mathematical model developed

with epidemiological and cost data from nine provinces of South Africa. Verguet determined the outcomes of female to male HIV transmission with a male circumcision intervention, and showed that an efficient intervention would reduce the infection outcome by 20%, whereas a 50%-efficient intervention would reduce 6% in infection outcome in a year.

Induction therapy is an HIV/AIDS treatment regime that hopes to benefit patients by decreasing drug resistance and reducing the overall number of drugs that must be taken. In order to minimize drug resistance, induction-maintenance (IM) therapy strategies begin with a period of intensified antiretroviral therapy (induction phase), followed by a simplified, long-term regimen (maintenance phase) [126, 127, 128, 18]. Previous work with induction therapy failed due to uncalculated latently infected cells and imperfect adherence [127, 18]. Havlir *et al.* [127] investigated whether a less-intensive maintenance regimen could sustain viral suppression after an initial response to combination therapy with indinavir, zidovudine and lamivudine. HIV-infected subjects with fewer than 200 copies of HIV RNA per milliliter of plasma after 16, 20 and 24 weeks were assigned to either continue triple-drug therapy, indinavir alone, or a combination of zidovudine and lamivudine. They found that 23% of those on either mono or dual therapy had a loss of viral suppression (at least 200 copies of HIV RNA per milliliter on two consecutive measurements during maintenance therapy), whereas only 4% had loss of viral suppression while maintaining triple-drug therapy. Descamps *et al.* compared maintenance therapy with the same triple-drug therapy, and looked at maintenance therapy with zidovudine-lamivudine and zidovudine-indinavir therapy. They identified gene mutations during maintenance therapy, but identified that early and late virologic failure appeared to be related more to problems of adherence and antiretroviral potency, respectively, than to selection of resistant mutant viruses. Subsequently, Curlin *et al.* [19] showed that a longer induction phase decreases the probability that viruses resistant to maintenance therapy will emerge. Their studies showed that the probability of success (maintain-

ing a suppressed, circulating, free-virus population for a period of at least 3 years after the end of induction therapy) varied with the length and time of the induction phase [19]. They showed that induction therapy would have to last at least 180 days for cocktails containing two RTI-like drugs and a PI-like drug [19, 20].

Vaccination has proven effective in reducing the spread of diseases such as Hepatitis A, Hepatitis B, measles, etc. A vaccine for HIV has not yet been created. Vaccination against HIV is an attractive solution, but poses many difficulties [129]. The main problem is the nature of the infection itself. HIV is a virus that proliferates extremely rapidly (half life of two days) and causes sustained infection in the face of strong cytotoxic T cell and antibody responses [130]. Since mutation occurs in each individual differently, recognition of the virus by antibodies and cytotoxic T lymphocytes is more difficult (or even impossible). Furthermore, the provirus that is invisible to the immune system might prevent the T and B cells from clearing the virus even if a vaccine is present [130]. Also, the main cause of HIV is still unknown, so creating a vaccine that increases the level of the cytotoxic T lymphocytes for example may not be enough. There are different kinds of vaccines that can be created. Creating a live, attenuated vaccine might cause more harm than good, and causes concern over the safety of pursuing this approach for HIV [131]. Another approach which is currently being used is a DNA vaccine [131]. This vaccine is not as strong as a protein vaccine. These new vaccines elicit T cells capable of recognizing and killing virus-infected cells [131]. Another vaccine that was tested in 2007 used carriers, adjuvants and novel carbohydrate antigen constructs in order to overcome weak immunological responses to carbohydrate-rich surface antigens [132]. The most common target to creating a vaccine for HIV/AIDS is by comparing it with the original source: chimpanzees. Chimps carry the Simian Immunodeficiency Virus (SIV) but are not negatively affected by the virus. The env genes of HIV-1 and SIV encode proteins bearing a high degree of structural similarity, and sharing an identical suite of essential functions [133]. The env complexes formed by these proteins are present on the surface of virus-producing

cells and virions, where they are the primary targets of the host neutralizing antibody response [133]. Other studies have triggered a protein contained in the virus. A protein such as tat does not mutate, but has been proven essential for the integration of the virus in a cell [134]. Their work focuses on triggering a part of the protein genome that will hopefully inhibit the effect of integration of the virus, and thus stop the virus from entering an immune cell.

Since a vaccine has not yet been developed, many studies have shown the impact of introducing an HIV vaccine. Dorigatti and Pugliese [135] analyzed a model to find exact conditions under which vaccination may lead to a shift in competitive balance in favour of a virus strain. They showed under certain conditions that there always exists a range of vaccination rates under which a coexistence equilibrium exists. Lou *et al.* [136] developed a mathematical model using a sex-role-preference framework to predict HIV infection in the men who have sex with men population, and evaluated different intervention strategies such as antiretroviral drugs and vaccination. They showed that the effects of a potential vaccine are worse than that of antiretroviral therapy, even if the vaccine efficacy is as high as 70%. Smith? and Schwartz [36] developed a mathematical model to describe a post-infection HIV vaccination program to regularly boost cytotoxic T-lymphocytes. They showed that, for an asymptotically stable periodic orbit, the vaccination frequency can be chosen so that the average number of infected $CD4^+$ T cells can be made arbitrarily low. Konrad *et al.* [137] presented a model describing the interaction between cytotoxic T cells, wild-type virus and resistant virus. They included mutation, and included the cytotoxic T cells as an impulse. The impact of imperfect adherence to the vaccination regimen was addressed, and the number of vaccinations that can be missed was calculated. Gumel *et al.* [138] developed a staged-progression HIV model to investigate the potential impact of an imperfect vaccine. They calculated the basic reproductive number, and showed that an imperfect vaccine can eliminate HIV in a given community if it can reduce the reproduction number to a value less than unity. Smith and Blower [139]

showed that a disease-modifying HIV vaccine that provides only a low degree of protection against infection and/or generate high fitness ratio will have a high probability of making the infection worse.

In very few cases, genetic variation in either virus or host show slower disease progression. Genetic variation in HLA type of the host modifies the disease outcome [140]. Studies show that individuals resistant to HIV secrete high levels of chemokines CCL3, CCL4 and CCL5 in response to the inoculation with HIV [62]. This blocks infection due to the competition of the chemokine co-receptors binding and the virus for the cell-surface receptor CCR5. These individuals are usually homozygous for a non-functional variant of CCR5 caused by a 32-base-pair deletion [62]. This may help in finding a cure for HIV, and finding ways to stop infection through sexual transmission. This genetic variation may also help to slow down the rate of progression of the virus.

Even though HIV kills close to two million people worldwide every year, there has been a lot of progress in controlling the spread of the disease. The World Health Organization (WHO) estimates that half the proportion of people living in poor countries will suffer from hunger by 2015 [8]. The percentage of underweight children is estimated to have declined from 25% in 1990 to 16% in 2010 [8]. Malnutrition is a major factor in disease death, meaning decreases in the number of people who suffer from hunger will help control the spread of HIV. Health, HIV and human rights are inextricably linked [107]. Also, WHO predicts that by 2015 the proportion of people without sustainable access to safe drinking water and basic sanitation will be halved [8]. Globally, the percentage of world's population with access to safe drinking-water increased from 77% to 87% [8]. These improvements have reduced the annual death rates in children by 35% from 1990 [8].

Behaviour change is also averting new HIV infections, especially among young people, sex workers and their clients, people who inject drugs, men who have sex with men and transgender people [6, 141]. Access to HIV prevention services has

empowered individuals and communities to act in earnest against the disease. In countries with generalized epidemics, a combination of behaviour changes, including reductions in numbers of sexual partners, increases in condom use, and delayed age of first sex, have reduced new infections (incidence) in several countries [6, 141]. Globally, contraceptive use has been on the rise, annually increasing 0.2% since 2000 [8]. In Cambodia, condom use among sex workers and their clients increased from about 40% in 1997 to current levels of over 90%, and there are approximately 48 thousand fewer new HIV infections annually [6]. In Dhaka, Bangladesh, harm-reduction programmes have been credited with slowing the spread of HIV among young people who inject drugs [6, 141]. People who inject drugs also need equitable access to non-discriminatory health and social services. Marshall *et al.* [142] developed an agent-based model to examine how combinations of interventions among injecting and non-injecting drug users may reduce and potentially eliminate HIV transmission among drug-using populations. The model included three populations: injecting and non-injecting drug users, and non-drug users who interact with each other and within risk networks and engage in sexual contact. They included HIV prevention interventions such as syringe exchange programs, substance-abuse treatment and HIV testing. Initial antiretroviral therapy is included in a stochastic manner. Their model closely approximated HIV trajectories in injecting and non-injecting drug users observed in New York city between 1992 and 2002 showing that a combination of interventions dramatically reduces HIV prevalence.

While some countries have made impressive gains in achieving health-related targets, others are falling behind [8]. Improvement has been made in the quality of life of HIV-positive lives and reduction of AIDS-related deaths by introducing antiretroviral treatment. Behaviour change programmes are crucial in order to bring down new HIV infections. Smith? *et al.* [143] developed a mathematical model that predicts eradication or persistence of HIV/AIDS on a world scale. They showed that even if HIV/AIDS can be eradicated in a specific region (continent, country etc)

independently, travel/immigration of susceptibles (not infectives) could still sustain the epidemic. A lot more work needs to be done in order to fully control the spread of HIV.

Appendix B

Additional information; Section 3.1

Simulation details and extra comments for the manuscript in Section 3.1; Miron and Smith? [3]

Numerical Simulations: The software used to plot the figures in the manuscript presented in Section 3.1 [3] was Matlab.

Figure 1 is a plot of the curve

$$s(t) = \frac{R(t)}{R(t) + IC_{50}},$$

the inhibition of viral replication (page 3 of manuscript). The values used to plot this curve are presented in Figure 4 and Table 1.

Figures 2 and 3 are plots of an exponentially decaying function including impulses. Between impulses, we plot an exponential decaying function (solutions to the dynamics of the drug on page 5 of the manuscript). At an impulse, we increase the drug by a factor of R^i, and then use this as the new initial condition. We run, with these new initial conditions, the exponential decaying function until the next impulse, and so on. We used $R^i = 1.5$, $d_R = 1$ and $\tau = 0.5$. The differences between the figures is that for, Figure 2b, we allow for a longer period of time where no impulses occur. Therefore, after taking n drugs, we plot an exponentially decaying function for 7 missed doses. And then we again reset the initial conditions by including an increase

in the drug and continue in the same way as described above. Figure 3 includes a line that indicates the average drug concentration.

The parameters and initial conditions used to plot Figures 4–10 are presented in Figure 4 and Table 1. We used *ode*45 to solve the system of ordinary differential equations between the three regions. Again, we reset the initial conditions when an impulse occurs, meaning we add R^i to the solution of the drug and do not change any other solution (since the impulse only affects the drug). We then run the ordinary differential equations again.

Figure 11 is a plot of the curve described by Equation 1 (the number of missable doses, h_1) on page 8 of the manuscript. The parameter values are presented in Table 1.

Sensitivity Analysis: Since parameters vary from patient to patient, we explore a more in-depth sensitivity analysis of the effect each parameter has on the number of missable doses using Latin hypercube sampling (LHS). We also assess the variability in the number of missable doses to key parameters using partial rank correlation coefficients (PRCCs).

For each parameter in our model (there are n parameters), we assigned a uniform probability distribution. Given the lack of available data to estimate parameters, this is a reasonable choice [144]. We then generated a Latin hypercube sample of size $\mathcal{N}$ for each parameter, which results in a Latin hypercube matrix (of size $N \times n$) representation for parameter space. A model output (in our case, the number of missable doses, h_1) is generated for each row of the Latin hypercube matrix; a new column is appended to the Latin hypercube matrix, resulting in a new matrix of size $N \times (n + 1)$. We then checked scatterplots of the model output against each parameter to ensure that we obtained monotonic relationships. This is a necessary step for PRCCs. To obtain PRCCs, each column is ranked; the lowest value gets a rank of 1, next lowest a rank of 2, and so on, to reduce the effect of nonlinear data. Repeated values are assigned an average rank. PRCCs measure the linear

relationship between model output and one input parameter after the linear effects of other parameters have been removed. Thus, to calculate PRCCs, we form two regression models: one between output and the $n-1$ parameters, the other between the parameter of interest and the $n-1$ parameters. The PRCC is then the correlation coefficient of the residuals of these two models.

Figure B.1 shows the partial rank correlation coefficient sensitivity analysis for 1000 runs. The range of parameters used are given in Table B.1 below. All relevant parameters are varied against h_1. The sample values, units and references can be found in Table 1 in the manuscript [3].

Table B.1. Range of parameters.

Parameter/state variable	Range
R_i	1 – 15
d_R	0.5 – 1.5
τ	0.1 – 1
ϵ	0.01 – 0.5
R_2	0.5 – 1.5

Clearly h_1 is most sensitive to the time between doses, τ, the drug clearance rate, d_R, and the dosage, R^i (Figure B.1). The effect of each parameter on h_1 can also be seen in Figures B.2–B.6 for τ, d_R, R_i, R_2 and ϵ, respectively.

Figures B.2–B.6 show that increasing the time between doses or increasing the dosage allows for a higher number of missable doses during a drug holiday (Figures B.2 and B.4). We also see that increasing the drug clearance rate decreases the number of missable doses that are allowed during a drug holiday (Figure B.3). The LHS of the remaining two parameters are approximately uniformly scattered (Figures B.5 and B.6).

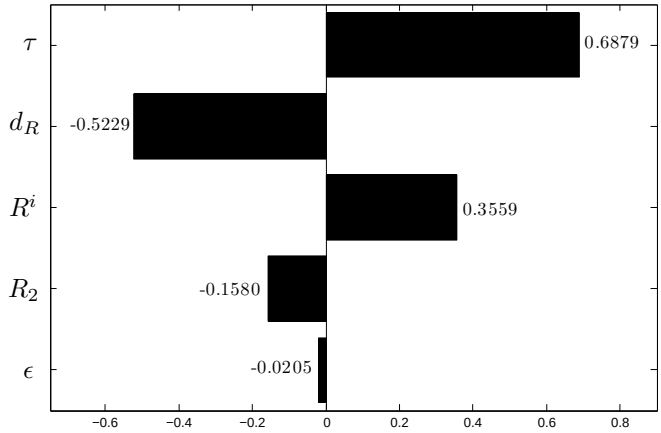

Figure B.1: Partial rank correlation coefficients for the number of missable doses, h_1, for all parameters.

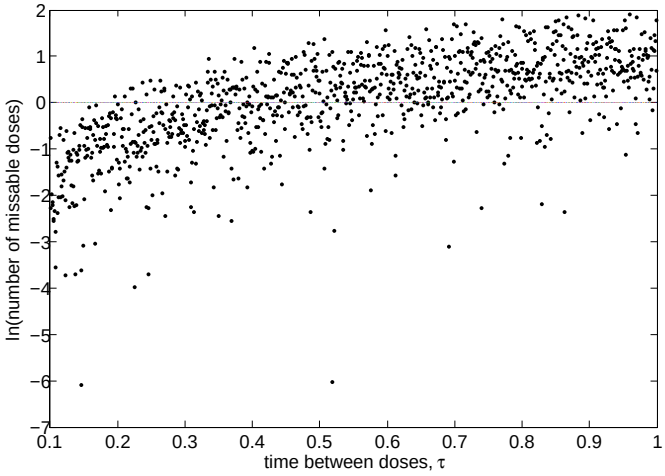

Figure B.2: The effect of the time between doses on h_1.

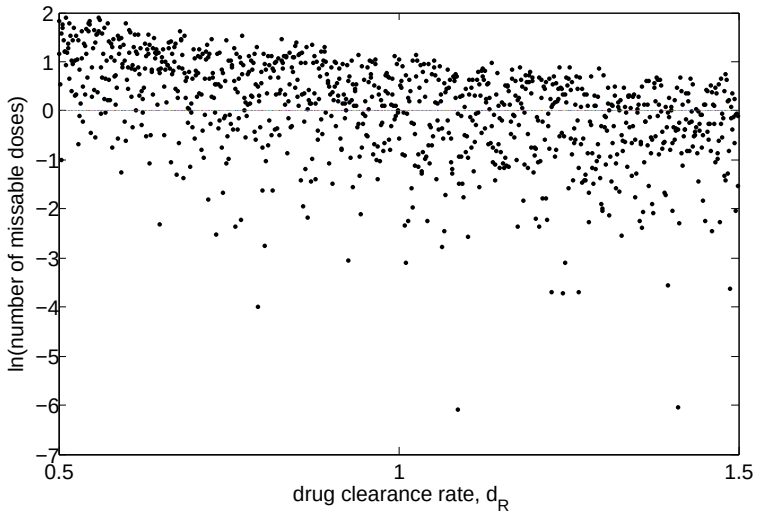

Figure B.3: The effect of the drug clearance rate on h_1.

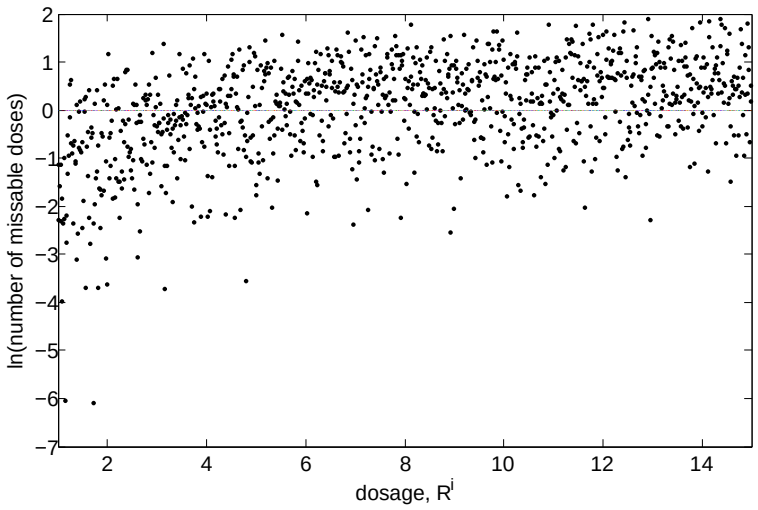

Figure B.4: The effect of the dosage on h_1.

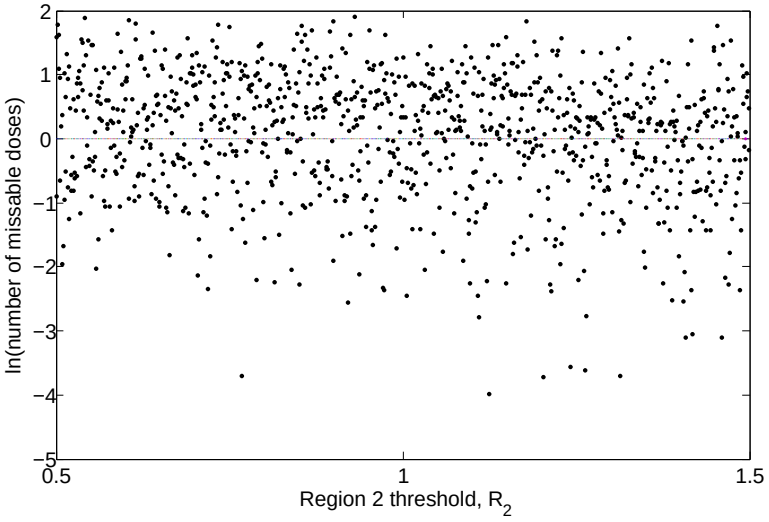

Figure B.5: The effect of the Region 2 threshold on h_1.

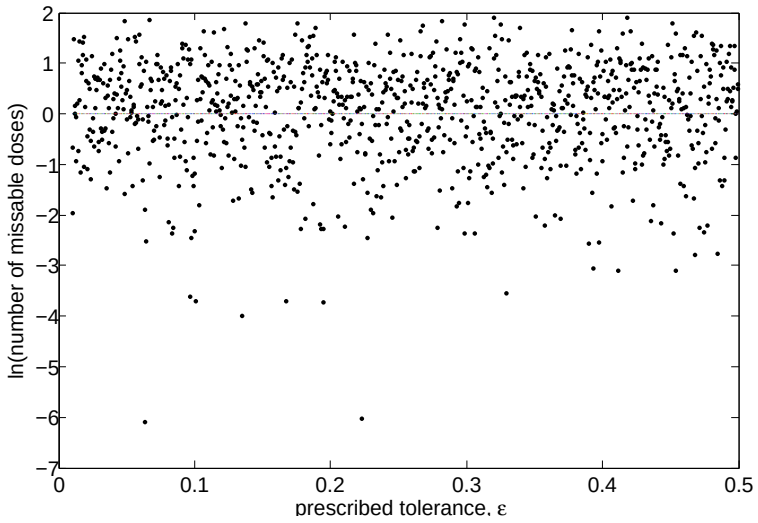

Figure B.6: The effect of the prescribed tolerance on h_1.

Errata:

1. The inequality before equation (2) is reversed (page 9). It should be

$$e^{-n_2 d_r \tau} \quad < \quad -\frac{\epsilon_2(1-e^{-d_r\tau})}{R_2(1-e^{-d_r\tau}) - R^i e^{-d_r\tau}}.$$

2. On page 13, paragraph 4, line 5, the brackets should read (35.7% of HIV RNA increase).

Appendix C

Region 1: Low drug levels; Miron and Smith? [4]

The following Appendix shows more details of the work presented in Region 1 of the manuscript in Chapter 3.2. We include many steps that are omitted in the manuscript. This Appendix only includes extra details on finding the mathematical results, thus it is only used to complete the manuscript. The Appendix does not include all of the manuscript.

The subregion model for Region 1 is given by

$$\begin{aligned}
\frac{dV_I}{dt} &= n_I\omega T_I - d_V V_I - r_I T_S V_I \\
\frac{dV_Y}{dt} &= n_I\omega T_Y - d_V V_Y - r_Y T_S V_Y \\
\frac{dV_N}{dt} &= n_I(1-\omega)(T_I + T_Y) - d_V V_N \\
\frac{dT_S}{dt} &= \lambda - r_I T_S V_I - r_Y T_S V_Y - d_S T_S \\
\frac{dT_I}{dt} &= r_I T_S V_I - d_I T_I \\
\frac{dT_Y}{dt} &= r_Y T_S V_Y - d_I T_Y.
\end{aligned} \tag{C.0.1}$$

C.1 Disease-free equilibrium

The disease-free equilibrium shown in the article is computed by setting the right hand side of the equations (C.0.1) equal to zero.

C.1.1 Basic reproductive number

In order to compute the basic reproductive number, we compute the FV^{-1} matrix, and find its eigenvalues. We have that

$$F = \begin{pmatrix} 0 & 0 & 0 & 0 \\ 0 & 0 & 0 & 0 \\ r_I\overline{T}_S & 0 & 0 & 0 \\ 0 & r_Y\overline{T}_S & 0 & 0 \end{pmatrix}$$

$$V = \begin{pmatrix} d_V + r_I\overline{T}_S & 0 & -n_I\omega & 0 \\ 0 & d_V + r_Y\overline{T}_S & 0 & -n_I\omega \\ 0 & 0 & d_I & 0 \\ 0 & 0 & 0 & d_I \end{pmatrix},$$

and that

$$V^{-1} = \begin{pmatrix} \frac{1}{d_V + r_I\overline{T}_S} & 0 & \frac{n_I\omega}{d_I(d_V + r_I\overline{T}_S)} & 0 \\ 0 & \frac{1}{d_V + r_Y\overline{T}_S} & 0 & \frac{n_I\omega}{d_I(d_V + r_Y\overline{T}_S)} \\ 0 & 0 & \frac{1}{d_I} & 0 \\ 0 & 0 & 0 & \frac{1}{d_I} \end{pmatrix}.$$

We have that F is a non-negative matrix, and we need to show that V is a non-singular M-matrix. We have, by definition (see [154]); if A is a real, square matrix with non-positive off-diagonal elements, each of the following is a necessary and sufficient condition for A to be an M-matrix:

a) Each principle minor of A is positive.

b) A is nonsingular, and $A^{-1} \geqq 0$.

c) Each real characteristic root of A is positive.

d) There is a row vector x with positive entries such that $xA > 0$.

We will now prove that V is an M-matrix.

Proof: We have that V is a real, square matrix with non-positive off-diagonal elements. We also have that

a) Since V is a square matrix, the principle minors of V are obtained by deleting the n-k rows and the n-k columns with the same numbers. We have the following principle minors:

$$D_1 = d_V + r_I \overline{T}_S > 0,$$

$$D_2 = \det \begin{vmatrix} d_V + r_I \overline{T}_S & 0 \\ 0 & d_V + r_Y \overline{T}_S \end{vmatrix} > 0$$

$$D_3 = \det \begin{vmatrix} d_V + r_I \overline{T}_S & 0 & -n_I \omega \\ 0 & d_V + r_Y \overline{T}_S & 0 \\ 0 & 0 & d_I \end{vmatrix} > 0$$

$$D_4 = \det \begin{vmatrix} d_V + r_I \overline{T}_S & 0 & -n_I \omega & 0 \\ 0 & d_V + r_Y \overline{T}_S & 0 & -n_I \omega \\ 0 & 0 & d_I & 0 \\ 0 & 0 & 0 & d_I \end{vmatrix} > 0$$

Therefore each of the principle minors of V are positive.

b) V is nonsingular since $\det V \neq 0$, and $V^{-1} \geqq 0$ (see V^{-1} above).

c) Each real characteristic root of V is positive since the roots of V are given by $d_V + r_I\overline{T}_S, d_V + r_Y\overline{T}_S, d_I, d_I$

d) Let $x = \begin{bmatrix} \frac{d_I}{n_I\omega} & \frac{d_I}{n_I\omega} & \frac{n_I\omega}{d_I} & \frac{n_I\omega}{d_I} \end{bmatrix}$. Then

$$xV = \begin{bmatrix} \frac{d_I}{n_I\omega} & \frac{d_I}{n_I\omega} & \frac{n_I\omega}{d_I} & \frac{n_I\omega}{d_I} \end{bmatrix} \begin{bmatrix} d_V + r_I\overline{T}_S & 0 & -n_I\omega & 0 \\ 0 & d_V + r_Y\overline{T}_S & 0 & -n_I\omega \\ 0 & 0 & d_I & 0 \\ 0 & 0 & 0 & d_I \end{bmatrix}$$

$$= \begin{bmatrix} \frac{d_I}{n_I\omega}(d_V + r_I\overline{T}_S) \\ \frac{d_I}{n_I\omega}(d_V + r_Y\overline{T}_S) \\ n_I\omega - d_I \\ n_I\omega - d_I \end{bmatrix},$$

which is positive since $n_I\omega - d_I > 0$. Therefore, there is a row vector x with positive entries such that $xV > 0$.

∎

This results in the following

$$FV^{-1} = \begin{pmatrix} 0 & 0 & 0 & 0 \\ 0 & 0 & 0 & 0 \\ \frac{r_I\overline{T}_S}{d_V + r_I\overline{T}_S} & 0 & \frac{n_I\omega r_I\overline{T}_S}{d_I(d_V + r_I\overline{T}_S)} & 0 \\ 0 & \frac{r_Y\overline{T}_S}{d_V + r_Y\overline{T}_S} & 0 & \frac{n_I\omega r_Y\overline{T}_S}{d_I(d_V + r_Y\overline{T}_S)} \end{pmatrix}.$$

The spectral radius of FV^{-1} shown in the article is the basic reproductive number.

C.1.2 Local stability analysis

The Jacobian matrix at the disease-free equilibrium is given by

$$J = \begin{bmatrix} -d_V - r_I T_S & 0 & 0 & 0 & n_I\omega & 0 \\ 0 & -d_V - r_Y T_S & 0 & 0 & 0 & n_I\omega \\ 0 & 0 & -d_V & 0 & n_I(1-\omega) & n_I(1-\omega) \\ -r_I T_S & -r_Y T_S & 0 & -d_S & 0 & 0 \\ r_I T_S & 0 & 0 & 0 & -d_I & 0 \\ 0 & r_Y T_S & 0 & 0 & 0 & -d_I \end{bmatrix}.$$

If we factor out $(-d_V - \mu)(-d_S - \mu)$ knowing these eigenvalues are negative, we have the following for the characteristic equation

$$\begin{aligned} 0 &= (-d_I - \mu)(-d_V - r_I T_S - \mu) \det \begin{vmatrix} -d_V - r_Y T_S & n_I\omega \\ r_Y T_S & -d_I \end{vmatrix} \\ &\quad + n_I \omega r_I T_S \det \begin{vmatrix} -d_V - r_Y T_S & n_I\omega \\ r_Y T_S & -d_I \end{vmatrix} \\ &= \Big[(-d_I - \mu)(-d_V - r_I T_S - \mu) + n_I \omega r_I T_S\Big] \det \begin{vmatrix} -d_V - r_Y T_S & n_I\omega \\ r_Y T_S & -d_I \end{vmatrix} \end{aligned}$$

Solving the polynomial, we get

$$d_I d_V + d_I r_I T_S + \mu(d_V + r_I T_S d_I) + \mu^2 + n_I \omega r_I T_S = 0$$

where all coefficients of the second order polynomial are positive.

Solving the matrix, we get

$$\begin{aligned} 0 &= (-d_V - r_Y T_S - \mu)(-d_I - \mu) - n_I \omega r_Y T_S \\ &= \mu^2 + \mu(d_V + r_Y T_S + d_I) + d_I d_V + d_I r_Y T_S - n_I \omega r_Y T_S. \end{aligned}$$

In this case, we have for the constant coefficient

$$\begin{aligned} d_I d_V + d_I r_Y T_S - n_I \omega r_Y T_S &= \frac{1}{d_S}(d_I d_V d_S + r_I \lambda d_I - d_I(d_V d_S + r_Y \lambda) R_{0,1,b}) \\ &= \frac{d_I d_V d_S + r_Y \lambda d_I}{d_S}(1 - R_{0,1,b}) \end{aligned}$$

The results in the article follow for the stability of the disease-free equilibrium.

C.2 Endemic equilibria

The endemic equilibria are computed by setting the right hand side of the equations (C.0.1) equal to zero and having $V_I \neq 0$ for the wild-type equilibrium and $V_Y \neq 0$ for the mutant equilibrium.

Note: We state that the wild-type and mutant equilibria exist if $R_{0,1} > 1$. The equilibria exist if $R_{0,1} < 1$ but are negative, meaning they are biologically irrelevant.

C.2.1 Local stability analysis

The Jacobian matrix at the wild-type equilibrium is given by

$$J = \begin{bmatrix} -d_V - r_I T_S & 0 & 0 & -r_I V_I & n_I\omega & 0 \\ 0 & -d_V - r_Y T_S & 0 & 0 & 0 & n_I\omega \\ 0 & 0 & -d_V & 0 & n_I(1-\omega) & n_I(1-\omega) \\ -r_I T_S & -r_Y T_S & 0 & -r_I V_I - d_S & 0 & 0 \\ r_I T_S & 0 & 0 & r_I V_I & -d_I & 0 \\ 0 & r_Y T_S & 0 & 0 & 0 & -d_I \end{bmatrix}.$$

If we factor out $(-d_V - \mu)$ since this eigenvalue is negative, we have the following for the characteristic equation

$$0 = (-d_V - r_Y T_S - \mu) \det \begin{vmatrix} -d_V - r_I T_S & -r_I V_I & n_I\omega & 0 \\ -r_I T_S & -r_I V_I - d_S & 0 & 0 \\ r_I T_S & r_I V_I & -d_I & 0 \\ 0 & 0 & 0 & -d_I \end{vmatrix}$$

$$+ n_I\omega \begin{vmatrix} -d_V - r_I T_S & 0 & -r_I V_I & n_I\omega \\ -r_I T_S & -r_Y T_S & -r_I V_I - d_S & 0 \\ r_I T_S & 0 & r_I V_I & -d_I \\ 0 & r_Y T_S & 0 & 0 \end{vmatrix}$$

$$= \Big[(-d_I - \mu)(-d_V - r_Y T_S - \mu) - n_I\omega r_Y T_S\Big] \det \begin{vmatrix} -d_V - r_I T_S & -r_I V_I & n_I\omega \\ -r_I T_S & -r_I V_I - d_S & 0 \\ r_I T_S & r_I V_I & -d_I \end{vmatrix}$$

Solving the polynomial we get

$$0 = \mu^2 + \mu(d_V + r_I\overline{T}_S + d_I) + d_I(d_V + r_Y T_S) - n_I\omega r_Y T_S$$

In this case, we have for the constant coefficient

$$\begin{aligned} d_I d_V + r_Y T_S(d_I - n_I\omega) &= d_I d_V - \frac{r_Y d_V d_I}{r_I(n_I\omega - d_I)}(n_I\omega - d_I) \\ &= \frac{d_I d_V(r_I - r_Y)}{r_I} \end{aligned}$$

where all coefficients of the second order polynomial are positive.

Solving the matrix, we get

$$\begin{aligned} 0 &= r_I T_S(-r_I V_I(-d_I - \mu) - r_I V_I n_I\omega) + (-r_I V_I - d_S - \mu)((-d_V - r_I T_S\mu)(-d_I - \mu) - r_I T_S n_I\omega) \\ &= \mu^3 + \mu^2(r_I\overline{V}_I + d_S + d_I + d_V + r_I\overline{T}_S) + \mu((d_V + r_I\overline{T}_S)d_S + (r_I\overline{V}_I + d_S)d_I + d_V r_I\overline{V}_I) \\ &\quad - d_I(r_I V_I + d_S + d_V + r_I T_S) + r_I V_I T_S d_I + d_S r_I T_S n_I\omega - d_I(r_I + d_S)(d_V + r_I T_S) \end{aligned}$$

In this case, we have for the constant coefficient

$$\begin{aligned}
&d_I(r_I V_I r_I \overline{T}_S + r_I V_I d_V + r_I T_S d_S + d_S d_S) - r_I V_I r_I T_S d_I - d_S r_I T_S n_I \omega - d_S r_I T_S (n_I \omega - d_I) \\
&\quad = d_I d_V r_I V_I \\
&\quad = d_I d_V r_I \frac{d_S d_V + r_I \lambda}{r_I d_V} (R_{0,1,a} - 1) \\
&\quad = d_I (d_S d_V d_I + r_I \lambda)(R_{0,1,a} - 1).
\end{aligned}$$

We also need to show that if we have $\mu^3 + a_2\mu^2 + b_2\mu + c_2 = 0$, that $a_2 b_2 - c_2 > 0$. In this case, we have

$$\begin{aligned}
a_2 b_2 - c_2 &= (r_I \overline{V}_I + d_S + d_I + d_V + r_I \overline{T}_S)(d_S(d_V + r_I \overline{T}_S) + (r_I \overline{V}_I + d_S) d_I + d_V r_I \overline{V}_I) \\
&\quad - d_I d_V r_I V_I \\
&= (r_I \overline{V}_I + d_S + d_I + r_I \overline{T}_S)(d_S(d_V + r_I \overline{T}_S) + (r_I \overline{V}_I + d_S) d_I + d_V r_I \overline{V}_I) \\
&\quad + d_V (d_S(d_V + r_I \overline{T}_S) + d_S d_I + d_V r_I \overline{V}_I) \\
&> 0
\end{aligned}$$

The results in the article follow for the stability of the wild-type equilibrium.

The Jacobian matrix at the mutant equilibrium is given by

$$J = \begin{bmatrix}
-d_V - r_I T_S & 0 & 0 & 0 & n_I \omega & 0 \\
0 & -d_V - r_Y T_S & 0 & -r_Y V_Y & 0 & n_I \omega \\
0 & 0 & -d_V & 0 & n_I(1-\omega) & n_I(1-\omega) \\
-r_I T_S & -r_Y T_S & 0 & -r_Y V_Y - d_S & 0 & 0 \\
r_I T_S & 0 & 0 & 0 & -d_I & 0 \\
0 & r_Y T_S & 0 & r_Y V_Y & 0 & -d_I
\end{bmatrix}.$$

If we factor out $(-d_V - \mu)$ since this eigenvalue is negative, we have the following for

the characteristic equation

$$0 = (-d_V - r_I T_S - \mu) \det \begin{vmatrix} -d_V - r_Y T_S & -r_Y V_Y & 0 & n_I \omega \\ -r_Y T_S & -r_Y V_Y - d_S & 0 & 0 \\ 0 & 0 & -d_I & 0 \\ r_Y T_S & r_Y V_Y & 0 & -d_I \end{vmatrix}$$

$$- n_I \omega \begin{vmatrix} 0 & -d_V - r_Y T_S & -r_Y V_Y & n_I \omega \\ -r_I T_S & -r_Y T_S & -r_Y V_Y - d_S & 0 \\ r_I T_S & 0 & 0 & 0 \\ 0 & r_Y T_S & r_Y V_Y & -d_I \end{vmatrix}$$

$$= \Big[(-d_I - \mu)(-d_V - r_I T_S - \mu) - n_I \omega r_I T_S \Big] \det \begin{vmatrix} -d_V - r_Y T_S & -r_Y V_Y & n_I \omega \\ -r_Y T_S & -r_Y V_Y - d_S & 0 \\ r_Y T_S & r_Y V_Y & -d_I \end{vmatrix}$$

The characteristic polynomial for the mutant equilibrium is the same as the wild-type equilibrium except r_I and V_I are interchanged with r_Y and V_Y. The results in the article follow for the stability of the mutant equilibrium.

Appendix D

Region 2: Intermediate drug levels; Miron and Smith? [4]

The following Appendix shows more details of the work presented in Region 2 of the manuscript in Chapter 3.2. We include many steps that are omitted in the manuscript. This Appendix only includes extra details on finding the mathematical results, thus it is only used to complete the manuscript. The Appendix does not include all of the manuscript.

The subregion model for Region 2 is given by

$$
\begin{aligned}
\frac{dV_I}{dt} &= n_I\omega T_I - d_V V_I - r_I T_S V_I - r_I T_{PN} V_I \\
\frac{dV_Y}{dt} &= n_I\omega (T_Y + T_{PY}) - d_V V_Y - r_Y T_S V_Y - r_Y T_{PN} V_Y \\
\frac{dV_N}{dt} &= n_I(1-\omega)(T_I + T_Y + T_{PY}) + n_I T_{PI} - d_V V_N \\
\frac{dT_S}{dt} &= \lambda - r_I T_S V_I - r_Y T_S V_Y - d_S T_S - r_P P T_S + m_P T_{PN} \\
\frac{dT_I}{dt} &= r_I T_S V_I - d_I T_I - r_P P T_I + m_P T_{PI} \\
\frac{dT_Y}{dt} &= r_Y T_S V_Y - d_I T_Y - r_P P T_Y + m_P T_{PY} \\
\frac{dT_{PN}}{dt} &= r_P P T_S - m_P T_{PN} - r_Y T_{PN} V_Y - r_I T_{PN} V_I - d_S T_{PN} \\
\frac{dT_{PI}}{dt} &= r_P P T_I - m_P T_{PI} + r_I T_{PN} V_I - d_I T_{PI} \\
\frac{dT_{PY}}{dt} &= r_P P T_Y - m_P T_{PY} + r_Y T_{PN} V_Y - d_I T_{PY}.
\end{aligned}
\tag{D.0.1}
$$

D.1 Disease-free equilibrium

The disease-free equilibrium shown in the article is computed by setting the right hand side of the equations (D.0.1) equal to zero.

D.1.1 Basic reproductive number

In order to compute the basic reproductive number, we compute the FV^{-1} matrix, and find its eigenvalues. We have that

$$F = \begin{pmatrix} 0 & 0 & 0 & 0 & 0 & 0 \\ 0 & 0 & 0 & 0 & 0 & 0 \\ r_I\overline{T}_S & 0 & 0 & 0 & 0 & 0 \\ 0 & r_Y\overline{T}_S & 0 & 0 & 0 & 0 \\ r_I\overline{T}_{PN} & 0 & 0 & 0 & 0 & 0 \\ 0 & r_Y\overline{T}_{PN} & 0 & 0 & 0 & 0 \end{pmatrix}$$

$$V = \begin{pmatrix} d_V + r_I\overline{T}_S + r_I\overline{T}_{PN} & 0 & -n_I\omega & 0 & 0 & 0 \\ 0 & d_V + r_Y\overline{T}_S + r_Y\overline{T}_{PN} & 0 & -n_I\omega & 0 & -n_I\omega \\ 0 & 0 & d_I + r_P P & 0 & -m_P & 0 \\ 0 & 0 & 0 & d_I + r_P P & 0 & -m_P \\ 0 & 0 & -r_P P & 0 & m_P + d_I & 0 \\ 0 & 0 & 0 & -r_P P & 0 & m_P + d_I \end{pmatrix},$$

and that $V^{-1} = [V_1^{-1}|V_2^{-1}]$ where

$$V_1^{-1} = \begin{pmatrix} \frac{1}{d_V + r_I\overline{T}_S + r_I\overline{T}_{PN}} & 0 & \frac{n_I\omega(m_P + d_I)}{d_I(d_I + r_P P^* + m_P)(r_I T_S^* + r_I T_{PN}^* + d_V)} \\ 0 & \frac{1}{d_V + r_Y\overline{T}_S + r_Y\overline{T}_{PN}} & 0 \\ 0 & 0 & \frac{m_P + d_I}{d_I(d_I + r_P P + m_P)} \\ 0 & 0 & 0 \\ 0 & 0 & \frac{r_P P}{d_I(d_I + r_P P + m_P)} \\ 0 & 0 & 0 \end{pmatrix}$$

$$V_2^{-1} = \begin{pmatrix} 0 & \frac{n_I\omega m_P}{d_I(d_I+r_PP^*+m_P)(r_IT_S^*+r_IT_{PN}^*+d_V)} & 0 \\ \frac{n_I\omega}{d_I(d_V+r_Y\overline{T}_S+r_Y\overline{T}_{PN})} & 0 & \frac{n_I\omega}{d_I(d_V+r_Y\overline{T}_S+r_Y\overline{T}_{PN})} \\ 0 & \frac{m_P}{d_I(d_I+r_PP+m_P)} & 0 \\ \frac{m_P+d_I}{d_I(d_I+r_PP+m_P)} & 0 & \frac{m_P}{d_I(d_I+r_PP+m_P)} \\ 0 & \frac{d_Ir_PP}{d_I(d_I+r_PP+m_P)} & 0 \\ \frac{r_PP}{d_I(d_I+r_PP+m_P)} & 0 & \frac{d_Ir_PP}{d_I(d_I+r_PP+m_P)} \end{pmatrix}.$$

We have that F is a non-negative matrix, and that V is a non-singular M-matrix (this can be shown in a similar fashion as was done in Appendix A).

This results in the following: $FV^{-1} = [FV_1^{-1}|FV_2^{-1}]$ where

$$FV_1^{-1} = \begin{pmatrix} 0 & 0 & 0 \\ 0 & 0 & 0 \\ \frac{r_IT_S}{d_V+r_IT_S+r_IT_{PN}} & 0 & \frac{n_I\omega r_I\overline{T}_S(m_P+d_I)}{d_I(d_I+r_PP^*+m_P)(r_IT_S^*+r_IT_{PN}^*+d_V)} \\ 0 & \frac{r_Y\overline{T}_S}{d_V+r_Y\overline{T}_S+r_Y\overline{T}_{PN}} & 0 \\ \frac{r_IT_{PN}}{d_V+r_IT_S+r_YT_{PN}} & 0 & \frac{n_I\omega r_I\overline{T}_{PN}(m_P+d_I)}{d_I(d_I+r_PP^*+m_P)(r_IT_S^*+r_IT_{PN}^*+d_V)} \\ 0 & \frac{r_YT_{PN}}{d_V+r_YT_S+r_YT_{PN}} & 0 \end{pmatrix}$$

$$FV_2^{-1} = \begin{pmatrix} 0 & 0 & 0 \\ 0 & 0 & 0 \\ 0 & \frac{n_I\omega r_I\overline{T}_Sm_P}{d_I(d_I+r_PP^*+m_P)(r_IT_S^*+r_IT_{PN}^*+d_V)} & 0 \\ \frac{n_I\omega r_Y\overline{T}_S}{d_I(d_V+r_Y\overline{T}_S+r_Y\overline{T}_{PN})} & 0 & \frac{n_I\omega r_Y\overline{T}_S}{d_I(d_V+r_Y\overline{T}_S+r_Y\overline{T}_{PN})} \\ 0 & \frac{n_I\omega r_I\overline{T}_{PN}m_P}{d_I(d_I+r_PP^*+m_P)(r_IT_S^*+r_IT_{PN}^*+d_V)} & 0 \\ \frac{n_I\omega r_YT_{PN}}{d_I(d_V+r_YT_S+r_YT_{PN})} & 0 & \frac{n_I\omega r_YT_{PN}}{d_I(d_V+r_YT_S+r_YT_{PN})} \end{pmatrix}.$$

The spectral radius of FV^{-1} shown in the article is the basic reproductive number.

D.1.2 Local stability analysis

The Jacobian matrix at the disease-free equilibrium is given by $J = [J_1|J_2]$, where

$$J_1 = \begin{bmatrix} -d_V - r_I T_S - r_I T_{PN} & 0 & 0 & 0 \\ 0 & -d_V - r_Y T_S - r_Y T_{PN} & 0 & 0 \\ 0 & 0 & -d_V & 0 \\ -r_I T_S & -r_Y T_S & 0 & -d_S - r_P P \\ r_I T_S & 0 & 0 & 0 \\ 0 & r_Y T_S & 0 & 0 \\ -r_I T_{PN} & -r_Y T_{PN} & 0 & r_P P \\ r_I T_{PN} & 0 & 0 & 0 \\ 0 & r_Y T_{PN} & 0 & 0 \\ 0 & 0 & 0 & 0 \end{bmatrix}$$

$$J_2 = \begin{bmatrix} n_I\omega & 0 & 0 & 0 & 0 & 0 \\ 0 & n_I\omega & 0 & 0 & n_I\omega & 0 \\ n_I(1-\omega) & n_I(1-\omega) & 0 & n_I & n_I(1-\omega) & 0 \\ 0 & 0 & m_P & 0 & 0 & -r_P T_S \\ -d_I - r_P P & 0 & 0 & m_P & 0 & -r_P T_I \\ 0 & -d_I - r_P P & 0 & 0 & m_P & -r_P T_Y \\ 0 & 0 & -m_P - d_S & 0 & 0 & r_P T_S \\ r_P P & 0 & 0 & -m_P - d_I & 0 & r_P T_I \\ 0 & r_P P & 0 & 0 & -m_P - d_I & r_P T_Y \\ 0 & 0 & 0 & 0 & 0 & -d_P \end{bmatrix}.$$

If we factor out $(-d_V - \mu)$ and $(-d_P - \mu)$ knowing these eigenvalues are negative, we have the following for the characteristic equation

$$
\begin{aligned}
0 = {} & (-d_V - r_I T_S - r_I T_{PN} - \mu) \\
& \times \begin{vmatrix}
-d_V - r_Y T_S - r_Y T_{PN} & 0 & 0 & n_I\omega & 0 & 0 & n_I\omega \\
-r_Y T_S & -d_S - r_P P & 0 & 0 & m_P & 0 & 0 \\
0 & 0 - d_I - r_P P & 0 & 0 & m_P & 0 & \\
r_Y T_S & 0 & 0 & -d_I - r_P P & 0 & 0 & m_P \\
r_Y T_{PN} & r_P P & 0 & 0 & -m_P - d_S & 0 & 0 \\
0 & 0 & r_P P & 0 & 0 & -m_P - d_I & 0 \\
r_Y T_{PN} & 0 & 0 & r_P P & 0 & 0 & -m_P - d_I
\end{vmatrix} \\
& - n_I\omega \\
& \times \begin{vmatrix}
0 & -d_V - r_Y T_S - r_Y T_{PN} & 0 & n_I\omega & 0 & 0 & n_I\omega \\
-r_I T_S & -r_Y T_S & -d_S - r_P P & 0 & m_P & 0 & 0 \\
r_I T_S & 0 & 0 & 0 & 0 & m_P & 0 \\
0 & r_Y T_S & 0 & -d_I - r_P P & 0 & 0 & m_P \\
-r_I T_{PN} & r_Y T_{PN} & r_P P & 0 & -m_P - d_S & 0 & 0 \\
-r_I T_{PN} & 0 & 0 & 0 & 0 & -m_P - d_I & 0 \\
0 & r_Y T_{PN} & 0 & r_P P & 0 & 0 & -m_P - d_I
\end{vmatrix} \\
= {} & \Big[(-d_V - r_I T_S - r_I T_{PN} - \mu)\Big((-d_I - r_P P - \mu)(-m_P - d_I - \mu) - m_P r_P P\Big) \\
& + n_I\omega\Big(r_I T_S(m_P + d_I + \mu) + m_P r_I T_{PN}\Big)\Big] \\
& \times \begin{vmatrix}
-d_V - r_Y T_S - r_Y T_{PN} & 0 & n_I\omega & 0 & n_I\omega \\
-r_Y T_S & -d_S - r_P P & 0 & m_P & 0 \\
r_Y T_S & 0 & -d_I - r_P P & 0 & m_P \\
-r_Y T_{PN} & r_P P & 0 & -m_P - d_S & 0 \\
r_Y T_{PN} & 0 & r_P P & 0 & -m_P - d_I
\end{vmatrix}
\end{aligned}
$$

Solving the polynomial, we get

$$\begin{aligned}0 = \lambda^3 &+ \lambda^2(m_P + d_I + d_V + r_I T_S^* + r_I T_{PN}^* + d_I + r_P P^*) + \lambda(-(d_I + r_P P^*)(d_V + r_I T_S^* + r_I T_{PN}) \\ &- (m_P + d_I)(d_V + r_I T_S^* + r_I T_{PN}^* + d_I + r_P P^*) + m_P r_P P^* + n_I \omega r_I T_S^*) \\ &- m_P r_P P(d_V + r_I T_S + r_I T_{PN}) - n_I \omega r_I T_S (m_P + d_I) n_I \omega m_P r_I T_{PN} \\ &+ (m_P + d_I)(d_V + r_I T_S + r_I T_{PN})(d_I + r_P P)\end{aligned}$$

In this case, we have for the constant coefficient

$$\begin{aligned}&- n_I \omega (m_P (r_I T_{PN} + r_I T_S)) - d_I n_I r_I T_S + (r_I T_S + r_I T_{PN})(d_I (d_I + r_P P) + m_P + d_I) \\ &- d_V m_P r_P P - d_V (m_P + d_I)(d_I + r_P P) \\ &\quad = -R_{0,2,b} d_I (d_I + r_P P + m_P)(r_I T_{PN} + r_I T_S + d_V) + d_I (r_I T_{PN} + r_I T_S)(d_I + r_P P + m_P) \\ &\qquad - d_V m_P r_P P - d_V (m_P + d_I)(d_I + r_P P) \\ &\quad = d_I (r_I T_{PN}^* + r_I T_S^* + d_V)(d_I + r_P P^* + m_P)(1 - R_{0,2,b})\end{aligned}$$

where the positivity conditions are as described in the article. We also need to show that if we have $\mu^3 + a_1\mu^2 + b_1\mu + c_1 = 0$, that $a_1b_1 - c_1 > 0$. In this case, we have

$$\begin{aligned}
a_1b_1 - c_1 &= (m_P + d_I + d_V + r_IT_S^* + r_IT_{PN}^* + d_I + r_PP^*)((d_I + r_PP^*)(d_V + r_IT_S^* + r_IT_{PN}) \\
&\quad + (m_P + d_I)(d_V + r_IT_S^* + r_IT_{PN}^* + d_I + r_PP^*) - m_Pr_PP^* - n_I\omega r_IT_S^*) \\
&\quad - d_I(r_IT_{PN}^* + r_IT_S^* + d_V)(d_I + r_PP^* + m_P)(1 - R_{0,2,b}) \\
&= (m_P + d_I + d_V + r_IT_S^* + r_IT_{PN}^* + d_I + r_PP^*)(d_I(d_V + r_IT_S^* + r_IT_{PN}) \\
&\quad + r_PP^*(d_V + r_IT_S^* + r_IT_{PN}) + d_I(d_V + r_IT_S^* + r_IT_{PN}^* + d_I + r_PP^*) \\
&\quad + m_P(d_V + r_IT_S^* + r_IT_{PN}^* + d_I) - n_I\omega r_IT_S^*) \\
&\quad - d_I(r_IT_{PN}^* + r_IT_S^* + d_V)(d_I + r_PP^* + m_P)(1 - R_{0,2,b}) \\
&= (m_P + d_I + d_V + r_IT_S^* + r_IT_{PN}^* + d_I + r_PP^*)(d_I(d_V + r_IT_S^* + r_IT_{PN}) \\
&\quad + r_PP^*(d_V + r_IT_S^* + r_IT_{PN}) + d_I(d_V + r_IT_S^* + r_IT_{PN}^* + d_I + r_PP^*) \\
&\quad + m_P(d_V + r_IT_S^* + r_IT_{PN}^* + d_I) - n_I\omega r_IT_S^*) \\
&\quad - (d_I(r_IT_{PN}^* + r_IT_S^* + d_V)(d_I + r_PP^* + m_P) - n_I\omega(m_P(r_IT_{PN}^* + r_IT_S^*) + d_Ir_IT_S)) \\
&= (m_P + d_I + d_V + r_IT_S^* + r_IT_{PN}^* + d_I + r_PP^*)d_I(d_I + d_V + r_IT_S^* + r_IT_{PN} + m_P) \\
&\quad + (m_P + d_I + d_V + r_IT_S^* + r_IT_{PN}^* + d_I + r_PP^*)\Big((r_IT_{PN}^* + r_IT_S^* + d_V) \\
&\quad \times (d_I + r_PP^* + m_P) - n_I\omega r_IT_S\Big) - \Big(d_I(r_IT_{PN}^* + r_IT_S^* + d_V)(d_I + r_PP^* + m_P) \\
&\quad - n_I\omega(m_P(r_IT_{PN}^* + r_IT_S^*) + d_Ir_IT_S)\Big)
\end{aligned}$$

$$
\begin{aligned}
&= (m_P + d_I + d_V + r_I T_S^* + r_I T_{PN}^* + d_I + r_P P^*) d_I (d_I + d_V + r_I T_S^* + r_I T_{PN} + m_P) \\
&\quad + (m_P + d_I + d_V + r_I T_S^* + r_I T_{PN}^* + r_P P^*) \Big(\frac{n_I \omega (m_P (r_I T_{PN}^* + r_I T_S^*) + d_I r_I T_S)}{d_I R_{0,2,b}} \\
&\quad - n_I \omega r_I T_S \Big) + n_I \omega m_P (r_I T_{PN}^* + r_I T_S^*) \\
&= (m_P + d_I + d_V + r_I T_S^* + r_I T_{PN}^* + d_I + r_P P^*) d_I (d_I + d_V + r_I T_S^* + r_I T_{PN} + m_P) \\
&\quad + \frac{m_P + d_I + d_V + r_I T_S^* + r_I T_{PN}^* + r_P P^*}{d_I R_{0,2,b}} \Big(n_I \omega m_P (r_I T_{PN}^* + r_I T_S^*) \\
&\quad + n_I \omega d_I r_I T_S (1 - R_{0,2,b}) \Big) + n_I \omega m_P (r_I T_{PN}^* + r_I T_S^*),
\end{aligned}
$$

which is greater than zero if $R_{0,2} < 1$. The results follow in the article.

Solving the matrix in the characteristic polynomial, we get

$$
0 = \begin{vmatrix} -d_S - r_P P & m_P \\ r_P P & -m_P - d_S \end{vmatrix} \begin{vmatrix} -d_V - r_Y T_S - r_Y T_{PN} & n_I \omega & n_I \omega \\ r_Y T_S & -d_I - r_P P & m_P \\ r_Y T_{PN} & r_P P & -d_I - m_P \end{vmatrix}.
$$

Solving the 2×2 - matrix, we get

$$
\begin{aligned}
0 &= \lambda^2 + \lambda(d_S + r_P P + m_P + d_S) + (d_S + m_P)(d_S + r_P P) - r_P P m_P \\
&= \lambda^2 + \lambda(d_S + r_P P + m_P + d_S) + d_S(d_S + r_P P) + m_P d_S.
\end{aligned}
$$

In this case, all the coefficients are positive. Solving the 3×3 - matrix, we get

$$
\begin{aligned}
0 &= \lambda^3 + \lambda^2(r_P P^* + 2d_I + d_V + r_Y T_S^* + r_Y T_{PN}^* + m_P) + \lambda(-m_P r_P P^* - n_I \omega r_Y (T_S^* + T_{PN}^*) \\
&\quad + (r_P P^* + d_I)(d_V + r_Y T_S^* + r_Y T_{PN}^*) + (m_P + d_I)(r_P P^* + d_I + d_V + r_Y T_S^* + r_Y T_{PN}^*)) \\
&\quad - m_P r_P P (d_V + r_Y T_S^* + r_Y T_{PN}^*) - n_I \omega r_Y T_S (m_P + d_I) - n_I \omega m_P r_Y T_{PN} - n_I \omega r_Y T_S r_P P \\
&\quad - n_I \omega r_Y T_{PN} (d_I + r_P P) + (m_P + d_I)(d_I + r_P P)(d_V + r_Y T_S^* + r_Y T_{PN}^*).
\end{aligned}
$$

In this case, we have for the constant coefficient

$$\begin{aligned}
&(d_V + r_Y T_S + r_Y T_{PN})(-m_P r_P P + (m_P + d_I)(d_I + r_P P)) - n_I \omega \Big(r_Y T_S (m_P + d_I) \\
&+ m_P r_Y T_{PN} + r_Y T_S r_P P + r_Y T_{PN}(d_I + r_P P) \Big) \\
&\quad = (d_V + r_Y T_S + r_Y T_{PN})(d_I(d_I + r_P P) + m_P d_I) - n_I \omega (m_P + d_I + r_P P)(r_Y T_S + r_Y T_{PN}) \\
&\quad = d_I (r_Y T^*_{PN} + r_Y T^*_S + d_V)(d_I + r_P P^* + m_P)(1 - R_{0,2,a})
\end{aligned}$$

where the positivity conditions are as described in the article. We also need to show that if we have $\mu^3 + a_3\mu^2 + b_3\mu + c_3 = 0$, that $a_3 b_3 - c_3 > 0$. In this case, we have that a_3 and c_3 are similar to a_1 and c_1 except that r_Y is interchanged with r_I, respectively. We also have that the only difference other than r_Y and r_I being interchanged between b_3 and b_1, respectively, is that the negative term $-n_I \omega r_Y (T_S + T_{PN})$ in b_3 replaces the negative term $-n_I \omega r_Y T_S$ in b_1 (since the wild-type virus is only produced from susceptible cells with low drug, whereas the mutant virus is produced from both the susceptible cells with low and intermediate drug). Using these similarities, we get

$$\begin{aligned}
a_3 b_3 - c_3 = &(r_P P^* + 2d_I + d_V + r_Y T^*_S + r_Y T^*_{PN} + m_P)(-m_P r_P P^* - n_I \omega r_Y (T^*_S + T^*_{PN}) \\
&+ (r_P P^* + d_I)(d_V + r_Y T^*_S + r_Y T^*_{PN}) + (m_P + d_I)(r_P P^* + d_I + d_V + r_Y T^*_S + r_Y T^*_{PN})) \\
&- (d_V + r_Y T^*_S + r_Y T^*_{PN})[-m_P r_P P^* + (m_P + d_I)(d_I + r_P P^*)] - n_I \omega [r_Y T^*_S (m_P + d_I) \\
&+ m_P r_Y T^*_{PN} + r_Y T^*_S r_P P^* + r_Y T^*_{PN}(d_I + r_P P^*)] \\
= &(m_P + d_V + r_Y T^*_S + r_Y T^*_{PN} + d_I + r_P P^*) d_I (d_I + d_V + r_Y T^*_S + r_Y T_{PN} + m_P) \\
&+ d_I^2 (d_I + m_P) + d_I^2 (d_V + r_Y T_S + r_Y T_{PN}) + (m_P + d_I + d_V + r_Y T^*_S + r_Y T^*_{PN} \\
&+ d_I + r_P P^*) \Big((r_Y T^*_{PN} + r_Y T^*_S + d_V)(d_I + m_P) + d_I (r_Y T^*_{PN} + r_Y T^*_S + d_V) \\
&- n_I \omega r_Y (T_S + T_{PN}) \Big) - d_I n_I \omega (r_Y T^*_{PN} + r_Y T^*_S) + n_I \omega (m_P (r_Y T^*_{PN} + r_Y T^*_S) + d_I r_Y T_S)
\end{aligned}$$

$$
\begin{aligned}
&= (m_P + d_V + r_Y T_S^* + r_Y T_{PN}^* + d_I + r_P P^*) d_I (d_I + d_V + r_Y T_S^* + r_Y T_{PN} + m_P) \\
&\quad + (m_P + d_I + d_V + r_Y T_S^* + r_Y T_{PN}^* + d_I + r_P P^*) \Big((r_Y T_{PN}^* + r_Y T_S^* + d_V)(d_I + m_P) \\
&\quad + d_I (r_Y T_{PN}^* + r_Y T_S^* + d_V) - R_{0,2,a} d_I (d_V + r_Y T_S + r_Y T_{PN}) \Big) + d_I^2 (d_V + r_Y T_S + r_Y T_{PN}) \\
&\quad - d_I^2 (d_V + r_Y T_S + r_Y T_{PN}) R_{0,2,a} + d_I^2 (d_I + m_P) + n_I \omega (m_P (r_Y T_{PN}^* + r_Y T_S^*) + d_I r_Y T_S) \\
&= (m_P + d_V + r_Y T_S^* + r_Y T_{PN}^* + d_I + r_P P^*) d_I (d_I + d_V + r_Y T_S^* + r_Y T_{PN} + m_P) \\
&\quad + (m_P + d_I + d_V + r_Y T_S^* + r_Y T_{PN}^* + d_I + r_P P^*) (r_Y T_{PN}^* + r_Y T_S^* + d_V) \\
&\quad \times (m_P + r_P P^* + d_I (1 - R_{0,2,a})) + d_I^2 (d_V + r_Y T_S + r_Y T_{PN}) (1 - R_{0,2,a}) \\
&\quad + d_I^2 (d_I + m_P) + n_I \omega (m_P (r_Y T_{PN}^* + r_Y T_S^*) + d_I r_Y T_S)
\end{aligned}
$$

which is greater than zero if $R_{0,2} < 1$. The results in the article follow for the stability of the disease-free equilibrium.

D.2 Endemic equilibria

The endemic equilibria are computed by setting the right hand side of the equations (D.0.1) equal to zero and having $V_I \neq 0$ for the wild-type equilibrium and $V_Y \neq 0$ for the mutant equilibrium.

D.2.1 Local stability analysis

The Jacobian matrix at the wild-type equilibrium is given by $J = [J_1|J_2]$ where

$$J_1 = \begin{bmatrix} -d_V - r_I T_S - r_I T_{PN} & 0 & 0 & -r_I V_I \\ 0 & -d_V - r_Y T_S - r_Y T_{PN} & 0 & 0 \\ 0 & 0 & -d_V & 0 \\ -r_I T_S & -r_Y T_S & 0 & -r_I V_I - d_S - r_P P \\ r_I T_S & 0 & 0 & r_I V_I \\ 0 & r_Y T_S & 0 & 0 \\ -r_I T_{PN} & -r_Y T_{PN} & 0 & r_P P \\ r_I T_{PN} & 0 & 0 & 0 \\ 0 & r_Y T_{PN} & 0 & 0 \\ 0 & 0 & 0 & 0 \end{bmatrix}$$

$$J_2 = \begin{bmatrix} n_I\omega & 0 & -r_I V_I & 0 & 0 & 0 \\ 0 & n_I\omega & 0 & 0 & n_I\omega & 0 \\ n_I(1-\omega) & n_I(1-\omega) & 0 & n_I & n_I(1-\omega) & 0 \\ 0 & 0 & m_P & 0 & 0 & -r_P T_S \\ -d_I - r_P P & 0 & 0 & m_P & 0 & -r_P T_I \\ 0 & -d_I - r_P P & 0 & 0 & m_P & -r_P T_Y \\ 0 & 0 & -m_P - r_I V_I - d_S & 0 & 0 & r_P T_S \\ r_P P & 0 & r_I V_I & -m_P - d_I & 0 & r_P T_I \\ 0 & r_P P & 0 & 0 & -m_P - d_I & r_P T_Y \\ 0 & 0 & 0 & 0 & 0 & -d_P \end{bmatrix}.$$

If we factor out $(-d_P - \mu)$ since this eigenvalue is negative, we have the following for the characteristic equation

$$
\begin{aligned}
0 = r_Y T_{PN} n_I \omega
&\begin{vmatrix}
-d_V - r_I T_S - r_I T_{PN} & -r_I V_I & n_I\omega & -r_I V_I & 0 & 0 \\
-r_I T_S & -r_I V_I - d_S - r_P P & 0 & m_P & 0 & 0 \\
r_I T_S & r_I V_I & -d_I - r_P P & 0 & m_P & 0 \\
0 & 0 & 0 & 0 & 0 & m_P \\
-r_I T_{PN} & r_P P & 0 & -m_P - r_I V_I - d_S & 0 & 0 \\
r_I T_{PN} & 0 & r_P P & r_I V_I & -m_P - d_I & 0
\end{vmatrix} \\
- r_Y T_{PN} n_I \omega
&\times \begin{vmatrix}
-d_V - r_I T_S - r_I T_{PN} & -r_I V_I & n_I\omega & 0 & -r_I V_I & 0 \\
-r_I T_S & -r_I V_I - d_S - r_P P & 0 & 0 & m_P & 0 \\
r_I T_S & r_I V_I & -d_I - r_P P & 0 & 0 & m_P \\
0 & 0 & 0 & -d_I - r_P P & 0 & 0 \\
-r_I T_{PN} & r_P P & 0 & 0 & -m_P - r_I V_I - d_S & 0 \\
r_I T_{PN} & 0 & r_P P & 0 & r_I V_I & -m_P - d_I
\end{vmatrix} \\
- r_P P(-d_V - r_Y T_S - r_Y T_{PN} - \mu)
&\times \begin{vmatrix}
-d_V - r_I T_S - r_I T_{PN} & -r_I V_I & n_I\omega & -r_I V_I & 0 & 0 \\
-r_I T_S & -r_I V_I - d_S - r_P P & 0 & m_P & 0 & 0 \\
r_I T_S & r_I V_I & -d_I - r_P P & 0 & m_P & 0 \\
0 & 0 & 0 & 0 & 0 & m_P \\
-r_I T_{PN} & r_P P & 0 & -m_P - r_I V_I - d_S & 0 & 0 \\
r_I T_{PN} & 0 & r_P P & r_I V_I & -m_P - d_I & 0
\end{vmatrix}
\end{aligned}
$$

$$
+ r_P P n_I \omega \begin{vmatrix} -d_V - r_I T_S - r_I T_{PN} & 0 & -r_I V_I & n_I\omega & -r_I V_I & 0 \\ -r_I T_S & -r_Y T_S & -r_I V_I - d_S - r_P P & 0 & m_P & 0 \\ r_I T_S & 0 & r_I V_I & -d_I - r_P P & 0 & m_P \\ 0 & r_Y T_S & 0 & 0 & 0 & 0 \\ -r_I T_{PN} & -r_Y T_{PN} & r_P P & 0 & -m_P - r_I V_I - d_S & 0 \\ r_I T_{PN} & 0 & 0 & r_P P & r_I V_I & -m_P - d_I \end{vmatrix}
$$

$$
\times \begin{vmatrix} -d_V - r_I T_S - r_I T_{PN} & -r_I V_I & n_I\omega & 0 & -r_I V_I & 0 \\ 0 & 0 & 0 & n_I\omega & 0 & 0 \\ -r_I T_S & -r_I V_I - d_S - r_P P & 0 & 0 & m_P & 0 \\ r_I T_S & r_I V_I & -d_I - r_P P & 0 & 0 & m_P \\ -r_I T_{PN} & r_P P & 0 & 0 & -m_P - r_I V_I - d_S & 0 \\ r_I T_{PN} & 0 & r_P P & 0 & r_I V_I & -m_P - d_I \end{vmatrix}
$$

$$
+ (-m_P - d_I - \mu)(-d_I - r_P P - \mu)
$$

$$
\times \begin{vmatrix} -d_V - r_I T_S - r_I T_{PN} & 0 & -r_I V_I & n_I\omega & -r_I V_I & 0 \\ 0 & -d_V - r_Y T_S - r_Y T_{PN} & 0 & 0 & 0 & 0 \\ -r_I T_S & -r_Y T_S & -r_I V_I - d_S - r_P P & 0 & m_P & 0 \\ r_I T_S & 0 & r_I V_I & -d_I - r_P P & 0 & m_P \\ -r_I T_{PN} & -r_Y T_{PN} & r_P P & 0 & -m_P - r_I V_I - d_S & 0 \\ r_I T_{PN} & 0 & 0 & r_P P & r_I V_I & -m_P - d_I \end{vmatrix}
$$

$$
\begin{aligned}
&= \big(r_Y T_{PN} n_I \omega m_P - r_Y T_{PN} n_I \omega(-d_I - r_P P - \mu) - r_P P m_P(-d_V - r_Y T_S - r_Y T_{PN} - \mu) \\
&\quad + r_P P n_I \omega r_Y T_S - r_Y T_S n_I \omega(-m_P - d_I - \mu) + (-m_P - d_I - \mu)(-d_I - r_P P - \mu) \\
&\quad \times (-d_V - r_Y T_S - r_Y T_{PN} - \mu)\big) \\
&\quad \times \begin{vmatrix}
-d_V - r_I T_S - r_I T_{PN} & -r_I V_I & n_I\omega & -r_I V_I & 0 \\
-r_I T_S & -r_I V_I - d_S - r_P P & 0 & m_P & 0 \\
r_I T_S & r_I V_I & -d_I - r_P P & 0 & m_P \\
-r_I T_{PN} & r_P P & 0 & -m_P - r_I V_I - d_S & 0 \\
r_I T_{PN} & 0 & r_P P & r_I V_I & -m_P - d_I
\end{vmatrix}
\end{aligned}
$$

Solving the polynomial we get

$$
\begin{aligned}
0 &= \mu^3 + \mu^2(2d_I + r_P P^* + m_P + d_V + r_Y T_S^* + r_Y T_{PN}^*) + \mu((d_V + r_Y T_S^* + r_Y T_{PN}^*)[(m_P + d_I) \\
&\quad + (d_I + r_P P^*)] + (d_I + r_P P^*)(m_P + d_I) - r_Y T_S^* n_I \omega + m_P r_P P^* - r_Y T_{PN}^* n_I \omega) \\
&\quad - n_I \omega r_Y T_S^*(m_P + d_I) + (d_V + r_Y T_S^* + r_Y T_{PN}^*)(m_P d_I + d_I^2 + d_I r_P P^*) - r_P P^* n_I \omega r_Y T_S^* \\
&\quad - r_Y T_{PN}^* n_I \omega m_P - r_Y T_{PN}^* n_I \omega(d_I + r_P P^*)
\end{aligned}
$$

In this case, we have for the constant coefficient

$$
\begin{aligned}
&- n_I \omega r_Y T_S^*(m_P + d_I) + (d_V + r_Y T_S^* + r_Y T_{PN}^*)(m_P d_I + d_I^2 + d_I r_P P^*) - r_P P^* n_I \omega r_Y T_S^* \\
&- r_Y T_{PN}^* n_I \omega m_P - r_Y T_{PN}^* n_I \omega(d_I + r_P P^*) \\
&\quad = -n_I \omega(r_Y T_S(m_P + d_I + r_P P) + r_Y T_{PN}(m_P + d_I + r_P P)) \\
&\qquad + d_I(d_V + r_Y T_S^* + r_Y T_{PN}^*)(m_P + d_I + rPP) \\
&\quad = d_I(r_Y T_{PN}^* + r_Y T_S^* + d_V)(d_I + r_P P^* + m_P)(1 - R_{0,2,a})
\end{aligned}
$$

The results in the article follow for the stability of the wild-type equilibrium.

The Jacobian matrix at the mutant equilibrium is given by $J = [J_1|J_2]$ where

$$J_1 = \begin{bmatrix} -d_V - r_I T_S - r_I T_{PN} & 0 & 0 & 0 \\ 0 & -d_V - r_Y T_S - r_Y T_{PN} & 0 & -r_Y V_Y \\ 0 & 0 & -d_V & 0 \\ -r_I T_S & -r_Y T_S & 0 & -r_Y V_Y - d_S - r_P P \\ r_I T_S & 0 & 0 & 0 \\ 0 & r_Y T_S & 0 & r_Y V_Y \\ -r_I T_{PN} & -r_Y T_{PN} & 0 & r_P P \\ r_I T_{PN} & 0 & 0 & 0 \\ 0 & r_Y T_{PN} & 0 & 0 \\ 0 & 0 & 0 & 0 \end{bmatrix}$$

$$J_2 = \begin{bmatrix} n_I\omega & 0 & 0 & 0 & 0 & 0 \\ 0 & n_I\omega & -r_Y V_Y & 0 & n_I\omega & 0 \\ n_I(1-\omega) & n_I(1-\omega) & 0 & n_I & n_I(1-\omega) & 0 \\ 0 & 0 & m_P & 0 & 0 & -r_P T_S \\ -d_I - r_P P & 0 & 0 & m_P & 0 & -r_P T_I \\ 0 & -d_I - r_P P & 0 & 0 & m_P & -r_P T_Y \\ 0 & 0 & -m_P - r_Y V_Y - d_S & 0 & 0 & r_P T_S \\ r_P P & 0 & 0 & -m_P - d_I & 0 & r_P T_I \\ 0 & r_P P & r_Y V_Y & 0 & -m_P - d_I & r_P T_Y \\ 0 & 0 & 0 & 0 & 0 & -d_P \end{bmatrix}.$$

If we factor out $(-d_P - \mu)$ since this eigenvalue is negative, we have the following for

the characteristic equation

$$
\begin{aligned}
0 = {} & (-d_I - r_P P - \mu)(-m_P - d_I - \mu)(-d_V - r_I T_S - r_I T_{PN} - \mu) \\
& \times \begin{vmatrix}
-d_V - r_Y T_S - r_Y T_{PN} & -r_Y V_Y & n_I\omega & -r_Y V_Y & n_I\omega \\
-r_Y T_S & -r_Y V_Y - d_S - r_P P & 0 & m_P & 0 \\
r_Y T_S & r_Y V_Y & -d_I - r_P P & 0 & m_P \\
-r_Y T_{PN} & r_P P & 0 & -m_P - r_Y V_Y - d_S & 0 \\
r_Y T_{PN} & 0 & r_P P & r_Y V_Y & -m_P - d_I
\end{vmatrix} \\
& - r_Y T_S n_I \omega (-m_P - d_I - \mu) \\
& \times \begin{vmatrix}
-d_V - r_Y T_S - r_Y T_{PN} & -r_Y V_Y & n_I\omega & -r_Y V_Y & n_I\omega \\
-r_Y T_S & -r_Y V_Y - d_S - r_P P & 0 & m_P & 0 \\
r_Y T_S & r_Y V_Y & -d_I - r_P P & 0 & m_P \\
-r_Y T_{PN} & r_P P & 0 & -m_P - r_Y V_Y - d_S & 0 \\
r_Y T_{PN} & 0 & r_P P & r_Y V_Y & -m_P - d_I
\end{vmatrix} \\
& - m_P (-d_V - r_I T_S - r_I T_{PN} - \mu) \\
& \times \begin{vmatrix}
-d_V - r_Y T_S - r_Y T_{PN} & -r_Y V_Y & 0 & n_I\omega & -r_Y V_Y & n_I\omega \\
-r_Y T_S & -r_Y V_Y - d_S - r_P P & 0 & 0 & m_P & 0 \\
r_Y T_S & r_Y V_Y & 0 & -d_I - r_P P & 0 & m_P \\
-r_Y T_{PN} & r_P P & 0 & 0 & -m_P - r_Y V_Y - d_S & 0 \\
0 & 0 & r_P P & 0 & 0 & 0 \\
r_Y T_{PN} & 0 & 0 & r_P P & r_Y V_Y & -m_P - d_I
\end{vmatrix}
\end{aligned}
$$

$$
\begin{aligned}
&+ m_P n_I \omega \\
&\times \begin{vmatrix}
0 & -d_V - r_Y T_S - r_Y T_{PN} & -r_Y V_Y & n_I\omega & -r_Y V_Y & n_I\omega \\
-r_I T_S & -r_Y T_S & -r_Y V_Y - d_S - r_P P & 0 & m_P & 0 \\
0 & r_Y T_S & r_Y V_Y & -d_I - r_P P & 0 & m_P \\
-r_I T_{PN} & -r_Y T_{PN} & r_P P & 0 & -m_P - r_Y V_Y - d_S & 0 \\
r_I T_{PN} & 0 & 0 & 0 & 0 & 0 \\
0 & r_Y T_{PN} & 0 & r_P P & r_Y V_Y & -m_P - d_I
\end{vmatrix} \\
&= \big(r_I T_{PN} n_I \omega m_P - r_P P m_P(-d_V - r_Y T_S - r_Y T_{PN} - \mu) - r_I T_S n_I \omega(-m_P - d_I - \mu) \\
&+ (-m_P - d_I - \mu)(-d_I - r_P P - \mu)(-d_V - r_I T_S - r_I T_{PN} - \mu) \big) \\
&\times \begin{vmatrix}
-d_V - r_Y T_S - r_Y T_{PN} & -r_Y V_Y & n_I\omega & -r_Y V_Y & n_I\omega \\
-r_Y T_S & -r_Y V_Y - d_S - r_P P & 0 & m_P & 0 \\
r_Y T_S & r_Y V_Y & -d_I - r_P P & 0 & m_P \\
-r_Y T_{PN} & r_P P & 0 & -m_P - r_Y V_Y - d_S & 0 \\
r_Y T_{PN} & 0 & r_P P & r_Y V_Y & -m_P - d_I
\end{vmatrix}
\end{aligned}
$$

Solving the polynomial we get

$$
\begin{aligned}
0 = {} & \mu^3 + \mu^2(2d_I + r_P P^* + m_P + d_V + r_I T_S^* + r_I T_{PN}^*) + \mu((d_V + r_I T_S^* + r_I T_{PN}^*)[(m_P + d_I) \\
& + (d_I + r_P P^*)] + (d_I + r_P P^*)(m_P + d_I) - r_I T_S^* n_I \omega - m_P r_P P^*) - n_I \omega r_I T_S^*(m_P + d_I) \\
& + (d_V + r_I T_S^* + r_I T_{PN}^*)(m_P + d_I)(d_I + r_P P^*) - r_P P^* m_P(d_V + r_I T_S^* + r_I T_{PN}^*) - m_P n_I \omega r_I T_{PN}^*
\end{aligned}
$$

In this case, we have for the constant coefficient

$$
\begin{aligned}
& - n_I \omega r_I T_S^*(m_P + d_I) + (d_V + r_I T_S^* + r_I T_{PN}^*)(m_P + d_I)(d_I + r_P P^*) \\
& - r_P P^* m_P(d_V + r_I T_S^* + r_I T_{PN}^*) - m_P n_I \omega r_I T_{PN}^* \\
& \quad = -n_I \omega(m_P(r_I T_S + r_T T_{PN}) + d_I r_I T_S) + d_I(d_V + r_Y T_S^* + r_Y T_{PN}^*)(m_P + d_I + rPP) \\
& \quad = d_I(r_I T_{PN}^* + r_I T_S^* + d_V)(d_I + r_P P^* + m_P)(1 - R_{0,2,b})
\end{aligned}
$$

The results in the article follow for the stability of the mutant equilibrium.

Appendix E

Region 3: High drug levels; Miron and Smith? [4]

The following Appendix shows more details of the work presented in Region 3 of the manuscript in Chapter 3.2. We include many steps that are omitted in the manuscript. This Appendix only includes extra details on finding the mathematical results, thus it is only used to complete the manuscript. The Appendix does not include all of the manuscript.

Note: We have that $r_P \geq r_{PP}$. Such is the case since drug absorption is greater when the cell goes from no drug to intermediate levels, than from intermediate levels to high levels (drug absorption saturates when drug levels are high). We also have no transition from T_S to T_{PPN}. This is because when a cell with no drug initially absorbs drug, the intake gradually increases from no drug, to intermediate drug, to high drug. The cell will not go from no drug to high levels without passing through intermediate levels.

The subregion model for Region 3 is given by

$$
\begin{aligned}
\frac{dV_I}{dt} &= n_I\omega T_I - d_V V_I - r_I T_S V_I - r_I T_{PN} V_I - r_I T_{PPN} V_I \\
\frac{dV_Y}{dt} &= n_I\omega(T_Y + T_{PY}) - d_V V_Y - r_Y T_S V_Y - r_Y T_{PN} V_Y - r_Y T_{PPN} V_Y \\
\frac{dV_N}{dt} &= n_I(1-\omega)(T_I + T_Y + T_{PY}) + n_I(T_{PI} + T_{PPI} + T_{PPY}) - d_V V_N \\
\frac{dT_S}{dt} &= \lambda - r_I T_S V_I - r_Y T_S V_Y - d_S T_S - r_P P T_S + m_P T_{PN} \\
\frac{dT_I}{dt} &= r_I T_S V_I - d_I T_I - r_P P T_I + m_P T_{PI} \\
\frac{dT_Y}{dt} &= r_Y T_S V_Y - d_I T_Y - r_P P T_Y + m_P T_{PY} \\
\frac{dT_{PN}}{dt} &= r_P P T_S - m_P T_{PN} - r_Y T_{PN} V_Y - r_I T_{PN} V_I - d_S T_{PN} - r_{PP} P T_{PN} + m_{PP} T_{PPN} \\
\frac{dT_{PI}}{dt} &= r_I T_{PN} V_I + r_P P T_I - m_P T_{PI} - r_{PP} P T_{PI} + m_{PP} T_{PPI} - d_I T_{PI} \\
\frac{dT_{PY}}{dt} &= r_Y T_{PN} V_Y + r_P P T_Y - m_P T_{PY} - r_{PP} P T_{PY} + m_{PP} T_{PPY} - d_I T_{PY} \\
\frac{dT_{PPN}}{dt} &= r_{PP} P T_{PN} - m_{PP} T_{PPN} - r_Y T_{PPN} V_Y - r_I T_{PPN} V_I - d_S T_{PPN} \\
\frac{dT_{PPI}}{dt} &= r_I T_{PPN} V_I + r_{PP} P T_{PI} - m_{PP} T_{PPI} - d_I T_{PPI} \\
\frac{dT_{PPY}}{dt} &= r_Y T_{PPN} V_Y + r_{PP} P T_{PY} - m_{PP} T_{PPY} - d_I T_{PPY}.
\end{aligned}
\tag{E.0.1}
$$

E.1 Disease-free equilibrium

The disease-free equilibrium shown in the article is computed by setting the right hand side of the equations (E.0.1) equal to zero.

E.1.1 Basic reproductive number

In order to compute the basic reproductive number, we compute the FV^{-1} matrix, and find its eigenvalues. We have that

$$F = \begin{pmatrix} 0 & 0 & 0 & 0 & 0 & 0 & 0 & 0 \\ 0 & 0 & 0 & 0 & 0 & 0 & 0 & 0 \\ r_I\overline{T}_S & 0 & 0 & 0 & 0 & 0 & 0 & 0 \\ 0 & r_Y\overline{T}_S & 0 & 0 & 0 & 0 & 0 & 0 \\ r_I\overline{T}_{PN} & 0 & 0 & 0 & 0 & 0 & 0 & 0 \\ 0 & r_Y\overline{T}_{PN} & 0 & 0 & 0 & 0 & 0 & 0 \\ r_I\overline{T}_{PPN} & 0 & 0 & 0 & 0 & 0 & 0 & 0 \\ 0 & r_Y\overline{T}_{PPN} & 0 & 0 & 0 & 0 & 0 & 0 \end{pmatrix},$$

and $V = [V_1|V_2]$

$$V_1 = \begin{pmatrix} d_V + r_I\overline{T}_S + r_I\overline{T}_{PN} + r_I\overline{T}_{PPN} & 0 & -n_I\omega & 0 \\ 0 & d_V + r_Y\overline{T}_S + r_Y\overline{T}_{PN} + r_Y\overline{T}_{PPN} & 0 & -n_I\omega \\ 0 & 0 & d_I + r_P P & 0 \\ 0 & 0 & 0 & d_I + r_P P \\ 0 & 0 & -r_P P & 0 \\ 0 & 0 & 0 & -r_P P \\ 0 & 0 & 0 & 0 \\ 0 & 0 & 0 & -r_P P \end{pmatrix}$$

$$V_2 = \begin{pmatrix} 0 & 0 & 0 & 0 \\ 0 & -n_I\omega & 0 & 0 \\ -m_P & 0 & 0 & 0 \\ 0 & -m_P & 0 & 0 \\ m_P + d_I + r_{PP}P & 0 & -m_{PP} & 0 \\ 0 & m_P + d_I + r_{PP}P & 0 & -m_{PP} \\ -r_{PP}P & 0 & m_{PP} + d_I & 0 \\ 0 & -r_{PP}P & 0 & m_{PP} + d_I \end{pmatrix}.$$

We also have that $V^{-1} = [V_1^{-1}|V_2^{-1}|V_3^{-1}|V_4^{-1}]$ where

$$V_1^{-1} = \begin{pmatrix} \frac{1}{d_V + r_I\overline{T}_S + r_I\overline{T}_{PN} + r_I\overline{T}_{PPN}} & 0 \\ 0 & \frac{1}{d_V + r_Y\overline{T}_S + r_Y\overline{T}_{PN} + r_Y\overline{T}_{PPN}} \\ 0 & 0 \\ 0 & 0 \\ 0 & 0 \\ 0 & 0 \\ 0 & 0 \\ 0 & 0 \end{pmatrix}$$

$$V_2^{-1} = \begin{pmatrix} \frac{n_I\omega(d_I(d_I+r_{PP}P+m_P+m_{PP})+m_Pm_{PP})}{\psi_1} & 0 \\ 0 & \frac{n_I\omega(d_I(d_I+r_PP+m_P++r_{PP}P+m_{PP})+(r_PP+m_P)m_{PP})}{\psi_2} \\ \frac{d_I(d_I+r_{PP}P+m_P+m_{PP})+m_Pm_{PP}}{\psi_3} & 0 \\ 0 & \frac{d_I(d_I+r_{PP}P+m_P+m_{PP})+m_Pm_{PP}}{\psi_3} \\ \frac{r_PP(m_{PP}+d_I)}{\psi_3} & 0 \\ 0 & \frac{r_PP(m_{PP}+d_I)}{\psi_3} \\ \frac{r_PPr_{PP}P}{\psi_3} & 0 \\ 0 & \frac{r_PPr_{PP}P}{\psi_3} \end{pmatrix}$$

$$V_3^{-1} = \begin{pmatrix} \frac{n_I\omega m_P(m_{PP}+d_I)}{\psi_1} & 0 \\ 0 & \frac{n_I\omega(d_I(m_P+r_PP+d_I)+m_{PP}(r_PP+m_P+d_I))}{\psi_2} \\ \frac{m_P(m_{PP}+d_I)}{\psi_3} & 0 \\ 0 & \frac{m_P(m_{PP}+d_I)}{\psi_3} \\ \frac{d_I(r_PP+d_I+m_{PP})+r_PPm_{PP}}{\psi_3} & 0 \\ 0 & \frac{d_I(r_PP+d_I+m_{PP})+r_PPm_{PP}}{\psi_3} \\ \frac{r_{PP}P(r_PP+d_I)}{\psi_3} & 0 \\ 0 & \frac{r_{PP}P(r_PP+d_I)}{\psi_3} \end{pmatrix}$$

$$V_4^{-1} = \begin{pmatrix} \frac{n_I\omega m_Pm_{PP}}{\psi_1} & 0 \\ 0 & \frac{n_I\omega m_{PP}(r_PP+m_P+d_I)}{\psi_2} \\ \frac{m_{PP}m_P}{\psi_3} & 0 \\ 0 & \frac{m_{PP}m_P}{\psi_3} \\ \frac{m_{PP}(r_PP+d_I)}{\psi_3} & 0 \\ 0 & \frac{m_{PP}(r_PP+d_I)}{\psi_3} \\ \frac{d_I(r_PP+d_I+m_{PP})+r_PPm_{PP}}{\psi_3} & 0 \\ 0 & \frac{d_I(r_PP+d_I+m_P+r_{PP}P)+r_PPr_{PP}P}{\psi_3} \end{pmatrix},$$

where

$$\psi_1 = d_I(d_V + r_I T_S^* + r_I T_{PN}^* + r_I T_{PPN}^*)\Big(d_I(d_I + r_P P^* + m_P + r_{PP} P^* + m_{PP}) + m_P m_{PP} + r_P P^* m_{PP} + r_P P^* r_{PP} P^*\Big)$$

$$\psi_2 = d_I(d_V + r_Y T_S^* + r_Y T_{PN}^* + r_Y T_{PPN}^*)\Big(d_I(d_I + r_P P^* + m_P + r_{PP} P^* + m_{PP}) + m_P m_{PP} + r_P P^* m_{PP} + r_P P^* r_{PP} P^*\Big)$$

$$\psi_3 = d_I(d_I(d_I + r_P P + m_P + + r_{PP} P + m_{PP}) + m_P m_{PP}).$$

We have that F is a non-negative matrix, and that V is a non-singular M-matrix (this can be shown in a similar fashion as was done in Appendix A).

This results in the following: $FV^{-1} = [FV_1^{-1}|FV_2^{-1}|FV_3^{-1}|FV_4^{-1}]$ where

$$FV_1^{-1} = \begin{pmatrix} 0 & 0 \\ 0 & 0 \\ \frac{r_I T_S}{d_V + r_I \overline{T}_S + r_I \overline{T}_{PN} + r_I \overline{T}_{PPN}} & 0 \\ 0 & \frac{r_Y T_S}{d_V + r_Y \overline{T}_S + r_Y \overline{T}_{PN} + r_Y \overline{T}_{PPN}} \\ \frac{r_I T_{PPN}}{d_V + r_I \overline{T}_S + r_I \overline{T}_{PN} + r_I \overline{T}_{PPN}} & 0 \\ 0 & \frac{r_Y \overline{T}_{PN}}{d_V + r_Y \overline{T}_S + r_Y \overline{T}_{PN} + r_Y \overline{T}_{PPN}} \\ \frac{r_I T_{PPN}}{d_V + r_I \overline{T}_S + r_I \overline{T}_{PN} + r_I \overline{T}_{PPN}} & 0 \\ 0 & \frac{r_Y \overline{T}_{PN}}{d_V + r_Y \overline{T}_S + r_Y \overline{T}_{PN} + r_Y \overline{T}_{PPN}} \end{pmatrix}$$

$$FV_2^{-1} = \begin{pmatrix} 0 & 0 \\ 0 & 0 \\ \frac{r_I T_S n_I \omega (d_I(d_I + r_{PP} P + m_P + m_{PP}) + m_P m_{PP})}{\psi_1} & 0 \\ 0 & \frac{r_Y T_S n_I \omega (d_I(d_I + r_P P + m_P + r_{PP} P + m_{PP}) + m_{PP}(m_P + r_P P))}{\psi_2} \\ \frac{r_I T_{PN} n_I \omega (d_I(d_I + r_{PP} P + m_P + m_{PP}) + m_P m_{PP})}{\psi_1} & 0 \\ 0 & \frac{r_Y T_{PN} n_I \omega (d_I(d_I + r_P P + m_P + r_{PP} P + m_{PP}) + m_{PP}(m_P + r_P P))}{\psi_2} \\ \frac{r_I T_{PPN} n_I \omega (d_I(d_I + m_P + r_{PP} P + m_{PP}) + m_{PP}(m_P + r_P P))}{\psi_1} & 0 \\ 0 & \frac{r_Y T_{PPN} n_I \omega (d_I(d_I + m_P + r_P P + r_{PP} P + m_{PP}) + m_{PP}(m_P + r_P P))}{\psi_2} \end{pmatrix}$$

$$FV_3^{-1} = \begin{pmatrix} 0 & 0 \\ 0 & 0 \\ \frac{r_I T_S n_I \omega m_P (m_{PP}+d_I)}{\psi_1} & 0 \\ 0 & \frac{r_Y T_S n_I \omega (d_I (m_P + r_P P + d_I) + m_{PP}(r_P P + m_P + d_I))}{\psi_2} \\ \frac{r_I T_{PN} n_I \omega m_P (m_{PP}+d_I)}{\psi_1} & 0 \\ 0 & \frac{r_Y T_{PN} n_I \omega (d_I (d_I + r_P P + m_P + m_{PP}) + m_{PP}(m_P + r_P P))}{\psi_2} \\ \frac{r_I T_{PPN} n_I \omega d_I (r_P P + d_I + m_{PP}) + r_P P m_{PP}}{\psi_1} & 0 \\ 0 & \frac{r_Y T_{PPN} n_I \omega d_I (d_I + r_P P + m_P + m_{PP}) + m_{PP}(m_P + r_P P)}{\psi_2} \end{pmatrix}$$

$$FV_4^{-1} = \begin{pmatrix} 0 & 0 \\ 0 & 0 \\ \frac{r_I T_S n_I \omega m_P m_{PP}}{\psi_1} & 0 \\ 0 & \frac{r_Y T_S n_I \omega m_{PP}(r_P P + m_P + d_I)}{\psi_2} \\ \frac{r_I T_{PN} n_I \omega m_{PP} m_P}{\psi_1} & 0 \\ 0 & \frac{r_Y T_{PN} n_I \omega m_{PP}(m_P + r_P P + d_I)}{\psi_2} \\ \frac{r_I T_{PPN} n_I \omega m_{PP} m_P}{\psi_1} & 0 \\ 0 & \frac{r_Y T_{PPN} n_I \omega m_{PP}(r_P P + d_I + m_P)}{\psi_2} \end{pmatrix},$$

where ψ_1, ψ_2 and ψ_3 are described as before. The spectral radius of FV^{-1} shown in the article is the basic reproductive number.

Appendix F

Region 4: Region of viral elimination; Miron and Smith? [4]

The following Appendix shows more details of the work presented in Region 4 of the manuscript in Chapter 3.2. We include many steps that are omitted in the manuscript. This Appendix only includes extra details on finding the mathematical results, thus it is only used to complete the manuscript. The Appendix does not include all of the manuscript.

Region 4 is a subset of the subregion model (E.0.1) for Region 3.

F.1 Disease-free equilibrium

The disease-free equilibrium in Region 4 shown in the article is found by letting $P^* \to \infty$ in the disease-free equilibrium for Region 3.

F.1.1 Local stability analysis

The Jacobian matrix at the disease-free equilibrium is given by $J = [J_1|J_2|J_3]$, where

$$J_1 = \begin{bmatrix} -d_V - r_I T_{PPN} & 0 & 0 & 0 \\ 0 & -d_V - r_Y T_{PPN} & 0 & 0 \\ 0 & 0 & -d_V & 0 \\ 0 & 0 & 0 & -d_S - r_P P \\ 0 & 0 & 0 & 0 \\ 0 & 0 & 0 & 0 \\ 0 & -r_Y T_{PN} & 0 & r_P P \\ 0 & 0 & 0 & 0 \\ 0 & 0 & 0 & 0 \\ -r_I T_{PPN} & -r_Y T_{PPN} & 0 & 0 \\ r_I T_{PPN} & 0 & 0 & 0 \\ 0 & r_Y T_{PPN} & 0 & 0 \\ 0 & 0 & 0 & 0 \end{bmatrix}$$

$$J_2 = \begin{bmatrix} n_I\omega & 0 & 0 & 0 \\ 0 & n_I\omega & 0 & 0 \\ n_I(1-\omega) & n_I(1-\omega) & 0 & n_I \\ 0 & 0 & m_P & 0 \\ -d_I - r_P P & 0 & 0 & m_P \\ 0 & -d_I - r_P P & 0 & 0 \\ 0 & 0 & -m_P - d_S - r_{PP} P & 0 \\ r_P P & 0 & 0 & -m_P - d_I - r_{PP} P \\ 0 & r_P P & 0 & 0 \\ 0 & 0 & r_{PP} P & 0 \\ 0 & 0 & 0 & r_{PP} P \\ 0 & 0 & 0 & 0 \\ 0 & 0 & 0 & 0 \end{bmatrix}$$

$$J_3 = \begin{bmatrix} 0 & 0 & 0 & 0 & 0 \\ n_I\omega & 0 & 0 & 0 & 0 \\ n_I(1-\omega) & 0 & n_I & n_I & 0 \\ 0 & 0 & 0 & 0 & 0 \\ 0 & 0 & 0 & 0 & 0 \\ m_P & 0 & 0 & 0 & 0 \\ 0 & m_{PP} & 0 & 0 & 0 \\ 0 & 0 & m_{PP} & 0 & 0 \\ -m_P - d_I - r_{PP}P & 0 & 0 & m_{PP} & 0 \\ 0 & -m_{PP} - d_S & 0 & 0 & 0 \\ 0 & 0 & -m_{PP} - d_I & 0 & 0 \\ r_{PP}P & 0 & 0 & -m_{PP} - d_I & 0 \\ 0 & 0 & 0 & 0 & -d_P \end{bmatrix}.$$

If we factor out $(-d_V-\mu)$ and $(-d_P-\mu)$ knowing these eigenvalues are negative, we have the following for the characteristic equation

$$
\begin{aligned}
0 = \Big[&(-m_P-d_S-r_{PP}P-\mu)\\
&\times\begin{vmatrix}
-d_V-r_YT_{PPN} & n_I\omega & n_I\omega & 0 & 0\\
0 & -d_I-r_PP & m_P & 0 & 0\\
0 & r_PP & -d_I-m_P-r_{PP}P & 0 & m_{PP}\\
-r_YT_{PPN} & 0 & 0 & -m_{PP}-d_S & 0\\
r_YT_{PPN} & 0 & r_{PP}P & 0 & -m_{PP}-d_I
\end{vmatrix}\\
&+\begin{vmatrix}
-d_V-r_YT_{PPN} & n_I\omega & 0 & n_I\omega & 0\\
0 & -d_I-r_PP & 0 & m_P & 0\\
0 & r_PP & 0 & -d_I-m_P-r_{PP}P & m_{PP}\\
-r_YT_{PPN} & 0 & r_{PP}P & 0 & 0\\
r_YT_{PPN} & 0 & 0 & r_{PP}P & -m_{PP}-d_I
\end{vmatrix}\\
&\times m_{PP}\Big]\\
&\times\Big[(-d_V-r_IT_{PPN}-\mu)(-d_S-r_PP-\mu)(-d_I-r_PP-\mu)\big(-r_{PP}Pm_{PP}\\
&-(-m_{PP}-d_I-\mu)(-m_P-d_I-r_{PP}P-\mu)\big)-m_Pr_PP(-d_V-r_IT_{PPN}-\mu)\\
&\times(-d_S-r_PP-\mu)(-m_{PP}-d_I-\mu)+n_I\omega m_Pm_{PP}r_IT_{PPN}(-d_S-r_PP-\mu)\Big]\\
&-n_I\omega m_Pm_{PP}r_IT_{PPN}m_Pr_{PP}(-m_{PP}-d_S-\mu)\\
&\times\begin{vmatrix}
-d_V-r_YT_{PPN}-\mu & n_I\omega & n_I\omega & 0\\
0 & -d_I-r_PP-\mu & m_P & 0\\
0 & r_PP & -m_P-r_{PP}P-d_I-\mu & m_{PP}\\
r_YT_{PPN} & 0 & r_{PP}P & -m_{PP}-d_I-\mu
\end{vmatrix}
\end{aligned}
$$

$$
\begin{aligned}
= \Bigg[& \Big((-d_V - r_I T_{PPN} - \mu)(-d_S - r_P P - \mu)(-d_I - r_P P - \mu)\big(- r_{PP} P m_{PP} \\
& - (-m_{PP} - d_I - \mu)(-m_P - d_I - r_{PP} P - \mu)\big) - m_P r_P P(-d_V - r_I T_{PPN} - \mu) \\
& \times (-d_S - r_P P - \mu)(-m_{PP} - d_I - \mu) + n_I \omega m_P m_{PP} r_I T_{PPN}(-d_S - r_P P - \mu)\Big) \\
& \times \Big((-m_P - d_S - r_{PP} P - \mu)(-m_{PP} - d_S - \mu) - m_{PP} r_{PP} P \Big) \\
& - n_I \omega m_P m_{PP} r_I T_{PPN} m_P r_{PP}(-m_{PP} - d_S - \mu) \Bigg] \\
\times & \begin{vmatrix}
-d_V - r_Y T_{PPN} - \mu & n_I \omega & n_I \omega & 0 \\
0 & -d_I - r_P P - \mu & m_P & 0 \\
0 & r_P P & -m_P - r_{PP} P - d_I - \mu & m_{PP} \\
r_Y T_{PPN} & 0 & r_{PP} P & -m_{PP} - d_I - \mu
\end{vmatrix}.
\end{aligned}
$$

Solving the polynomial and dividing each term by P^{*4}, we get

$$
\begin{aligned}
0 = {} & \mu^3 + \mu^2(2m_{PP} + d_S + d_I + d_V + r_I T^*_{PPN}) + \mu(m_{pp}(d_S + d_V + r_I T^*_{PPN}) \\
& + (d_I + m_{PP})(d_V + r_I T^*_{PPN}) + d_S(d_I + m_{PP} + d_V + r_I T^*_{PPN})) + m_{PP} d_S(d_V + r_I T^*_{PPN}) \\
& + d_S(d_I + m_{PP})(d_V + r_I T^*_{PPN}),
\end{aligned}
$$

where the positivity conditions in the article are satisfied. We also need to show that if we have $\mu^3 + b_1\mu^2 + b_2\mu + b_3 = 0$, that $b_1 b_2 - b_3 > 0$. In this case, we have

$$
\begin{aligned}
b_1 b_2 - b_3 = {} & (2m_{PP} + d_S + d_I + d_V + r_I T^*_{PPN})(m_{pp}(d_S + d_V + r_I T^*_{PPN}) \\
& + (d_I + m_{PP})(d_V + r_I T^*_{PPN}) + d_S(d_I + m_{PP} + d_V + r_I T^*_{PPN})) \\
& - m_{PP} d_S(d_V + r_I T^*_{PPN}) - d_S(d_I + m_{PP})(d_V + r_I T^*_{PPN}) \\
= {} & (2m_{PP} + d_S + d_I + d_V + r_I T^*_{PPN})(m_{pp}(d_S + d_V + r_I T^*_{PPN}) \\
& + d_I(d_V + r_I T^*_{PPN}) + d_S(d_I + m_{PP})) + (2m_{PP} + d_I + d_V + r_I T^*_{PPN}) \\
& \times (m_{PP}(d_I + m_{PP}) + d_S(d_V + r_I T^*_{PPN})),
\end{aligned}
$$

which is greater than zero. The results follow in the article.

Solving the matrix in the characteristic polynomial, we get

$$
\begin{aligned}
0 = (-d_I - r_P P - \mu) &\begin{vmatrix} -d_V - r_Y T_{PPN} & n_I\omega & 0 \\ 0 & -m_P - r_{PP}P - d_I & m_{PP} \\ r_Y T_{PPN} & r_{PP}P & -m_{PP} - d_I \end{vmatrix} \\
- m_P &\begin{vmatrix} -d_V - r_Y T_{PPN} & n_I\omega & 0 \\ 0 & r_{PP}P & m_{PP} \\ r_Y T_{PPN} & 0 & -m_{PP} - d_I \end{vmatrix} \\
= (-d_I - r_P P - \mu)&(-d_V - r_Y T_{PPN} - \mu)((-m_P - r_{PP}P - d_I - \mu)(-m_{PP} - d_I - \mu) \\
&- m_{PP} r_{PP} P) + (-d_I - r_P P - \mu) n_I \omega m_{PP} r_Y T_{PPN} - m_P r_P P(-d_V - r_Y T_{PPN} - \mu) \\
&\times (-m_{PP} - d_I - \mu) - m_P n_I \omega m_{PP} r_Y T_{PPN}
\end{aligned}
$$

If we divide each term by P^{*2} and take $P^* \to \infty$, we get

$$0 = \lambda^2 + \lambda(d_V + r_Y T^*_{PPN} + d_I) + (d_V + r_Y T^*_{PPN}) d_I.$$

The results in the article follow for the stability of the disease-free equilibrium.

Appendix G

Additional information; Section 3.2

Simulation details and positivity conditions for the manuscript in Section 3.2; Miron and Smith? [4]

Numerical Simulations: The software used to plot the figures in the manuscript presented in Section 3.2 [4] was Matlab.

Figure 2 is a plot of the curve

$$s(t) = \frac{R(t)}{R(t) + IC_{50}},$$

the inhibition of viral replication (page 3 of manuscript in Section 3.1). The values used to plot this curve can be found in Table 2 of the manuscript in Section 3.2 and in Table C.1 below.

Table C.1. Parameters used in Figure 2.

Parameter/state variable	Units	Range	References
P^i	μM	15.5	[145]
d_P	days^{-1}	24 ln(2)/(6.2)	[22]
τ	days	0.5	[145]
IC_{50}	μM	0.02	[145]

Figure 3 plots the equations from page 26 of the manuscript [4]. All the parameters are presented in Table 2.

The parameters and initial conditions used to plot Figure 4 are presented in Table 2. We used *ode*45 to solve the ordinary differential system between the three regions. We reset the initial conditions when an impulse occurs, meaning we add P^i to the drug equation and do not change any other solution (since the impulse only affects the drug). We then run the ordinary differential equations again.

Figures 6–9 are derived from the same procedures as explained in Appendix B (Sensitivity Analysis).

Positivity of Solutions: We will now show the positivity of solutions. We will show this for the entire system, meaning the results follow for each subregion (Regions 1, 2 and 3). We prove that if $V_I(0) \geq 0, V_Y(0) \geq 0, V_{NI}(0) \geq 0, T_S(0) \geq 0, T_I(0) \geq 0, T_Y(0) \geq 0, T_{PN}(0) \geq 0, T_{PI}(0) \geq 0, T_{PY}(0) \geq 0, T_{PPN}(0) \geq 0, T_{PPI}(0) \geq 0, T_{PPY}(0) \geq 0$, then these variables stay nonnegative in $t > 0$.

Proof of positivity: Note that we can write our equations as $x' = F(x) - G(x)$ where $F(x) = \{n_I\omega T_I, n_I\omega(T_Y + T_{PY}), n_I(1-\omega)(T_I + T_Y + T_{PY}) + n_I(T_{PI} + T_{PPI} + T_{PPY}, \lambda + m_P T_{PN}, r_I T_S V_I + m_P T_{PI}, r_Y T_S V_Y + m_P T_{PY}, \alpha_1 r_P P T_S + m_{PP} T_{PPN}, r_I T_{PN} V_I + \alpha_1 r_P P T_I + m_{PP} T_{PPI}, r_Y T_{PN} V_Y + \alpha_1 r_P P T_Y + m_{PP} T_{PPY}, \alpha_2 r_{PP} P T_{PN}, r_I T_{PPN} V_I + \alpha_2 r_{PP} P T_{PI}, r_Y T_{PPN} V_Y + \alpha_2 r_{PP} P T_{PY}\}$ and all remaining terms are in $G(x)$. Now notice that, in $x \geq 0$, $F(x) \geq 0$ and, for each x_i, $G_i(x) = 0$ if $x_i = 0$. Thus if the moving point $\{x_1, x_2, x_3, x_4, x_5, x_6, x_7, x_8, x_9, x_{10}, x_{11}, x_{12}\}$ is in the nonnegative space, then no compartment of $F(x)$ is negative, and if the point is on any "plane" $x_i = 0$, then that compartment cannot become negative (because $x_i = F_i(x) - G_i(x) \geq 0$). Considering that the right-hand sides are polynomials, this proves the invariance of the positive space of our system.

Errata: *Equilibrium T cell counts:* The total uninfected T cell count for Region 2 (page 25, paragraph 2), should be an inequality instead of an equality. It should

read

$$T_S^* + T_{PN}^* \leq T_S^* + \frac{r_P P^* T_S^*}{m_P + d_S}.$$

Discussion Figures 4 and 5 (page 27): Figures 4 and 5 describe trajectories either remaining within a region (Figure 4, page 42) or crossing multiple regions (Figure 5, page 43). Since impulses are included, we expect sudden changes in the behaviour of the trajectories when an impulse occurs. For example, in Figure 4(a), the cusp is actually just a corner since no impulses occur (in Region 1). Figure 5(c) appears to have two impulses, but this is misleading. The dynamics are such that trajectories seem to increase in both the wild-type and mutant initially (mostly wild-type, since we are moving from Region 1 to Region 2), then an impulse occurs that drives the wild-type and mutant towards zero. There is a second cusp that seems to occur where we do not have an impulse. In this case, we have a corner that seems to indicate leaving Regions 3/4 (see Figure G.1 for a close up). We enter Region 2, where we have an increase in the mutant population, and then fall into Region 1, where we have an increase in the wild-type population.

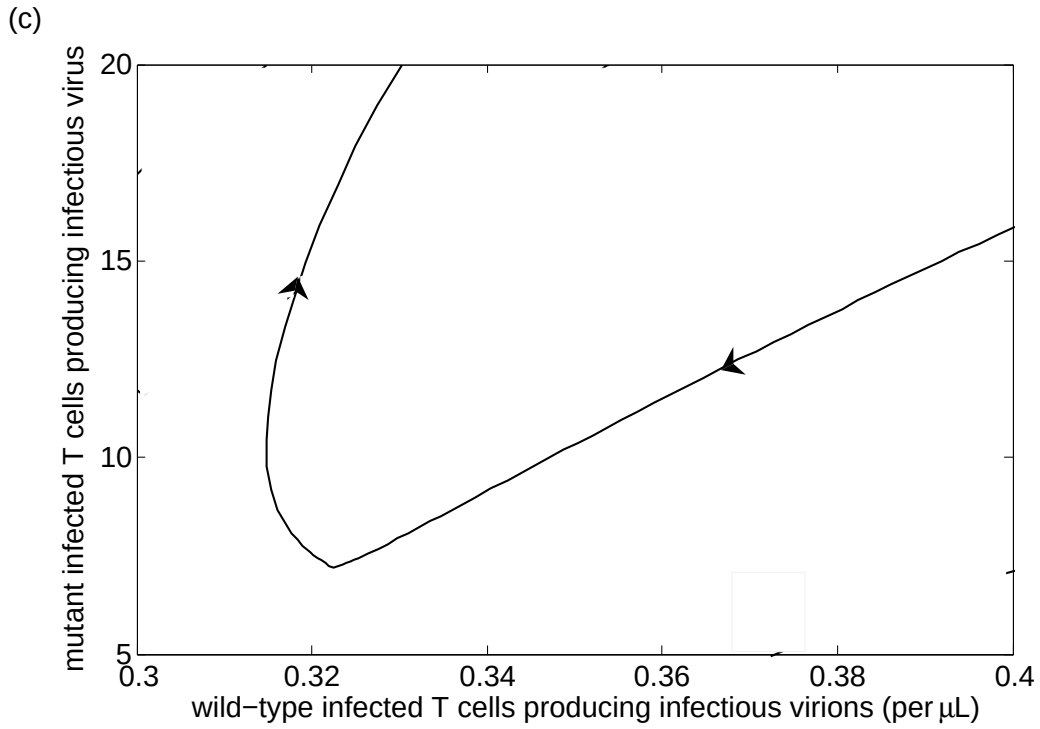

Figure G.1: Closer look at Figure 5(c) in manuscript: The behaviour when trajectories of drug concentrations cross all regions.

Appendix H

Rift Valley Fever

H.1 Etiology

RVF is a member of the Bunyavridae family of viruses; all five genera in this family are pathogenic [47, 50]. RVF belongs to the Phlebovirus genus, which is one of three arthropod-borne genera in Bunyavridae [47, 50]. Most members of Phlebovirus are transmitted by sandflies; however, RVF is typically transmitted by mosquitoes under natural circumstances [46, 51]. RVF's nucleocapsid is sphere-shaped, encased in a bilayered lipid envelope and encrusted with glycoprotein spikes [50]. House et al. state that RVF is approximately 90-100 nm in diameter [50], while Gerdes states that it can reach 120 nm in diameter [47]. There are three segments to RVF's single-stranded ribonucleic genome [47, 50].

H.2 Vectors

RVF is transmitted to vertebrate hosts by an extremely wide variety of arthropod vectors: over 40 species of mosquitoes from eight different genera have been isolated in the field [46, 51]. Mosquitoes appear to be the primary vector in RVF transmission

and are involved with its maintenance; sandflies are capable of transmitting the virus in a laboratory setting [46, 47, 51]. Mosquitoes belonging to the Aedes genus are an important vector, as they may vertically transmit infection to their young through transovarial transmission, enabling the maintenance of RVF during interepizootic periods [47, 48]. Culex species and those belonging to Eretmapodites are believed to be strongly involved with epizootic outbreaks; no evidence has been found to indicate that Culex spp. are capable of transovarial transmission [47, 48]. RVF can also be transmitted through aerosol exposure from handling infected carcasses; laboratory workers, veterinarian, and individuals involved with meat processing are particularly vulnerable to this form of infection [45, 46, 47, 48, 51].

A vector's ability to transmit a virus is based on a number of intrinsic and extrinsic factors; as such, not all vectors are equally competent or capable of transmission [47]. In order for a mosquito to successfully transmit the virus to a vertebrate host, the mosquito itself must be susceptible to oral infection. Once the mosquito is infected, the virus must be capable of disseminating beyond the mosquito's midgut to its salivary glands [46, 47, 51]. This is not always possible, as different mosquito species have different biological barriers [46, 47, 51]. For example, Turell et al. found that vector competence in Culex species was mostly determined by the midgut escape barrier, while competence was limited by salivary gland barriers in Aedes [51]. Extrinsic factors such as temperature and rainfall have an extremely important impact on the vector capacity of different mosquitoes as they affect their susceptibility and ability to transmit infection; these factors also influence host availability and density [41, 43, 47, 48, 149].

H.3 Hosts

RVF has a very wide range of viable vertebrate hosts, as one might expect when considering the diversity of its vectors [52]. RVF's most significant amplifier hosts

are domestic ruminants such as sheep and cattle [46, 47, 51, 52]. Newborn lambs and kids are most susceptible to disease, followed by calves and sheep [47, 50]. Moderate disease occurs in adult cattle, sheep, goats, humans, water buffalo and rats; humans and ruminants are capable of developing enough viraemia to infect mosquitos [47, 50]. Camels, horses, pigs, cats, dogs, guinea pigs, rabbits, hedgehogs and monkeys are susceptible, but do not necessarily display clinical disease [47, 50]. Birds, with the exception of pigeons and chickens, and rerptiles are believed to be resistant to infection [47, 50]. Balkhy & Memish [52] state that fatality in adult cattle and sheep can be as high as 30%, while young animals may experience 100% fatality. Gerdes [50] states that disease is most significant in young animals, particularly lambs and kids, which may experience 70-100% mortality. Newborns typically experience 100% fatality and most epidemics are defined by high incidences of fetal death, or as Gerdes wrote: abortion storms [50].

RVF tends to localize in the liver of humans and animals; it may also localize in other organs such as the brain and spleen [47, 50]. Both animals and humans may experience fever and hepatitis [52]. Abortion is a medically and economically significant manifestation of RVF in susceptible animal hosts [47, 50, 52]. Clinical disease varies with host species and is generally most severe in younger hosts [47, 50]. For example, clinical disease in lambs is characterized by 90-100% mortality, weakness, anorexia and listlessness, while adult cattle typically display fever and experience mortality rates of 10% at most [47]. Prior to the Egyptian outbreak in 1977, clinical disease in humans had mostly been asymptomatic or quite mild, often manifesting as with influenza-like symptoms, febrile illness and occasionally retinitis [46, 47, 50, 52]. Although the majority of clinical disease continues to be mild, complications such as encephalitis may occur and less than 1% of cases may present as a potentially fatal haemorrhagic fever [46, 47, 50, 52].

In order for a vector-borne emerging infectious disease to become endemic in a new location, there must be a sufficient number of susceptible hosts and competent

vectors [53]. Due to RVF's large range of viable hosts and vectors, its potential to establish itself elsewhere is especially high compared to other vector-borne diseases. Gaff *et al.* [54] modelled RVF's transmission using an ordinary differential equation model for two populations of mosquito species — those that can transmit vertically and those that cannot — and one population of domestic livestock animals with disease-dependent mortality. They analyzed the model to find the stability of the disease-free equilibrium and tested which model parameters affect the stability most significantly. By changing the values for contact rates and death rates associated with cattle, the authors showed that, for any given contact rate, there is a low level of endemic prevalence, meaning the disease could persist if introduced in an isolated system.

H.4 Epidemiology

Outbreaks of RVF are cyclical and are characterized by epizootic periods and interepizootic periods [47, 50, 51]. In order for an epizootic period to occur, there must be a significant number and density of effective vectors and susceptible amplifying hosts [47]. The duration and maintenance of the transmission cycle during interepizootic periods are dependent on geographic location, climatic conditions and available host and vector species [41, 47, 50, 51].

Interepizootic periods tend to be shorter in wetter climates [50]. RVF is believed to be maintained during interepizootic periods through enzootic cycles, transovarial transmission and possibly through ruminant migration [50]. Aedes mosquitoes are floodwater mosquitoes that typically lay their eggs on dry substrate where they remain dormant for extended periods of time until flooding events; species capable of transovarial transmission enable the persistence of the virus [41, 44, 47, 50, 51]. In northern and western Africa, endemic cycles are enabled by vectors that breed on stagnant water and are active year round [50].

The effects of environmental conditions on the spread of the disease [150, 151], demonstrate that the incidence of many vector-borne infectious diseases shows seasonality, and extreme weather events are frequently accompanied by additional outbreaks. Bicout and Sabatier [150] constructed a model showing the effects of rainfall trajectories on RVF mosquito vectors in the course of time. They assessed the prevalence of RVF in a population of susceptible hosts as a consequence of rainfall. Spatial spread of the virus was also examined by Favier *et al.* [152] to assess the possibility of endemicity without wild animals providing a permanent virus reservoir. They showed that endemicity without a permanent virus reservoir would be impossible in a single site except when there is a strictly periodic rainfall pattern; however, it would be possible when there are herd movements and there is sufficient inter-site variability in rainfall, which drives mosquito emergence.

Epidemics are typically initiated by the appearance and increased activity of large populations of vectors [50]. RVF's vectors and the virus itself are ectothermic; as such, their reproductive capacity and success are directly related to climate [42]. In sub-Saharan Africa where transovarial transmission occurs, epidemics are strongly correlated with significant flooding events, such as those related to heavy rainfall from warm ENSO events [41, 42, 44, 47, 50, 51]. In areas where transovarial transmission does not occur, epidemics are not necessarily correlated with heavy rainfall events and may be initiated by migration of infected animals, anthropogenic activity such as dam building or irrigation, mosquitoes blown in by the wind from endemic areas or even as a result of increased host susceptibility induced by other diseases [39, 45, 49, 50, 149]. Outbreaks may be controlled through costly vaccination and vector-control programs [41, 47]. Gaff *et al.* [153] extended their original model [54] in order to compare efficacy of vaccination with alternative countermeasures such as managing mosquito population or destroying infected livestock. The model was also modified by including logistic growth for the mosquito population. Their results suggested that livestock vaccination and culling offered the greatest benefit in terms of reducing livestock

morbidity and mortality.

H.5 Discussion: RVF's Potential to Spread

RVF's 1977 outbreak in Egypt established its potential as an emerging infectious disease due to its expansion beyond its native sub-Saharan range and because of its increased virulence in human hosts. The success of an emerging disease is defined by its ability to disseminate and establish itself outside its natural boundaries [39].

In order for a vector-borne emerging infectious disease to become endemic in a new location, there must be a sufficient number of susceptible hosts and competent vectors [47]. Due to RVF's large range of viable hosts and vectors, its potential to establish itself elsewhere is especially high in respect to other vector borne diseases. A number of studies have demonstrated that many European and North American mosquitoes, including floodwater species possibly capable of transovarial transmission, can become viremic and are able to transmit the virus under laboratory settings [45, 46, 47].

Dissemination from established populations to novel ones is called microbial traffic, a process that is frequently exasperated by anthropogenic activity [39]. Increased microbial traffic resulting from international trade and travel are particular concerns for RVF due the virus' ability to create significant viraemia in both livestock and humans; Meegan, for example, postulated that RVF disseminated to Egypt via the movement of UN troops [49]. In 1992, House et al. [47] wrote that the international trade of live, and potentially viremic, animals posed a significant threat and deemed it fortuitous that RVF had not yet established itself in the Arabian Peninsula. The Arabian Peninsula's fortunes changed in 2000 when not one, but two outbreaks of RVF occurred with the highest human case fatality rate to date [52]. Anthropogenic change to natural ecosystem processes is also a driving process behind the emergence of infectious disease; in RVF's case, dam construction and agricultural activity such as

irrigation have played a particularly important role in its success [39, 40]. Agricultural and economic development can expose new populations to disease through proximity, or create favourable conditions for an outbreak; in RVF's case, dam construction and irrigation can increase flooding, enabling an outbreak by allowing mosquito vectors to reach a sufficiently high density [39, 44]. Flooding activity resulting from the completion of the Aswan dam is believed to have enabled the 1977 outbreak in Egypt [52]. This trend was also notably observed in the Mauritanian outbreak of 1987, which followed the construction of the Diama dam along the Senegal River [39, 52]. Global climate change also has great potential to affect incidences of RVF outbreaks as many of its vectors are strongly affected by climatic variability [42].

H.6 Conclusion

Since its identification in 1931, RVF has spread from sub-Saharan Africa all the way to the Arabian Peninsula. RVF's potential to spread outside its current range is of great concern due to the plausibility of that situation and because of its ability to cause both economic and human loss. This potential is based on the availability of viable hosts and vectors, as well as appropriate environmental conditions. Preparedness, recognition of the clinical signs and an active disease-reporting system will all be necessary to moderate the consequences of any outbreaks in novel environments [47].

Appendix I

Additional information; Section 5.1

Simulation details and extra comments for the manuscript in Section 5.1; Miron and Smith? [5]

Numerical Simulations: The software used to plot the figures in the manuscript presented in Section 5.1 was Matlab.

Figure 2 is a plot of the curve presented by equation (68) in the manuscript. The total livestock population is assumed to be 1000. All the parameters are presented in Table 2 of the manuscript.

The parameters used to plot Figure 3–6 are presented in Table 2 in the manuscript. The initial conditions are assumed to be 1000 for the susceptible and livestock populations, 10,000 for the susceptible mosquito population and 10 for the infected mosquito population. All other initial conditions are set to zero. For Figures 5 and 6, the impulses occur after 230 days. We used $d_3 = 1/5$ for the figures where $R_0 < 1$, and we used $d_3 = 1/20$ for the figures where $R_0 > 1$. We used *ode*45 to numerically solve the ordinary differential equations. We reset the initial conditions when an impulse occured, meaning we add the impulse conditions presented by the difference equations (6)–(8) in the manuscript. We then ran the ordinary differential equations again. Table I.1 shows the parameters used for the impulse conditions.

Table I.1. Range of parameters.

Parameter	Value
r_1	0.1
r_2	0.4
r_3	0.98
p_1	0.1
p_2	0.4
p_3	0.01
c	10

Figure 7 is derived from the same procedures as explained in Appendix B (Sensitivity Analysis). Figure 8 plots the coefficients described by equations (37)–(39). The parameters used are presented in Table 2 of the manuscript. Figure 9 plots the curves

$$y = x^3$$

$$y = Ax + B,$$

where A and B are described by equations (51) and (52) in the manuscript. The parameters used are presented in Table 2 of the manuscript.

Errata:

1. Table 1. The units for β_{LH} should be days^{-1}.

2. On page 9, paragraph 1 of Section 3, line 5, it should read "In the case of RVF, we only consider sufficiently small perturbations away from the disease-free equilibrium because the disease is **not** present in North America."

3. On page 9, paragraph 2 of Section 3, line 2, it should read "For fixed parameters and **fixed state variables**, the stability changes as the mosquito death rate d_M varies."

4. On page 12, first paragraph, line 3, it should read "A fraction p_1 of the population dies and is replaced with an equal fraction."

5. On page 12, last paragraph, line 1, it should read "r_3 is the fraction of decrease in the mosquito population."

6. In the last sentence of Section 5.1, bottom of page 15, we say "The infection does not completely eradicate the virus, which suggests that the endemic equilibrium is stable." In this case, we are talking about how, when $R_0 > 1$, the infection is not completely eradicated. It is not the infection that eradicates a virus. This sentence is meant to further explain that, since the infected populations persist for $R_0 > 1$, the endemic equilibrium is stable.

7. We also need to highlight a discrepancy in the last sentence of Section 5.3, pages 17–18. We say "R_0 is most sensitive to the mosquito death rate, as Figure 7(b) shows". Figure 7(a) is the partial rank correlation coefficient sensitivity analysis on R_0 for all parameters, whereas Figure 7(b) is the the effect of the disease death rate on R_0 using Latin Hypercube Sampling. We thus have that Figure 7(a) shows that R_0 is most sensitive to the mosquito death rate. Figure 7(b) only shows the effect of the disease death rate on R_0, and not that R_0 is most sensitive to the disease death rate.

8. On page 21, paragraph 2, there is a discrepancy from an earlier version of the paper. It should read "The sufficient and necessary condition given in Section A.2 to have eigenvalues with negative real part (ensuring that the disease-free equilibrium is stable) is $0.15 < d_M < 0.68$, where d_M is the mosquito death rate." The next three sentences should be ignored since this was later proven in the recent version of the manuscript.

Bibliography

[1] Bainov, D., Simeonov, P. 1993. *Impulsive differential equations: periodic solutions and applications* UK: Longman Scientific & Technical.

[2] Lakshmikantham, V., Bainov, D., Simeonov, P. 1989. *Theory of impulsive differential equations* SG: World Scientific Publishing Co. Pte. Ltd.

[3] Miron, R. E., Smith?, R. J. 2010. Modeling imperfect adherence to HIV induction therapy. *BMC Infectious Diseases* **10**:6.

[4] Miron, R.E., Smith?, R.J. 2014. Resistance to protease inhibitors in a model of HIV-1 infection with impulsive drug effects. *Bulletin of Mathematical Biology.* **76**:1, 59-97.

[5] Miron, R. E., Giordano, G. A., Kealey, A. D., Smith?, R. J. 2012. A multi-season transmission model for Rift Valley Fever: Invasion analysis in North America. *Population Studies on Modeling Infectious Diseases.* (in press).

[6] UNAIDS World AIDS Day Report. How to get to zero: Faster. Smarter. Better. 2011. *Joint United Nations Programme on HIV/AIDS (UNAIDS)*

[7] Wahl, A., Swanson, M.D., Nochi, T., Olesen, R., Denton, P.W., Chateau, M., Garcia, J.V. 2012. Human Breast Milk and Antiretrovirals Dramatically Reduce Oral HIV-1 Transmission in BLT Humanized Mice. *PLoS Pathog* **8**(6): e1002732.

[8] World Health Organization. Millennium Development Goals: progress towards the health-related Millennium Development Goals. May 2011.

[9] Mbirimtengerenji, N.D. 2007. Is HIV/AIDS epidemic outcome of poverty in Sub-Saharan Africa? *Croat Med.* **48**, 605-17.

[10] Oni, A.A. 2005. Education: An antidote for the spread of HIV/AIDS. *Journal of the Association of Nurses in AIDS care* **16**:2, 40-48.

[11] Dempster, C, (2002, April 9). Rape - Silent war on South African women. BBC News.

[12] Janeway, C., Travers, P., Walport, M., Shlomchik, M. 2006. *Immunobiology: the immune system in health and disease, 6th edition.* GS: Garland Science, Taylor & Francis Group, pg. 461-50.

[13] NBC news. New HIV strain detected in Cameroon woman. August 2, 2009. *Associated Press.* Washington.

[14] De Clercq, E. 2009. Anti-HIV drugs: 25 compounds approved within 25 years after the discovery of HIV. *International Journal of Antimicrobial Agents* **33**(4), 307-320.

[15] Bartlett, J. A. 2002. Addressing the challenges of adherence. *J. Acq. Immun. Def. Synd.* **29**, Suppl. 1, 2-10.

[16] Smith?, R.J. 2006. Adherence to antiretroviral HIV drugs: how many doses can you miss before resistance emerges? *Proceedings of the Royal Society of London Series B: Biological Sciences* **273**(1586), 617-624.

[17] Havlir D.V., Marschner I.C., Hirsch M.S., Collier A.C., Tebas P., Bassett R.L., Ioannidis J.P., Holohan M.K., Leavitt R., Coone G., Richman D.D. 1998. Maintenance antiretroviral therapies in HIV infected patients with undetectable

plasma HIV RNA after triple-drug therapy. AIDS Clinical Trials Group Study 343 Team. *N Engl J Med* **339**, 1261-1268.

[18] Descamps D, Flandre P, Calvez V, Peytavin G, Meiffrédy V, Collin G, Delaugerre C, Robert-Delmas S, Bazin B, Aboulker JP, Pialoux G, Raffi, F, Brun-Vézinet F. 2000. Mechanisms of virologic failure in previously untreated HIV-infected patients from a trial of induction-maintenance therapy. *JAMA* **283**, 205-211.

[19] Curlin M, Iyer S, Mittler J. 2007. Optimal timing and duration of induction therapy for HIV-1 infection. *PLoS Comput Biol* **3**(7), e133.

[20] Havlir D, Hellmann NS, Petropoulos CJ, Whitcomb JM, Collier AC, Hirsch MS, Tebas P, Sommadossi JP, Richman DD. 2000. Drug Susceptibility in HIV infection after Viral Rebound in Patients Recieving Indinavir-Containing Regimens. *JAMA* **283**, 299-234.

[21] Smith, R.J., Wahl, L.M. 2004. Distinct effects of protease and reverse transciptase inhibition in an immunological model of HIV-1 infection with impulsive drug effects. *Bull. Math. Biol.* **66**, 1259-1283.

[22] Smith, R.J., Wahl, L.M. 2005. Drug resistance in an immunological model of HIV-1 infection with impulsive drug effects. *Bulletin of Mathematical Biology* **67**, 783-813.

[23] Perelson, A.S., Nelson, P.W. 1999. Mathematical Analysis of HIV-1 Dynamics in Vivo. *Society for Industrial and Applied Mathematics.* **41**: 1, 344.

[24] Heffernan, J.M., Wahl, L.M. 2005. Monte Carlo estimates of natural variation in HIV infection. *Journal of Theoretical Biology.* **236**, 137153.

[25] Heffernan, J.M., Wahl, L.M. 2006. Natural variation in HIV infection: Monte Carlo estimates that include CD8 effector cells. *Journal of Theoretical Biology.* **243**, 191204.

[26] Wang, Y., Zhou, Y., Brauer, F., Heffernan, J.M. 2012. Viral dynamics model with CTL immune response incorporating antiretroviral therapy. *J. Math. Biol.* DOI 10.1007/s00285-012-0580-3.

[27] Pearson, J.E., Krapivsky, P., Perelson, A.S. 2011. Stochastic theory of early viral infection: continuous versus burst production of virions. *PLoS Comput. Biol.* **7**:2, 117.

[28] de Leenheer, P., Smith, H.L. 2003. Virus dynamics: a global analysis. *SIAM J. Appl. Math.* **63**, 13131327.

[29] Qesmi, R., Wu, J., Wu, J., Heffernan, J.M. 2010. Influence of backward bifurcation in a model of hepatitis B and C viruses. *Mathematical Biosciences.* doi:10.1016/j.mbs.2010.01.002.

[30] Callaway, D.S., Perelson, A.S. 2002. HIV-1 Infection and Low Steady State Viral Loads. *Bulletin of Mathematical Biology.* **64**, 2964.

[31] Stancevic, O., Angstmann, C.N., Murray, J.M., Henry, B.I. 2013. Turing Patterns from Dynamics of Early HIV Infection. *Bull. Math. Biol.* **75**, 774795.

[32] Wanga, Y., Zhou, Y., Wub, J., Heffernan, J. 2009. Oscillatory viral dynamics in a delayed HIV pathogenesis model. *Mathematical Biosciences.* **219**, 104112.

[33] Yuan, Z., Zou, X. 2013. Global threshold dynamics in an HIV virus model with nonlinear infection rate and distributed invasion and production delays. *Mathematical Biosciences and Engineering.* **10**: 2, 483-498.

[34] Smith?, R.J., Aggarwala, B.D. 2009. Can the viral reservoir of latently infected $CD4^+$ T cells be eradicated with antiretroviral HIV drugs? *Journal of Mathematical Biology.* **59**(5), 697-715.

[35] Krakovska, O., Wahl, L.M. 2007. Optimal drug treatment regimens for HIV depend on adherence. *Journal of Theoretical Biology* **246**(3), 499509.

[36] Smith?, R.J., Schwartz, E.J. 2008. Predicting the potential impact of a cytotoxic T-lymphocyte HIV vaccine: how often should you vaccinate and how strong should the vaccine be? *Mathematical Biosciences* **212**, 180-187.

[37] Lou, J., Smith?, R.J. 2011. Modelling the effects of adherence to the HIV fusion inhibitor enfuvirtide. *Journal of Theoretical Biology* **268**(1), 1-13.

[38] Lou, J., Lou, Y., Wu, J. 2012. Threshold virus dynamics with impulsive antiretroviral drug effects. *Journal of Mathematical Biology* **65**(4), 623-52.

[39] Morse, S. S. 1995. Factors in the Emergence of Infectious Diseases. *Emerging Infectious Diseases* **1**, 7-15.

[40] Despommiers, D., Ellis, B. R., Wilcox, B. A. 2007. The Role of Ecotones in Emerging Infectious Diseases. *EcoHealth* **3**, 281-289.

[41] Anyamba, A., Chretien, J. P., Smalla, J., Tuckera, C. J., Formentyc, P. B., Richardsond, J. H., Britche, S. C., Schnabelf, D. C., Ericksonb, R. L., Linthicume, K. J. 2009. Prediction of a Rift Valley fever outbreak. *PNAS* **106**, 955-959.

[42] Patz, J. A., Campbell-Lendrum, D., Holloway, T., Foley, J. A. 2005. Impact of regional climate change on human health. *Nature* **438**, 310-317.

[43] Porphyre, T., Bicout, D. J., Sabatier, P. 2005. Modelling the abundance of mosquito vectors versus flooding dynamics. *Ecological Modelling* **183**, 173-181.

[44] Favier, C., Chalvet-Monfray, Sabatier, P., Lancelot, R., Fontenille, D, Dubois, M. A. 2006. Rift Valley fever in West Africa: the role of space in endemicity. *Tropical Medicine and International Health* **12**, 1878-1888.

[45] Moutailler, S., Krida, G., Schaffner, F., Vazeille, M., Failloux, A.-B. 2008. Potential Vectors of Rift Valley Fever Virus in the Mediterranean Region. *Vector-Borne and Zoonotic Diseases* **8**, 749-753.

[46] Turell, M. J., Dohm, D. J., Mores, C. N., Terracina, L., Wallette Jr., D. L., Hribar, L. J., Pecor, J. E., Blow, J. A. 2008. Potential for North American Mosquitoes to Transmit Rift Valley Fever Virus. *Journal of the American Mosquito Control Association* **24**, 502-507.

[47] House, J. A., Turell, M. J., Mebus, C. A. 1992. Rift Valley fever: present status and risk to the Western Hemisphere.*Annals New York Academy of Sciences* **653**, 233-242.

[48] Traoré-Lamizana, M., Fontenille, D., Diallo, M. Ba, Y., Zeller, H. G., Mondo, M., Adam, F., Thonon, J., Maiga, A. 2001. Arbovirus Surveillance from 1990-1995 in the Barkedji Area (Ferlo) of Senegal, a Possible Natural Focus of Rift Valley Fever Virus. *Journal of Medical Entomology* **38**, 480-491.

[49] Meegan, J. M. 1980. The Rift Valley fever epizootic in Egypt 1977-78 1. Description of the epizootic and virological studies. *Transactions of the Royal Society of Tropical Medicine and Hygiene* **73**, 618-623.

[50] Gerdes, G. H. 2004. Rift Valley Fever. Revue scientifique et technique - Office International des Epizooties, **23**, 613-623.

[51] Turell, M. J., Linthicum, K. J., Patrican, L. A., Davies, F. G., Kairo, A., Bailey, C. L. 2008. Vector Competence of Selected African Mosquito (Diptera:

Culicidae) Species for Rift Valley Fever Virus. *Journal of Medical Entomology* **45**, 102-108.

[52] Balkhy, H. H., Memish, Z. A. 2003. Rift valley fever: an uninvited zoonosis in the Arabian peninsula. *International Journal of Antimicrobial Agents* **21**, 153-157.

[53] House, J.A., Turell, M.J., Mebus, C.A. 1992. Rift Valley Fever: present status and risk to the Western Hemisphere. *Annals New York Academy of Sciences* **653**, 233-242.

[54] Gaff, H.D., Hartley, D.M., Leahy, N.P. 2007. An Epidemiological Model of Rift Valley Fever. *Electronic Journal of Differential Equations* **2007**, 1-12.

[55] Trigg, P.I. and Kondrachine, A.V. 1998. Commentary: Malaria control in the 1990s. *Bulletin of the World Health Organization* **76**, 11-16.

[56] Mabaso, M.L., Sharp, B., and Lengeler, C. 2004. Historical review of malarial control in southern Africa with emphasis on the use of indoor residual house-spraying. *Tropical Medicine and International Health* **9**, 846-856.

[57] Macintyre, K., Keating, J., Okbaldt, Y.B., et al. 2006. Rolling out insecticide treated nets in Eritrea: Examining the determinants of possession and use in malarious zones during the rainy season. *Tropical Medicine and International Health* **11**, 824-833.

[58] Al-Arydah, M. and Smith?, R. 2011. Controlling malaria with indoor residual spraying in spatially heterogeneous environments. *Mathematical Biosciences and Engineering* **8**(4), 889-914.

[59] Leviyang, S. 2012. Sampling HIV intrahost genealogies based on a model of acute stage CTL response. *Bull Math Biol.* **74**(3), 509-35.

[60] Simonov, M., Rawlings, R.A., Comment, N., Reed, S.E., Shi, X., Nelson, P.W. 2012. Modeling adaptive regulatory T-cell dynamics during early HIV infection. *PLoS One* **7**(4), e33924.

[61] Center for Disease Control and Prevention. HIV transmitted from a living organ donor. New York City, 2009.

[62] van Manen, D., Delaneau, O., Kootstra, N.A., Boeser-Nunnink, B.D., Limou, S., Bol, S.M., Burger, J.A., Zwinderman, A.H., Moerland, P.D., van 't Slot, R., Zagury, J-F., van 't Wout, A.B., Schuitemaker, H. 2011. Genome-Wide Association Scan in HIV-1-Infected Individuals Identifying Variants Influencing Disease Course. *PLoS ONE* **6**(7), e2208.

[63] Lacerda, M., Scheffler, K., Seoighe, C. 2010. Epitope discovery with phylogenetic hidden Markov models. *Mol Biol Evol.* **27**(5), 1212-20.

[64] Lee, B., Sharron, M., Montaner, L.J., Weissman, D., Doms, R.W. 1999. Quantification of CD4, CCR5, and CXCR4 levels on lymphocyte subsets, dendritic cells, and differentially conditioned monocyte-derived macrophages. *Pro. Nat. Aca. of Sci. of USA* **96**(9), 5215-5220.

[65] Seibert, S.A., Howell, C.Y., Hughes, M.K., Hughes, A.L. 1995. Natural Selection on the gag, pal, and eltv Genes of Human Immunodeficiency Virus 1 (HIV-l). *Mol. Biol. Evol.* **12**(5), 803-813.

[66] Mills, J., Masur, H. 1990. AIDS-Related Infections. *Scientific American*

[67] Maplanka, C. 2007. AIDS: is there an answer to the global pandemic? The immune system in HIV infection and control. *Viral Immunology* **20**, 331-42.

[68] Shiri, T., Welte, A. 2008. Transient antiretroviral therapy selecting for common HIV-1 mutations substantially accelerates the appearance of rare mutations. *Theor Biol Med Model.* **5**, 25.

[69] Shi, V., Tridane, A., Kuang, Y. 2008. A viral load-based cellular automata approach to modeling HIV dynamics and drug treatment. *J Theor Biol.* **253**(1), 24-35.

[70] Huang, Y., Wu, H., Acosta, E.P. 2010. Hierarchical Bayesian inference for HIV dynamic differential equation models incorporating multiple treatment factors. *Biom J.* **52**(4), 470-86.

[71] von Wyl, V., Cambiano, V., Jordan, M.R., Bertagnolio, S., Miners, A., Pillay, D., Lundgren, J., Phillips, A.N. 2012. Cost-Effectiveness of Tenofovir Instead of Zidovudine for Use in First-Line Antiretroviral Therapy in Settings without Virological Monitoring. *PLoS One* **7**(8).

[72] Wagner, B.G., Blower, S. 2012. Universal Access to HIV Treatment versus Universal 'Test and Treat': Transmission, Drug Resistance & Treatment Costs. *PLoS One* **7**(9).

[73] Heye, T.B., Tadesse, B.T., Yalew, A.W. 2012. Predictors of treatment failure and time to detection and switching in HIV-infected Ethiopian children receiving first line anti-retroviral therapy. *BMC Infect Dis.* **12**(1).

[74] Mohanty, U., Dixit, N.M. 2008. Mechanism-based model of the pharmacokinetics of enfuvirtide, an HIV fusion inhibitor. *J Theor Biol.* **251**(3), 541-51.

[75] Bhunu, C.P., Garira, W., Magombedze, G. 2009. Mathematical analysis of a two strain HIV/AIDS model with antiretroviral treatment. *Acta Biotheor.* **57**(3), 361-81.

[76] Rosenbloom, D.I., Hill, A.L., Rabi, S.A., Siliciano, R.F., Nowak, M.A. 2012. Antiretroviral dynamics determines HIV evolution and predicts therapy outcome. *Nat Med.*

[77] Wu, J., Yan, P., Archibald, C. 2007. Modelling the evolution of drug resistance in the presence of antiviral drugs. *BMC Public Health.* **7**, 300.

[78] Rong, L., Gilchrist, M.A., Feng, Z., Perelson, A.S. 2007. Modeling within-host HIV-1 dynamics and the evolution of drug resistance: trade-offs between viral enzyme function and drug susceptibility. *J Theor Biol.* **247**(4), 804-18.

[79] Rong, L., Feng Z., Perelson, A.S. 2007. Emergence of HIV-1 drug resistance during antiretroviral treatment. *Bull Math Biol. 69*(6), 2027-60.

[80] Kitayimbwa, J.M., Mugisha, J.Y., Saenz, R.A. 2012. The role of backward mutations on the within-host dynamics of HIV-1. *J Math Biol.*

[81] World Health Organization, UNICEF, UNAIDS, UNFPA. HIV transmission through breastfeeding. A review of available evidence. An undate from 2001 to 2007.

[82] Cremin I, Alsallaq R, Dybul M, Piot P, Garnett G, Hallett TB. 2013. The new role of antiretrovirals in combination HIV prevention: a mathematical modelling analysis. *AIDS* **27**(3), 447-58.

[83] Wahl, L.M., Nowak, M.A. 2000. Adherence and drug resistance: predictions for therapy outcome. *Proc R Soc B* **267**, 835-843.

[84] Philips, A.N., Youle, M., Johnson, M., Loveday, C. 2001. Use of stochastic model to develop understanding of the impact of different patterns of antiretroviral drug use on resistance development. *AIDS* **15**, 2211-2220.

[85] Tchetgen, E., and Kaplan, E.H., Friedland, G.H. 2001. Public health consequences of screening patients for adherence to highly active antiretroviral therapy. *J AIDS* **26**, 118-129.

[86] Huang, Y., Rosenkranz, S., Wu, H. 2003. Modeling HIV dynamics and antiviral response with consideration of time-varying drug exposures, adherence and phenotypic sensitivity. *Math Biosci* **184**, 165-186.

[87] Huang, Y., Liu, D., Wu H. 2004. Hierarchical Bayesian methods for estimation of parameters in longitudinal HIV dynamic system. *Biometrics* **62**, 413-423.

[88] Ferguson, N.M., Donnelly, C.A., Hooper, J., Ghani, A.C., Fraser, C., Bartley, L.M. 2005. Adherence to antiretroviral therapy and its impact on clinical outcome in HIV-infected patients. *J R Soc Interface* **2**, 349-363.

[89] Vernazza, P., Hirschel, B., Bernasconi, E., Flepp, M. 2008. Les personnes sropositives ne souffrant d'aucune autre MST et suivant un traitement antiretroviral efficace ne transmettent pas le VIH par voie sexuelle. *Bulletin des mdecins suisses* **89**.

[90] Hart, C.E., Lennox, J.L., Pratt-Palmore, M., Wright, T.C., Schinazi, R.F., Evans-Strickfaden, T., Bush, T.J., Schnell, C., Conley, L.J., Clancy, K.A., Ellerbrock, T.V. 1999. Correlation of Human Immunodificiency Virus Type 1 RNA levels in blood and female genital tract. *The journal of infectious diseases* **179**, 871-882.

[91] Wilson, D.P., Law, M.G., Grulich, A.G., Cooper, D.A., Kaldor, J.M. 2008. Relation between HIV viral load and infectiousness: a model-based analysis. *Lancet* **372**, 314-320.

[92] Wilson, D.P., 2010. Correspondence. *AIDS* **24**(2), 2891-2893.

[93] Boily, M.-C.Bastos, F.I.,Desai, K.Msse, B. 2004. Changes in the Transmission Dynamics of the HIV Epidemic After the Wide-Scale Use of Antiretroviral Therapy Could Explain Increases in Sexually Transmitted Infections: Results From Mathematical Models. *Sexually Transmitted Diseases* **31**(2), 100-113.

[94] Marks, G., Crepaz, N., Jassen, R.S. 2006. Estimating sexual transmission of HIV from persons aware and unaware that they are infected with the virus in the USA. *AIDS* **20**(10), 1447-1450.

[95] Smith? R.J., Aggarwala, B.D. 2010. HIV: the invisible epidemic of the United States healthcare system. *Social Theory and Health* **8**, 83-94.

[96] Lewis, S. HIV/AIDS in Africa: gender inequality is fatal, pg. 4-12.

[97] Clark, S. 2004. Early marriage and HIV risks in sub-Saharan Africa. *Stud. Fam. Plann.* **35**(3), 149-160.

[98] Diouf, N. 2004. Polygamy hangs on in Africa. *The Milwaukee Journal Sentinel*.

[99] Ramjee, G., Gouws, E. 2002. Prevalence of HIV among truck drivers visiting sex workers in KwaZulu-Natal, South Africa. *Sex Transm. Dis.* **29**(1), 44-49.

[100] Bwayo, J., Plummer, F., Omari, M., Mutere, A., Moses, S., Ndinya-Achola, J., Velentgas, P., Kreiss, J. 1994. Human Immunodeficiency Virus Infection in Long-Distance Truck Drivers in East Africa. *Archives of Internal Medicine* **154**(12).

[101] Ho, J.L., He, S., Hu, A., Geng, J., Dasile, F.G., Almeida, M.G., Saito, A.Y., Laurence, J., Johnson, W.D. Jr. 1995. Neutrophils from human immunodeficiency virus (HIV)-seronegative donors induce HIV replication from HIV-infected patients' mononuclear cells and cell lines: and in vitro model of HIV transmission facilitated by Chlamydia trachomatis. *Journal of Experimental medicine* **181**, 1493-1505.

[102] Laga, M., Manoka, A., Kivuvu, M., Malele, B., Tuliza, M., Nzila, N., Goeman, J., Behets, F., Batter, V., Alary, M., Heyward, W.L., Ryder, R.W., Piot, R. 1993. Non-ulcerative sexually transmitted diseases as risk factors for HIV-1 transmission in women: results from a cohort study. *AIDS* **7**(1), 95-102.

[103] McGowan, J.P., Shah, S.S., Ganea, C.E., Blum, S., Ernst, J.A., Irwin, K.L., Olivo, N., Weidle, P.J. 2004. Risk Behaviour for Transmission of Human Immunodeficiency Virus (HIV) among HIV-seropositive individuals in an urban setting. *Clinical Infectious Diseases* **38**(1), 122-127.

[104] Meel, B.L., 2003. The myth of child rape as a cure for HIV/AIDS in Transkei: A case report. *Medicine, Science and the law* **43**(1), 85-88.

[105] Meier, E. 2002. Child Rape in South Africa. *Pediatr. Nurs.* **28**, 532-535.

[106] Herek, G., Glunt, E. 1988. An Epidemic of Stigma. *American Psychologist* **43**, 886-891.

[107] Patton, C. 2011. Rights Language and HIV Treatment: Universal Care or Population Control? *Rhetoric Society Quarterly* **41**(3), 250-266.

[108] Cummins J., Dezzutti, C. 2000. Sexual HIV-1 transmission and mucosal defense mechanisms *AIDS* **2**, 144-154.

[109] Parker, R., Aggleton, P. 2003. HIV and AIDS-related stigma and discrimination: a conceptual framework and implications for action. *Social Science & Medicine* **57**, 13-24.

[110] World Health Organization (2005, November 21) HIV infection rates decreasing in several countries but global number of people living with HIV continues to rise WHO.

[111] Watson, C. 1988. An open approach to AIDS. Uganda. *Afr Rep.*, 32-4.

[112] Jones, S. 1991. Uganda battles AIDS on all fronts. Medical aid. *New Afr.*.

[113] Joshi, H., Lenhart, S., Albright, K., Gipson, K. 2008. Modeling the effect of information campaigns on the HIV epidemic in Uganda. *Math Biosci Eng.* **5**(4), 757-70.

[114] Kassa S.M., Ouhinou A. 2011. Epidemiological models with prevalence dependent endogenous self-protection measure. *Math Biosci.* **229**(1), 41-9.

[115] Waetjen, T., Mar, G. 2010. Traditions desire: The politics of culture in the rape trial of Jacob Zuma. *concerned Africa scholars* **84**.

[116] Page-Shafer, K., 2002. Risk of HIV transmission attributable to oral sex among men who have sex with men and in the population of men who have sex with men. *AIDS* **16**, 2350-2352.

[117] Kalichman, S.C., Rompa, D., Cage, M., DiFonzo, K., Simpson, D., Austin, J., Luke, W., Buckles, J., Kyomugisha, F., Benotsch, E., Pinkerton, S., Graham, J. 2001. Effectiveness of an intervention to reduce HIV transmission risks in HIV-positive people. *American Journal of Preventive Medicine* **21**(2), 84-92.

[118] Weinhardt, L.S., Carey, M.P., Johnson, B.T., Bickham, N.L. 1999. Effects of HIV counselling and testing on sexual risk behaviour: A meta-analytic review of published research, 1985-1997. *American Journal of Public Health* **89**.

[119] Mukandavire, Z., Garira, W. 2007. Effect of public health educational campaigns and the role of sex workers on the spread of HIV/AIDS among heterosexuals. *Theoretical Pop. Bio.* **72**(13), 346-356.

[120] Smith?, R.J., Magnet, S. 2007. The introduction of vaginal microbicides must also target men. *Journal of men's health and gender* **4**(1), 81-84.

[121] Davis, K., Weller, S. 1999. Condom effectiveness in reducing heterosexual HIV transmission (Review). *The cocharane collaboration*, Wiley.

[122] Smith, R.J., Bodine, E.N., Wilson, D.P., Blower, S.M. 2005. Evaluating the potential impact of vaginal microbicides to reduce the risk of acquiring HIV in female sex workers. *AIDS* **19**, 413-421.

[123] Quinn, T. et al. 2000. Viral load and heterosexual transmission of human immunodeficiency virus type 1. *The New England journal of medicine* **342**.

[124] Weiss, H.A., Quigley, M.A., Hayes, R.J. 2000. Male circumcision and risk of HIV infection in sub-Saharan Africa: a systematic review and meta-analysis. *AIDS* **14**, 2361-2370.

[125] Verguet, S. 2013. Efficient and equitable HIV prevention: A case study of male circumcision in South Africa. *Cost Eff Resour Alloc* **11**(1).

[126] Reijers, M.H., Weverling, G.J., Jurriaans, S., Wit, F.W., Weigel, H.M., Ten Kate, R.W., Mulder, J.W., Frissen, P.H., van Leeuwen, R., Reiss, P., Schuitemaker, H., de Wolf, F., Lange, J.M. 1998. Maintenance therapy after quadruple induction therapy in HIV-1 infected individuals: Amsterdam Duration of Antiretroviral Medication study. *Lancet* **352**, 185-190.

[127] Havlir, D.V., Marschner, I.C., Hirsch, M.S., Collier, A.C., Tebas, P., Bassett, R.L., Ioannidis, J.P., Holohan, M.K., Leavitt, R., Coone, G., Richman, D.D. 1998. Maintenance antiretroviral therapies in HIV infected patients with undetectable plasma HIV RNA after triple-drug therapy. AIDS Clinical Trials Group Study 343 Team. *N Engl J Med* **339**, 1261-1268.

[128] Pialoux, G., Raffi, F., Brun-Vezinet, F., Meiffrédy, V., Flandre, P., Gastaut, J.-A., Dellamonica, P., Yeni, P., Delfraissy, J.-F., Aboulker, J.-P. 1998. A randomized trial of three maintenance regimens given after three months of induction therapy with zidovudine, lamivudine, and indinavir in previously untreated HIV-1-infected patients. Trilege (Agence Nationale de Recherches sur le SIDA 072) Study Team. *N Engl J Med* **339**, 1269-1276.

[129] Emini, E., Koff, W. 2004. Developing an AIDS Vaccine: Need, Uncertainty, Hope. *Science* **304**(5679), 1913-1914.

[130] Campbell, N., Reece, J. 2002. *Biology.* Benjamin Cummings, pg. 335, 393, 919-21, 438, 455, 832-33.

[131] Donnelly, J.J., Ulmer, J.B., Liu, M.A. 1996. DNA vaccines. *Life Science* **60**(3), 163-172.

[132] Robinson, H.L. 2007. HIV/AIDS Vaccines: 2007. *Clin. Pharm. Thera.* **82**, 686-693.

[133] Koff, W.C., Johnson, P.R., Watkins, D.I., Burton, D.R., Lifson, J.D., Hasenkrug, K.J., McDermott, A.B., Schultz, A., Zamb, T.J., Boyle, R., Desrosiers R.C. 2006. HIV vaccine design: insights from live attenuated SIV vaccines. *Nature Immunology* **7**, 19-23.

[134] Faller, E., McVey, M., Kakal, J., MacPherson, P. 2006. Interleukin-7 receptor expression on CD8 T-cells is downregulated by the HIV Tat protein. *J. Acquir. Im. Defic. Syndr.* **43**.

[135] Dorigatti I., Pugliese A. 2011. Analysis of a vaccine model with cross-immunity: when can two competing infectious strains coexist? *Math Biosci.* **234**(1), 33-46.

[136] Lou J, Wu J, Chen L, Ruan Y, Shao Y. 2009. A sex-role-preference model for HIV transmission among men who have sex with men in China. *BMC Public Health* **9** Suppl 1.

[137] Konrad, B.P., Vaidya, N., Smith?, R.J. 2011. The impact of mutation to a cytotoxic T-lymphocyte HIV vaccine. *Mathematical Population Studies* **18**(2), 122-149.

[138] Gumel A.B., McCluskey C.C., van den Driessche P. 2006. Mathematical study of a staged-progression HIV model with imperfect vaccine. *Bull Math Biol.* **68**(8),2105-28.

[139] Smith, R.J., Blower, S.M. 2004. Could disease-modifying HIV vaccines cause population-level perversity? *The Lancet Infectious Diseases* **4**, 636-639.

[140] Bultimore, D., 1995. Lessons from people with nonprogressive HIV infection. *N. Engl. J. Med.* **332**, 259-60.

[141] Patton, C. 1990. Inventing African AIDS. *new formations* NUMBER 10, 25-39.

[142] Marshall, B.D., Paczkowski, M.M., Seemann, L., Tempalski, B., Pouget, E.R., Galea, S., Friedman, S.R. 2012. A complex systems approach to evaluate HIV prevention in metropolitan areas: preliminary implications for combination intervention strategies. *PLoS One* **7**(9), e44833.

[143] Smith?, R.J., Li, J., Gordon, R., Heffernan, J.M. 2009. Can we spend our way out of the AIDS epidemic? A World Halting AIDS Model. *BMC Public Health* **9**(Suppl 1), S15.

[144] Marino, S., Hogue, I.B., Ray, C.J., Kirschner, D.E. 2008. A methodology for performing global uncertainty and sensitivity analysis in systems biology. *J Theor Biol.* **254**(1), 178-196.

[145] AIDSinfo Drug Database. Ritonavir. Revised July 2013. AbbVie Inc. http://aidsinfo.nih.gov/drugs/244/ritonavir/33/professional

[146] Roche, J.P. 2002. The New York Academy of Medicine Print Media Coverage of Risk-Risk Tradeoffs Associated with West Nile Encephalitis and Pesticide Spraying. *Journal of Urban Health: Bulletin of the New York Academy of Medicine* **79**(4).

[147] Karpati, A.M., Perrin M.C., Matte, T., Leighton, J., Schwartz, J., Barr, G. 2004. Pesticide Spraying for West Nile Virus Control and Emergency Department Asthma Visits in New York City, 2000. *Environ Health Perspect.* **112**(11), 11831187.

[148] Mostashari, F., Kulldorff, M., Hartman, J.J., Miller, J.R., Kulasekera, V. 2003. Dead Bird Clusters as an Early Warning System for West Nile Virus Activity. *Emerg Infect Dis.* **9**(6), 641646.

[149] Muturui, E, J., Shililu, J. I., Gu, W., Jacob, B. G., Githure, J. I., Novak, R. J. 2007. Larval habitat dynamics and diversity of Culex mosquitoes in rice agro-ecosystems in Mwea, Kenya. *American Journal of Tropical and Medicine* **76**, 95-102.

[150] Bicout, D.J., Sabatier, P. 2004. Mapping Rift Valley Fever Vectors and Prevalence Using Rainfall Variations. *Vector-borne and Zoonotic diseases* **4** (1).

[151] Zell, R. 2004. Global climate change and the emergence/re-emergence of infectious diseases. *Int. J. Med. Microbiol.* **293** (37), 16-26.

[152] Favier, C., Chalvet-Monfray, K., Sabatier, P., Lancelot, R., Fontenille, D., Dubois, M.A. 2006. Rift Valley Fever in West Africa: the role of space in endemicity. *Tropical Medicine and International Health* **11** (12), 1878-1888.

[153] Gaff, H.D., Burgess, C., Jackson, J., Niu, T., Papelis, Y., Hartley, D. 2011. Mathematical Model to Assess the Relative Effectiveness of Rift Valley Fever Countermeasures. *International Journal of Artificial Life Research* **2**(2), 1-18.

[154] Crabtree, D.E. 1966. Characteristic roots of M-matrices. *A.M.S.*, 1435